CARES/LIFE Ceramics Analysis and Reliability Evaluation of Structures Life Prediction Program

Noel N. Nemeth
Glenn Research Center, Cleveland, Ohio

Lynn M. Powers
Case Western Reserve University, Cleveland, Ohio

Lesley A. Janosik and John P. Gyekenyesi
Glenn Research Center, Cleveland, Ohio

Since its founding, NASA has been dedicated to the advancement of aeronautics and space science. The NASA Scientific and Technical Information (STI) Program Office plays a key part in helping NASA maintain this important role.

The NASA STI Program Office is operated by Langley Research Center, the Lead Center for NASA's scientific and technical information. The NASA STI Program Office provides access to the NASA STI Database, the largest collection of aeronautical and space science STI in the world. The Program Office is also NASA's institutional mechanism for disseminating the results of its research and development activities. These results are published by NASA in the NASA STI Report Series, which includes the following report types:

- TECHNICAL PUBLICATION. Reports of completed research or a major significant phase of research that present the results of NASA programs and include extensive data or theoretical analysis. Includes compilations of significant scientific and technical data and information deemed to be of continuing reference value. NASA's counterpart of peer-reviewed formal professional papers but has less stringent limitations on manuscript length and extent of graphic presentations.

- TECHNICAL MEMORANDUM. Scientific and technical findings that are preliminary or of specialized interest, e.g., quick release reports, working papers, and bibliographies that contain minimal annotation. Does not contain extensive analysis.

- CONTRACTOR REPORT. Scientific and technical findings by NASA-sponsored contractors and grantees.

- CONFERENCE PUBLICATION. Collected papers from scientific and technical conferences, symposia, seminars, or other meetings sponsored or cosponsored by NASA.

- SPECIAL PUBLICATION. Scientific, technical, or historical information from NASA programs, projects, and missions, often concerned with subjects having substantial public interest.

- TECHNICAL TRANSLATION. English-language translations of foreign scientific and technical material pertinent to NASA' mission.

Specialized services that complement the STI Program Office's diverse offerings include creating custom thesauri, building customized databases, organizing and publishing research results . . . even providing videos.

For more information about the NASA STI Program Office, see the following:

- Access the NASA STI Program Home Page at *http://www.sti.nasa.gov*

- E-mail your question via the Internet to help@sti.nasa.gov

- Fax your question to the NASA Access Help Desk at 301–621–0134

- Telephone the NASA Access Help Desk at 301–621–0390

- Write to:
  NASA Access Help Desk
  NASA Center for AeroSpace Information
  7121 Standard Drive
  Hanover, MD 21076

CARES/LIFE Ceramics Analysis and Reliability Evaluation of Structures Life Prediction Program

Noel N. Nemeth
Glenn Research Center, Cleveland, Ohio

Lynn M. Powers
Case Western Reserve University, Cleveland, Ohio

Lesley A. Janosik and John P. Gyekenyesi
Glenn Research Center, Cleveland, Ohio

This document was initially released in 1993. The formal numbered publication was delayed until 2003.

TABLE OF CONTENTS

Introduction

Advanced ceramic components designed for gasoline, diesel, and turbine heat engines are leading to lower engine emissions, higher fuel efficiency, and more compact designs due to their low density and ability to retain strength at high temperatures. Ceramic materials are also used for wear parts (nozzles, valves, seals, etc.), cutting tools, grinding wheels, bearings, and coatings. Currently, research is focused on improving ceramic material properties and processing, lowering associated manufacturing costs, properly characterizing material properties, and developing a mature and validated brittle material design methodology. The emerging materials, particularly silicon nitride and silicon carbide, consist of abundant and nonstrategic constituents and have the potential for competing with traditional metals in many demanding applications. For advanced heat engines, ceramic components have already demonstrated functional abilities at temperatures reaching 1371 °C -- well beyond the operational limits of most metallic materials.

Unfortunately, ceramics also have several inherent undesirable properties which must be considered in the design procedure. The most deleterious of these properties is that ceramics are brittle materials. This lack of ductility and yielding capability leads to low strain tolerance, low fracture toughness, and large variations in observed fracture strength. When a load is applied, the absence of significant plastic deformation or microcracking causes large stress concentrations to occur at microscopic flaws, which are unavoidably present as a result of materials processing operations or inservice environmental factors. The observed scatter in component strength is caused by the variable severity of these flaws and by the behavior of sudden catastrophic crack growth which occurs when the crack driving force or energy release rate reaches a critical value. In addition, the ability of a ceramic component to sustain a load degrades over time due to a variety of effects such as oxidation, creep, stress corrosion, and cyclic fatigue. Stress corrosion and cyclic fatigue result in a phenomenon called subcritical crack growth (SCG). SCG initiates at a pre-

existing flaw and continues until a critical length is reached, causing catastrophic propagation. The SCG failure mechanism is a load-induced phenomenon over time. It can also be a function of chemical reaction, environment, debris wedging near the crack tip, and deterioration of bridging ligaments.

Once the factors that contribute to material failure have been identified and characterized, ceramic components can be designed for service applications using an appropriate brittle material design methodology. For this purpose the integrated design computer program CARES/LIFE (Ceramics Analysis and Reliability Evaluation of Structures LIFE) has been developed to predict the fast-fracture and/or lifetime reliability of monolithic structural ceramic components subjected to thermomechanical and/or proof test loading. This design methodology combines the statistical nature of strength-controlling flaws with fracture mechanics to allow for multiaxial stress states, concurrent flaw populations, and subcritical crack growth. CARES/LIFE is an extension of the CARES program (Powers, Starlinger, and Gyekenyesi, 1992) (Nemeth, Manderscheid, and Gyekenyesi, 1990) (Pai, and Gyekenyesi, 1988) (Gyekenyesi, and Nemeth, 1987) (Gyekenyesi, 1986), which predicts the fast-fracture reliability of monolithic ceramic components. The fundamental subsets of the program include: (a) fast-fracture reliability analysis, (b) inert (fast-fracture) statistical material parameter estimation, (c) crack growth laws to account for static and cyclic fatigue, (d) conversion of cyclic boundary loading to an equivalent static state, (e) static, dynamic, and cyclic fatigue parameter estimation, (f) fatigue parameter compatibility relationships for various stress states, fracture criteria, and failure probability models, and (g) the effect of proof testing on component service probability of failure.

Because ceramics fail due to the presence of microscopic flaws, examination of fracture surfaces can reveal the nature of failure. Fractography of broken samples has shown that these flaws can be characterized into two general categories: (1) defects internal or intrinsic to the

material volume (volume flaws) and (2) defects extrinsic to the material volume (surface flaws). Intrinsic defects are a result of materials processing. Extrinsic flaws can result from grinding or other finishing operations, from chemical reaction with the environment, or from the internal defects intersecting the external surface. The different physical nature of these flaws results in dissimilar failure response to identical loading situations. Consequently, separate criteria must be employed to describe the effects of the applied loads on the component surface and volume.

Because of the statistical nature of these flaw populations, the size of stressed material surface area and volume (known as the size effect) affects the strength. By increasing component size, the average strength is reduced because of the increased probability of having a weaker flaw. Generally, for metals, the variation of strength is small, and thus the scaling effect is negligible; however, for materials that display large variations of strength, this effect is not trivial. Hence, if a ceramic design is based on material parameters obtained from smaller size test pieces, then the effects of scaling must be taken into account, otherwise a nonconservative design will result.

Another consequence of the random distribution of flaws is that failure of a complex component may not be initiated at the point of highest nominal stress. A particularly severe flaw may be located at a region of relatively low stress, yet still be the cause of component failure. For this reason, the entire field solution of the stresses should be considered. Clearly, it is not adequate to predict reliability based only on the most highly stressed point.

Traditional analysis of the failure of materials uses a deterministic approach, where failure is assumed to occur when some allowable stress level or equivalent stress is exceeded. The most widely used of these theories are the maximum normal stress, maximum normal strain, maximum shear stress, and maximum distortional energy criteria of failure. These phenomenological failure theories have been reasonably successful when applied to ductile materials such as metals. However, these methods do not account for observed variations in ceramic component fracture

stress. Therefore, to assure high reliability in brittle material design, large factors of safety are required. This does not allow for optimization of design since the physical phenomena that determine fracture response are not properly modeled.

Because of its lack of a proper physical basis, the traditional approach to design is not adequate to predict failure of brittle materials. Consequently, Griffith (Griffith, 1921) (Griffith, 1924) proposed a fracture theory where failure was due to the presence of cracks of specified size and shape distributed randomly throughout the material. He assumed that no interaction takes place between adjacent cracks and that failure occurs at the flaw with the least favorable orientation relative to the macroscopic loading. The Griffith energy balance criterion for fracture states that crack growth will occur if the energy release rate reaches a critical value. Griffith's theory provides a sound physical basis to describe the rupture process in an isotropic brittle continuum. However, it omits the effect of component size on strength because the crack length is not treated as a probabilistic quantity.

Reliability analysis is essential for accurate failure prediction and efficient structural utilization of brittle materials subjected to arbitrary stress states. When coupled with the weakest-link model (Weibull (151), 1939), this approach takes into account not only the size effect and loading system, but also the variability in strength due to defect distributions. A statistical theory of failure can be readily incorporated into the finite element method of structural analysis since each element can be made arbitrarily small such that the element stress gradient is negligible. Component integrity is computed by calculating element-by-element reliability and then determining the component survivability as the product of the individual element reliabilities.

For fast-fracture reliability analysis, the first probabilistic approach used to account for the scatter in fracture strength and the size effect of brittle materials was introduced by Weibull (Weibull (151), 1939) (Weibull (153), 1939) (Weibull, 1951). This approach is based on the

previously developed weakest-link theory (WLT) (Pierce, 1926) (Kontorova, 1940) (Frenkel, and Knotorova, 1943), which is primarily attributed to Pierce, who proposed it while modeling yarn failure. The weakest-link theory is analogous to pulling a chain, where catastrophic failure occurs when the weakest link in the chain is broken. Unlike Pierce, who assumed a Gaussian distribution of strength, Weibull assumed a unique probability density function known as the Weibull distribution. It has been shown (Shih; 1980) that the three-parameter Weibull distribution is a more accurate approximation of ceramic material behavior than the Gaussian or other distributions. Since three-parameter behavior is rarely observed in as-processed monolithic ceramics, the CARES/LIFE program uses the two-parameter Weibull model in which the threshold stress (the value of applied stress below which the failure probability is zero) is taken as zero. The reliability predictions obtained using the two-parameter model are more conservative than those obtained with the three-parameter model.

To predict the fast-fracture material response under multiaxial stress states by using statistical parameters obtained from flexural or uniaxial test specimens, Weibull proposed calculating the risk of rupture by averaging the tensile normal stress raised to an exponent in all directions over the area of a unit radius sphere (volume flaws) (Weibull(151), 1939) or over the contour of a unit radius circle (surface flaws) (Gross, 1989). Although this approach is intuitively plausible, it is somewhat arbitrary. In addition, it lacks a closed-form solution, and therefore, requires computationally intensive numerical modeling. Subsequently, Barnett and Freudenthal (Barnett, et al., 1967) (Freudenthal, 1968) proposed an alternative approach usually referred to as the principle of independent action (PIA) model for finding the failure probability in multidimensional stress fields. This principle states that the Weibull survival probability of a uniformly stressed material element experiencing multiaxial loading is equal to the product of the survival probabilities for each of the tensile principal stresses applied individually. The PIA fracture theory is the weakest-link statistical

equivalent of the maximum stress failure theory. The Weibull method of averaging the tensile normal stress and the principle of independent action model have been the most popular methods for polyaxial stress state analysis, and they have been widely applied in brittle material design (Margetson, 1976) (Paluszny, and Wu, 1977) (DeSalvo, 1970) (Wertz, and Heitman, 1980) (Dukes, 1971).

However, the Weibull and PIA hypotheses do not specify the nature of the defect causing failure, and consequently, there is no foundation for extrapolating to conditions different from the original test specimen configuration. Consequently, the accuracy of these theories has been questioned, and other statistical models have been introduced (Batdorf, and Crose, 1974) (Evans, and Jones, 1978) (Batdorf, 1976). The ideas developed by Batdorf and Crose (Batdorf, and Crose, 1974) are important because they provide a physical basis for incorporating the effect of multiaxial stresses into the weakest-link theory. They describe material volume and surface imperfections as randomly oriented, noninteracting discontinuities (cracks) with an assumed regular geometry. This enables the contributions of shear and normal forces to the fracture process to be explicitly treated. Failure is assumed to occur when the effective stress on the weakest flaw reaches a critical level. The effective stress is a combination of normal and shear stresses acting on the flaw. It is a function of the assumed crack configuration, the existing stress state, and the fracture criterion employed. Accounting for the presence of shear on the crack plane reduces the normal stress needed for fracture, yielding a more accurate reliability analysis than that of the shear-insensitive crack model (Weibull's method). Unlike in the deterministic Griffith failure criterion, the size of the crack in the probabilistic approach need not be considered because it is associated with the strength of the material.

The search for an accurate fracture criterion to predict fast-fracture response to monotonically increasing loads leads to the field of fracture mechanics. Many authors have discussed the stress

distribution around cavities of various types under different loading conditions, and numerous criteria have been proposed to describe impending failure. Paul and Mirandy (Paul, and Mirandy, 1976) extended Griffith's maximum tensile stress criterion for biaxial loadings to include three-dimensional effects due to Poisson's ratio and flaw geometry, which could not be accounted for in Griffith's previous two-dimensional analysis. Other investigators (Giovan, and Sines, 1979) (Batdorf, 1982) (Stout, and Petrovic, 1984) (Petrovic, and Stout, 1984) have compared results from the most widely accepted mixed-mode fracture criteria with each other and with selected experimental data. No prevailing consensus has emerged regarding a best theory. Also, most of the criteria predict somewhat similar results, despite the divergence of initial assumptions. Therefore, the authors of this report concluded that several alternatives would be available for the sake of comparison but that the semi-empirical equation developed by Palaniswamy and Knauss (Palaniswamy, and Knauss, 1978) and Shetty (Shetty, 1987) provides the most flexibility to fit the available experimental data. In addition, Shetty's criterion can account for the out-of-plane flaw growth that is observed under mixed-mode loadings. Finally, several different flaw geometries are provided, but the penny-shaped and semicircular crack configurations are recommended as the most accurate representations of volume and surface defects, respectively.

A wide variety of materials, including ceramics, exhibit the phenomenon of delayed fracture or fatigue. Under the application of a loading function of magnitude smaller than that which induces short term failure, there is a regime where subcritical crack growth occurs and this can lead to eventual component failure in service. SCG is a complex process involving a combination of simultaneous and synergistic failure mechanisms. These can be grouped into two catagories: (1) crack growth due to corrosion, and (2) crack growth due to mechanical effects arising from cyclic loading. Stress corrosion is due to a stress-dependent chemical interaction between the material and its environment. Water, for example, has a pronounced deleterious effect on the strength of glass

and alumina. Higher temperatures also tend to accelerate this process. Mechanically induced cyclic fatigue is dependent only on the number of load cycles and not on the duration of the cycle. This phenomenon can be caused by a variety of effects, such as debris wedging or the degradation of bridging ligaments, but essentially it is based on the accumulation of some type of irreversible damage that tends to enhance the crack growth. Service environment, material composition, and material microstructure determine if a brittle material will display one, none, or some combination of these fatigue mechanisms.

Because of the complex nature of SCG, models that have been developed tend to be semi-empirical and approximate the behavior of subcritical crack growth phenomenologically. Theoretical and experimental work in this area has demonstrated that lifetime failure characteristics can be described by consideration of the crack growth rate versus the stress intensity factor (or the range in the stress intensity factor). This is graphically depicted as the logarithm of the rate of crack growth versus the logarithm of the mode I stress intensity factor. Curves of experimental data show three distinct regimes or regions of growth. The first region indicates threshold behavior of the crack, where below a certain value of stress intensity the crack growth is zero. The second region shows an approximately linear relationship of stable crack growth. The third region indicates unstable crack growth as the materials critical stress intensity factor is approached. For the stress corrosion failure mechanism, these curves are material and environment sensitive. This model, using conventional fracture mechanics relationships, satisfactorily describes the failure mechanisms in materials where at high temperatures, plastic deformations and creep behave in a linear visco-elastic manner (Evans, and Wiederhorn, 1974). In general, at high temperatures and low levels of stress, failure is best described by creep rupture which generates new cracks (Wiederhorn, and Fuller, 1985). Creep and material healing mechanisms are not addressed in the CARES/LIFE code.

The most often cited models in the literature regarding SCG are based on power law formulations. Other theories, most notably Wiederhorn's (Wiederhorn, Fuller, and Thomson, 1980), have not achieved such widespread usage, although they may also have a reasonable physical foundation. Power law formulations are used to model both the stress corrosion phenomenon and the cyclic fatigue phenomenon. This modeling flexibility, coupled with their widespread acceptance, make these formulations the most attractive candidates to incorporate into a design methodology. A power law formulation is obtained by assuming the second crack growth region is linear and that it dominates over the other regions. Three power law formulations are useful for modeling brittle materials: the power law, the Paris law, and the Walker law. The power law (Evans, and Wiederhorn, 1974) (Wiederhorn, 1974) describes the crack velocity as a function of the stress intensity factor, and implies that the crack growth is due to stress corrosion. For cyclic fatigue, either the Paris law (Paris, 1963) or Walker's (Walker, 1970) (Dauskardt, et al., 1992) modified formulation of the Paris law is used to model the subcritical crack growth. The Paris law describes the crack growth per load cycle as a function of the range in the stress intensity factor. The Walker equation relates the crack growth per load cycle to both the range in the crack tip stress intensity factor and the maximum applied crack tip stress intensity factor. It is useful for predicting the effect of the R-ratio (the ratio of the minimum cyclic stress to the maximum cyclic stress) on the material strength degradation.

Because SCG operates on the pre-existing flaws in the material, the fast-fracture statistical theories discussed previously are required to predict the time-dependent reliability for brittle materials. The SCG model is combined with the two-parameter Weibull cumulative distribution function to characterize the component failure probability as a function of service lifetime. The effects of multiaxial stresses are considered by using the principle of independent action (PIA) model, the Weibull normal stress averaging method (NSA), or the Batdorf theory.

Lifetime reliability analysis accounting for subcritical crack growth under cyclic and/or sustained loads is essential for the safe and efficient utilization of brittle materials in structural design. Current life design methodology assumes SCG of mixed-mode loading is based on a power function relationship existing between the crack propagation rate and the equivalent mode I stress intensity factor (Boehm, 1989) (Hamanaka, et al., 1987) (Homada, and Teramae, 1990) (Thiemeier, 1989) (Sturmer, et al., 1990) (Sturmer, et al., 1991). The literature is sparse regarding crack velocity measurements for mixed-mode loadings of brittle materials. When a crack is subjected to a combined mode loading, it extends in a curved or kinked path that reorients the crack to a pure mode I coplanar extension at the crack tip (Shetty, and Rosenfield, 1991). The models of Boehm, Hamanaka, Homada, Thiemeier, and Sturmer do not consider this more complex behavior due to paucity of available data. The approach taken by these researchers is reasonable if the duration where mixed-mode loading exists at the crack tip is small compared to the duration where the crack tip is extending in pure mode I. In any event, the formulations they adopted will tend to be conservative.

For corrosion-assisted SCG, time-dependent reliability analysis for a component subjected to various cyclic boundary load conditions can be simplified by transforming that type of loading to an equivalent static state. The conversion, through the use of a constant called the g-factor (Evans, 1980) (Mencik, 1984), satisfies the requirement that both systems will cause the same crack growth. Implicit in this conversion is the validity of the crack growth power law. The probability of failure is then obtained with respect to the transformed equivalent static state.

Prior to placing a component in service, confidence that it will perform reliably is usually demonstrated through proof testing. To a great extent, this is the accepted way to assure the reliability of a component (Evans, and Wiederhorn, 1974) (Wiederhorn, 1974) (Ritter, Oates, Fuller, and Wiederhorn, 1980) (Fuller, Wiederhorn, Ritter, and Oates, 1980) (Srinivasan, and Seshadri,

1982). Ideally, the boundary load conditions applied to a component under proof testing simulate those conditions a component would be subjected to in service and the proof test loads are appropriately greater in magnitude over some fixed time interval. The significance of proof testing is that it enables specimens with a certain minimum flaw size or larger to be eliminated from the strength distribution. Thus, an attenuated probability of failure is obtained and the survived components can be placed in service with greater confidence in their integrity. In practice, however, it is often difficult, expensive, or impossible for the proof test load conditions to exactly simulate the service load conditions; there can exist misalignment between the loads, or the proof test and the service load are different multiaxial stress states. This situation can be accounted for when proof testing design methodology is incorporated into the statistical fracture theories for polyaxial stress states (Service, and Ritter, 1985) (Hamanaka, Suzuki, and Sakai, 1990) (Brukner-Foit, Heger, and Munz, to be published). An attenuated probability of failure is computed for the survived components, however a minimum life of assured reliability may no longer be relavent.

The primary objective of this report is to describe a public domain computer program that is coupled with the general purpose finite element codes MSC/NASTRAN[1], ANSYS[2], and ABAQUS[3] for predicting the fast-fracture and/or service lifetime failure probability of monolithic ceramic components. Potential enhancements to the code include the capability for transient analysis, three-parameter Weibull statistics, creep and oxidation modeling, flaw anisotropy, and parameter regression for multiple specimen sizes.

This report functions as both a users' and a programmers' manual. The user can focus primarily on the first five sections of this manual for background information and for detailed

---

[1]MacNeal-Schwendler Corporation, Los Angeles, CA.

[2]Swanson Analysis Systems, Inc., Houston, PA.

[3]Hibbitt, Karlsson, and Sorenson, Inc., Providence, RI.

descriptions of the program capabilities, setup and execution, input, and output. A users' guide has been prepared to facilitate execution of the CARES/LIFE program. In addition, seven example problems are included in the section **Example Problems** to further illustrate program input, output, and interpretation of results. These examples also provide program validation and verification. It is strongly recommended that the user read the theoretical sections as well for a better understanding of the probabilistic fast-fracture and time-dependent theories employed. All of these sections are essential to a programmer who may wish to modify the source code. In addition, a list of symbols has been included to aid the reader.

Program Capability and Description

The CARES/LIFE integrated design computer program predicts the reliability and the failure probability of a monolithic ceramic component as a function of its service life. CARES/LIFE couples commercially available finite element programs, such as MSC/NASTRAN, ANSYS, or ABAQUS with probabilistic design methodologies to account for material failure from subcritical crack growth (SCG) of preexisting flaws. The code is written in FORTRAN 77 and is divided into three separately executable modules which perform: (1) statistical analysis and characterization of experimental data obtained from the fracture of standard laboratory specimens; (2) neutral data base generation from the MSC/NASTRAN, ABAQUS, and ANSYS finite element analysis programs; and (3) time-dependent reliability evaluation of thermomechanically loaded ceramic components. Proof test effects on a survived component are included along with the consequences of off-axis and multiaxial loading. Figure 1 illustrates the operational flow of the program. Finite element heat transfer and linear-elastic stress analysis are used to determine the temperature and stress distributions in the component. Component reliability for volume (intrinsic) flaws is determined from finite element stress, temperature, and volume output from two-dimensional, three-dimensional or axisymmetric elements. Reliability for surface (extrinsic) flaws is calculated from shell element stress, temperature, and area data. CARES/LIFE produces an optional PATRAN file containing risk-of-rupture intensities (a local measure of reliability) for graphical rendering of the structure's critical regions.

The phenomenon of subcritical crack growth (SCG) is modeled with the power law, the Paris law, and the Walker law. The power law (Evans, and Wiederhorn, 1974) (Wiederhorn, 1974) describes the crack velocity as a function of the stress intensity factor. For cyclic fatigue, either the Paris law (Paris, 1963) or Walker's (Walker, 1970) (Dauskardt, et al., 1992) modified formulation of the Paris law is used to model the subcritical crack growth. The Paris law relates the crack growth

per load cycle to the range in the stress intensity factor. The Walker equation relates the crack growth per load cycle to both the range in the crack tip stress intensity factor and the maximum applied crack tip stress intensity factor. This formulation accounts for the effect of the R-ratio (minimum cycle stress to maximum cycle stress) on lifetime. The power law and the Paris law require two experimentally derived fatigue parameters N and B which are material/environmental constants. The Walker equation requires three material/environmental constants N, B, and Q. Steady-state cyclic loading is accounted for by using the Walker law, the Paris law, or by employing g-factors (Mencik, 1984) in conjunction with the power law. The g-factor approach equates variable cyclic loadings to equivalent static loadings. CARES/LIFE includes the sinusoidal, square, and sawtooth loading waveforms. Typically, the use of g-factors is appropriate for flat T-curve materials (T-toughness resistance).

The probabilistic nature of material strength and the effects of multiaxial stresses are modeled by using either the principle of independent action (PIA), the Weibull normal stress averaging method, or the Batdorf theory. The Batdorf theory combines linear elastic fracture mechanics with the weakest-link mechanism. It requires a user-selected flaw geometry and a mixed-mode fracture criterion to describe volume or surface strength limiting defects. The combination of a particular flaw shape and fracture criterion results in an effective stress, which is a function of the far-field stresses, and acts on the crack plane. Figure 2 shows the fracture criteria and flaw geometries available to the user for both surface and volume flaw analysis. The simple PIA fracture theory does not require a crack geometry. When the PIA model is used, only tensile principal stresses can contribute to failure. The Weibull normal stress averaging (NSA) method is independent of crack geometry. The mode I (opening mode) crack growth is considered, and mode II (sliding mode) and mode III (tearing mode) effects are neglected. The combination of a particular flaw shape and fracture criterion results in an effective stress involving far-field principal stresses in terms of

normal and shear stresses acting on the crack plane. CARES/LIFE includes the total strain energy release rate theory (coplanar crack extension) (Batdorf, and Heinisch, 1978). Out-of-plane crack extension criteria are approximated by a simple semi-empirical equation (Palaniswamy, and Knauss, 1978) (Shetty, 1987). This equation involves a parameter that can be varied to model the maximum tangential stress theory (Erdogan, and Sih, 1963), the minimum strain energy density criterion (Sih, 1974), the maximum strain energy release rate theory (Hellen, and Blackburn, 1975) (Ichikawa, 1991), or experimental results. For comparison, Griffith's maximum tensile stress analysis for volume flaws is also included. The highlighted boxes in figure 2 show the recommended fracture criteria and flaw shapes. If the normal stress acting on the flaw plane is compressive, then no crack growth is assumed to occur.

In CARES/LIFE, if the maximum principal stress is compressive, then the corresponding element reliability is set equal to unity. Typically, brittle materials are much stronger in compression than in tension. It is assumed that the lower tensile strength limit will predominate over the higher compressive limit for a typical component design. If the compressive stresses are significant, they should be checked against limiting values by other methods.

For fast fracture, the probabilistic nature of material strength is described by the two-parameter Weibull cumulative distribution function, which incorporates weakest-link theory. This relation postulates that inherent material flaws in the component body (volume flaws) and on its surface (surface flaws) govern the strength response. The component reliability is determined by integrating the stress over the body. The Weibull stress-volume integral is a function of the scale parameter, σ_o, and the shape parameter, m. The scale parameter corresponds to the stress level at which 63.21 percent of specimens with unit volume or area would fracture. The characteristic strength, σ_θ, is similar to the Weibull scale parameter except that it includes the effect of the

specimen volume or area. The shape parameter (or Weibull modulus), denoted by m, is a

dimensionless quantity and measures the degree of strength dispersion of the flaw distribution.

Weibull material parameters, the Batdorf crack density coefficient, and fatigue parameters are

estimated from rupture strength data of naturally flawed specimens. The parameters are obtained

from the fracture stresses of specimens whose geometry and loading configurations are held constant

(30 or more specimens are recommended). A similar number is recommended for fatigue

experiments. The CARES/LIFE program includes closed form solutions for the three- and

four-point modulus-of-rupture (MOR) bending bar (Baratta, Matthews, and Quinn, 1987) and the

pure tensile specimen (Liu, and Brinkman, 1986) under isothermal conditions. For other

conventional specimen geometries, material parameters can be estimated via effective volume and

area calculations (a finite element model of the specimen geometry and loading is required).

Since the material parameters are a function of temperature, various constant-temperature data

sets can be simultaneously input and the corresponding parameter estimates will be calculated and

made available for component reliability analysis. Linear interpolation is performed to obtain values

at intermediate temperatures. More sophisticated interpolation techniques are not used due to the

potential of obtaining erroneous results. Each constant-temperature data set can consist of up to 999

specimens. In addition, each specimen can be identified by its mode of failure-either volume flaw,

surface flaw, or some other mode -- so that parameter estimates for competing failure modes can be

obtained.

CARES/LIFE estimates fatigue parameters from naturally flawed specimens ruptured under

static, cyclic, or dynamic loading (CARES/LIFE does not estimate the Walker R-ratio sensitivity

exponent, Q). Cyclic fatigue parameter evaluation assumes steady state loading and a constant R-

ratio throughout the specimen. Fatigue parameters can be calculated using either the median value

technique (Jakus, Coyne, and Ritter, 1978), a least squares regression technique, or a median

deviation regression method which is somewhat similar to trivariant regression (Jakus, Coyne, and Ritter, 1978). The median value technique is a well known estimation procedure based on regression of the median values of the fatigue data at the various stressing levels or rates. The least squares regression technique involves a regression on all the fatigue data to establish the parameters. The median deviation procedure involves minimizing the median deviation of the scatter in the data versus the crack growth exponent N. In the CARES/LIFE code this minimization is accomplished by maximizing the time-dependent Weibull modulus versus the crack growth exponent N. The fast-fracture strength distribution Weibull modulus, m, and characteristic strength, σ_θ, are optionally estimated from the fatigue data for a failure time of one second with constant stress rate loading (or a lifetime of $1/(N+1)$ cycles). The fatigue data is transformed to an equivalent fast-fracture strength distribution. This enables goodness-of-fit testing and using an outlier test. The resulting goodness-of-fit statistics are applied to the original fatigue data. If inert strength fracture data is simultaneously input, then the Weibull parameters for this data override those calculated from time-dependent data.

For inert strength fracture (fast-fracture) data, parameter estimation of the biased Weibull modulus and characteristic strength σ_θ can be performed for unimodal or concurrent surface and volume flaw populations by using least-squares analysis (Johnson, 1964) or the maximum likelihood method (Nelson, 1982). Because estimates of Weibull parameters are obtained from a finite amount of data, they contain an inherent uncertainty that can be characterized by bounds in which the true parameters are likely to lie. Methods have been developed to evaluate confidence limits that quantify this range with a level of probability as a function of sample size. For the maximum likelihood method with a complete sample, unbiasing factors for the shape parameter m, and 5- and 95-percent confidence limits for m and the characteristic strength σ_θ, are provided (Thoman, Bain, and Antle, 1969). For a censored sample, an asymptotic approximation of the 90-percent confidence

.

limits is calculated. No unbiasing of parameters or estimation of confidence limits is given when the least-squares option is requested.

CARES/LIFE includes a test that will identify potential bad data (outliers) from the time-dependent or inert strength fracture experiments. This test, known as the Stefansky outlier test (Stefansky, 1972) (Neal, Vangel, and Todt, 1987), is based on the normal distribution and, therefore, its application to the Weibull distribution is not rigorous. However, it serves as a useful guideline to the user. Data detected as outliers are flagged with a warning message, and any further action is left to the discretion of the user.

The ability of the hypothesized distribution to reasonably fit the empirical data is measured with the Kolmogorov-Smirnov (K-S) and Anderson-Darling (A-D) goodness-of-fit tests. These tests are extensively discussed by D'Agostino and Stephens (D'Agostino, and Stephens, 1986). The tests quantify discrepancies between the experimental data and the estimated Weibull distribution by a significance level associated with the hypothesis that the data were generated from the proposed distribution. The A-D test is more sensitive than the K-S test to discrepancies at low and high probabilities of failure. The calculated significance levels are based on the assumption that the Weibull parameters are chosen independent of the experimental data. For inert strength data the Kanofsky-Srinivasan 90-percent confidence band values (Kanofsky, and Srinivasan, 1972) about the Weibull line are given as an additional test of the goodness-of-fit of the data to the Weibull distribution.

CARES/LIFE automatically calculates the other material parameters necessary for the reliability analysis. The biased estimate of the shape parameter and the estimated characteristic strength are used along with the specimen geometry to calculate the Weibull scale parameter. The Batdorf normalized crack density coefficient is computed from the selected fracture criterion, crack

geometry, and the biased estimate of the shape parameter. The computation of the material/environmental fatigue parameters is detailed in the **Theory** section.

To ensure compatibility of failure probabilities for surface and volume flaw specimens, the relationships between the fatigue parameters (N and B) and the various failure criteria have been established. From test specimen data (uniaxial tension, 3- and 4-point bend) compatibility is derived by equating the risk of rupture of the uniaxial Weibull model to the risk of rupture of the PIA, NSA or the Batdorf shear-sensitive models. This satisfies the requirement that for a uniaxial stress state, all models produce the same probability of failure as the uniaxial Weibull model. The value of N is invariant and the value of B is adjusted to satisfy this condition.

Finite element analysis is an ideal mechanism for obtaining the stress distribution needed to calculate the survival probability of a structure. Each element can be made arbitrarily small, such that the stresses can be taken as constant throughout each element (or subelement). In CARES/LIFE the reliability calculations are performed at the Gaussian integration points of the element or, optionally, at the element centroid. Using the element integration points enables the element to be divided into sub-elements, where integration point sub-volumes, sub-areas, and sub-temperatures are calculated. The location of the Gaussian integration point in the finite element, and the corresponding weight functions are considered when the subelement volume/area is calculated. The number of subelements in each element depends on the integration order chosen, and the element type. If the probability of survival for each element is assumed to be a mutually exclusive event, the overall component reliability is the product of all the calculated element (or sub-element) survival probabilities.

The component reliability analysis module of the CARES/LIFE program uses finite element elastostatic output to calculate time-dependent reliability for each element. Volume-flaw-based reliability is calculated from the previously determined volume flaw material strength parameters

and the output of the stresses, volumes, and temperatures for each solid element. Volume flaw analysis can be performed using brick, wedge, and tetrahedron isoparametric solid elements, triangular (and optionally quadrilateral) axisymmetric isoparametric elements, and triangular and quadrilateral isoparametric shell elements. For the MSC/NASTRAN finite element analysis code, the supported element types are HEXA, PENTA, TETRA, TRIAX6, QUAD4, QUAD8, TRIA3, and TRIA6. The capability to use shell elements with volume flaw analysis is a restricted option requiring a zero stress gradient through the element thickness. Surface-flaw-based reliability is calculated from the surface flaw material strength parameters and individual shell element output of the two-dimensional surface stresses, areas, and temperatures. Surface flaw analysis can be performed using quadrilateral and triangular isoparametric shell elements. Modeling with axisymmetric elements is not permitted for surface flaw reliability analysis. For the MSC/NASTRAN finite element analysis code, the supported element types are QUAD4, QUAD8, TRIA3, and TRIA6. Shell elements are used to identify external surfaces of solid elements that correspond to the component external surfaces important to the reliability analysis. Shell elements with exclusively membrane properties and negligible thickness (and hence stiffness) are used.

Provision is made in CARES/LIFE to permit the use of the cyclic symmetry modeling option in MSC/NASTRAN or similar mesh reduction schemes done via component symmetry. CARES/LIFE also permits the analysis of simultaneously occurring flaw populations in a given finite element model (multiple ceramic materials or multiple flaw population capability). Elements not designated as brittle materials are ignored in the reliability computations. Temperature-dependent statistical material properties are linearly interpolated at each individual element temperature. Element and nodal identification numbers can be arbitrary. The risk-of-rupture intensity is also calculated for each element, and these values are sorted to determine the maximum values. Element risk-of-rupture intensities are written to a data file for processing

with a graphical interpreter such as PATRAN (only available if the finite element mesh has been generated via PATRAN preprocessing).

Proof test methodology is incorporated into the PIA, the Weibull normal stress averaging, and the Batdorf theories, accounting for the effect of multiaxial stresses. With the Weibull normal stress averaging and the Batdorf theory, the proof test load need not closely simulate the actual service conditions on the component. This is important because it allows reliability analysis to be performed when proof test stresses have not been applied in the same direction and/or location as the service load stresses. CARES/LIFE simultaneously processes two finite element analysis neutral files containing the stress analysis results for the proof test and the service load conditions. The duration of the proof test and the service load are also considered and each load situation can have different material-environmental constants (Weibull and fatigue parameters).

For a steady-state cyclic load, component reliability analysis can be performed if the ratio of the minimum cycle stress to the maximum cycle stress is constant throughout the component. When this ratio is not constant throughout the component, two finite element result files are required for the reliability analysis. These two files represent the extremes of the cyclic load range. The capability of performing transient analysis is also planned for a future update of CARES/LIFE. If temperature cycling is present, resulting in a variation of material properties as a function of time, the most severe set of parameters will be used in the analysis with the Paris law or the Walker equation.

The CARES/LIFE coding architecture has been designed into a modular format to facilitate ease of use, specialization of function, and access to additional finite element codes with a minimization of effort (Powers, Starlinger, and Gyekenyesi, 1992). The algorithm is split into three separately executable module types: (1) the finite element data interface modules; (2) the material parameter estimation module; and (3) the component reliability evaluation module. With the first

set of modules, results from finite element analysis (available in the form of standard output files and/or plot data files) are interpreted. Modules are available for the ABAQUS, ANSYS, and MSC/NASTRAN finite element programs, which are named ABACARES, ANSCARES, and NASCARES, respectively. These interpreter programs write element or subelement stress tensors, volumes (or surface areas for shell elements), and temperatures into a formatted (ASCII) neutral data base. This feature enables easy data transfer between different computer systems and avoids repeated (time consuming) executions of the interpreter program. The structure of the neutral data base is optimized with respect to memory. The finite element data is arranged within the neutral data base using the following hierarchy-- element groups, elements and subelements.

The second module, named C4PEST, performs the statistical analysis and estimates inert strength Weibull parameters and fatigue parameters from fracture data of naturally flawed specimens. The parameter estimates are placed in a data file for subsequent use by the third module, named C4LIFE, which reads this file and the neutral data base created from the finite element interpreter program to calculate the component reliability. C4LIFE will read two neutral data base files simultaneously if proof testing or cyclic loading is invoked. Although all the modules in CARES/LIFE are separately executed, they are easily coupled through command files to sequentially execute without user intervention. Modularization of the program minimizes the memory overhead, creates a more comprehensible code, and decreases the need to repeatedly process finite element results files.

The component reliability evaluation module (C4LIFE) and the finite element data interface module NASCARES use a blank common technique to adjust memory size for a particular problem. As such, there is no limitation on the total number of elements that can be used in a model. However, larger memory capacity is required for larger problems. A minimum of 2 megabytes of memory are necessary to execute the programs. The introduction of one large blank common array

(instead of several fixed-dimension arrays) in each routine allows the user to easily adapt the program to the problem size as well as to the available computational resources. The size of the blank common array is adjusted by resetting one parameter (MTOT) at the beginning of the module main program. This capability enables executing the program on PC systems and workstations. Individual arguments within the blank common array are addressed via pointers, which are integer variables whose values are internally adjusted within the program to optimize memory. The finite element interface modules ABACARES and ANSCARES use fixed dimension arrays instead of the blank common technique. Integer parameters are declared at the beginning of the main module and the subroutines to fix the array sizes. Initial settings support a maximum of 2000 solid and 2000 shell elements.

The material parameter estimation module (C4PEST) does not use the blank common technique, due to the large amount of variable arguments (and hence pointers) required and the reduced need to conserve computer memory. Instead, array sizes are declared with parameters initialized at the beginning of each subroutine. These parameters correspond to the number of materials (LM), the number of temperature sets (KL), and the maximum number of specimens used for each temperature (IJK). Module C4PEST has the initial settings of LM = 100, KL = 15, and IJK = 999. Adjustment of these array sizing parameters must be identically done for every subroutine within the C4PEST module.

Because input files may be quite large and require a significant amount of execution time, CARES/LIFE is designed to run in a batch mode environment. Therefore all program input are contained in control and data files. Data files refer to finite element analysis results files and neutral data base files. Control files refer to files containing control indices required to control program execution, material definitions - such as fracture criterion and specimen data or temperature dependent material parameters, and flags for printing and postprocessing (e.g. writing the element

risk of rupture intensities to a PATRAN data file). Description and specification of data within these files, as well as preparation of the finite element problem and program execution are explained in the following sections of this manual.

Input Information

The CARES/LIFE program consists of three separate executable modules: (1) CARES neutral data base creation module (module name of NASCARES, ANSCARES, and ABACARES for the MSC/NASTRAN, ANSYS, and ABAQUS finite element analysis programs, respectively); (2) fatigue parameter and Weibull parameter estimation module C4PEST; and (3) component reliability analysis module C4LIFE. Figure 3 shows the required input files for the various modules to perform a complete analysis (the default file names are shown in the figure). The required input information for each of these modules will be discussed in detail. In addition, the preparation of an MSC/NASTRAN finite element analysis problem for subsequent reliability analysis with CARES/LIFE will be discussed. For details of preparing a structural model with ANSYS or ABAQUS, consult the appropriate manuals/papers which are available.

MSC/NASTRAN Finite Element Analysis

NASTRAN (NASA STRuctural ANalysis) is a large, comprehensive, general purpose finite element computer code for structural analysis which was developed under NASA sponsorship to fill the need for a universally available analysis program. It was initially released into the public domain in 1969 through COSMIC (COmputer Software Management and Information Center). In addition to the NASA-supported version, which is commonly called COSMIC/NASTRAN, there are several enhanced proprietary versions of this program. The most widely known of these proprietary versions is MSC/NASTRAN, which was developed and is maintained by the MacNeal-Schwendler Corporation. This version of NASTRAN includes a consistent set of isoparametric two- and three-dimensional elements, rigid elements, superelements for substructural analysis, improved cyclic symmetry, and numerical analysis and computer science enhancements. MSC/NASTRAN is widely

.

used by many of the world's largest corporations, government laboratories, and commercial data centers.

MSC/NASTRAN creates and manipulates a data base to solve problems by matrix structural analysis. It includes rigid formats: that is, an ordered execution of a set of DMAP (Direct Matrix Abstraction Programming) instructions. The CARES/LIFE program utilizes results from only a very small fraction of available NASTRAN analysis capability. Since fast-fracture mechanical design of high-performance ceramic components requires temperature and stress solutions only, static analysis results from Solution Sequence 61 and Rigid Format 47 (in case of cyclic symmetry) are most often used. Beginning with version 66, MSC/NASTRAN has introduced new structured solution sequences. These solutions are useful because DMAP routines are organized to be compatible with any other structured solution sequence. Solutions numbered 100 and higher are structured. SOL 101 - SESTATIC and SOL 114 - CYCSTATX may be used in place of SOL 61 and SOL 47, respectively.

The MSC/NASTRAN program is controlled by user-specified input data. The functions of the MSC/NASTRAN input can be logically described as: (1) Providing user control over the MSC/NASTRAN executive functions - the EXECUTIVE CONTROL DECK, (2) Providing user control over program input and output - the CASE CONTROL DECK, and (3) Defining the physical problem consisting of the finite element model, including constraints and loading conditions - the BULK DATA DECK. Details of preparing a MSC/NASTRAN structural model with the selected elements can be found in Schaeffer (Schaeffer, 1979) and in the appropriate MacNeal-Schwendler NASTRAN manuals. It is assumed that analysts using the CARES/LIFE program are fully familiar with MSC/NASTRAN and its capabilities in solving heat transfer and stress analysis problems.

A new version of MSC/NASTRAN is made available to the user community every year. Currently Version 67 is being used on the NASA Lewis computer; consequently, it was the version used to solve the example problems summarized in the EXAMPLE PROBLEM section of this manual. A word of caution is in order at this point. Occasionally, coding errors arise in NASTRAN which, when reported to MacNeal-Schwendler Corporation, are usually corrected in later releases. MSC/NASTRAN Version 64 and earlier versions had coding errors in calculating TRIAX6 element volumes. These errors were supposedly corrected in Version 66. Also, for a HEXA or PENTA element, significant error can be introduced in the calculation of the element volume when the element geometry has a large amount of curvature, especially when a coarse mesh is used. Finally, errors in stress computation occurred with Version 64 shell elements when nonuniform temperatures were imposed on a given element's nodes. This error should also have been corrected in Version 65, and it does appear that this problem has been fixed.

The following is an example of the MSC/NASTRAN EXECUTIVE CONTROL DECK which is recommended to obtain satisfactory input for CARES/LIFE postprocessing for a typical problem involving static analysis:

NASTRAN DAYLIMIT = -1

ID CERAMIC,FRACTURE

APP DISP

SOL 101

TIME 30

CEND

For problems that are modeled with cyclic symmetry, Solution Sequence 101 is replaced by Solution Sequence 114.

It is assumed that the user is familiar with MSC/NASTRAN, so each statement will not be explained herein. Previously, for CARES 1 and CARES 2, Solution Sequence 61-SUPERELEMENT STATICS (or SOL 101, in version 66) and Rigid Format 47-CYCLIC STATICS (or SOL 114) were used for the analysis because element volumes and areas can be obtained through a PARAM card located in the BULK DATA. Since the element (and subelement) volumes/areas are now calculated by the NASCARES finite element interface module, a limit on which solution sequences may be used is no longer present.

For the CASE CONTROL DECK, a typical problem without the cyclic symmetry option would contain

```
TITLE = USER OPTION
SUBTITLE = USER OPTION
SEALL = ALL
SPC = 10
MPC = 11
LOAD = 12
DISP = ALL
STRESS(PRINT) = ALL
ECHO = SORT
    .
    .
    .

BEGIN BULK
```

A problem with the cyclic symmetry option would typically contain

```
TITLE = USER OPTION
SUBTITLE = USER OPTION
SET 2 = 0
HARMONICS = 2
SPC = 1
LOAD = 10
SET 5 = 1
NOUTPUT = 5
DISP = ALL
SET 8 = 1 THRU 1000 EXCEPT 200 THRU 300
STRESS (PRINT) = 8
ECHO = SORT
    .                    .
    .
```

BEGIN BULK

The following three items are important to note. First, multiple load subcases are not defined. CARES/LIFE does not handle stress output from multiple subcases at this time; therefore, separate NASTRAN executions are required for each loading condition. Second, element stresses are routed to the printout file when STRESS(PRINT)=ALL is specified. All element stresses must be placed in the print file. Last, ECHO=SORT will send the sorted BULK DATA to the print file. CARES/LIFE reads the necessary BULK DATA, such as material ID, element connectivity, and nodal temperatures, from the print file.

Selected cards from the BULK DATA deck are:

```
BEGIN BULK
PARAM,EST,1
TEMPD,2,70.0
TEMP...
    .
    .
    .
GRID...
    .
    .
    .
CHEXA...
    .
    .
    .
CPENTA...
    .
    .
    .
CTETRA...
    .
    .
    .
CQUAD8...
    .
    .
    .
CTRIA6...
    .
```

.
.
.

PSOLID...

.
.

PSHELL...

.
.
.

ENDDATA

The PARAM,EST card will output element volumes and areas to the NASTRAN printout file. As noted previously, this card only functions for some solution sequences or rigid formats. The TEMPD card is required if some grid points do not have an explicit temperature assignment. All nodes must have an associated temperature, either through a TEMP, TEMP*, or TEMPD card. Since this version of CARES/LIFE does not examine cards for their subcase identity, caution must be exercised not to allow multiple temperature cases. Nodal temperatures are used by CARES/LIFE to obtain the average element or subelement temperatures, which are not routinely available in MSC/NASTRAN.

General guidelines for modeling will now be discussed. Ceramics are extremely sensitive to geometric discontinuities and resulting stress concentrations. Solid elements have the best capability for modeling regions of high stress gradients, such as fillets and corners, and for outputting detailed stress maps. A study on the accuracy of NASTRAN solid elements (Case, and Vandegrift, 1984) concluded that quadratic elements are probably the most accurate and efficient in analyzing three-dimensional structures, especially with potential extremes in element aspect ratios. CARES/LIFE utilizes results from isoparametric two- and three-dimensional, as well as axisymmetric, finite elements. The HEXA, PENTA, TETRA, and TRIAX6 elements are used for volume-based reliability analysis, and the QUAD8, QUAD4, TRIA6, and TRIA3 elements are used for surface-based reliability analysis. The TRIAX6 element is a special case because it is axisymmetric, and

therefore, it cannot be used for surface reliability analysis since the QUAD8 and TRIA6 elements cannot be attached to the modeled component surface. For typical designs, the three-dimensional HEXA, PENTA, and TETRA elements should be used to model the whole ceramic structure, including thin cross sections such as blades.

The use of the two-dimensional shell elements for surface reliability analysis is primarily to identify the corresponding external surfaces of the component. Note that shell elements used for structural modeling cannot be processed correctly by the NASCARES interface module unless NASCARES is modified to read both upper and lower surface stress states. These elements can be excluded from the reliability analysis by using a different material property identification number. The shell elements are needed by NASCARES to identify the model surface and to obtain corresponding two-dimensional stress states, areas, and surface temperatures. The shell elements are attached to the appropriate faces of the solid elements, consistent with the component external surfaces. Shell elements and solid elements should use the same nodes. An external quadrilateral face of a solid element should have a QUAD8 element attached to its nodes. The triangular face of a PENTA element should share nodes with a TRIA6 element. The shell elements should not contribute significantly to the structural stiffness of the model. This is achieved by specifying shell elements with membrane properties only and with a small thickness. Therefore, a typical PSHELL card would be

PSHELL,101,300,.000001

The entry 101 in field 2 represents the PSHELL identification number as it appears in the element connectivity card (CQUAD8 or CTRIA6). The entry 300 in field 3 is the material identification number for the membrane properties material card. The entry 0.000001 in field 4 is the thickness of the element; a small nonzero value is used so that the element stiffness contribution is negligible relative to the solid element. Material identification numbers for bending and

transverse shear are left blank, so that those effects are excluded. The PSOLID property card is used for the solid elements and is defined in the usual manner.

After execution of the MSC/NASTRAN problem, the analyst should have a print file containing the sorted BULK DATA, element stresses and general problem information. At this point, all the information required from MSC/NASTRAN to determine the component reliability is present.

Finite Element Interface Modules Input Information

The results from a finite element analysis (available in the form of standard output files and/or plot data files) have to be interpreted by an interface program for subsequent reliability analysis with CARES/LIFE. Due to the different formats used for output of the results in each finite element program, this interpreter program has to be adapted to the specific finite element software used; therefore, for each finite element software package, a separate interface program is prepared. The interface program writes the results of the finite element analysis into a file known as the neutral data base. Three interface program modules have been developed to process MSC/NASTRAN, ANSYS, and ABAQUS finite element analysis output files for subsequent reliability analysis with CARES/LIFE: NASCARES, ANSCARES, and ABACARES, respectively.

Certain information must be available from the finite element output file for processing with the interface modules. To ensure that this data is available, the user must include the appropriate flags in the finite element input file so that the data necessary for a reliability analysis is included in the finite element output file. Since this is dependent on the particular finite element software package being used, the details of the pertinent information have been addressed in a series of papers which discuss the NASCARES, ANSCARES, and ABACARES interface modules individually (Powers, Starlinger, and Gyekenyesi, 1992) (Pintz, 1989) (Edwards, Powers, ..., 1992).

The interface modules process finite element temperatures, stresses, and volumes/areas from the finite element analysis output files. If this information is not available in the finite element output file, the execution of the interface program will be terminated. If the interface program is successfully executed, a neutral data base file with the default name CARES.NEU (or PROOF.NEU, if the options of proof testing or cyclic loading are requested) will be generated. The CARES.NEU file represents the static service loading on the component or the maximum cyclic load condition. The file PROOF.NEU represents the static proof test load on the component or the minimum cyclic load condition. The contents, organization, and format of the neutral data base file are discussed in detail in the **Output Information** section.

CARES/LIFE Input File Preparation

To control the execution of the CARES/LIFE modules C4PEST and C4LIFE, the user must prepare an input file (designated as file C4PEST.INP in fig. 3) consisting of the Master Control Input and the Material Control Input. The Master Control Input is a set of control indices which directs the overall program execution. It specifies whether material parameter analysis and/or reliability analysis of a finite element model will be performed. It also specifies the number of brittle material statistical characterizations. The Material Control Input consists of control indices and either the rupture data required to estimate the fatigue and statistical material parameters or direct input of the parameter values themselves, for various temperatures. This input category includes the choices of fracture criteria and flaw shapes shown in figure 2. On the tape or disks provided with the program is a file called TEMPLET.INP that can be used to construct an input file for a particular problem. It is assumed that the CARES/LIFE user has access to a full-screen editor where block manipulations and character editing can be easily done (the resulting file should be in a plain ASCII or similar character based format).

The input to modules C4PEST and C4LIFE is keyword driven. The keywords can be present in any order within each input section (except for temperature dependent input, which must be organized into ascending order of temperature). Keywords must start in the first column of the file. The beginning of this file is reproduced in figure 4. Note that underneath each keyword a location is given that specifies where the data value or values are input. An explanation of each keyword is provided to the right, and a list of available choices is given, if applicable. If integer input is required, then the input field is defined between asterisks (*), and entries must be right justified. Real number input is read in an F10.4 or E18.10 format, and asterisks are not present to define the field width. A maximum of 30 lines between keywords is allowed before an error message is generated, and therefore, the user can insert short notes as desired. The Master Control Input is always located at the beginning of the input file.

The CARES/LIFE modules C4PEST and C4LIFE both begin execution by searching for the keywords associated with the Master Control Input. The end of the Master Control Input occurs when the $ENDX keyword is encountered. Following the Master Control Input, the modules C4PEST and C4LIFE search for keywords specific to the Material Control Input. The $ENDM and $ENDT keywords signal the end of temperature independent and temperature dependent data, respectively. Keywords not found between these $END_ intervals may assume default values (specific default values are indicated in the TEMPLET.INP file). Because CARES/LIFE has a multiple material capability, each section of input for a particular material is separated by a $ENDT card. The TEMPLET.INP file has only one material characterized. Modifying the file for more materials involves block copying the Material Control Input sections of the original file, appending them to the end of the file, and modifying the copied input values accordingly (as well as appropriately modifying the Master Control Input selections regarding the number of materials in the reliability analysis). The user is advised to keep an unaltered copy of the TEMPLET.INP file as

a backup. Details on specific input preparation are described in the **Master Control Input** and **Material Control Input** sections of this manual. Each keyword is discussed in these sections, and the format field for the input is denoted in parentheses next to the keyword as well as the appropriate module to which the keyword pertains. It is useful to note that input files previously used with the CARES fast-fracture code can also be used with CARES/LIFE without modification.

C4PEST Module Input Information

The module C4PEST performs analysis on specimen rupture data to estimate Weibull and fatigue parameters as well as calculate the other statistical measures as described in section Program Capability and Description. The default input file name for the C4PEST module is C4PEST.INP. This file contains two categories of input: (1) Master Control Input, and (2) Material Control Input (which includes temperature-dependent material fracture data). See the sections **C4PEST module Master Control Input** and **C4PEST module Material Control Input** for a detailed explanation of the input options of the C4PEST.INP file.

The output from the C4PEST module is placed in the two files (with the default names of) C4PEST.OUT and CARES.INP. C4PEST.OUT is the results file listing the estimated fatigue and statistical material parameters as well as other relevant information (goodness-of-fit results, outlier test, confidence intervals, etc...). The CARES.INP file is the corresponding input file to the C4LIFE module. This file echoes the Master Control Input and the Material Control Input from the C4PEST.INP file, except that the temperature dependent specimen fracture data is replaced with the temperature dependent Weibull and fatigue parameters (direct parameter input option). The C4LIFE module requires the temperature dependent material parameters as input. It is important to understand that the CARES.INP input file for module C4LIFE is automatically prepared by module

C4PEST from the C4PEST.INP file (the user is not required to prepare this file, although the user may desire to edit this file and make changes prior to executing the C4LIFE module).

C4PEST module Master Control Input. - The Master Control Input section from the TEMPLET.INP file is reproduced in figure 4. If parameter keywords are omitted, they assume default values as defined in figure 4. Available keywords may be specific to only one of the two modules C4PEST or C4LIFE, however, keywords not recognized by a particular module are ignored. Keywords that will be used with the C4LIFE module should be specified in the input file C4PEST.INP (for the C4PEST module) because they will automatically be reproduced in file CARES.INP when module C4PEST is executed.

INTERP (4X,I1) [C4PEST] The control index **INTERP** is to give the user the option to print material parameters at interpolated levels of temperature. If interpolated values are requested, then Lagrange polynomials are used to calculate these values at five intermediate levels between each user input temperature. These values are output in the CARES.INP file. Since the C4LIFE module linearly interpolates between the temperatures specified in the CARES.INP file, these additional values are provided so as to improve the accuracy of the interpolation. The potential penalty for requesting Lagrangian interpolated values is that poor results may be obtained, therefore interpolated values should always be verified before proceeding with reliability analysis.

IPRINT (4X,I1) [C4PEST and C4LIFE] The keyword **IPRINT** controls the printing of element stresses and experimental fracture stresses. It gives the user the option to control the length of the program output. If **IPRINT** = 0, the element stresses and/or specimen fracture data are not printed. If **IPRINT** = 1, all element stresses and/or fracture data are echoed in the program output.

NE (4X,I1) [C4PEST and C4LIFE] NE is a keyword to control program execution. If NE is zero, then component reliability analysis will not be performed. If the NE control index is 3 (or non zero) then subsequent component reliability analysis using the C4LIFE module is assumed.

NGP (4X,I2) [C4PEST and C4LIFE] NGP controls the number of Gaussian integration points that are used in the Batdorf reliability calculations in module C4LIFE. It is also used in the integration to obtain the Batdorf normalized crack density coefficient $\bar{k}_B$ in module C4LIFE and to numerically calculate g-factors when closed form solutions are not possible (such as for the sine wave). The input values can be either 15, 30 or 50. Entries of 30 or 50 will give improved accuracy but with the penalty of larger CPU requirements.

NMATS, NMATV (4X,I2) [C4PEST and C4LIFE] The keyword NMATS represents the number of materials for which surface flaw analysis is performed. NMATV represents the number of materials for which volume flaw analysis is performed. NMATS is associated with shell elements, and NMATV is associated with either solid, shell, or axisymmetric elements. This association is achieved via the finite element material ID numbers (see keyword definition MATID in the Material Control Input section). A component consisting of one material may have one set of statistical material parameters to characterize the surface and another set for the volume, for which NMATS = 1 and NMATV = 1. Statistical material parameters are a function of processing, microstructure, and environment. The CARES/LIFE program modules are capable of analyzing a single material with multiple statistical material characterizations or many materials with multiple statistical material characterizations. For example, if a single material component has two different surface finishes, then NMATS = 2 is used because two different sets of statistical material

parameters are required. The only constraint is that the total of **NMATS** + **NMATV** must be less than 101.

TITLE (72A1) [C4PEST and C4LIFE] The input associated with the **TITLE** keyword is reproduced in the program output files C4PEST.OUT and CARES.OUT for problem identification.

TIME (E10.4) [C4PEST and C4LIFE] The keyword **TIME** allows the user to specify the duration of the service loading on the component. This input should be in units of seconds (for power law) or cycles (for the Paris law and Walker law). If **TIME** = 0.0 then fast-fracture reliability is calculated.

$ENDX [C4PEST and C4LIFE] The keyword **$ENDX** signifies the end of the MASTER CONTROL INPUT.

   C4PEST module Material Control Input. - A sample of the Material Control Input from the TEMPLET.INP file is reproduced in figures 5 and 6. Note that the Material Control Input actually consists of two different data partitions. The data contained in both figures 5 and 6 are for a single material. In figure 5, temperature independent control indices, material constants, and geometric variables are shown. In figure 6, the temperature-dependent fracture data are listed. The temperature-dependent fracture data or temperature-dependent values of the Weibull and fatigue parameters are always placed immediately following the temperature independent control indices for that material. The total number of Material Control Input sections must be equal to the sum of **NMATS** + **NMATV** from the Master Control Input. Note that keywords that are not found assume default values. Available keywords may be specific to only one of the two modules C4PEST or

C4LIFE. However, all keywords that will be used with module C4LIFE should be specified in file C4PEST.INP because they will automatically be printed in file CARES.INP when module C4PEST is executed.

It should also be noted that the material Poisson's ratio is a required input (for shear sensitive Batdorf models only). Other temperature-dependent physical and mechanical properties - such as Young's modulus, thermal conductivity, thermal coefficient of expansion, and specific heat - are required for finite element analysis but are not used for reliability evaluation. It is assumed that Poisson's ratio is constant and temperature independent in the reliability evaluations.

C4PEST module Material- and specimen-dependent (temperature independent) data: The following keywords are the control indices, material indices, and geometric variables necessary for calculation of volume and surface flaw statistical parameters as shown in figure 5.

DL1, DL2, DH, DW (F10.4) [C4PEST] If **ID1** = 2 or 5 (that is, if statistical material parameters are to be determined from three- or four-point MOR flexure specimens), then the specimen dimensions must be input. All dimensions must be input in units consistent with the finite element analysis. **DL1** represents the length between the two outer symmetrical loads. **DL2** is the length between the two inner central loads, **DH** is the total height of the test specimen cross section, and **DW** is the total width of the test specimen cross section. Note that when **DL2** is set to zero, then the solution for three-point bending is obtained, and when **DL1** and **DL2** are of equal value then the pure bending beam solution is obtained. This input selection is specific to the C4PEST module.

ID1 (4X,I1) [C4PEST and C4LIFE] **ID1** is a control index for specifying the form of the data to be input for obtaining the statistical material parameters. Either the Weibull shape and scale

parameters are directly specified (**ID1** = 3) or experimental fracture data are input (**ID1** = 1, 2, 4, or 5). The fracture data can be from three-point modulus-of-rupture bend bars (**ID1**= 2 or 5), four-point modulus-of-rupture bend bars (**ID1** = 2 or 5) or tensile test specimens (**ID1** = 1 or 4). Optionally, the fracture data can be from any specimen geometry (**ID1** = 1 or 4), however this would require that the specimen effective volume or area (see **VAGAGE** keyword) be input. If the fracture data are assumed to be all from one failure mode (all volume flaws or all surface flaws), then **ID1** = 1 or 2 can be chosen. If **ID1** = 1 or 2, then CARES assumes that the fracture origins are consistent with the **ID4** input index. If **ID1** = 4 or 5, then fracture origins must be supplied with the fracture data. The **ID1** keyword is primarily for the C4PEST module. This input value must be set to a positive integer, when used with the C4LIFE module. Note that if module C4PEST is run prior to module C4LIFE, then **ID1** is automatically set to the value of 3 when module C4PEST creates the CARES.INP input file for module C4LIFE.

ID2 (4X,I1) [C4PEST and C4LIFE] The control index **ID2** is for selection of a fracture criterion. Note that some caution must be exercised here because the maximum tensile stress criterion (**ID2** = 2) is only used with volume flaw analysis (**ID4** must be set to 1). All choices available, except the PIA model, are used with the Batdorf integration routines. Shetty's mixed-mode fracture criterion (**ID2** = 5) is recommended for both surface and volume flaw analysis (see also keyword C).

ID3 (4X,I1) [C4PEST and C4LIFE] The **ID3** control index is for selection of a crack geometry. Note that caution must be exercised here since some of the available choices are applicable either for surface flaw analysis or for volume flaw analysis only. For instance, the penny-shaped crack is only applicable for volume flaw analysis. The shear sensitive notch crack and the semi-circular edge crack are only applicable for surface flaw analysis. The Griffith crack is available for both

surface and volume flaw analysis. The penny-shaped crack is recommended for volume flaw analysis and the semicircular crack is recommended for surface flaw analysis. See figure 2 for a matching of crack geometry with fracture criteria.

ID4 (4X,I1) [C4PEST and C4LIFE] **ID4** specifies if parameter estimation and subsequent component reliability analysis is volume or surface flaw based. The value input must be consistent with the **ID2** and **ID3** selections. From the fracture data supplied by the user, the Weibull shape and scale parameters, along with the normalized Batdorf crack density coefficient consistent with the **ID4** input value, are estimated and are subsequently made available for processing with finite element data. The entry for **ID4** must be consistent with the finite element analysis material card ID specified in **MATID**.

IKBAT (4X, I1) [C4PEST and C4LIFE] **IKBAT** selects the method of calculating the normalized Batdorf crack density coefficient, $\overline{k_B}$. If **IKBAT** = 0, then the crack density coefficient is set to the value that is the solution for the normal stress fracture criterion, regardless of the fracture criterion and crack geometry selected by the user for subsequent component analysis. If **IKBAT** = 1, then the crack density coefficient is calculated based on the fracture criterion and crack geometry selected by the **ID2** and **ID3** keywords. **IKBAT** = 0 gives more conservative reliability predictions than **IKBAT** = 1 does. Setting **IKBAT** = 1 is recommended.

OUTLIE (F10.4) [C4PEST] The input associated with the **OUTLIE** keyword corresponds to the significance level for which outliers of a sample distribution are to be detected. This keyword is specific to the C4PEST module. The value input can range between 0.1 (corresponding to a significance level of 0.1 percent) and 10.0 (corresponding to a significance level of 10.0 percent).

An outlier detected at the 1.0 percent level of significance indicates that there is a 1.0 percent chance that the data point is actually a member of the flaw population, and a 99.0 percent chance that the data point is an outlier. The outlier test is based on a normal distribution (symmetrical distriution about the mean) and does not rigorously apply to the Weibull distribution (skewed distribution about the mean). Results from the outlier test serve only to warn the user. Detected outliers should not be discarded or censored without proper justification (results from the outlier test alone does not constitute sufficient justification to remove or censor data).

MATID (1X,I7) [C4PEST and C4LIFE] **MATID** is the material identification number associated with the statistical material parameter data. The value input should correspond to the material identification number listed in the CARES/LIFE neutral data base file for a given element. Therefore, the value for **MATID** must match the material ID designated in the finite element analysis. If only parameter estimation is being performed, then **MATID** should be an arbitrary integer value.

MLORLE (4X,I1) [C4PEST] The **MLORLE** input is only used with the C4PEST module and is active for fast-fracture and time-dependent data (see keyword **SOL** in the section **Temperature-dependent fracture or statistical material parameters data; the Data Table form of input**). It is the control index for the method of estimation of Weibull parameters. For fast-fracture data these parameters correspond to shape parameter m and characteristic strength σ_θ. For static and cyclic fatigue data this corresponds to a time-dependent Weibull modulus $\tilde{m}$ and characteristic time t_θ. For dynamic fatigue data this corresponds to a time-dependent Weibull

modulus $\tilde{m}$ (N + 1) and characteristic time $t_{\theta d}$. See section **Theory** for a definition of these terms.

PR (F10.4) [C4PEST and C4LIFE] **PR** is Poisson's ratio. It is assumed to be temperature independent.

TITLE (72A1) [C4PEST and C4LIFE] The input associated with the **TITLE** keyword is reproduced in the program output files C4PEST.OUT and C4LIFE.OUT for material identification.

VAGAGE (F10.4) [C4PEST] **VAGAGE** is the gage volume or gage area of a tensile test specimen. This quantity can also be input in the Data Table (see section **Temperature-dependent fracture or statistical material parameters data; the Data Table form of input**). If **ID4** = 2 and **ID1** = 1 or 4 (that is, if surface flaw analysis is specified and the statistical material parameters are to be determined from specimen fracture data), then the gage surface area or effective area of the specimen must be specified. If **ID4** = 1 and **ID1** = 1 or 4 (that is, if volume flaw analysis is specified and the statistical material parameters are to be determined from specimen fracture data), then the gage volume or effective volume of the specimen must be specified. It is recommended that the Data Table be used to input this quantity since the effective volume or area can be temperature dependent quantities. See keyword **PFCONV** used with module C4LIFE for additional information.

$ENDM [C4PEST and C4LIFE] The keyword **$ENDM** signifies the end of a section of the Material Control Input. The temperature-dependent specimen fracture data or the Weibull shape and scale parameters are assumed to immediately follow.

C4PEST module temperature-dependent fracture or statistical material parameters

data: Immediately following the **$ENDM** keyword, which signals the end of the material's temperature-independent data, the temperature-dependent experimental fracture data or material parameters are input. Data must be arranged so that they correspond to ascending order of temperature. These data enable interpolation of the statistical material parameters to other temperatures. Figure 6 shows an example of the input for experimental fracture stress data for module C4PEST. The essential feature of figure 6 is that the data is organized in a table, called the Data Table (**DTABLE**) for a discrete temperature. The tabular input format for the Data Table is an upgrade feature from the previous CARES codes. It is therefore recommended that the Data Table format is always used, however for completeness the input style associated with the CARES codes is maintained with CARES/LIFE (input files prepared for CARES1, CARES2, or CARES3 can be used with CARES/LIFE). The Data Table is fully described in the following section of this manual (see section titled **Temperature-dependent fracture or statistical material parameters data; the Data Table form of input**).

The keywords used with experimental fracture stresses (i.e. **DTABLE, MOR,** and **NUT**) are only recognized by the C4PEST module. The material parameters calculated from this module are output in the CARES.INP data file for subsequent use by the C4LIFE module. A sample of the temperature dependent data section of the CARES.INP file is shown in figure 7. An explanation of all the keywords, including a separate section describing the Data Table, is provided in the following text.

DTABLE [C4PEST] This keyword denotes the beginning of the Data Table for a given temperature. The **$ENDD** marks the end of the Data Table. See the section titled

Temperature-dependent fracture or statistical material parameters data; the Data Table form of input for a complete description of this input format.

MOR (3A1,3E18.10) or (3E18.10) [C4PEST] The input format associated with this keyword is not recommended with the CARES/LIFE code, but is included for completeness. It was previously used with the CARES1, CARES2, and CARES3 codes. **MOR** indicates that experimental inert fracture stresses (fast-fracture data) will be input. Fracture stresses can be input in random order for each temperature; however, the number of entries must correspond with the **NUT** keyword. There are two styles of input. If **ID1** = 1 or 2 (that is, if the fracture data are assumed to be a complete sample), then fracture stresses only are input. The input format is 3E18.10. If **ID1** = 4 or 5 (that is, if the fracture origins and the fracture stresses are to be input), then the input format is 3A1,3E18.10. The 3A1 represents three fields of single alphanumeric characters. This field is for fracture origin input. An "S" indicates a surface flaw origin. A "V" represents a volume flaw origin. A "U" indicates an unknown flaw origin. Each fracture stress has a corresponding fracture origin. Each line of fracture data consists of three fracture origins followed by their respective failure stresses. Fracture data values should be unique, and multiple identical values should not be input (change one value slightly). This keyword is specific to the C4PEST module.

NUT (3X,I3) [C4PEST] The input format associated with this keyword is not recommended with the CARES/LIFE code but is included for completeness. **NUT** is the sample size of the experimental fracture data for the temperature indicated by **TEMP** (or **TDEG**) and always precedes the **MOR** keyword. **NUT** is specified if **ID1** does not equal 3 (statistical material parameters are not being directly input). Different numbers of specimens are permitted at different temperatures. This keyword is specific to the C4PEST module.

PARAM (2E18.10) [C4PEST and C4LIFE] **PARAM** signals that the Weibull shape parameter, m, and Weibull scale parameter, σ_o, will be input for the temperature indicated by the **TEMP** (or **TDEG**) keyword. Referring to figure 7, the Weibull shape and then the Weibull scale parameters are entered at the indicated space with a format of 2E18.10 (denoted by M and SP, respectively in the figure). The Weibull shape parameter is dimensionless. The Weibull scale parameter has units of stress × (volume)$^{1/m_v}$ for volume flaw analysis and units of stress × (area)$^{1/m_s}$ for surface flaw analysis.

TEMP or **TDEG** (F10.4) [C4PEST and C4LIFE] **TEMP** (or **TDEG**) is the input keyword for the temperature of the fracture data or of the statistical material parameters that immediately follow. Temperature can be specified in any units but must be consistent with the finite element analysis.

$ENDT [C4PEST and C4LIFE] The keyword **$ENDT** signals the end of the temperature-dependent data. Another section of the Material Control Input follows, if required.

Temperature-dependent fracture or statistical material parameters data; the Data Table form of input: The Data Table describes an input format for the time-dependent and fast-fracture rupture data, an example of which is shown in figure 6. This is the recommended input style for the C4PEST module. One Data Table exists for each discrete temperature level. Data Tables are arranged in ascending order of temperature. Input within the Data Table is keyword driven. A brief description of these keywords is shown in figure 6. A line of input in the Data Table is broken up into five input areas, denoted by TEST, FLAW, FIELD1, FIELD2, and FIELD3. TEST is the input area for the keyword. FLAW is the input area for integer data associated with the **SOL** and **CYCLIC** keywords and fracture origin data for the **FAST, STAT, CYCL,** and **DYNA** keywords.

FIELD1, FIELD2, and FIELD3 define input areas for real number inputs such as temperature, fracture times, stressing rates, etc. Blank entries for the TEST, FLAW and FIELD1 input areas assume the identity of the previous line or some other previously defined (default) value. The specific rules are explained for the individual keywords.

CYCL The **CYCL** keyword indicates that steady state cyclic fatigue data will be input. The fracture origin is assigned in the FLAW field. Only a single entry is allowed in this field (placement is arbitrary). An entry of S, U, or V indicates either a surface, unknown or volume flaw, respectively. A blank entry will default the flaw origin to the type consistent with the **ID4** keyword. If **ID4** = 1, then a volume flaw is assigned. If **ID4** = 2, then a surface flaw is assigned. An entry of U could indicate an unknown flaw origin, an unspecified competing failure mode, or an unfailed (truncated or run out) specimen. It is recommended that data censoring be used only when **SOL** = 2 and even then results should be verified, if possible, by other means. The magnitude of the extreme fiber stress (or maximum stress in the component) is input in FIELD1. For cyclic loading this corresponds to the peak (maximum) cyclic stress at the highest stressed point in the specimen. If this field is blank or the entry is less than 1.0E-30, then the value from the last user specified FIELD1 entry for a **CYCL** card is used. The specimen times to failure (in seconds) for the power law or cycles to failure for the Paris and Walker laws are input in FIELD2 and/or FIELD3 (see the **CYCLIC** keyword). A blank entry or an entry whose value is less than 1.0E-30 is ignored. Both FIELD2 and FIELD3 entries are assigned the fracture origin input in the FLAW field.

CYCLIC The presence of this keyword signals that fatigue parameter B_w is to be calculated from steady state cyclically loaded specimen data. The data for the individual rupture specimen is input via the **CYCL** keyword. The crack growth law and cycle waveform are input in the FLAW field

(the Paris law and Walker law are independent of the cycle waveform). The R-ratio (the minimum cycle stress divided by the maximum cycle stress) is input in FIELD1. It is assumed that the R-ratio is invariant (constant) at every location in the specimen. Alternatively the user may also directly input a g-factor in FIELD1 provided the FLAW field contains an entry of 1. Negative values for the R-ratio are allowed to be input; however for the Paris and Walker laws a warning message is issued in this situation. A negative value of the R-ratio will predict additional strength degradation for the Paris and Walker laws. For the power law no crack extension occurs when the normal stress acting on the flaw is compressive. The traditional fracture mechanics approach assumes that no additional strength degradation occurs due to the presence of compressive stresses for any of the crack growth laws. For component reliability analysis CARES/LIFE may or may not predict additional strength degradation for negative R-ratios. The user is advised to examine the options listed with the **CYCLIC** keyword described in the **Material- and specimen-dependent (temperature independent) data** section of the Master Control Input. If the power law is selected then the period of the cycle in units of seconds must be input in FIELD2 and the loading exponent imposed on the waveform is optionally input in FIELD3. The FIELD3 input for the power law is specifically for calculation of the g-factor for rotating components where the angular speed varies with time and has a waveform indicated with the FLAW field input (an input value of 2.0 is for a rotational load, an input value of 1.0 calculates the g-factor in the usual way). If a value of 0 is entered in the FLAW field, then the Paris and Walker laws are selected. The value of the Walker R-ratio sensivity exponent, Q, is input in FIELD3. For this case if FIELD3 is left blank or a value is zero is entered then the Paris law is implimented. If a positive nonzero real number is entered in FIELD3 then the Walker law is implimented.

DTABLE This keyword denotes the beginning of the Data Table for a given temperature. The **$ENDD** marks the end of the Data Table.

DYNA The **DYNA** keyword indicates that dynamic fatigue (constant stress rate) data will be input. The fracture origin is assigned in the FLAW field. Only a single entry is allowed in this field (placement is arbitrary). An entry of S, U, or V indicates either a surface, unknown or volume flaw, respectively. A blank entry will default the flaw origin to the type consistent with the **ID4** keyword. If **ID4** = 1 then a volume flaw is assigned. If **ID4** = 2 then a surface flaw is assigned. An entry of U could indicate an unknown flaw origin, an unspecified competing failure mode, or an unfailed (truncated or run out) specimen. *It is recommended that data censoring be used only when* **SOL** = *2 and even then results should be verified, if possible, by other means.* The stressing rate (stress/second) at the highest stressed point in the component is input in FIELD1. If this field is blank or the entry is less than 1.0E-30, then the value from the last user specified FIELD1 entry for a **DYNA** card is used. The specimen ultimate failure stresses (at the highest stressed point in the component) are input in FIELD2 and/or FIELD3. A blank entry or an entry whose value is less than 1.0E-30 is ignored. Both FIELD2 and FIELD3 entries are assigned the fracture origin input in the FLAW field.

FAST The **FAST** keyword indicates that inert strength or fast-fracture data will be input. The fracture origin is assigned in the FLAW field. Only a single entry is allowed in this field (placement is arbitrary). An entry of S, U, or V indicates either a surface, unknown or volume flaw, respectively. A blank entry will default the flaw origin to the type consistent with the **ID4** keyword. If **ID4** = 1 then a volume flaw is assigned. If **ID4** = 2 then a surface flaw is assigned. An entry of U could indicate an unknown flaw origin or an unspecified competing failure mode. The specimen

ultimate failure stresses (at the highest stressed point in the specimen) are input in FIELD1 and/or FIELD2 and/or FIELD3. A blank entry or an entry whose value is less than 1.0E-30 is ignored. The FIELD1, FIELD2 and FIELD3 entries are assigned the fracture origin input in the FLAW field. Fast-fracture and fatigue data may both be simultaneously present in the Data Table. Weibull parameters determined from fast-fracture data will override Weibull parameters estimated soley from the fatigue data.

PARAM The keyword **PARAM** signals that the Weibull shape and scale parameter will be input for the temperature indicated by the **TEMP** keyword. The Weibull shape parameter m is input in FIELD1. The Weibull scale parameter is entered in FIELD2. The Weibull shape parameter is dimensionless. The Weibull scale parameter has units of stress $\times$ (volume)$^{1/m_v}$ for volume flaw analysis and units of stress $\times$ (area)$^{1/m_s}$ for surface flaw analysis. The characteristic strength can be optionally input in FIELD3. Note FIELD2 or FIELD3 can be left blank. Values input via the **PARAM** keyword override Weibull parameters generated from fatigue data.

RANGE The **RANGE** keyword is used to specify a range of values for the crack growth exponent N in which to search for a solution when the median deviation estimation technique (**ISOL** = 2) is selected. If **RANGE** is not invoked, then the default range of 2.1 to 150.0 is assumed. The bounds of the range are input in FIELD1 and FIELD2, in any order. The limitation of the numerical solution method is that convergence on a value has a tolerance of 0.001 of the span of the range. Consequently, if further accuracy (in absolute terms) is required then the range bounds must be decreased. Numerical problems may be encountered for values of N approaching 2.0 and for large values of N. If a solution is returned that has a value identical to one of the range bounds, then the

search range must be expanded (or shifted). There is no guarantee that an obtained solution is unique.

RSTRES and +STRES These keywords are not used with parameter estimation from specimen rupture data (not used with module C4PEST), but rather are transfered to the CARES.INP file when the module C4PEST is executed (see the keyword **RSTRES** in section **Temperature-dependent fracture or statistical material parameters data**). If material residual stresses (not loading induced) are present, the keyword **RSTRES** allows the user to input a stress tensor that is added to the mechanically induced stresses in the component (it is not added to the fracture stresses of the experimental fracture specimens). This option requires a consistent material reference frame (neutral file stresses should be organized in a material coordinate system reference frame). The stresses are input in two lines. The **RSTRES** keyword uses FIELD1, FIELD2, and FIELD3, for the X, Y, and Z components, respectively. The continuation line uses the **+STRES** keyword with FIELD1, FIELD2, FIELD3 for the XY, YZ, and ZX components, respectively. For shell elements only the X, Y, and XY components are used. The **RSTRES** option is recommended only when **IPRINC** = 2, otherwise the user is limited to input of hydrostatic stresses (X = Y = Z; 0.0 = XY = YZ = ZX) in order to obtain valid results.

STAT The **STAT** keyword indicates that static fatigue data will be input. The fracture origin is assigned in the FLAW field. Only a single entry is allowed in this field (placement is arbitrary). An entry of S, U, or V indicates either a surface, unknown or volume flaw, respectively. A blank entry will default the flaw origin to the type consistent with the **ID4** keyword. If **ID4** = 1, then a volume flaw is assigned. If **ID4** = 2, then a surface flaw is assigned. An entry of U could indicate an unknown flaw origin, an unspecified competing failure mode, or an unfailed (truncated or run

out) specimen. It is recommended that data censoring be used only when **SOL** = 2 and even then results should be verified, if possible, by other means. The magnitude of the extreme fiber stress (or maximum stress in the component) is input in FIELD1. If this field is blank or the entry is less than 1.0E-30, then the value from the last user specified FIELD1 entry for a **STAT** card is used. The specimen times to failure (in seconds) are input in FIELD2 and/or FIELD3. A blank entry or an entry whose value is less than 1.0E-30 is ignored. Both FIELD2 and FIELD3 entries are assigned the fracture origin input in the FLAW field.

SOL This keyword is used to select the method of solution for obtaining the time-dependent power law parameters (see figure 6) from fatigue specimen data. The choice is input in the FLAW field of the Data Table and can be placed anywhere within the field. If the **SOL** keyword is not specified, then the default is the median value technique (**SOL** = 0) using least squares linear regression. Note if **SOL** = 0 that data assigned fracture origins not consistent with the **ID4** index are ignored (don't censor data with this option). The median value technique is the least accurate estimation procedure available in CARES/LIFE.

If **SOL** = 1, then the least squares regression technique is invoked. This technique performs linear regression on all the fatigue data (as opposed to only the median values) to establish the crack growth exponent N.

When **SOL** = 2, the median deviation method is chosen. The median deviation method uses Weibull analysis to minimize the scatter in the data to establish the crack growth exponent N. As such, two different solution routes are possible, maximum likelihood or least squares, depending on the setting of the **MLORLE** keyword in the temperature independent section of the Material Control Input. The **RANGE** keyword should be used with this solution option. Data censoring is

allowed although caution should be exercised in interpreting results (especially if competing failure modes have dissimilar crack growth exponents).

For the least squares, median value, and median deviation technique the inert strength distribution Weibull modulus m and a characteristic strength σ_θ, is optionally estimated from the fatigue data. If inert strength fracture data is simultaneously input, then the Weibull parameters for this data override those calculated from time dependent data.

TEMP This keyword is used to denote temperature. The temperature is input in FIELD1. Only one assignment of temperature is permitted in the Data Table. Data Tables must be arranged in ascending order of temperature.

TPARAM The keyword **TPARAM** signals that the power law parameters N and B_w (and optionally Q for the Walker law) will be input for the temperature indicated by **TEMP**. The crack growth exponent N and the constant B_w are entered in FIELD1 and FIELD2, respectively. The Walker R-ratio sensitivity exponent Q is optionally entered in FIELD3. The crack growth exponent is dimensionless. The crack growth constant has units of (second $\times$ (stress)^2) for the power law and (cycle $\times$ (stress)^2) for the Paris and Walker laws. The Walker R-ratio sensivity exponent is dimensionless.

VAGAGE The keyword **VAGAGE** represents the gage volume or area of a tensile test specimen. Equivalently, it also represents the fast-fracture effective volume, V_e, or area, A_e, of some arbitrary specimen geometry and loading (hence it becomes a temperature dependent quantity). See the section titled **Material Strength Characterization** of the section **Theory** for a definition. The effective volume and area are used in the calculation of the Weibull scale parameter, σ_o. If **ID4** = 2

and **ID1** = 1 or 4 (that is, if surface flaw analysis is specified and the statistical material parameters are to be determined from specimen fracture data), then the gage surface area or fast-fracture effective area of the specimen must be specified. If **ID4** = 1 and **ID1** = 1 or 4 (that is, if volume flaw analysis is specified and the statistical material parameters are to be determined from specimen fracture data), then the gage volume or fast-fracture effective volume of the specimen must be specified. The effective volume or surface area are input in FIELD1. Consult the section **Material Strength Characterization** of this manual for the definition of the effective volume and area.

VAGTIM The keyword **VAGTIM** represents the gage volume or area of a tensile test specimen. Equivalently it also represents the stress-normalized effective volume, V_{ef}, or area, A_{ef}, of some arbitrary specimen geometry and loading (hence it becomes a temperature dependent quantity). See the section titled **Material Failure Characterization For Static, Cyclic Or Dynamic Loading** of the section **Theory** for a definition. The stress-normalized effective volume and area are used in the calculation of the fatigue parameter, B_w. If **ID4** = 2 and **ID1** = 1 or 4 (that is, if surface flaw analysis is specified and the fatigue parameters are to be determined from specimen fracture data), then the gage surface area or stress-normalized effective area of the specimen must be specified. If **ID4** = 1 and **ID1** = 1 or 4 (that is, if volume flaw analysis is specified and the fatigue parameters are to be determined from specimen fracture data), then the gage volume or stress-normalized effective volume of the specimen must be specified. The stress normalized effective volume or surface area are input in FIELD1.

$ENDD This keyword signals the end of the Data Table for a given temperature.

.

C4LIFE Module Input Information

The output from the C4PEST module is placed in the two files (with the default names of) C4PEST.OUT and CARES.INP. The CARES.INP file is the corresponding input file to the C4LIFE module. This file echoes the Master Control Input and the Material Control Input from the C4PEST.INP file, except that the temperature dependent specimen fracture data is replaced with the temperature dependent Weibull and fatigue parameters (direct parameter input option). The C4LIFE module requires the temperature dependent material parameters as input. It is important to understand that the CARES.INP input file for module C4LIFE is automatically prepared by module C4PEST from the C4PEST.INP file (the user is not required to prepare this file, although the user may desire to edit this file and make changes prior to executing the C4LIFE module).

The module C4LIFE performs the reliability analysis of the component from the CARES.NEU and optionally PROOF.NEU neutral data base files along with the CARES.INP input file (default file names are shown). The overall structure and input options of the CARES.INP file are similar to those for the C4PEST.INP file. Refer to the **C4LIFE module Master Control Input** and **C4LIFE module Material Control Input** sections of this manual for further information regarding the individual input items. As previously stated, the CARES.INP file is typically generated from the C4PEST module (as opposed to the user manually preparing this file). The CARES.NEU and PROOF.NEU neutral data base files are generated from the module NASCARES (for MSC/NASTRAN), ANSCARES (for ANSYS), or ABACARES (for ABAQUS). The NASCARES, ANSCARES, or ABACARES programs only create one neutral data base file per execution. The file PROOF.NEU represents the static proof test load on the component or a cyclic load on the component. The C4LIFE module can be executed without the PROOF.NEU file. The CARES.NEU file represents the static service loading on the component or a cyclic load condition and is always a required input file for the C4LIFE module. For cyclic loads the file CARES.NEU

would contain the maximum stresses and the file PROOF.NEU would contain the minimum stresses due to the cyclic load. If the R-ratio is constant throughout the component then only the CARES.NEU neutral file containing the maximum cyclic stresses is needed for the reliability analysis (the R-ratio is then input by the user).

C4LIFE module Master Control Input. - The Master Control Input section from the TEMPLET.INP file is reproduced in figure 4. If parameter keywords are omitted, they assume default values as defined in figure 4. Available keywords may be specific to only one of the two modules C4PEST or C4LIFE, however, keywords not recognized by a particular module are ignored. Keywords that will be used with the C4LIFE module should be specified in the input file C4PEST.INP (for the C4PEST module) because they will automatically be reproduced in file CARES.INP when module C4PEST is executed.

FACTOR (E10.4) [C4LIFE] The keyword **FACTOR** allows the user to input a loading factor to multiply all element (or subelement) stresses. These adjusted values are used to calculate the subsequent reliability. Note, adjusted stresses are not echoed in the program output. This keyword is specific to the C4LIFE module.

IPOST (4X,I1) [C4LIFE] The control index **IPOST** is for PATRAN postprocessing of the module C4LIFE component reliability analysis. If **IPOST** = 1 then a data file of averaged (average of the subelements of an element) element risk-of-rupture intensities is created (default file name is CARES.PAT). Note that use of this file requires that the finite element mesh was created with the PATRAN program (i.e., the phase II model data is still available). If **IPOST** = 0 then this file is not created. The **IPOST** keyword is specific to the C4LIFE module.

IPRINC (4X,I1) [C4LIFE] **IPRINC** is the control index for passing stresses to the reliability algorithms. If **IPRINC** = 1 then the principal stresses calculated in subroutine EIGEN are used. This is a requirement for the PIA model. If **IPRINC** = 2 then the stress tensor is passed to the Batdorf models. This option allows consideration of the effect of proof testing or cyclic loading when the boundary load direction and/or location changes (**IPROOF** = 1 should also be specified). This keyword is specific to the C4LIFE module.

IPRINT (4X,I1) [C4PEST and C4LIFE] The keyword **IPRINT** controls the printing of element stresses and experimental fracture stresses. It gives the user the option to control the length of the program output. If **IPRINT** = 0, the element stresses and/or specimen fracture data are not printed. If **IPRINT** = 1, all element stresses and/or fracture data are echoed in the program output.

IPROOF (4X,I1) [C4LIFE] The control index **IPROOF** is used as a flag signaling whether one or two neutral data base files are to be read by the C4LIFE module. If **IPROOF** = 0, then only one file is to be read. This file (CARES.NEU) contains either the stress analysis of the static load or the peak stresses of the cyclic load. In this case, for cyclic loading the R-ratio (min/max cycle stress) is assumed constant throughout the component and the appropriate loading information must be input using the **CYCLIC** keyword. If **IPROOF** = 1 then two neutral files are to be read (CARES.NEU and PROOF.NEU). These neutral files will either represent proof testing or cyclic loading. For reliability analysis with proof testing, then the proof test neutral data base file is PROOF.NEU and the service load neutral file is CARES.NEU. The PROOF.NEU and CARES.NEU files contain the stress analyses of the proof test load and service load, respectively. For reliability analysis with cyclic loading where the R-ratio is not constant throughout the component, then two neutral data base files are required to compute the R-ratio on an element-by-element basis. In this case, the

PROOF.NEU neutral data base file contains the minimum cyclic stresses and the CARES.NEU neutral data base file contains the maximum cyclic stresses. The **IPRINC** and **TIMEPT** keywords are also required if **IPROOF** = 1. In this case **IPRINC** = 2 should be used for either proof test or cyclic loading. For proof testing, the **TIMEPT** keyword is used to assign the duration of the proof test and the **TIME** keyword is used to assign the duration of the of service load. For cyclic loading, **TIMEPT** and **TIME** are assigned the same value.

NE (4X,I1) [C4PEST and C4LIFE] **NE** is a keyword to control program execution. If **NE** is zero, then component reliability analysis will not be performed. If the **NE** control index is 3 (or non zero) then subsequent component reliability analysis using the C4LIFE module is assumed.

NGP (4X,I2) [C4PEST and C4LIFE] **NGP** controls the number of Gaussian integration points that are used in the Batdorf reliability calculations in module C4LIFE. It is also used in the integration to obtain the Batdorf normalized crack density coefficient $\bar{k}_B$ in module C4LIFE and to numerically calculate g-factors when closed form solutions are not possible (such as for the sine wave). The input values can be either 15, 30 or 50. Entries of 30 or 50 will give improved accuracy but with the penalty of larger CPU requirements.

NMATS, NMATV (4X,I2) [C4PEST and C4LIFE] The keyword **NMATS** represents the number of materials for which surface flaw analysis is performed. **NMATV** represents the number of materials for which volume flaw analysis is performed. **NMATS** is associated with shell elements, and **NMATV** is associated with either solid, shell, or axisymmetric elements. This association is achieved via the finite element material ID numbers (see keyword definition **MATID** in the **Material Control Input** section). A component consisting of one material may have one set of

statistical material parameters to characterize the surface and another set for the volume, for which **NMATS** = 1 and **NMATV** = 1. Statistical material parameters are a function of processing, microstructure, and environment. The CARES/LIFE program modules are capable of analyzing a single material with multiple statistical material characterizations or many materials with multiple statistical material characterizations. For example, if a single material component has two different surface finishes, then **NMATS** = 2 is used because two different sets of statistical material parameters are required. The only constraint is that the total of **NMATS** + **NMATV** must be less than 101.

NS (3X,I3) [C4LIFE] Because it's possible that a finite element model consists of only a fraction of the total ceramic component (model reduction via symmetry), the **NS** keyword allows for multiplication of the model geometry by the appropriate number of times when the reliability of the entire component is desired. For cyclic symmetry, **NS** corresponds to the number of segments required to reproduce the whole component. Specifically **NS** is used to multiply element or subelement volumes and areas in the reliability calculations. This keyword is only used with the C4LIFE module.

TITLE (72A1) [C4PEST and C4LIFE] The input associated with the **TITLE** keyword is reproduced in the program output files C4PEST.OUT and CARES.OUT for problem identification.

TIME (E10.4) [C4PEST and C4LIFE] The keyword **TIME** allows the user to specify the duration of the service loading on the component. This input should be in units of seconds (for power law) or cycles (for the Paris law and Walker law). If **TIME** = 0.0 then fast-fracture reliability is calculated.

TIMEPT (E10.4) [C4LIFE] The keyword **TIMEPT** is used to specify the duration of the loading for the optional neutral data base file PROOF.NEU (defaulted name). This option is activated when the keyword **IPROOF** is set equal to 1. If cyclic loading is assumed then the value input should equal the value input for the **TIME** keyword. For proof test reliability analysis the keyword **TIMEPT** allows the user to specify the duration of the proof test loading on the component. In this particular case the value input must be in units of seconds (since Paris law, Walker law, or g-factors have not been made as input options with proof testing). Only static loadings are assumed for the proof test and service condition. If **TIMEPT** = 0.0 then only the fast-fracture proof test loading is considered. The **TIMEPT** keyword is used only with the C4LIFE module.

$ENDX [C4PEST and C4LIFE] The keyword **$ENDX** signifies the end of the MASTER CONTROL INPUT.

C4LIFE module Material Control Input. - A sample of the Material Control Input from the TEMPLET.INP file is reproduced in figures 5 and 7. Note that the Material Control Input actually consists of two different data partitions. The data contained in both figures 5 and 7 are for a single material. In figure 5, temperature independent control indices, material constants, and geometric variables are shown. In figure 7, the temperature-dependent Weibull and fatigue parameters are listed. The temperature-dependent Weibull and fatigue parameters are always placed immediately following the temperature independent control indices for that material. The total number of Material Control Input sections must be equal to the sum of **NMATS** + **NMATV** from the Master Control Input. Note that keywords that are not found assume default values. Available keywords may be specific to only one of the two modules C4PEST or C4LIFE. However, all

keywords that will be used with module C4LIFE should be specified in file C4PEST.INP because they will automatically be printed in file CARES.INP when module C4PEST is executed.

It should also be noted that the material Poisson's ratio is a required input (for shear sensitive Batdorf models only). Other temperature-dependent physical and mechanical properties - such as Young's modulus, thermal conductivity, thermal coefficient of expansion, and specific heat - are required for finite element analysis but are not used for reliability evaluation. It is assumed that Poisson's ratio is constant and temperature independent in the reliability evaluations.

C4LIFE module Material- and specimen-dependent (temperature independent) data: The following keywords are the control indices, material indices, and geometric variables necessary for calculation of volume and surface flaw statistical parameters as shown in figure 5.

C (F10.4) [C4PEST and C4LIFE] The value of the empirical constant $\bar{C}$ that is required for Shetty's mixed-mode fracture criterion (noncoplanar strain energy release rate criterion) is assigned using the C keyword. This fracture criterion is specified with the **ID2** keyword in the Master Control Input (**ID2** =5).

CYCLIC (4X,I1,/,E10.4,/,E10.4,/,E10.4) [C4LIFE] Invoking the **CYCLIC** keyword in the temperature independent section of the Material Control Input indicates that the component reliability analysis performed with module C4LIFE will also include the effects of cyclic fatigue degradation (see also the **CYCLIC** keyword described in the section titled **Temperature-dependent fracture or statistical material parameters data; the Data Table form of input,** which is used to estimate fatigue parameters from cyclic fatigue rupture data using module C4PEST). The integer input (IWAVE) designates the crack growth law (Paris and Walker laws, or the power law) and the

loading cycle waveform (square, sawtooth, and sine). The real number input (RCYC) assigns the R-ratio (the minimum cycle stress divided by the maximum cycle stress) for the material. This input assumes the value of the R-ratio is constant at every point in the body and that only one neutral data base file is being processed (**IPROOF** = 0). If two neutral data base files are to be examined (**IPROOF** = 1) then the input for RCYC is ignored. This is because the R-ratio is now computed for each element in the model (by comparing the two neutral files). Negative values for the R-ratio are allowed to be input (via **RCYC**) when **IPROOF** = 0; however for the Paris and Walker laws this means that additional material degradation is predicted due to the compressive stress component (an appropriate warning message is issued). When **IPROOF**= 1 and a negative R-ratio is computed at an element; no additional degradation due to the compressive stresses is assumed (equivalent to the R-ratio having a value of zero) for all the crack growth laws (this is the additional fracture mechanics approach). The real number input for the period of the cycle (PERIOD) is associated with the power law and must be in units of seconds. Using the **CYCLIC** keyword with the power law means that g-factors, which equate the cyclic loading to an equivalent static loading situation are to be computed. It is useful to know that when the power law is invoked with the sawtooth waveform and the value of RCYC is set to zero, then the g-factor is 1/N+1, which is equivalent to dynamic (constant stress rate) loading. The user is warned that calculating g-factors with a sine wave is numerically intensive when processing two neutral files (**IPROOF** = 1) with the Batdorf model (when **ID2** is not equal to 4). If the power law is selected then the loading exponent QCYC is optionally input. The QCYC input for the power law is specifically for calculation of the g-factor for rotating components where the angular speed varies with time and has a waveform indicated with the QCYC value input (an input value of 2.0 is for a rotational load, an input value of 1.0 calculates the g-factor in the usual way).

.

ID1 (4X,I1) [C4PEST and C4LIFE] **ID1** is a control index for specifying the form of the data to be input for obtaining the statistical material parameters. Either the Weibull shape and scale parameters are directly specified (**ID1** = 3) or experimental fracture data are input (**ID1** = 1, 2, 4, or 5). The fracture data can be from three-point modulus-of-rupture bend bars (**ID1**= 2 or 5), four-point modulus-of-rupture bend bars (**ID1** = 2 or 5) or tensile test specimens (**ID1** = 1 or 4). Optionally, the fracture data can be from any specimen geometry (**ID1** = 1 or 4), however this would require that the specimen effective volume or area (see **VAGAGE** keyword) be input. If the fracture data are assumed to be all from one failure mode (all volume flaws or all surface flaws), then **ID1** = 1 or 2 can be chosen. If **ID1** = 1 or 2, then CARES assumes that the fracture origins are consistent with the **ID4** input index. If **ID1** = 4 or 5, then fracture origins must be supplied with the fracture data. The **ID1** keyword is primarily for the C4PEST module. This input value must be set to a positive integer, when used with the C4LIFE module. Note that if module C4PEST is run prior to module C4LIFE, then **ID1** is automatically set to the value of 3 when module C4PEST creates the CARES.INP input file for module C4LIFE.

ID2 (4X,I1) [C4PEST and C4LIFE] The control index **ID2** is for selection of a fracture criterion. Note that some caution must be exercised here because the maximum tensile stress criterion (**ID2** = 2) is only used with volume flaw analysis (**ID4** must be set to 1). All choices available, except the PIA model, are used with the Batdorf integration routines. Shetty's mixed-mode fracture criterion (**ID2** = 5) is recommended for both surface and volume flaw analysis (see also keyword **C**).

ID3 (4X,I1) [C4PEST and C4LIFE] The **ID3** control index is for selection of a crack geometry. Note that caution must be exercised here since some of the available choices are applicable either for surface flaw analysis or for volume flaw analysis only. For instance, the penny-shaped crack is

only applicable for volume flaw analysis. The shear sensitive notch crack and the semi-circular edge crack are only applicable for surface flaw analysis. The Griffith crack is available for both surface and volume flaw analysis. The penny-shaped crack is recommended for volume flaw analysis and the semicircular crack is recommended for surface flaw analysis. See figure 2 for a matching of crack geometry with fracture criteria.

ID4 (4X,I1) [C4PEST and C4LIFE] **ID4** specifies if parameter estimation and subsequent component reliability analysis is volume or surface flaw based. The value input must be consistent with the **ID2** and **ID3** selections. From the fracture data supplied by the user, the Weibull shape and scale parameters, along with the normalized Batdorf crack density coefficient consistent with the **ID4** input value, are estimated and are subsequently made available for processing with finite element data. The entry for **ID4** must be consistent with the finite element analysis material card ID specified in **MATID**.

IKBAT (4X, I1) [C4PEST and C4LIFE] **IKBAT** selects the method of calculating the normalized Batdorf crack density coefficient, $\overline{k_B}$. If **IKBAT** = 0, then the crack density coefficient is set to the value that is the solution for the normal stress fracture criterion, regardless of the fracture criterion and crack geometry selected by the user for subsequent component analysis. If **IKBAT** = 1, then the crack density coefficient is calculated based on the fracture criterion and crack geometry selected by the **ID2** and **ID3** keywords. **IKBAT** = 0 gives more conservative reliability predictions than **IKBAT** = 1 does. Setting **IKBAT** = 1 is recommended.

MATID (1X,I7) [C4PEST and C4LIFE] **MATID** *is the material identification number associated with the statistical material parameter data. The value input should correspond to the material*

identification number listed in the CARES/LIFE neutral data base file for a given element. Therefore, the value for **MATID** must match the material ID designated in the finite element analysis. If only parameter estimation is being performed, then **MATID** should be an arbitrary integer value.

PR (F10.4) [C4PEST and C4LIFE] **PR** is Poisson's ratio. It is assumed to be temperature independent.

PFCONV (F10.4) [C4LIFE] When a non-zero value is input ($0.000001 <$ **PFCONV** < 0.999999), then the Weibull scale parameter, σ_o, as well as the effective volume, V_e, or area, A_e, of the finite element model of the component is computed (a neutral data base file is required and **IPROOF** = 0). The real number assigned to **PFCONV** corresponds to some level of probability of failure of the component. The value input must correspond with the specified loading on the finite element model. The user is warned that the calculated Weibull scale parameter requires that the effective volume and area are invariant quantities versus the magnitude of the loading (this fact should be verified for non standard specimen geometries). Appropriately modifying the input Weibull modulus (via the **PARAM** keyword) to a value of Nm/(N-2) will yield the stress normalized effective volume, V_{ef}, and stress normalized effective area, A_{ef}. The computed effective volume and area can be used as input for **VAGAGE** (see section **Temperature-dependent fracture or statistical material parameters data; the Data Table form of input**) with module C4PEST. The computed stress normalized effective volume and area can be used as input for **VAGTIM** (see section **Temperature-dependent fracture or statistical material parameters data; the Data Table form of input**) with module C4PEST. The **PFCONV** keyword requires that the specimen model is isothermal or that the material properties are invariant over the range of temperature

loading. For the user this means that material properties for a range of different temperatures should not be input (only one set of parameters for one temperature should be input). This keyword is only active with the C4LIFE module.

TITLE (72A1) [C4PEST and C4LIFE] The input associated with the **TITLE** keyword is reproduced in the program output files C4PEST.OUT and C4LIFE.OUT for material identification.

$ENDM [C4PEST and C4LIFE] The keyword **$ENDM** signifies the end of a section of the Material Control Input. The temperature-dependent specimen fracture data or the Weibull shape and scale parameters are assumed to immediately follow.

C4LIFE module temperature-dependent fracture or statistical material parameters data:
Immediately following the **$ENDM** keyword, which signals the end of the material's temperature-independent data, the temperature-dependent Weibull and fatigue parameters are input. Data must be arranged so that they correspond to ascending order of temperature. These data enable interpolation of the statistical material parameters to other temperatures. Figure 7 shows an example of the input for these parameters module C4LIFE. An explanation of these keywords is provided in the following text.

PARAM (2E18.10) [C4PEST and C4LIFE] **PARAM** signals that the Weibull shape parameter, m, and Weibull scale parameter, σ_o, will be input for the temperature indicated by the **TEMP** (or **TDEG**) keyword. Referring to figure 7, the Weibull shape and then the Weibull scale parameters are entered at the indicated space with a format of 2E18.10 (denoted by M and SP, respectively in the figure). The Weibull shape parameter is dimensionless. The Weibull scale parameter has units

of stress × (volume)$^{1/m_V}$ for volume flaw analysis and units of stress × (area)$^{1/m_S}$ for surface flaw analysis.

RSTRES (3E18.10,/,3I8.10) [C4LIFE] If material residual stresses (not loading induced) are present, the keyword **RSTRES** allows the user to input a stress tensor that is added to the mechanically induced stresses in the component (it is not added to the fracture stresses of the experimental fracture specimens). This option requires a consistent material reference frame (neutral file stresses should be organized in a material coordinate system reference frame). The stresses are input in two lines having a 3E18.10 format with the X, Y, Z, components on the first line and the XY, YZ, and ZX components on the second line, respectively. For shell elements only the X, Y, and XY components are used. The **RSTRES** option should be used only when **IPRINC** = 2, otherwise the user is limited to input of hydrostatic stresses (X = Y = Z; 0.0 = XY = YZ = ZX) in order to obtain valid results.

TEMP or **TDEG** (F10.4) [C4PEST and C4LIFE] **TEMP** (or **TDEG**) is the input keyword for the temperature of the fracture data or of the statistical material parameters that immediately follow. Temperature can be specified in any units but must be consistent with the finite element analysis.

TPARAM (3E18.10) [C4LIFE] **TPARAM** signals that the power law or Paris law fatigue parameters N and B_w will be input for the temperature indicated by **TEMP** (or **TDEG**). The Walker law fatigue parameters N, B_w, and Q (where Q is the dimensionless Walker R-ratio sensitivity exponent) are also input with this keyword. Referring to figure 7, the crack growth exponent N and then the constant B_w are entered at the indicated space with a format of 2E18.10. The crack growth exponent N is dimensionless. The crack growth constant B_w has units of

(second × (stress)^2) for the power law or (cycle × (stress)^2) for the Paris and Walker laws. The IWAVE control parameter of the **CYCLIC** keyword (see the section titled **C4LIFE module Material- and specimen-dependent (temperature independent) data** of the Master Control Input) controls the choice of crack growth law. If IWAVE = 1 or the **CYCLIC** keyword is not present in the input file then the power law is automatically assumed with static fatigue. If IWAVE > 1, then the power law is used with cyclic loading. If IWAVE = 0 and the input field for Q (36X,E18.10) is left blank or has a zero entry then the Paris law is implemented. If IWAVE = 0 and the input field for Q (36X,E18.10) is a positive nonzero real number then the Walker is law is implemented.

$ENDT [C4PEST and C4LIFE] The keyword **$ENDT** signals the end of the temperature-dependent data. Another section of the Material Control Input follows, if required.

Execution of the CARES/LIFE Program

The CARES/LIFE integrated design computer program has two primary objectives: (1) postprocessing MSC/NASTRAN, ANSYS, or ABAQUS finite element static analysis output to predict component reliability and (2) analysis of specimen fracture data to determine estimates of the statistical material and/or fatigue parameters. To facilitate user interaction with the program, CARES/LIFE is divided into three separately executable modules which perform: (1) statistical analysis and characterization of experimental data obtained from the fracture of laboratory specimens; (2) neutral data base generation from the MSC/NASTRAN, ANSYS, or ABAQUS finite element analysis programs; and (3) time-dependent reliability evaluation of thermomechanically loaded ceramic components. Although all three modules in the CARES/LIFE program are separately executed, they may easily be coupled through command files to sequentially execute without user intervention. The disks which are provided with this manual include the source code for each of the three modules comprising the CARES/LIFE program. The CARES/LIFE program modules are programmed in standard FORTRAN 77 and must be compiled by the user before they can be executed. The CARES/LIFE code requires that input files for all three modules be prepared prior to execution. Specific examples of the files associated with each of the three modules are presented in the **Users' Guide** section, along with an explanation of how the variables in the files are designated and/or manipulated. In addition, the **Users' Guide** section contains several examples of templet file keyword settings which illustrate the keywords necessary for performing parameter estimation and component reliability analysis with the C4PEST and C4LIFE modules.

Output Information

The output from the CARES/LIFE program consists of separate input/output files created from the various independent program modules--C4LIFE, C4PEST, and the finite element interface programs ABACARES, ANSCARES, and NASCARES. The ABACARES, ANSCARES, and NASCARES programs couple to the finite element analysis codes ABACUS, ANSYS, and MSC/NASTRAN, respectively. These interface programs and the parameter estimation program C4PEST each produce a data file that input into the C4LIFE program to predict component reliability. The C4LIFE program outputs two files, one of which is a results file and the other is a PATRAN compatible data file of the element risk-of-rupture intensities, which enables graphical rendering of the structures critical regions. The contents of the input/output files from each CARES/LIFE module are described in the following three sections of this manual.

Finite Element Interface Modules Output Information

The results from the finite element analysis (available in the form of standard output files and/or plot data files) have to be interpreted by an interface program. Due to the different formats used for output of the results in each finite element program this interpreter program has to be adapted to the specific finite element software used; therefore, for each finite element software package a separate interface program is prepared. The interface program writes the results of the finite element analysis into a file known as the neutral data base (the default name of this file is CARES.NEU or also PROOF.NEU).

The concept of a neutral data base allows for the coupling of CARES/LIFE to several finite element packages. A further advantage of this approach is the ease of transfer of this database (ASCII file) to different computer systems. Its salient feature is that it has a common format (hence the word neutral) for all finite element programs. The contents of this file include the stress tensors

and temperatures at the element Gaussian integration points as well as volumes or areas associated with these integration points. Only one finite element load case is permitted in the file (it is expected that future versions of CARES/LIFE will allow multiple load cases); therefore for proof testing or cyclic fatigue then two separate neutral files are required (CARES.NEU and PROOF.NEU). For proof testing, one neutral file contains the proof test loading case and the other neutral file contains the service loading case. For cyclic fatigue each neutral file would represent one extreme in the range of imposed loading on the component over a cycle. The finite element interface program creates only one neutral data base file per execution.

Appendix B shows a sample of the organization of the neutral data base. The structure of the file is optimized with respect to memory. The finite element data is arranged using the following hierarchy: element groups, elements, and subelements. A subelement refers to the volume or area associated with a particular element Gaussian integration point. The stress state is assumed constant within the domain of the subelement. The element group data contain information regarding the number of elements within the group. Interpreter control parameters, such as the number of element groups to be considered in the reliability analysis, flags for accounting for volume and surface flaw analysis, etc., precede the finite element data.

The introduction of comment lines (defined by 'COM' as the first 3 characters of an input line) allows for a more friendly substructuring of the neutral data base. Based on the global hierarchy outlined above, the neutral file data is arranged into records with standard FORTRAN formats: the first record (format A80) specifies the title for the particular reliability evaluation. The next entry (format 2I5) contains the number of element groups NUMEL (both volume as well as surface (shell) elements) to be considered in the reliability analysis and the flag NUMELB indicating combined volume as well as surface flaw reliability analysis for shell elements.

Depending on the parameter NUMEL, a loop over all element groups is started with the next statement (format 4I5): the identification number of the element group considered (INUEG), the element type (IEGTYP) corresponding to PATRAN element type codes, the number of elements within this element group (IGREL) and a shell element type indicator (ISHELL) have to be input. If shell elements are used in the analysis, the indicator ISHELL has to be set to 1. Information pertaining to the element level is read in a loop over the number of elements (INVEQ) within the element group considered (format 4I5,3F15.0).

The element level data contains the identification number of the element considered (IELNUM), the number of subelements within this element (ISUBEL), the material identification number for volume flaw analysis (MATINP), the material identification number for surface flaw analysis (MAT2), the element volume (ELVOL), the element thickness (ELTHIC) only in case of shell elements, and the averaged temperature of this element (ELTEMP). The identification number of the element should be the same as the corresponding element number in the finite element mesh, if further postprocessing of the reliability results are planned. The number of subelements within this element depends on the Gaussian integration order chosen in the finite element analysis and on the element type. If stress data is only available at the center of the element (standard case in NASTRAN analyses prepared for previous CARES versions), one subelement is specified (ISUBEL=1). The material identification numbers must correspond to the material numbers used in the finite element analysis as well as the material numbers in the control file (containing the Weibull parameters). Element volume and element temperature are necessary only for element group information summaries in the printout file. For the reliability evaluation the subelement data are directly used.

A third loop is started for reading at the subelement level. In case of volume type elements (ISHELL=0 on Element Group Entry) the identification number of the subelement (ISUNUM), the

subelement volume (SUBVOL), the subelement temperature (SUBTEM) and the full stress tensor at the integration point (defined by σ_{xx}, σ_{yy}, σ_{zz}, σ_{xy}, σ_{yz} and σ_{xz} in the local coordinate system) have to be specified (format I5,5F15.0,/,35X,3F15.0).

In the case of shell type elements (ISHELL=1 on Element Group Entry) plane stress conditions are assumed. For that reason only σ_{xx}, σ_{yy} and σ_{xy} are necessary for the definition of the subelement stress tensor. Instead of the subelement volume, the subelement area has to be specified (I5,5F15.0): ISUNUM, SUBAREA, SUBTEM, σ_{xx}, σ_{yy} and σ_{xy}.

Typically, subelement volumes and areas are not included with standard finite element output. Thus, the volume or area of each subelement (corresponding to a Gauss integration point) is calculated in the interpreter program using the shape functions inherent to the element type. In the usual context of finite element methods, the volume of a three-dimensional element, (i. e., brick, wedge, pyramid, or tetrahedron), the volume of an axisymmetric element (i. e., quadrilateral or triangular), and the area of a shell element (i. e., quadrilateral or triangle) are calculated after transformation into the natural coordinate space (Bathe, 1982). See section **Theory** (and also Powers, Starlinger, and Gyekenyesi, 1992) for information regarding calculation of subelement volumes and areas.

C4PEST Module Output Information

The C4PEST module reads specimen rupture data from the C4PEST.INP input file (C4PEST.INP is the default file name) and subsequently estimates the inert strength (fast-fracture) Weibull parameters as well as the fatigue parameters. This information is output in two separate files. One output file contains the results of the analysis (default file name C4PEST.OUT), which includes parameter estimates, outlier testing, goodness-of-fit statistics, etc... The other file is a data file (default file name CARES.INP), which is input into the C4LIFE module. It contains the

parameter estimates along with program control indices. The CARES.INP file is an exact copy of the C4PEST.INP input file, except that the specimen rupture data is replaced with the parameter estimates (via keywords **PARAM, TPARAM,** and **TEMP** as described in section **Temperature-dependent fracture or statistical material parameters data**). The section **Input Information** provides a description of the contents of this data file.

The results file C4PEST.OUT contains a summary of the parameter estimation analysis performed by the C4PEST module. The beginning of this file contains an echo of the choices selected (or default values) from the Master Control Input. The PRINTA subroutine echoes these data. The results of the analysis of each flaw population for a corresponding material follow, starting with the echo of the Material Control Input (from the PRINTB subroutine). The time-dependent data and analysis are output first (PRINTQ subroutine) and the inert strength (fast-fracture) data and analysis are output second (PRINTP subroutine).

The time-dependent specimen data is output in ascending order of temperature (which is also the way it must be input in file C4PEST.INP). The specimen dimensions are given at each temperature for either four-point bending, three-point bending, tensile specimen gage volume, tensile specimen gage area, specimen effective volume or specimen effective area (effective volume and area are calculated for some arbitrary specimen geometry as prescribed with the keyword **PFCONV** in the Master Control Input). The specimen effective volume or area can change with temperature if the Weibull modulus changes with temperature (see section **Material Strength Characterization**).

A summary of the cyclic fatigue control data (see keyword **CYCLIC** in section **Temperature-dependent fracture or statistical material parameters data; the Data Table form of input**) is given. This output echoes the user's selections for the crack growth law (power law, Paris law, or Walker law), the cycle waveform (power law only), the period of the cycle, and the R-

ratio (the ratio of minimum cycle stress to maximum cycle stress). The R-ratio is assumed invariant at all locations in the specimen (for the C4LIFE module the R-ratio may vary throughout the component). If the power law is selected then the g-factor is calculated for the waveform and printed (see section **Cyclic Fatigue**). The g-factor can be viewed as a multiplication factor of time (for cyclic loading) to obtain an equivalent failure time for a static (invariant) load. CARES/LIFE calculates the g-factor based on this static stress having a magnitude equal to the maximum cycle stress. The C4PEST module determines the value of the fatigue parameter B_w using the g-factor (see section **Evaluation of Fatigue Parameters from Naturally Flawed Specimens**) and the maximum cyclic failure stresses in the specimens.

Prior to the printing of the specimen rupture data, if the median deviation solution is used the bounds of the range to search for a solution for the crack growth exponent N is listed (see keyword **RANGE** and **SOL** in section **Temperature-dependent fracture or statistical material parameters data; the Data Table form of input**). The total number of specimens and the testing temperature is printed, followed by a table echoing the fatigue specimen fracture data. For static and cyclic fatigue data the table includes the maximum stress and the duration of loading in units of seconds for the power law and cycles for the Paris and Walker laws. The data are ranked according to the highest rupture stress followed by the smallest duration for which the load is applied. For dynamic fatigue the data are ranked according to the lowest stressing rate followed by to the lowest fracture stress. The ranking according to this hierarchy is indicated by the integer in parenthesis. The failure origin is indicated with a "V" for volume flaw, an "S" for surface flaw, and a "U" for an unknown flaw origin.

The time-dependent specimen fracture data are transformed to equivalent inert (fast-fracture) strengths (see section **Evaluation of Fatigue Parameters from Inherently Flawed Specimens**), which are then printed in a table. The transformation depends on the estimated fatigue parameters

and the Weibull modulus m' and characteristic strength σ_θ' estimated solely from the fatigue data. This approach depends on the extrapolation of the time dependent rupture data to an equivalent fast-fracture time and should be used with caution. The characteristic strength σ_θ' is arbitrarily defined as the value of the specimen failure stress where the probability of failure is 0.6321 and the time to failure is 1.0 second for dynamic loading (constant stress rate loading). For static loading this is equivalent to a time to failure of 1/(N+1) seconds and for cyclic loading its 1/(N+1) cycles. The transformed inert strengths are arranged in ascending order of magnitude. The integer number in parenthesis cross references to the original specimen data of the previous table.

Using the Stefansky outlier test any transformed inert strength data value that deviates substantially from the rest of the data is detected as an outlier, and its corresponding significance level is printed. The lower the significance level, the more extreme is the deviation of the data point from the rest of the distribution. A 1-percent significance level indicates that there is a 1-in-100 chance that the data point is actually a member of the same population as the other data, assuming a normal distribution (the skewness of the Weibull distribution can falsely influence results, causing a data point to have a lower significance level than it should). Detected outliers can be cross referenced to the original specimen data. The results from the outlier test should only be considered as a warning to the user and any subsequent action should be carefully considered. Plotting the data on a Weibull scale helps in confirming the identity of outliers. It is recommended that outliers not be removed from the data set unless the significance level is below 1-percent and a physical justification can found for such action. Detected outliers may indicate a competing failure mode is present.

With the conclusion of the specimen data (specimen geometry, specimen fracture data, transformed fracture data, and outlier test) versus temperature, a table containing the estimated

fatigue parameters N and A_c (or A_d) along with statistical parameters m' and σ_θ' obtained

solely from the fatigue data follow. The fatigue parameter B_w is not included in this particular

table since the calculated value may depend on additional fast-fracture data given later. Listed in

order of increasing temperature, the failure mode of the flaw population is identified, either volume

or surface, the type of experiment is identified, either "STAT" for static fatigue, "CYCL" for cyclic

fatigue, or "DYNA" for dynamic fatigue, and the solution method "SOL" is printed. The fatigue

exponent is under the column marked "N" and the natural logarithm of the fatigue constant A_c, or

A_d (whichever is appropriate) is under the column marked "LN A". A_c and A_d are determined based

on a 50.0 percent probability of failure (they describe the median behavior of the data). The

remaining columns of estimated parameters pertain to the statistical distribution of the fatigue data

(the Weibull parameters estimated directly from the fatigue data). These values depend on the

Weibull parameter estimation method (see keyword **MLORLE** in section **Material- and specimen-**

dependent (temperature-independent) data) as much as they depend on the particular fatigue

parameter estimation method. The columns marked "M BIASED" and "M UNBIASED" indicate

the transformed inert distribution biased and unbiased Weibull modulus m', respectively.

Unbiasing of the Weibull modulus is not provided if least-squares estimation is used (**MLORLE** =

1). For maximum likelihood estimation the unbiasing is based on factors from Thoman, Bain, and

Antle (Thoman, Bain, and Antle, 1969). The column marked "CHAR. STR." indicates the

characteristic strength σ_θ' of the transformed inert data. As previously explained this characteristic

strength is arbitrarily defined as the value of the failure stress where the probability of failure is

0.6321 and the time to failure is 1.0 second for dynamic loading (constant stress rate loading). For

static loading this is equivalent to a time to failure of $1/(N+1)$ seconds and for cyclic loading its

1/(N+1) cycles. The columns with the headings "MEAN" and "STD. DEV." are the Weibull mean and standard deviation of the inert distribution parameters m' and σ'_θ.

Following the table of the parameter estimates is the results from the Kolmogorov-Smirnov and Anderson-Darling goodness-of-fit testing on the transformed inert strength data and the Weibull parameters m' and σ'_θ. These values of the goodness-of-fit statistics are applied to the original fatigue data. The Kolmogorov-Smirnov (K-S) goodness-of-fit test is done for each data point, and the corresponding K-S statistics (D^+ and D^-) and significance level are listed. Similarly, the K-S statistic D for the overall population is printed along with the significance level. This overall statistic is the absolute maximum of individual specimen data D^+ and D^- factors. For the Anderson-Darling (A-D) goodness-of-fit test, the A-D statistic A^2 is determined for the overall population and its associated significance level is printed. The lower the significance level, the worse is the fit of the experimental data to the proposed distribution. For these tests, a 1-percent level of significance is interpreted as a 1-in-100 chance that the specimen fracture data were generated from the estimated distribution. A word of caution must be inserted regarding the interpretation of the printed significance levels. These values are based on the assumption that the fatigue and Weibull parameters are determined independent of the experimental data. This assumption is not true here and therefore the printed values for the significance level may need revision. The significance level for these tests should be viewed as a relative measure of goodness-of-fit and not as an absolute measure. Further research is required in order to resolve this inconsistency.

If fast-fracture (inert strength) experimental data is input (see keyword **FAST** in section **Temperature-dependent fracture or statistical material parameters data; the Data Table form of input**), then the results of the Weibull analysis versus temperature is printed (via subroutine PRINTP). The specimen dimensions are given at each temperature for either four-point bending,

three-point bending, tensile specimen gage volume, tensile specimen gage area, specimen effective volume or specimen effective area (effective volume and area are calculated for some arbitrary specimen geometry as prescribed with the keyword **PFCONV** in the Master Control Input). The specimen effective volume or area can change with temperature if the Weibull modulus changes with temperature (see section **Material Strength Characterization**). The inert strengths are arranged in ascending order of magnitude with proper failure mode identification. An "S" indicates a surface flaw, a "V" indicates a volume flaw, and a "U" indicates an unknown flaw origin. Following this table the Stefansky outlier test is used to check for outliers in the inert strength data (the previous comments regarding the interpretation of the results of the outlier test also apply here). Any value that deviates substantially from the rest of the data is detected as an outlier, and its corresponding significance level is printed. Detected outliers may indicate a competing failure mode is present.

After the fast-fracture specimen data (specimen geometry, specimen fracture data, and outlier test) a table containing the estimated Weibull statistical parameters follow. The estimation method is identified, either least-squares or maximum likelihood (see keyword **MLORLE** in section **Material- and specimen-dependent (temperature-independent) data**) prior to beginning the table. The parameters are listed in order of increasing temperature and the failure mode of the flaw population is identified, either volume or surface. The columns marked "M BIASED" and "M UNBIASED" indicate the fast-fracture distribution biased and unbiased Weibull modulus m, respectively. Unbiasing of the Weibull modulus is not provided if least-squares estimation is used. For maximum likelihood estimation the unbiasing is based on factors from Thoman, Bain, and Antle (Thoman, Bain, and Antle, 1969). The columns identified with "UP M" and "LOW M" indicate the ninety percent confidence bounds of the Weibull modulus. These bounds are only applicable for the maximum likelihood procedure and are also based on factors developed by Thoman, Bain, and

Antle (Thoman, Bain, and Antle, 1969). The column marked "CHAR. STR." indicates the characteristic strength σ_θ of the specimen data. The characteristic strength is the value of the fracture stress where the probability of failure is 0.6321. The columns identified with "UP C.S." and "LOW C.S." indicate the ninety percent confidence bounds of the characteristic strength. These bounds are only applicable for the maximum likelihood procedure and again are based on factors developed by Thoman, Bain, and Antle (Thoman, Bain, and Antle, 1969). As a rule of thumb the confidence bounds are significantly larger (as a fraction of the estimated parameter) for the Weibull modulus than for the characteristic strength. The columns with the headings "MEAN" and "STD. DEV." are the Weibull mean and standard deviation of the fast-fracture distribution parameters m and σ_θ.

The Kolmogorov-Smirnov (K-S) goodness-of-fit test is done for each fast-fracture data point, and the corresponding K-S statistics (D^+ and D^-) and significance level are listed. Similarly, the K-S statistic D for the overall population is printed along with the significance level. For the Anderson-Darling (A-D) goodness-of-fit test, the A-D statistic A^2 is determined for the overall population and its associated significance level is printed. The previous comments regarding the interpretation of results of these tests also apply here.

The next table that is generated by C4PEST from the PRINTP subroutine contains data to construct Kanofsky-Srinivasan 90-percent confidence bands about the Weibull distribution. The table includes fast-fracture rupture stress data, the corresponding Weibull probability of failure values, the 90-percent upper and lower confidence band values about the Weibull line, and the median rank value for each data point. These statistical quantities are calculated with either tabular values or approximating polynomial functions. Experimental fracture data lying outside of these bands are an indication of poor fit to the Weibull distribution.

.

The last table generated for the material (from the PRINTP subroutine) lists the material parameters that are used in the component reliability calculations as a function of temperature. These values are passed to module C4LIFE via the CARES.INP file. The table lists the biased Weibull modulus m, the Weibull scale parameter σ_o, the fatigue exponent N, the fatigue constant B_w, and the crack growth law. The fatigue constant B_w is always printed regardless of the fracture criterion chosen (B_w is also printed in the CARES.INP data file for module C4LIFE). The C4LIFE program module will automatically calculate B_B from B_w for the chosen fracture criteria so that the user is not required to repeatedly run the C4PEST module every time a component reliability analysis is performed using a different fracture criteria (this statement is only true when the specimen is not multiaxially loaded). The values given in the table correspond to the experimental *temperatures input (and optionally to five additional interpolated sets of values between each input* temperature if the **INTER** keyword is set to 1 in the Master Control Input). If fatigue specimen rupture data is available but not fast-fracture specimen rupture data, then the table lists

m', σ_o', N', and B_w (in this case B_w is calculated using m' and σ_o'). If fatigue and fast-fracture

specimen rupture data is available (or the Weibull parameters are directly input using keyword **PARAM** in section **Temperature-dependent fracture or statistical material parameters data; the Data Table form of input**), then the table lists m, σ_o, N, and B_w (in this case B_w is

calculated using m and σ_o). The headings For this table are as follows; the Weibull modulus m is denoted by the column headed by "M", the scale parameter σ_o is headed by "SP", the fatigue exponent N is headed by "N" and the fatigue constant B_w is headed by "B".

C4LIFE Module Output Information

The C4LIFE module reads control indices, Weibull, and fatigue parameters from the CARES.INP file; the finite element information is read from the neutral file data base (or from two neutral files when proof testing or cyclic loading are considered). This information is used to predict component reliability. The results from this analysis is output in a file with the default name of CARES.OUT. A separate data file is also generated with the default name of CARES.PAT, containing the element risk-of-rupture intensities. This data file is PATRAN compatible so that graphical rendering of the components critical regions is possible.

The reliability analysis results file CARES.OUT begins with an echo of the choices selected (or default values) from the Master Control Input. The PRINTA subroutine echoes this data. For each flaw population of a material the Material Control Input is echoed for the temperature independent information (from the PRINTB subroutine) and then its printed for the temperature dependent material parameters (from the PRINTP subroutine). The crack growth law is identified followed by the material parameters which include the Weibull modulus m, the normalized Batdorf crack density coefficient $\overline{k_B}$, the Weibull scale parameter σ_o, and if the loading duration is non-zero (**TIME** > 0.0), then the fatigue exponent N and the fatigue constant B_B or B_w (whichever is appropriate). The Weibull modulus m is denoted by the column headed by "M", the normalized Batdorf crack density coefficient $\overline{k_B}$ column is headed by "K", the scale parameter σ_o is headed by "SP", the fatigue exponent N is headed by "N" and the fatigue constant B_B or B_w is headed by "B". Information on the selected fracture criterion and crack shape is printed for shear-sensitive fracture models. Crack shape is not required for the NSA (Batdorf shear-insensitive model) or for the PIA model, and it need not be identified for those cases.

Information regarding cyclic loading is echoed in the temperature independent section of the Master Control Input (see keyword **CYCLIC** in section **Material- and specimen dependent (temperature-independent) data**). This data includes the choices for the crack growth law (power law, Paris law, or Walker law) and cycle waveform. The period of the cycle (in seconds) and the R-ratio (ratio of minimum cycle stress to maximum cycle stress) is printed. The R-ratio is assumed constant throughout the component if only one neutral file is being processed (**IPROOF** = 0). If two neutral files are being processed (**IPROOF** = 1), then the R-ratio is computed at every subelement and for all crack orientations. In this case then the printed value for the R-ratio in the Master Control Input is ignored.

Following the echo of the contents of the CARES.INP input file (the Master Control Input and *Material Control Input) is the listing of the finite element analysis data read from the neutral file*. This data comes from the primary neutral file (default file name CARES.NEU). Any information regarding the (optional) second neutral file PROOF.NEU is not printed. Note two neutral files are used by C4LIFE only for the case of proof testing or cyclic loading (**IPROOF** = 1).

The output from the neutral file begins with an echo of the problem title that was input by the user. Next, tables are output showing each element number, averaged element temperature, and the (undeformed) element volume or area. This information is arranged according to element group. The total number of elements in the group and the group number is printed at the beginning of the table and the total element group volume or area is printed at the end of each table. Element groups are arranged according to element type and not to a particular material designation, therefore elements may be listed that are not used in the reliability analysis. If the element group pertains to solid type elements (brick, wedge, or tetrahedron) or two-dimensional axisymmetric elements (quadrilateral and triangular), then the element volumes are listed. If the element group pertains to shell elements (quadrilateral, triangular) then the element area is printed. Note that volume flaw

analysis may be performed with shell elements (assuming no through the thickness stress gradients exist), however element thicknesses or volumes are not output for this situation.

After the element group tables of temperatures, volumes and areas, the number of array elements used to store information in the blank common block **A** and the total size of this common block is listed. Blank common block **A** is the main storage array for material data and finite element data. This information is efficiently placed in this array through the use of integer addresses called pointers. The highest pointer number, which is the value listed in CARES.OUT, indicates the index of the array element where the last item of data is stored. The difference between this number and the limit (MTOT) or total size of the array indicates the amount of unused memory. The size of this array is controlled by the parameter MTOT, which is declared at the beginning of the C4LIFE source code. Increasing or decreasing the value of this parameter increases or decreases the amount of memory required to run this module. This is a user friendly feature added to enable tailoring the code to the available machine memory or to the size of the finite element problem. If the amount of memory allocated is insufficient to run the problem, then an error message is printed along with this table.

Since in a large finite element mesh the stress output could be excessive, printed element stress tables in CARES are optional (see keyword **IPRINT** in section **Master Control Input**). The stress analysis results are printed for each group of elements (from subroutine PRINTC). The element group number is identified along with the integer identification of the element type. As stated previously, the element stresses that are printed are from the primary neutral file and elements may be listed that are not used in the reliability analysis. This information can consist of either centroidal or subelement level stresses for each element. The subelement stress is the stress at the Gaussian integration point and therefore the number of subelements per element depends on the integration order of the element. The centroidal stress is the stress at the center of the element and

is the only data given for the element (considered the equivalent of one subelement per element). Using centroidal stresses will dramatically reduce execution time of the C4LIFE module, however the penalty is reduced accuracy in the reliability analysis when element stress gradients are present. The use of subelements to perform the reliability analysis is recommended. A compromise approach is to use centroidal stresses for preliminary design and subelement stresses for the final design. For each line of output the element number, and subelement number are identified along with the stresses and subelement temperature. The output stresses are either principal stresses or the tensor stresses read from the neutral file. Principal stresses are calculated when keyword **IPRINC** = 1 and tensor stresses are used when **IPRINC** = 2. Typical practice with isotropic monolithic materials is to use principal stresses, however for certain situations such as proof testing with off-axis loading or cyclic loading where the boundary loading conditions vary with time, then a global reference frame is required. For solid elements the three principal or the six tensor stress components are printed. For shell elements only two principal stresses are printed or the three tensor stress components are printed. For principal stresses these two components appear in the first and second principal stress columns, the third principal stress column has a zero value listed. For the tensorial stress components only the X, Y, and XY values are used, the other components YZ, and ZX have zero values listed.

The results of the reliability analysis follows the output of the element and subelement stresses. First the information is presented in tabular form for each flaw population of each material (from subroutine PRINTC) and then given for the whole component (from subroutine PRINTO). The component level information may include a summary of the reliabilities of all the elements depending on if more than one volume flaw population or more than one surface flaw population is specified. Any given finite element may have multiple flaw populations defined, and therefore several separate tables (representing the different flaw populations) are presented containing

reliability information regarding that same element. Thus for a particular material number (**MATID**) that references a finite element, there may be several concurrent flaw populations specified and the total element reliability is the product of the reliabilities of the individual flaw populations for that element. Reliability results are always presented at the element level and not at the subelement level. The element reliability is the product of the subelement reliabilities. The printout of element reliabilities can be suppressed via the **IPRINT** keyword in the Master Control Input.

The reliability analysis for each flaw population of each material is presented. The order in which this is given is identical to the order presented in the input file CARES.INP; therefore material results are listed without regard to the value of the identification number or whether the analysis is for volume flaws or surface flaws. Tables are provided for each element group and are arranged in ascending order of element number. Only elements with the same material ID as specified with the **MATID** keyword are listed. Information given for each element is the survival probability, the failure probability, the element averaged (if subelements are used) risk-of-rupture intensity, and the average element temperature material parameters. Using subelements means that the reliability analysis is done with the material parameters interpolated to the subelement temperature (although this information is never output). The element averaged material parameters include the Weibull modulus m, the normalized Batdorf crack density coefficient $\overline{k_B}$, the Weibull scale parameter σ_o, and if the loading duration is non-zero, then the fatigue parameters N and B_B. The Weibull modulus is denoted by the column headed by "M", the normalized Batdorf crack density coefficient column is headed by "K", the scale parameter is headed by "SP", the fatigue parameters are headed by "N" and by "B". Following each element group table is a summary of elements with the fifteen maximum risk-of-rupture intensity values and element ID's (the number of

.

values printed can be changed by adjusting parameter NPLV defined at the beginning of the main program).

Finally the survival probability of the flaw population of the material, which is the product of the element reliabilities, and the failure probability is printed along with the maximum effective stress found (the effective stress, σ_{Ie}, and not the effective stress transformed to a time value of zero, $\sigma_{Ieq,0}$). If the **PFCONV** keyword is activated (**PFCONV** = 1 and material parameters are given for only one temperature in the temperature dependent Material Control Input section of file CARES.INP), then the effective volume, effective area and scale parameter is determined for the material (for the flaw population). These calculations are based on the maximum principal stress found in the component and not on the maximum effective stress. For the non-coplanar crack extension fracture criteria the maximum effective stress can be larger than the highest principal stress. In order for these numbers to be valid the keywords **TIME** and **TIMEPT** must be set to zero. It is recommended that **PFCONV** option only be used for typical specimen geometries such as beams under flexure, C-rings, O-rings, tensile specimens, biaxially loaded specimens like ring-on-ring or pressure loaded, etc. For these geometries the effective volume and area are invariant versus applied loading. For other geometries this may not be true and thus separate analyses with at least two different magnitude of loading must be attempted with the C4LIFE module to verify that the effective volume and area are indeed invariant. For the calculation of the scale parameter of the material to be correct the value input for **PFCONV** must correspond to the failure probability associated with the imposed level of loading. The effective volume and area require that the Weibull modulus m be input. To obtain the stress normalized effective volume V_{ef} and area A_{ef} then a modified Weibull modulus of magnitude Nm/(N-2) is substituted for the Weibull modulus in the temperature dependent Master Control Input (in this case the calculated scale parameter has no meaning and the value input for the keyword **PFCONV** can be some arbitrary value).

If more than one volume flaw population or more than one surface flaw population is defined in the CARES.INP file (that is, if either keyword **NMATS** or **NMATV** is larger than one) then additional tables are generated at the element group level listing the element reliabilities, failure probabilities and risk-of-rupture intensities. All elements are listed for which reliability analysis was performed. If an element has more than one statistical flaw population defined for it, then the listed numbers represent the product of the survival probabilities for each of the flaw populations. The values shown for the risk-of-rupture intensities are the same values that are output to the PATRAN compatible data file CARES.PAT. Following the element group tables is a summary of elements with the fifteen maximum risk-of-rupture intensity values and element ID's (the number of values printed can be changed by adjusting parameter NPLV defined at the beginning of the main program). Also included is the probability of failure and survival over the component surface and/or volume, whichever is appropriate. Finally, the overall component probability of failure, as well as the component probability of survival, are printed.

Theory
Fast-Fracture Reliability Analysis

Introduction

The use of advanced ceramic materials in structural applications requiring high component integrity has led to the development of a time-dependent probabilistic design methodology. This method combines three major elements: (1) linear elastic fracture mechanics theory that relates the strength of ceramics to the size, shape, orientation, and growth of critical flaws; (2) extreme value statistics to obtain the characteristic flaw size distribution function, which is a material property; and (3) material microstructure. Inherent to this design procedure is that the requirement of total safety must be relaxed and that an acceptable failure probability must be specified.

The statistical nature of fracture in engineering materials can be viewed from two distinct models (Tracy, 1982). The first was presented by Weibull and used the weakest-link theory as originally proposed by Pierce (Pierce, 1926). The second model was also analyzed by Pierce (Pierce, 1926) and, in addition, by Daniels (Daniels, 1945). This second model is referred to as the "bundle" or "parallel" model. In the bundle model, a structure is viewed as a bundle of parallel fibers. Each fiber can support a load less than its breaking strength indefinitely but will break immediately under any load equal to or greater than its breaking strength. When a fiber fractures, a redistribution of load occurs and the structure may survive. Failure occurs when the remaining fibers can no longer support the increased load. The weakest-link model assumes that the structure is analogous to a chain with n links. Each link may have a different limiting strength. When a load is applied to the structure such that the weakest link fails, then the structure fails. Observations show that advanced monolithic ceramics closely follow the weakest-link theory (WLT). A component fails when an equivalent stress at a flaw reaches a critical value which depends on the

fracture mechanics criterion, crack configuration, crack orientation, and the crack density function of the material. In comparison with the bundle model, WLT is, in most cases, more conservative.

Weibull's WLT model does not consider failure caused by purely compressive stress states. Phenomenological observations indicate that compressive stresses do not play a major role in the failure of ceramic structures since the compressive strength of brittle materials is significantly greater than their tensile strength. The effect of a predominant compression on failure is assumed negligible in the CARES/LIFE program. This is done by comparing compressive and tensile principal stresses in each finite element. When a principal compressive stress exceeds three times the maximum principal tensile stress in a given element, the compressive stress state predominates, and the corresponding element reliability is set equal to unity.

One of the important features of WLT is that it predicts a size effect. The number and severity of flaws present in a structure depends on the material volume and surface area. The largest flaw in a big specimen is expected to be more severe than the largest flaw in a smaller specimen. Another consequence of WLT is that component failure may not be initiated at the point of highest nominal stress (Davies, 1973), as would be true for ductile materials. A large flaw may be located in a region far removed from the most highly stressed zone. Therefore, the complete stress solution of the component must be considered.

Classical WLT does not predict behavior in a multiaxial stress state. A number of concepts such as the PIA, Weibull's normal stress averaging method, and Batdorf's model have been applied to account for polyaxial stress state response. Batdorf's model (Batdorf, and Crose, 1974) assumes the following: (1) microcracks in the material are the cause of fracture, (2) cracks do not interact, (3) each crack has a critical stress σ_{cr} which is defined as the stress normal to the crack plane which will cause fracture, and (4) fracture occurs under combined stresses when an effective stress σ_e acting on the crack is equal to σ_{cr}. For an assumed crack shape, σ_e can be obtained through

the application of a fracture criterion. These concepts are used in conjunction with techniques to obtain various statistical material parameters necessary for fast-fracture reliability analysis.

Volume Flaw Reliability Analysis

Consider a stressed component containing many flaws, and assume that failure is due to any number of independent and mutually exclusive mechanisms (links). Each link involves an infinitesimal probability of failure ΔP_{fV}. Discretize the component into n incremental links. The probability of survival P_{sV} of the ith link is

$$(P_{sV})_i = [1 - (\Delta P_{fV})]_i \tag{1}$$

where the subscript V denotes volume-dependent terms. The resultant probability of survival of the whole structure is the product of the individual probabilities of survival

$$
\begin{aligned}
P_{sV} &= \prod_{i=1}^{n}(P_{sV})_i = \prod_{i=1}^{n}\left[1 - (\Delta P_{fV})\right]_i \\
&\cong \prod_{i=1}^{n}\exp\left[-(\Delta P_{fV})_i\right] = \exp\left[-\sum_{i=1}^{n}(\Delta P_{fV})_i\right]
\end{aligned}
\tag{2}
$$

Assume the existence of a function $N_V(\sigma)$, referred to as the crack density function, representing the number of flaws per unit volume having a strength equal to or less than σ. Under a uniform tensile stress, σ, the probability of failure of the ith link, representing the incremental volume ΔV_i, is

$$(\Delta P_{fV})_i = \left[N_V(\sigma)\ \Delta V\right]_i \tag{3}$$

and substituting into equation (2), the resultant probability of survival is

$$P_{sV} = \exp[-N_V(\sigma) \, V] \tag{4}$$

and the probability of failure is

$$P_{fV} = 1 - \exp[-N_V(\sigma) \, V] \tag{5}$$

where V is the total volume. If the stress is a function of location then

$$P_{fV} = 1 - \exp\left[-\int_V N_V(\sigma) \, dV\right] = 1 - \exp(-B_V) \tag{6}$$

A term called the risk of rupture by Weibull and denoted by the symbol B_V is commonly used in reliability analysis. Equations similar to (5) and (6) are applicable to surface-distributed flaws where surface area replaces volume and the flaw density function is surface area dependent.

Weibull introduced a three-parameter power function for the crack density function $N_V(\sigma)$,

$$N_V(\sigma) = \left[\frac{\sigma - \sigma_{uV}}{\sigma_{oV}}\right]^{m_V} \tag{7}$$

where σ_{uV} is the threshold stress parameter, which is usually taken as zero for ceramics. This parameter is the value of applied stress below which the failure probability is zero. When this parameter is zero, the two-parameter Weibull model is obtained. The scale parameter σ_{oV} then corresponds to the stress level where 63.2 percent of specimens with unit volumes would fracture. The scale parameter has dimensions of stress x (volume)$^{1/m_V}$, where m_V is the shape parameter (Weibull modulus), a dimensionless parameter that measures the degree of strength variability. As m_V increases, the dispersion is reduced. For large values of m_V ($m_V > 40$), such as those obtained for ductile metals, the magnitude of the scale parameter corresponds to the material ultimate

strength. These three statistical parameters are material properties, and they are temperature and processing dependent.

Three-parameter behavior is rarely observed in as-processed monolithic ceramics, and statistical estimation of the three material parameters is very involved. The CARES/LIFE program uses the two-parameter model. The subsequent reliability predictions are more conservative than for the three-parameter model since we have taken the minimum strength of the material as zero.

The two-parameter crack density function is expressed as

$$N_V(\sigma) = \left[\frac{\sigma}{\sigma_{oV}} \right]^{m_V} = k_{wV}\sigma^{m_V} \tag{8}$$

and when equation (8) is substituted into equation (6), the failure probability becomes

$$P_{fV} = 1 - \exp\left(-k_{wV}\int_V \sigma^{m_V}dV\right) \tag{9}$$

where $k_{wV} = (\sigma_{oV})^{-m_V}$ is the uniaxial Weibull crack density coefficient. Various methods have been developed to calculate σ_{oV} and m_V for a given material by using fracture strength data from simple uniaxial specimen tests (Pai, and Gyekenyesi, 1988).

The two most common techniques for using uniaxial data to calculate P_{fV} in polyaxial stress states are the PIA method (Barnett, et al, 1967) (Freudenthal, 1968) and the Weibull normal tensile stress averaging method (Weibull, 1939, two references). In the PIA model, the principal stresses $\sigma_1 \geq \sigma_2 \geq \sigma_3$ are assumed to act independently. If all principal stresses are tensile, the probability of failure according to this approach is

$$P_{fV} = 1 - \exp\left[-k_{wV}\int_V (\sigma_1^{m_V} + \sigma_2^{m_V} + \sigma_3^{m_V})dV\right] \tag{10}$$

Compressive principal stresses are assumed not to contribute to the failure probability. It has been shown that this equation yields nonconservative estimates of P_{fV} in comparison with the Weibull normal stress method (Batdorf, 1977).

The failure probability using the Weibull normal tensile stress averaging method, which has been described through an integral formulation (Gross, and Gyekenyesi, 1989), can be calculated from

$$P_{fV} = 1 - \exp\left(-\int_V k_{wpV} \, \overline{\sigma_n}^{m_V} dV\right) \tag{11}$$

where

$$\overline{\sigma_n}^{m_V} = \frac{\int_A \sigma_n^{m_V} dA}{\int_A dA}$$

The area integration is performed in principal stress space over the surface A of a sphere of unit radius for regions where σ_n, the projected normal stress on the surface, is tensile. The polyaxial Weibull crack density coefficient is k_{wpV}. The relationship between k_{wpV} and k_{wV} is found by equating the failure probability for uniaxial loading to that obtained for the polyaxial stress state when the latter is reduced to a uniaxial condition. The result is

$$k_{wpV} = (2m_V + 1) \, k_{wV} \tag{12}$$

Batdorf and Crose (Batdorf, and Crose, 1974) proposed a statistical theory in which attention is focused on cracks and their failure under stress. Flaws are taken to be uniformly distributed and randomly oriented in the material bulk. Fracture is assumed to depend only on the tensile stress acting normal to the crack plane; hence, shear insensitivity is inherent to the model. Subsequently,

Batdorf and Heinisch (Batdorf, and Heinisch, 1978) included the detrimental effects of shear traction on a flaw plane. Their method applies fracture mechanics concepts by combining a crack geometry and a mixed-mode fracture criterion to describe the condition for crack growth. Adopting this approach, the CARES/LIFE program contains several fracture criteria and flaw shapes for volume and surface analyses (fig. 2).

Consider a small, uniformly stressed material element of volume ΔV. The incremental probability of failure under the applied state of stress Σ can be written as the product of two probabilities,

$$\Delta P_{fV}(\Sigma, \sigma_{cr}, \Delta V) = \Delta P_{1V} P_{2V} \tag{13}$$

where ΔP_{1V} is the probability of the existence in ΔV of a crack having a critical stress between σ_{cr} and $\sigma_{cr} + \Delta \sigma_{cr}$. As previously noted, critical stress is defined as the remote, uniaxial fracture strength of a given crack in mode I loading. The second probability, P_{2V}, denotes the probability that a crack of critical stress σ_{cr} will be oriented in a direction such that an effective stress σ_e (which is a function of fracture criterion, stress state, and crack configuration) satisfies the condition $\sigma_e \geq \sigma_{cr}$. The effective stress is defined as the equivalent mode I stress a flaw would experience when subjected to a multiaxial stress state that results in modes I, II, and III crack surface displacements.

The strength of a component containing a flaw population is related to the critical flaw size, which is implicitly used in statistical fracture theories. Batdorf and Crose (Batdorf, and Crose, 1974) describe ΔP_{1V} as

$$\Delta P_{1V} = \Delta V \, \frac{dN_V(\sigma_{cr})}{d\sigma_{cr}} \, d\sigma_{cr} \tag{14}$$

and P_{2v} is expressed as

$$P_{2v} = \frac{\Omega(\Sigma,\sigma_{cr})}{4\pi} \tag{15}$$

where $N_v(\sigma_{cr})$ is the Batdorf crack density function and $\Omega(\Sigma,\sigma_{cr})$ is the area of the solid angle projected onto the unit radius sphere in principal stress space containing all the crack orientations for which $\sigma_e \geq \sigma_{cr}$. The constant 4π is the surface area of a unit radius sphere and corresponds to a solid angle containing all possible flaw orientations.

The probability of survival in a volume element ΔV_i is

$$(P_{sV})_i = \exp\left\{-\Delta V\left[\int_0^{\sigma_{e_{max}}} \frac{\Omega(\Sigma,\sigma_{cr})}{4\pi} \frac{dN_v(\sigma_{cr})}{d\sigma_{cr}} d\sigma_{cr}\right]\right\}_i \tag{16}$$

where $\sigma_{e_{max}}$ is the maximum effective stress a randomly oriented flaw could experience from the given stress state. Hence, the component failure probability is

$$P_{fV} = 1 - \exp\left\{-\int_V\left[\int_0^{\sigma_{e_{max}}} \frac{\Omega(\Sigma,\sigma_{cr})}{4\pi} \frac{dN_v(\sigma_{cr})}{d\sigma_{cr}} d\sigma_{cr}\right] dV\right\} \tag{17}$$

The Batdorf crack density function $N_v(\sigma_{cr})$ is a material property, independent of stress state, and is usually approximated by a power function (Batdorf, and Heinisch, 1978). This leads to the Batdorf crack density function of the form

$$N_v(\sigma_{cr}) = k_{BV}\sigma_{cr}^{m_v} \tag{18}$$

where the material Batdorf crack density coefficient k_{BV} and the Weibull modulus m_v are evaluated from experimental inert strength fracture data. Batdorf and Crose (Batdorf, and Crose, 1974) initially proposed a Taylor series expansion for $N_v(\sigma_{cr})$, but this method has computational

difficulties. A more convenient integral equation approach was formulated and extended to the use of data from four-point MOR bar tests (Rufin, Samos, and Bollard, 1984). Note that $N_V(\sigma_{cr})$ has units of inverse volume.

Although the Weibull (eq. (8)) and Batdorf (eq. (18)) crack density functions are similar in form, they are not the same. The Weibull function simply depends on the applied stress distribution, σ, and is the only term other than the volume necessary to calculate P_{fV}. The Batdorf function depends on the mode I strength of the crack, σ_{cr}, which is probabilistic and must be integrated over a range of values for a given stress state. Furthermore, to obtain P_{fV}, a crack orientation function, P_{2V}, must be considered in addition to the density function and the volume. Finally, the Batdorf coefficient k_{BV} cannot be calculated from inert strength data until a fracture criterion and crack shape are chosen-in contrast to the Weibull coefficient k_{wV}, which depends only on the data.

To determine a component probability of failure, P_{2V} (eq. (15)) has to be evaluated for each elemental volume ΔV_i, within which a uniform stress state Σ is assumed. The solid angle $\Omega(\Sigma,\sigma_{cr})$ depends on the selected fracture criterion, the crack configuration, and the applied stress state. For multiaxial stress states, with few exceptions, $\Omega(\Sigma,\sigma_{cr})$ must be determined numerically. For a sphere of unit radius (fig. 8), an elemental surface area of the sphere is $dA = \sin\alpha \, d\beta \, d\alpha$. Project onto the spherical surface the equivalent (effective) stress $\sigma_e(\Sigma,\alpha,\beta)$. The solid angle $\Omega(\Sigma,\sigma_{cr})$ is the area of the sphere containing all of the projected equivalent stresses satisfying $\sigma_e \geq \sigma_{cr}$. Noting the symmetry of σ_e in principal stress space, and addressing the first octant of the unit sphere, then

$$\Omega(\Sigma,\sigma_{cr}) = \int_0^{\frac{\pi}{2}} \left(\int_0^{\frac{\pi}{2}} \sin\alpha \, d\alpha \right) d\beta \ H(\sigma_e,\sigma_{cr}) \tag{19}$$

where

$$H(\sigma_e,\sigma_{cr}) = 1 \qquad \sigma_e \geq \sigma_{cr}$$
$$H(\sigma_e,\sigma_{cr}) = 0 \qquad \sigma_e < \sigma_{cr}$$

Substituting into equation (17) and integrating with respect to σ_{cr}, the component failure probability

becomes (Batdorf, Fundamentals of the Statistical Theory of Fracture, 1980)

$$P_{fV} = 1 - \exp\left[-\frac{2}{\pi} \int_V \left(\int_0^{\frac{\pi}{2}} \int_0^{\frac{\pi}{2}} N_V(\sigma_e) \sin\alpha \; d\alpha \; d\beta\right) dV\right] \qquad (20)$$

where

$$N_V(\sigma_e) = k_{BV} \; \sigma_e^{m_V}(x,y,z,\alpha,\beta)$$

For a given element, $\sigma_e(x,y,z,\alpha,\beta)$ is the projected equivalent stress over the unit radius sphere in

principal stress space as shown in figure 8.

Equation (20) circumvents the involved numerical integration of $\Omega(\Sigma,\sigma_{cr})$ as developed in the

original CARES program (Nemeth, Manderscheid, and Gyekenyesi, 1990). Equations (17) and (20)

are equivalent formulations; however, equation (20) is more convenient for computational purposes

with few exceptions (Batdorf and Crose, 1974). Therefore, CARES/LIFE applies equation (20) to

obtain the component probability of failure.

Assuming a shear-insensitive condition, fracture occurs when $\sigma_n = \sigma_e \geq \sigma_{cr}$, where σ_n is the

normal tensile stress on the flaw plane. However, it is known from fracture mechanics analysis that

for a flat crack, a shear stress τ applied parallel to the crack plane (mode II or III) also contributes

to fracture. Therefore, the effective stress σ_e is a function of both σ_n and τ.

Selecting an arbitrary plane in principal stress space (fig. 8) and imposing equilibrium

conditions yields the following equations:

$$\sigma^2 = (\sigma_1\ell)^2 + (\sigma_2 m)^2 + (\sigma_3 n)^2 \qquad (21)$$

$$\sigma_n = \sigma_1 \ell^2 + \sigma_2 m^2 + \sigma_3 n^2 \tag{22}$$

and

$$\tau^2 = \sigma^2 - \sigma_n^2 \tag{23}$$

where σ is the total traction vector acting on the crack plane and the direction cosines ℓ, m, and n are given in figure 8 in terms of trigonometric functions of α and β.

From the selected fracture criterion and crack configuration, σ_e is obtained as a function of Σ, α, and β. Batdorf and Heinisch (Batdorf, and Heinisch, 1978) give effective stress expressions for two flaw shapes by using both Griffith's maximum tensile stress criterion and Griffith's total coplanar strain energy release rate criterion G_T. Arranged in order of increasing shear sensitivity, for the maximum tensile stress criterion the effective stress equations are

$$\sigma_e = \frac{1}{2}\left(\sigma_n + \sqrt{\sigma_n^2 + \tau^2}\right) \tag{24}$$

for a Griffith flaw and

$$\sigma_e = \frac{1}{2}\left\{\sigma_n + \sqrt{\sigma_n^2 + \left[\frac{\tau}{(1 - 0.5\nu)}\right]^2}\right\} \tag{25}$$

for a penny-shaped flaw, where ν is Poisson's ratio.

The total coplanar strain energy release rate criterion is calculated from

$$G_T = G_I + G_{II} + G_{III} \tag{26}$$

where G is the energy release rate for various crack extension modes. In terms of stress intensity factors, the effective stress equation can be derived from (plane strain condition assumed) enforcing the condition $G_T = G_C$, where G_C is the critical strain energy release rate. Thus,

$$K_{IC}^2 = K_I^2 + K_{II}^2 + \frac{K_{III}^2}{1 - \nu} \tag{27}$$

For a Griffith crack, assuming that modes I and II dominate the response with $K_I = \sigma_n \sqrt{\pi a}$ and $K_{II} = \tau \sqrt{\pi a}$, where 2a is the crack length, we have from equation (27)

$$\sigma_e = \sqrt{\sigma_n^2 + \tau^2} \tag{28}$$

For a penny-shaped crack at the critical point on the crack periphery, we have $K_I = 2\sigma_n \sqrt{a/\pi}$ and $K_{II} = (4\tau/(2-\nu)) \sqrt{a/\pi}$ (Sih, 1973), where a is now the crack radius. The resulting effective stress from equation (28) is

$$\sigma_e = \left\{ \sigma_n^2 + \left[\frac{\tau}{(1 - 0.5\nu)} \right]^2 \right\}^{1/2} \tag{29}$$

The equations given by Batdorf and Heinisch consider only self-similar (coplanar) crack extension. However, a flaw experiencing a multiaxial stress state usually undergoes crack propagation initiated at some angle to the flaw plane (noncoplanar crack growth). Shetty (Shetty, 1987) performed experiments on polycrystalline ceramics and glass where he investigated crack propagation as a function of an applied far-field multiaxial stress state. He modified an equation proposed by Palaniswamy and Knauss (Palaniswamy, and Knauss, 1978) so that it would empirically fit experimental data. This multimodal interaction equation takes the form

$$\frac{K_I}{K_{IC}} + \left[\frac{K_\delta}{\overline{C}\,K_{IC}}\right]^2 = 1 \tag{30}$$

where K_δ is either K_{II} or K_{III}, whichever is dominant, and $\overline{C}$ is a constant adjusted to best fit the data. Shetty (Shetty, 1987) found a range of values of $0.80 \leq \overline{C} \leq 2.0$ for the materials he tested which contained large induced flaws. As $\overline{C}$ increases, the response becomes progressively more shear insensitive.

Using this relationship with assumed modes I and II dominance for the Griffith crack yields

$$\sigma_e = \frac{1}{2}\left[\sigma_n + \sqrt{\sigma_n^2 + \left[\frac{2\tau}{\overline{C}}\right]^2}\right] \tag{31}$$

and for a penny-shaped crack, we obtain

$$\sigma_e = \frac{1}{2}\left[\sigma_n + \sqrt{\sigma_n^2 + \left[\frac{4\tau}{\overline{C}\,(2 - v)}\right]^2}\right] \tag{32}$$

For a Griffith crack when $\overline{C}$ =.80, .85, 1.0 and 1.15 equation (30) models, respectively, the following criteria: Maximum strain energy release rate (Ichikawa, 1991), maximum tangential stress (Erdogan, and Sih, 1963), maximum strain energy release rate (Hellen, and Blackburn, 1975) and co-linear crack extension.

Similarly, for a penny shaped crack with a material having a Poisson's ratio of about .22 and $\overline{C}$ =.80, .85, 1.05 and 1.10, equation (30) models, respectively, the following criteria: Maximum strain energy release rate (Ichikawa, 1991), maximum tangential stress, maximum strain energy release rate (Hellen, and Blackburn, 1975), and co-linear crack extension.

For a stressed component , the probability of failure is calculated from equation (20). The finite element method enables discretization of the component into incremental volume elements. CARES/LIFE evaluates the failure probability at the Gaussian integration points of the element or optionally at the element centroid. Using the element integration points subdivides the element into subelements, hence each V_i corresponds to the ith subelement. In the usual context of finite element methods, the volume of a three-dimensional element is calculated after transformation into the natural coordinate space (Bathe, 1982)

$$V = \int_{-1}^{1} \int_{-1}^{1} \int_{-1}^{1} \det J(r,s,t) \ dr \ ds \ dt \tag{33}$$

where J is the Jacobian operator and r,s,t are the natural coordinates. The subelement volume is defined as the contribution of the integration point to the element volume in the course of the numerical integration procedure. This means that the volume of each subelement (corresponding to a Gauss integration point) is calculated using the shape functions inherent to the element type. The stress state in each subelement is assumed uniform. Powers et al. (Powers, Starlinger, and Gyekenyesi, 1992) gives further details of the subelementing procedure as used in CARES/LIFE. The numerical solution of equation (20) takes the following form:

$$P_{fv} = 1 - \exp \left\{ -\frac{2}{\pi} k_{BV} \sum_{i=1}^{n} V_i \left[\int_A \sigma_e^{m_V}(\alpha,\beta) \ dA \right]_i \right\} \tag{34}$$

where n is the total number of subelements. If k_{BV} is element dependent, it would appear inside the brackets.

Surface Flaw Reliability Analysis

For surface flaw analysis (Gyekenyesi, and Nemeth, 1987), many of the equations from the **Volume Flaw Reliability Analysis** section remain the same, except that the statistical material parameters are a function of surface area instead of volume and the equivalent stresses are projected onto the contour of a circle of unit radius rather than onto the surface of a unit radius sphere. The cracks are assumed to be randomly oriented in the plane of the external boundary with their planes normal to the surface (Batdorf, and Heinisch, 1978).

For surface-flaw-induced failure in ceramic structures, the probability of failure for the two-parameter Weibull distribution, which is analogous in form to equation (9), is

$$P_{fS} = 1 - \exp\left(-k_{wS} \int_A \sigma^{m_s} \, dA\right) \tag{35}$$

where $k_{wS} = (1/\sigma_{oS})^{m_s}$ is the uniaxial Weibull surface crack density coefficient. The subscript S denotes the terms that are surface area dependent. Here σ_{oS} is the surface scale parameter with units of stress $\times$ (area)$^{1/m_s}$, and A is the stressed surface area. For biaxial stress states, the PIA model yields

$$P_{fS} = 1 - \exp\left[-k_{wS} \int_A \left(\sigma_1^{m_s} + \sigma_2^{m_s}\right) dA\right] \tag{36}$$

where σ_1 and σ_2 are the principal tensile in-plane stresses acting on the surface of the structure. For the Weibull normal stress averaging method, the failure probability is expressed as

$$P_{fS} = 1 - \exp\left(-k_{wpS} \int_A \overline{\sigma}_n^{m_s} \, dA\right) \tag{37}$$

where

$$\overline{\sigma_n}^{m_s} = \frac{\int_c \sigma_n^{m_s} \, dc}{\int_c dc}$$

Here k_{wpS} is the polyaxial Weibull crack density coefficient for surface flaws. The line integration is performed over the contour c of a unit radius circle where the projected normal stress σ_n is tensile. The relationship of k_{wpS} to k_{wS} is obtained by carrying out the integration in equation (37) for a uniaxial stress and equating the resultant failure probability to that of equation (35) (Pai, and Gyekenyesi, 1988). This results in

$$k_{wpS} = \frac{m_s \, \Gamma(m_s) \, \sqrt{\pi}}{\Gamma\left[m_s + \dfrac{1}{2}\right]} k_{wS} \tag{38}$$

where Γ is the gamma function. Equation (37) is the shear-insensitive case of the more general Batdorf polyaxial model.

For mixed-mode fracture due to surface flaws, the Batdorf polyaxial failure probability equation (analogous to eq. (17)) is

$$P_{fS} = 1 - \exp\left[\int_A \int_0^{\sigma_{max}} \frac{\omega(\Sigma, \sigma_{cr})}{2\pi} \frac{dN_S(\sigma_{cr})}{d\sigma_{cr}} \, d\sigma_{cr} dA\right] \tag{39}$$

where analogous to equations (14) and (15)

$$\Delta P_{lS} = \Delta A \frac{dN_S(\sigma_{cr})}{d\sigma_{cr}} d\sigma_{cr} \tag{40}$$

and

$$P_{2S} = \frac{\omega \ (\ \Sigma, \sigma_{cr})}{2\pi} \tag{41}$$

For randomly oriented cracks, $\omega(\Sigma, \sigma_{cr})$ is the total arc length on a unit radius circle in principal

stress space on which the projection of the equivalent stress satisfies $\sigma_e \geq \sigma_{cr}$, and 2π is the total arc

length of the circle. Similarly as with volume flaws, the Batdorf crack density function is

approximated by the power function,

$$N_S(\sigma_{cr}) = k_{BS} \sigma_{cr}^{m_s} \tag{42}$$

where k_{BS} is the Batdorf surface crack density coefficient.

A simplification of equation (39) is obtained by noting the following:

$$\omega(\Sigma, \sigma_{cr}) = \int_0^{2\pi} H(\sigma_e, \sigma_{cr}) \ d\alpha \tag{43}$$

where

$$H(\sigma_e, \sigma_{cr}) = 1 \qquad \sigma_e \geq \sigma_{cr}$$
$$H(\sigma_e, \sigma_{cr}) = 0 \qquad \sigma_e < \sigma_{cr}$$

Substituting into equation (39) and noting symmetry (for principal stress space), we obtain

$$P_{fs} = 1 \ -\exp[-\frac{2}{\pi} \int_A (\ \int_0^{\frac{\pi}{2}} N_S(\sigma_e) \ d\alpha) \ dA \ ] \tag{44}$$

where

$$N_S(\sigma_e) = k_{BS} \sigma_e^{m_s}(x,y,\alpha)$$

For a given element, $\sigma_e(x,y,\alpha)$ is the projected equivalent stress over the first quadrant of a unit

radius circle in principal stress space, as shown in figure 9. Equation (44) circumvents the

computation of $\omega(\Sigma, \sigma_{cr})$ and is used to obtain the component probability of failure in CARES/LIFE.

The finite element method enables discretization of the surface of the component into incremental area elements. CARES/LIFE evaluates the failure probability at the Gaussian integration points of shell elements or optionally at the element centroid. Using the element integration points subdivides the element into subelements, where each A_i corresponds to the ith subelement. The element or subelement area of a two-dimensional element is calculated in similar fashion to the method outlined for equation (33)

$$ A = \int_{-1}^{1} \int_{-1}^{1} \det J(r,s) \ dr \ ds \tag{45} $$

except a two dimensional natural coordinate space is used. Powers et al. (Powers, Starlinger, and Gyekenyesi, 1992) gives further details of the subelementing procedure as used in CARES/LIFE.

The stress state in each subelement is assumed uniform and the numerical formulation of equation (44) is

$$ P_{fs} = 1 - \exp\left(-2 \ \frac{k_{BS}}{\pi} \sum_{i=1}^{n} A_i \left[\int_0^{\frac{\pi}{2}} \sigma_e^{m_s}(\alpha) \ d\alpha \right]_i \right) \tag{46} $$

where n is the total number of subelements. If k_{BS} is element dependent it would appear inside the brackets.

For the plane stress condition, selecting an arbitrary plane and imposing equilibrium conditions yields the following equations:

$$ \sigma^2 = (\ \sigma_1 \ell\ )^2 + (\ \sigma_2 m\ )^2 \tag{47} $$

$$\sigma_n = \sigma_1 \ell^2 + \sigma_2 m^2 \tag{48}$$

and

$$\tau^2 = \sigma^2 - \sigma_n^2 \tag{49}$$

where σ is the total traction vector acting on the crack plane and the direction cosines m and n are given in figure 9 in terms of trigonometric functions of α.

Fracture occurs when the equivalent stress $\sigma_e \geq \sigma_{cr}$. For the shear-insensitive case, fracture depends only on the value of the normal tensile stress such that $\sigma_e = \sigma_n$. For shear-sensitive cracks and colinear crack extension, assuming a Griffith crack with $K_I = \sigma_n \sqrt{\pi a}$ and $K_{II} = \tau \sqrt{\pi a}$, we obtain as before

$$\sigma_e = \sqrt{\sigma_n^2 + \tau^2} \tag{50}$$

whereas for a Griffith notch subjected to plane strain conditions with $K_I = 1.1215 \, \sigma_n \sqrt{\pi a}$ and $K_{III} = \tau \sqrt{\pi a}$ (Sih, 1973), we obtain

$$\sigma_e = \sqrt{\sigma_n^2 + \frac{0.7951}{(1 - \nu)} \tau^2} \tag{51}$$

Note that the equivalent stress for the Griffith crack is dependent on modes I and II, whereas the equivalent stress for the Griffith notch is dependent on modes I and III (Gyekenyesi, and Nemeth, 1987).

For noncoplanar crack growth, from equation (30) the effective stress equations for the Griffith crack and Griffith notch, respectively, are

$$\sigma_e = \frac{1}{2}\left[\sigma_n + \sqrt{\sigma_n^2 + 4\left(\frac{\tau}{\overline{C}}\right)^2}\right] \tag{52}$$

and

$$\sigma_e = \frac{1}{2}\left[\sigma_n + \sqrt{\sigma_n^2 + 3.1803\left(\frac{\tau}{\overline{C}}\right)^2}\right] \tag{53}$$

For a semicircular surface crack, $K_I = 1.366\,\sigma_n\,\sqrt{a}$, $K_{II} = 1.241\,\tau\,\sqrt{a}$, and $K_{III} = 0.133\,\sqrt{a}$ (Smith, Emery, and Kobayashi, 1967) (Smith, and Sorenson, 1974). Since the contribution of K_{III} is small, it is neglected, and thus the effective stress for this case is

$$\sigma_e = \frac{1}{2}\left[\sigma_n + \sqrt{\sigma_n^2 + 3.301\left(\frac{\tau}{\overline{C}}\right)^2}\right] \tag{54}$$

For the same stress state and identical $\overline{C}$, the Griffith crack is the most shear sensitive, whereas the Griffith notch and the semicircular crack give almost identical predictions.

Material Strength Characterization

Ceramic inert strength due to inherent flaws is described by the simple Weibull uniaxial cumulative distribution function. For brittle materials, tensile strength, compressive strength, shear strength, flexural strength, and theoretical strength all have unique meanings and different values. The theoretical strength is defined as the tensile stress required to break atomic bonds, which typically ranges from 1/10th to 1/5th of the elastic modulus for ceramic materials. Because of processing flaws, this strength is never obtained. In an inert environment, a much more meaningful strength measurement is the inert strength or ultimate tensile strength in uniaxial tension or flexural testing. In flexural strength testing the bend strength σ_f of a ceramic is defined as the maximum tensile stress in the extreme fiber of a beam specimen (modulus of rupture, MOR). The main objective of the CARES/LIFE program is to characterize ceramic strength in terms of the MOR or pure uniaxial strength, and to use this information with appropriate analysis to predict component response under complex multiaxial stress states. This section deals with the calculation of the Weibull scale parameter, σ_o, and the Batdorf crack density coefficient, k_B. Closed form solutions for σ_o are given for the uniaxial tensile, and three- and four-point bending specimen geometries. Also, simplified Weibull equations are described that facilitate evaluation of Weibull parameters from experimental data. Procedures for obtaining Weibull parameters from experimental data are described in the following section titled **Estimation of Statistical Material Strength Parameters.**

Typically for brittle materials, the Weibull parameters are determined from simple specimen geometry and loading conditions, such as beams under flexure and either cylindrical or flat specimens under uniform uniaxial tension. For fast-fracture, in an inert environment, the flexural test failure probability can be expressed in terms of the extreme fiber fracture stress, σ_f, by using the two-parameter Weibull form given in equations (9) and (35):

.

$$P_f = 1 - \exp\left[-\left[\frac{\sigma_f}{\sigma_\theta}\right]^m\right] \qquad (55)$$

where m is the volume or area fast-fracture Weibull modulus and σ_θ is the volume or area specimen characteristic strength. The Weibull scale parameter σ_o (as defined in equations (7) and (35) for volume and surface cracks, respectively) is determined from σ_θ, m, the specimen geometry, and the loading configuration. The scale parameter σ_o is a material property, whereas σ_θ includes the effects of the specimen dimensions and stress distribution. The characteristic strength σ_θ is defined as the uniform stress or extreme fiber stress at which the probability of failure is 0.632 . The component failure behavior in fast-fracture, equation (55), is only a function of σ_f and the empirically determined parameters m and σ_θ. Procedures such as least squares or maximum likelihood analysis are used to estimate m and σ_θ from experimental fracture data as described in the section titled **Estimation of Statistical Material Strength Parameters**.

The uniaxial inert strength distribution for volume flaws (equation (9)) is expressed in terms of the extreme fiber fracture stress, σ_f, of the specimen by

$$P_{fV} = 1 - \exp\left\{-V_e \left(\frac{\sigma_f}{\sigma_{oV}}\right)^{m_V}\right\} \qquad (56)$$

where an effective volume, V_e, is defined by equating the risk of rupture, equation (9), with equation (55).

$$V_e = \int_V \left(\frac{\sigma(x,y,z)}{\sigma_f}\right)^{m_V} dV = \left(\frac{\sigma_{oV}}{\sigma_{\theta V}}\right)^{m_V} \qquad (57)$$

The effective volume is the equivalent volume under a uniform uniaxial tensile stress of magnitude σ_f that is needed to give an identical failure probability as the specimen. Comparing equations (55) and (56) the volume flaw scale parameter is solved as

$$\sigma_{oV} = \sigma_{\theta V} \, V_e^{1/m_V} \qquad (58)$$

For the four-point bend specimen geometry shown in figure 10, the tensile stress distribution in the specimen is

$$\sigma_x = \frac{4xy\sigma_f}{(L_1 - L_2)h} \qquad 0 \le x \le \frac{L_1 - L_2}{2}$$

$$\sigma_x = \frac{2y\sigma_f}{h} \qquad \frac{L_1 - L_2}{2} \le x \le \frac{L_1 + L_2}{2} \qquad (59)$$

$$\sigma_x = \frac{4(L_1 - x)y\sigma_f}{(L_1 - L_2)h} \qquad \frac{L_1 + L_2}{2} \le x \le L_1$$

Substituting equation (59) into equation (57) and solving for the effective volume we obtain

$$V_e = \frac{wh}{2} \frac{(L_1 + m_V L_2)}{(m_V + 1)^2} \qquad (60)$$

The effective volume for the three-point bend specimen geometry is obtained when $L_2 = 0$ in equation (60). For uniaxial tensile loading, the effective volume is equal to the gage volume V_g, which is the uniformly stressed region where fracture is expected to occur.

When a specimen is subjected to multiaxial stresses, the PIA and Batdorf theories are used to equate the specimen strength to the uniaxial stress state. For the PIA theory the effective volume used with equation (56) is

$$V_e = \left(\frac{1}{\sigma_f}\right)^{m_V} \int_V \left(\sigma_1^{m_V} + \sigma_2^{m_V} + \sigma_3^{m_V}\right) dV \qquad (61)$$

where $\sigma_1 \ge \sigma_2 \ge \sigma_3$ are functions of (x,y,z) and negative values are taken as zero. In this case σ_f represents the maximum principal stress found in the component. For the Batdorf theory the effective volume used with equation (56) is defined as

$$V_e = \frac{2\overline{k}_{BV}}{\pi} \int_V \left[\int_0^{\frac{\pi}{2}} \int_0^{\frac{\pi}{2}} \left(\frac{\sigma_e(x,y,z,\alpha,\beta)}{\sigma_f} \right)^{m_V} \sin\alpha \; d\alpha \; d\beta \right] dV \qquad (62)$$

where

$$\overline{k}_{BV} = \frac{k_{BV}}{k_{wV}} \qquad (63)$$

The term $\overline{k}_{BV}$ is the normalized Batdorf crack density coefficient for volume flaws. It is obtained

by equating the risks of rupture of equations (9) and (20), the polyaxial Batdorf theory to the

uniaxial Weibull model, for an imposed uniaxial stress state or, equivalently, by equating the

effective volumes in equations (57) and (62). Under a uniform uniaxial stress of magnitude σ_1, this

yields

$$\overline{k}_{BV} = \frac{\pi}{2 \int_0^{\frac{\pi}{2}} \int_0^{\frac{\pi}{2}} \left[\frac{\sigma_e(\sigma_1,\alpha,\beta)}{\sigma_1} \right]^{m_V} \sin\alpha \; d\alpha \; d\beta} \qquad (64)$$

This equation is evaluated numerically except for two special cases where a closed form solution is

known to exist. For the shear-insensitive fracture criterion

$$\left(\frac{\sigma_e(\sigma_1,\alpha,\beta)}{\sigma_1} \right) = \cos^2\alpha \qquad (65)$$

substituting into equation (64) then

$$\overline{k}_{BV} = 2m_V + 1 \qquad (66)$$

For the coplanar strain energy release rate criterion and the Griffith crack geometry

$$\left(\frac{\sigma_e(\sigma_1,\alpha,\beta)}{\sigma_1} \right) = \cos \alpha \tag{67}$$

again substituting into equation (64) gives

$$\bar{k}_{BV} = m_V + 1 \tag{68}$$

For surface flaws the uniaxial inert strength distribution (equation (35)) is expressed in terms of the extreme fiber fracture stress, σ_f, of the specimen by

$$P_{fS} = 1 - \exp\left\{ -A_e \left(\frac{\sigma_f}{\sigma_{oS}} \right)^{m_S} \right\} \tag{69}$$

where an effective area, A_e, is defined

$$A_e = \int_A \left(\frac{\sigma}{\sigma_f} \right)^{m_S} dA \tag{70}$$

Comparing equations (55) and (69) the surface flaw scale parameter is solved as

$$\sigma_{oS} = \sigma_{\theta S} A_e^{1/m_S} \tag{71}$$

Referring to equation (59) for the four-point bend specimen geometry (fig. 10), the tensile stress on the beam surface $y = h/2$, is

$$\left. \begin{array}{ll} \sigma_x = \dfrac{2x\sigma_f}{(L_1 - L_2)} & 0 \leq x \leq \dfrac{L_1 - L_2}{2} \\[3mm] \sigma_x = \sigma_f & \dfrac{L_1 - L_2}{2} \leq x \leq \dfrac{L_1 + L_2}{2} \\[3mm] \sigma_x = \dfrac{2(L_1 - x)}{(L_1 - L_2)} \sigma_f & \dfrac{L_1 + L_2}{2} \leq x \leq L_1 \end{array} \right\} \tag{72}$$

Substituting equation (72) and equation (59) for the side surface stress distributions into equation (70) and performing the integration, the effective area is obtained as

$$A_e = \left[\frac{\left[\frac{L_2}{L_1}\right]^{m_s + 1}}{(m_s + 1)^2} \right] \left[\frac{m_s \, w}{w + h} + 1 \right] (w + h) L_1 \tag{73}$$

The effective area for the three-point bending specimen geometry is obtained when $L_2 = 0$ in equation (73). For uniaxial tensile loading, the effective area is equal to the specimen gage area A_g, which is the total specimen surface area of interest.

When a specimen is subjected to multiaxial stresses, the PIA and Batdorf model risks of rupture are equated to the uniaxial Weibull risk of rupture given by equation (69). For the PIA model, the effective area used with equation (69) is

$$A_e = \left(\frac{1}{\sigma_f}\right)^{m_s} \int_A \left(\sigma_1(x,y)^{m_s} + \sigma_2(x,y)^{m_s}\right) dA \tag{74}$$

and σ_f represents the maximum principal stress found on the component. For the Batdorf theory the effective area used with equation (69) is

$$A_e = \frac{2\bar{k}_{BS}}{\pi} \int_A \left[\int_0^{\frac{\pi}{2}} \left(\frac{\sigma_e(x,y,\alpha)}{\sigma_f}\right)^{m_s} d\alpha \right] dA \tag{75}$$

where

$$\bar{k}_{BS} = \frac{k_{BS}}{k_{wS}} \tag{76}$$

The term $\bar{k}_{BS}$ is the normalized Batdorf crack density coefficient for surface flaws. In CARES/LIFE the normalized Batdorf crack density coefficient for surface flaws is found for a uniaxially loaded specimen by equating the risk-of-ruptures of equations (35) and (44), or equivalently by equating the effective areas in equations (70) and (75). For a uniform uniaxial stress of magnitude σ_1, this yields

$$\bar{k}_{BS} = \frac{\pi}{2 \int_0^{\frac{\pi}{2}} \left[\frac{\sigma_e(\sigma_1, \alpha)}{\sigma_1} \right]^{m_s} d\alpha} \tag{77}$$

This equation is evaluated numerically. A closed form solution is known to exist for the shear-insensitive fracture criterion (Gross, and Gyekenyesi, 1989). Since

$$\left(\frac{\sigma_e(\sigma_1, \alpha)}{\sigma_1} \right) = \cos^2 \alpha \tag{78}$$

substituting into equation (77) then

$$\bar{k}_{BS} = \frac{m_s \sqrt{\pi} \ \Gamma(m_s)}{\Gamma \left[m_s + \frac{1}{2} \right]} \tag{79}$$

For the shear-sensitive fracture criterion, Griffith crack geometry, and co-linear crack extension

$$\left(\frac{\sigma_e(\sigma_1, \alpha)}{\sigma_1} \right) = \cos \alpha \tag{80}$$

again substituting into equation (77) gives

$$\overline{k}_{BS} = \frac{\sqrt{\pi} \; m_S \; \Gamma\left(\dfrac{m_S}{2}\right)}{2 \; \Gamma\left(\dfrac{m_S + 1}{2}\right)} \tag{81}$$

Estimation of Statistical Material Strength Parameters

Selected statistical theories and equations for Weibull parameter estimation are explained in detail in the reference by Pai (Pai, and Gyekenyesi, 1988). The following is a brief description of these methods and how they are used in the CARES/LIFE code. For brittle materials the Weibull parameters are determined from repeated fracture experiments on nominally identical specimens. Typically this involves a simple geometry and loading condition, such as beams under flexure or specimens with either a round or rectangular cross section under uniform uniaxial tension. As a rule of thumb, a minimum of 30 specimens are required to obtain parameter estimates with a reasonably narrow standard deviation within which the true values of the parameters are likely to reside. Since each specimen carries a fixed cost, the experimentalist desires to use analytical methods that maximize the information that can be gained from a data sample while using the fewest possible number of specimens. CARES/LIFE accomplishes this by including efficient parameter estimation schemes as well as statistical measures to quantify the quality of the data.

For fast-fracture, the flexural test failure probability can be expressed in terms of the extreme fiber fracture stress σ_f by using a simplified two-parameter Weibull form as described by equation (55), where m is the volume or area Weibull modulus and σ_θ is the volume or area specimen characteristic strength. Although the statistical theories and parameter estimation methods outlined in the following discussion are expressed in terms of the fast-fracture strength distribution, these techniques are equally applicable to the time dependent distribution as well.

Before computing the estimates of the statistical parameters, it is essential to carefully examine the available specimen data to screen them for outliers. Very often, a data set may contain

one or more values which may not belong to the overall population. The statistical procedure used to detect the outliers at different significance levels is explained in Pai (Pai, and Gyekenyesi, 1988) and Stefansky (Stefansky, 1972). This outlier test assumes that the data are normally distributed and from a complete sample. Therefore, the application of this test to the Weibull distribution and censored statistics is only approximate. CARES/LIFE improves the original technique (Pai and Gyekenyesi, 1988) by numerically integrating the t-distribution to calculate the critical values (CV) for significance levels in the range of 0.0% to 10.0% with a resolution of 0.1% (polynomial approximating functions are no longer used).

Various methods are available to estimate the statistical material parameters from experimental data for the two-parameter Weibull distribution. The success of the statistical approach depends on how well the probability density function fits the data. Two popular techniques used to evaluate the characteristic strength and shape parameter (σ_θ and m) from inert strength data are the least-squares analysis and the maximum likelihood method. Least-squares analysis is a special case of the maximum likelihood method, where the error is normally distributed and has a zero mean and constant variance. The least-squares method is not suitable for calculating confidence intervals and unbiasing factors, which quantify the statistical uncertainties in the available data.

Equation (55) can be linearized by taking the natural logarithm twice yielding

$$\ell n \left[\ell n \left[\frac{1}{P_s} \right] \right] = \ell n \left[\ell n \left[\frac{1}{1 - P_f} \right] \right] = \ell n \left[\frac{1}{\sigma_\theta} \right]^m + m \ \ell n \ \sigma_f \qquad (82)$$

For the least-squares analysis, it is necessary to obtain the line of best fit with slope m and an intercept which, as seen in equation (82), is equal to $\ell n \left(\frac{1}{\sigma_\theta} \right)^m$. The failure probability, P_f, is

determined by conducting fracture tests on n specimens. The fracture stresses are ranked such that $\sigma_{f1} < \sigma_{f2} < ... < \sigma_{fi} < ... < \sigma_{fn}$. For rank regression analysis, the probability of failure of a specimen with rank i is

$$P_f(\sigma_{fi}) = \frac{i - 0.3}{n + 0.4} \tag{83}$$

By taking the partial derivative of the sum of the squared residuals with respect to m and σ_θ, and by equating the derivatives to zero, values of m and σ_θ are calculated.

With censored data, one cannot directly use the rank regression analysis as given in equation (83) because of the competing failure modes. To take into account the influence of the suspended items, Johnson (Johnson, 1964) developed the rank increment technique. For this technique, all observed fracture stresses are arranged in ascending order, and rank increment values are calculated for each failure stress from the following equation:

$$\text{Rank increment} = \frac{(n + 1) - (\text{previous adjusted rank})}{1 + (\text{number of items beyond present suspended item})} \tag{84}$$

In the CARES/LIFE program for volume flaw analysis, all fracture stresses designated as V's are considered as failure data; for surface flaw analysis, the S's are considered as failure data. The new adjusted rank values are obtained by adding the rank increment value to the previously adjusted rank. These adjusted rank values are then used to calculate the failure probability by using the median rank regression equation (83). Finally, the estimated Weibull parameters for m and σ_θ are obtained.

Since the distribution of errors from the data is not normal, the maximum likelihood method is often preferred in Weibull analysis. This method has certain inherent properties. The likelihood equation from which the maximum likelihood estimates (MLE's) are obtained will have a unique

solution. In addition, as the sample size increases, the solution converges to the true values of the parameters. Another feature of the maximum likelihood method is that there are no ranking functions or linear regression analysis when complete or censored samples are analyzed. The likelihood equation for a complete sample is given by

$$L = \prod_{i=1}^{n} \left[\frac{m}{\sigma_\theta} \right] \left[\frac{\sigma_{fi}}{\sigma_\theta} \right]^{m-1} \exp \left[- \left[\frac{\sigma_{fi}}{\sigma_\theta} \right]^m \right] \tag{85}$$

The values of m and σ_θ which maximize the likelihood function, L, are determined by taking the partial derivative of the logarithm of the likelihood function with respect to m and σ_θ. The estimated values, $\hat{m}$ and $\hat{\sigma}_\theta$, are obtained by equating the resulting expressions to zero and solving the simultaneous equations with the Newton-Raphson iterative technique. The MLE of m and σ_θ are designated by $\hat{m}_V$ and $\hat{\sigma}_{\theta V}$ and by $\hat{m}_S$ and $\hat{\sigma}_{\theta S}$ for volume flaw analysis and surface flaw analysis, respectively. For censored statistics we have

$$\frac{\sum\limits_{i=1}^{n} (\sigma_{fi})^{\hat{m}} \, \ell n(\sigma_{fi})}{\sum\limits_{i=1}^{n} (\sigma_{fi})^{\hat{m}}} - \frac{1}{r} \sum\limits_{i=1}^{r} \ell n(\sigma_{fi}) - \frac{1}{\hat{m}} = 0 \tag{86}$$

and

$$\hat{\sigma}_\theta = \left[\frac{\sum\limits_{i=1}^{n} \sigma_{fi}^{\hat{m}}}{r} \right]^{1/\hat{m}} \tag{87}$$

where r is the number of remaining specimens failed by the flaw mode for which parameters are being calculated. For a complete (uncensored) sample, r is replaced by n, which is the total size of the sample.

The MLE of the shape parameter is always a biased estimate that depends on the number of specimens in the sample. Unbiasing of the shape parameter estimate is desired to minimize the deviation between the sample and the true population. The unbiased estimate of m is obtained by multiplying the biased estimate with an unbiasing factor (Thoman, Bain, and Antle, 1969). The confidence intervals for complete samples can also be obtained (Thoman, Bain, and Antle, 1969). For censored samples, a rigorous method for obtaining confidence intervals has not yet been developed because of the complexity of competing failure modes. Confidence bounds for censored statistics are instead estimated in the CARES/LIFE code from the factors obtained from complete samples (Pai, and Gyekenyesi, 1988). Confidence bounds enable the user to estimate the uncertainty in the parameters as a function of the number of specimens. Bounds at a 90-percent confidence level, and therefore at 5 and 95 percentage points of distribution of the MLE's of the parameters, have been incorporated into the CARES/LIFE program, with data taken from Thoman, et al (Thoman, Bain, and Antle, 1969).

Subjective judgement is needed to test the goodness of fit of the data to the assumed distribution. When graphical techniques are used, it can be very difficult to decide if the hypothesized distribution is valid, especially for small sample sizes. Therefore, many statistical tests have been developed to quantify the degree of correlation of the experimental data to the proposed distribution.

In general, a statistic is a numerical value computed from a random sample of the total population. The difference between an empirical distribution function (EDF) and a hypothesized distribution function is called an EDF statistic. There are two major classes of EDF statistics, and they differ in the manner in which the functional (vertical) difference between the EDF and the proposed distribution function is considered. The Kolmogorov-Smirnov (K-S) goodness-of-fit statistic D belongs to the supremum class and is very effective for small samples. It uses the

largest vertical difference between the two distribution functions to determine the goodness of fit. For the K-S test, the sample is arranged in ascending order, and the empirical distribution function $F_n(x)$ is a step function obtained from the following expressions:

$$
\left.\begin{array}{ll}
F_n(x) = 0 & x < X_1 \\[6pt]
F_n(x) = \dfrac{i}{n} & X_i \leq x < X_{i+1} \text{ and } i = 1,2,3,\ldots,n-1 \\[6pt]
F_n(x) = 1 & X_n \leq x
\end{array}\right\} \tag{88}
$$

where $X_1 < X_2 < \ldots X_i \ldots < X_n$ are the ordered fracture stresses from a sample of size n. The statistic D is obtained by initially evaluating two other statistics, D^+ and D^- (the largest vertical differences when $F_n(x)$ is greater than the distribution function $F(x)$ (equation (55)) and the largest vertical differences when $F_n(x)$ is smaller than $F(x)$, respectively). All three statistics are calculated by using the following expressions:

$$
\begin{aligned}
D^+ &= \left| \frac{i}{n} - F(x)_i \right| \\[8pt]
D^- &= \left| F(x)_i - \frac{i - 1}{n} \right| \qquad i = 1,2,\ldots,n \\[6pt]
D &= \max(D^+, D^-)
\end{aligned} \tag{89}
$$

For ceramics design, the $F(x)_i$'s are equal to P_f's and are calculated from equation (55).

On the other hand, the Anderson-Darling statistic A^2 belongs to the quadratic class and is a more powerful goodness-of-fit statistic. It evaluates the discrepancy between the two distributions through squared differences and the use of an appropriate weighting function. The statistic A^2 is given by

$$
A^2 = -n - \left[\frac{1}{n}\right] \sum_{i=1}^{n} (2i - 1)\left\{\ell n\,[Z_i] + \ell n\,[1 - Z_{n+1-i}]\right\} \tag{90}
$$

In this case, the Z_i's are the predicted failure probabilities obtained from equation (55).

Corresponding significance levels α are calculated from the D and A^2 statistics. From previous surveys (Pai, and Gyekenyesi, 1988) there is no specific mention of an absolute accepted significance level. Therefore, the users must be subjective, using their own judgement in either accepting or rejecting the hypothesis that the data fit a Weibull distribution. However, a higher value of α indicates that the data fit the distribution more closely. In addition, Johnson and Tucker (Johnson, and Tucker, 1992) point out that the basis of the calculation of the significance level is relevant. In CARES/LIFE the significance level is calculated with the assumption that the Weibull parameters are calculated independent of the observed strength data. However, the Weibull parameters are actually estimates based on the experimental data and hence the assumption of independence is violated. Until appropriate corrections are available for the K-S and A-D tests, the user must be cautious in interpreting the calculated significance levels in CARES/LIFE. For now, it is recommended that the significance level be viewed as a relative measure of goodness-of-fit and not as an absolute measure.

For complete samples, the 90-percent Kanofsky-Srinivasan confidence band values about the proposed distribution are also calculated to ascertain the fit of the data. These values are similar to the K-S statistic D centered around the EDF. The bands are generated by

$$\text{Confidence bands} = [F(x) - K(n), F(x) + K(n)] \tag{91}$$

where F(x) is the failure probability obtained by substituting the Weibull parameters in equation (55). The Kanofsky functions, denoted by K(n), are described in Abernethy (Abernethy, 1983).

Some limitations are intrinsic to a purely statistical approach to design. One problem occurs when the design stress is well below the range of experimental data as shown in figure 11. Extrapolation of the Weibull distribution into this regime may yield erroneous results if other

phenomena are present. When two flaw populations exist concurrently, but only one (population A) is active in the strength regime tested, the predicted failure probability may be incorrect. Furthermore, if the threshold strength is not zero, the strength may be underestimated. Finally, an approach based only on statistics can allow for stress state effects only in an empirical fashion.

Theory
Time-Dependent Reliability Analysis

Introduction

For ceramics and glasses the ability to sustain a load degrades over time due to a variety of possible effects, such as oxidation, creep, stress corrosion, and cyclic fatigue. Stress corrosion and cyclic fatigue are representatives of a phenomenon called subcritical crack growth (SCG). SCG initiates on a pre-existing flaw and continues until a critical length is reached, causing catastrophic propagation. This occurs when the equivalent mode I stress intensity factor, K_{Ieq}, equals the fracture toughness, K_{IC}. The SCG failure mechanism is load induced over time. It can also be a function of chemical reaction with the environment, debris wedging near the crack tip, the progressive deterioration of bridging ligaments, etc. Because of this complexity, the models that have been developed tend to be semi-empirical and approximate the phenomenological behavior of subcritical crack growth.

The previous sections assumed no subcritical crack growth occurred prior to failure, and all failures were assumed independent of time and history of previous thermal-mechanical loadings. The effects of time-dependent subcritical crack growth on component reliability will now be addressed. Creep and material healing mechanisms are not addressed in CARES/LIFE. Proof testing (Evans and Weiderhorn, 1974) will improve the reliability of a survived component. This form of testing results in an attenuated probability of failure and a predicted minimum life expectancy of the survived components under the service load. This subject is discussed in the section, **Proof Testing Effect on Component Service Probability of Failure.**

For the analysis of time-dependent reliability, in addition to the Weibull shape and scale parameters, the material/environmental fatigue parameters (N and B) are required. The derivations that follow will develop the time-dependent probability of failure based on the mode I equivalent

stress distribution due to thermal-mechanical loading at time t_p, transformed to its equivalent stress distribution at time $t = 0$. Determination of the fatigue parameters is discussed in the section, **Evaluation of Fatigue Parameters from Inherently Flawed Specimens**.

Investigations in the area of mode I crack extension (Paris, and Sih, 1965) have resulted in the following relationship

$$K_{Ieq}(\Psi,t) = \sigma_{Ieq}(\Psi,t)\ Y\ \sqrt{a(\Psi,t)} \tag{92}$$

where Y is a function of crack geometry and can vary with subcritical crack growth; however, CARES/LIFE assumes Y is a fixed geometric constant. σ_{Ieq} is the equivalent mode I far field stress normal to a crack, a(t) is the appropriate crack length, and Ψ represents a location (x,y,z) within the body and the orientation (α,β) of the crack. In some models, such as the Weibull and PIA, Ψ represents a location only. The equations presented in this section are based on the Batdorf theory and the PIA model. For the Batdorf theory, $\Psi=(x,y,z,\alpha,\beta)$ for volume flaw analysis and $\Psi=(x,y,\alpha)$ for surface flaw analysis. For the PIA model, $\Psi=(x,y,z)$ for volume flaw analysis and $\Psi=(x,y)$ for surface flaw analysis.

The crack growth as a function of the equivalent mode I stress intensity factor can be expressed

$$\frac{da(\Psi,t)}{dt} = A\ K_{Ieq}^{N}(\Psi,t) \tag{93}$$

where A and N are material/environmental constants. From equations (92) and (93) we obtain

$$\frac{d\ a(\Psi,t)}{dt} = A\ \sigma_{Ieq}^{N}(\Psi,t)\ Y^{N}\ a(\Psi,t)^{N/2} \tag{94}$$

The relationship at time t between a(t) and a mode I critical effective stress, $\sigma_{Ieq,t}$ is

$$a(\Psi,t) = \left(\frac{K_{IC}}{Y}\right)^2 \sigma_{Ieq,t}^{-2}(\Psi,t) \tag{95}$$

Differentiating equation (95) and substituting into (94) results in

$$\int_{\sigma_{Ieq,0}}^{\sigma_{Ieq,f}} \sigma_{Ieq,t}^{N-3} d\sigma_{Ieq,t} = -A \ Y^2 \ \frac{K_{IC}^{N-2}}{2} \int_0^{t_f} \sigma_{Ieq}^N(\Psi,t) \ dt \tag{96}$$

where $\sigma_{Ieq,0}(\Psi)$ is the transformed critical equivalent stress distribution at t=0 and $\sigma_{Ieq,f} = \sigma_{Ieq}(\Psi,t_f)$ is the equivalent stress distribution in the component at time t=t_f. The transformation of the equivalent stress distribution at time t_f to its effective stress distribution $\sigma_{Ieq,0}(\Psi)$ at time t=0 (Thiemeier, 1989)(Sturmer, Schulz, and Wittig, 1991) is

$$\sigma_{Ieq,0}(\Psi) = \left[\frac{\int_0^{t_f} \sigma_{Ieq}^N(\Psi,t) \ dt}{B} + \sigma_{Ieq}^{N-2}(\Psi,t_f) \right]^{\frac{1}{(N-2)}} \tag{97}$$

where

$$B = \frac{2}{A \ Y^2 \ K_{IC}^{N-2} \ (N-2)} \tag{98}$$

N and B are the material/environmental fatigue parameters. The exponent N is dimensionless and B has units stress^2 × time. The determination of these parameters is addressed in the section **Evaluation of Fatigue Parameters from Inherently Flawed Specimens.**

Volume Flaw Reliability Analysis

CARES/LIFE computes the time-dependent reliability of a ceramic component assuming a crack density distribution which is a function of the critical effective stress distribution. The crack density coefficient is now time-dependent. For volume flaw analysis the crack density function is expressed

$$N_V(\sigma(\Psi)) = k_{BV} \, \sigma_{Ieq,0}^{m_V}(\Psi) \tag{99}$$

where k_{BV} and m_V are constants and the critical effective stress, $\sigma_{Ieq,0}$, is expressed as

$$\sigma_{Ieq,0}(\Psi) = \left[\frac{\int_0^{t_f} \sigma_{Ieq}^{N_V}(\Psi,t) \, dt}{B_{BV}} + \sigma_{Ieq}^{N_V-2}(\Psi,t_f) \right]^{\frac{1}{(N_V-2)}} \tag{100}$$

where N_V and B_{BV} are material fatigue parameters. Based on a probability of failure model, a subscripted fatigue parameter, such as B_{BV} for the Batdorf model, is computed. B_{BV} is directly proportional to B. The various model-dependent subscripted fatigue parameters are all directly proprotional to B. They are evaluated by satisfying the requirement that for a uniaxial stress state, all models produce the same probability of failure. For large values of N, all model fatigue parameters tend to B. The relationship between the B subscripted parameters is discussed in the section **Fatigue Parameter Risk of Rupture Compatibility.**

If the boundary load direction and/or location changes with time, the principal stress vectors change direction with respect to a fixed global coordinate system. If this occurs, the permanent reference axis becomes the fixed global coordinate system. The normal and shear stresses are computed with respect to the global coordinate system. The normal stress is

$$\sigma_n = l^2 \, \sigma_x + m^2 \, \sigma_y + n^2 \, \sigma_z + 2(lm \, \tau_{xy} + mn \, \tau_{yz} + nl \, \tau_{zx}) \tag{101}$$

and the shear stress is

$$\tau^2 = (l\ \sigma_x + m\ \tau_{yx} + n\ \tau_{zx})^2 + (l\ \tau_{xy} + m\ \sigma_y + n\ \tau_{zy})^2$$
$$+ (l\ \tau_{xz} + m\ \tau_{yz} + n\ \sigma_z)^2 - \sigma_n^2 \tag{102}$$

where l, m and n are the direction cosines, defined in figure 12. Symmetry conditions permit the integration of the equivalent mode I stress projection over the upper half of the spherical surface as shown in figure 12.

The probability of failure for the Batdorf model is

$$P_{fV}(t_f) = 1 - \exp\left[-\frac{k_{BV}}{2\pi} \int_V \int_0^{2\pi} \int_0^{\frac{\pi}{2}} [\sigma_{Ieq,0}(\Psi)]^{m_V} \sin\alpha\ d\alpha\ d\beta\ dV \right] \tag{103}$$

where $\sigma_{Ieq,0}(\Psi)$ is the critical effective stress distribution as given in equation (100). $\sigma_{Ieq,0}(\psi)$ is dependent on the appropriate fracture criterion, crack shape, and time t_f. The criteria and crack shapes available for time-dependent analysis are identical to those used for fast fracture. The fracture criteria are: Weibull's normal stress averaging (a shear-insensitive case of the Batdorf theory), maximum tensile stress, total coplanar strain energy release rate, and the noncoplanar (Shetty) criterion.

For the Principle of Independent Action (PIA) model, the probability of failure is

$$P_{fV}(t_f) = 1 - \exp\left[-k_{wV} \int_V \left(\sigma_{I1,0}^{m_V}(\Psi) + \sigma_{I2,0}^{m_V}(\Psi) + \sigma_{I3,0}^{m_V}(\Psi) \right) dV \right] \tag{104}$$

where

$$\sigma_{Ii,0}(\Psi) = \left[\frac{\int_0^{t_f} \sigma_i^{N_V}(x,y,z,t)\ dt}{B_{wV}} + \sigma_i^{N_V-2}(x,y,z,t_f) \right]^{\frac{1}{N_V-2}}.$$

and i=1,2,3. $\sigma_1(x,y,z,t)$, $\sigma_2(x,y,z,t)$ and $\sigma_3(x,y,z,t)$ are the principal tensile stress distributions.

In proof testing of components, off axis testing (proof test loading axis differs from service loading) frequently occurs requiring a fixed global coordinate system. This occurrence is discussed and analyzed in the **Proof Testing - Off-Axis Loading** section.

For a stressed component, the probability of failure is calculated from equation (103). The finite element method enables discretization of the component into incremental volume elements. CARES/LIFE evaluates the failure probability at the Gaussian integration points of the element or optionally at the element centroid. Using the element integration points subdivides the element into subelements, hence each V_i corresponds to the ith subelement. In the usual context of finite element methods, the volume of a three-dimensional element is calculated after transformation into the natural coordinate space (Bathe, 1982)

$$V = \int_{-1}^{1} \int_{-1}^{1} \int_{-1}^{1} \det J(r,s,t) \ dr \ ds \ dt \tag{105}$$

where J is the Jacobian operator and r,s,t are the natural coordinates. The subelement volume is defined as the contribution of the integration point to the element volume in the course of the numerical integration procedure. This means that the volume of each subelement (corresponding to a Gauss integration point) is calculated using the shape functions inherent to the element type. The stress state in each subelement is assumed uniform. Powers et al. (Powers, Starlinger, and Gyekenyesi, 1992) gives further details of the subelementing procedure as used in CARES/LIFE. The numerical solution of equation (103) takes the following form:

$$P_{fV}(t_f) = 1 - \exp\left[-\frac{k_{BV}}{2\pi} \sum_{i=1}^{n} V_i \left(\int_{0}^{2\pi} \int_{0}^{\frac{\pi}{2}} [\sigma_{Ieq,0}(\Psi)]^{m_V} \sin\alpha \ d\alpha \ d\beta \right)_i \right] \tag{106}$$

where n is the total number of subelements. If k_{BV} is element dependent, it would appear inside the brackets.

Surface Flaw Reliability Analysis

CARES/LIFE computes the time-dependent reliability of a ceramic component assuming a crack density distribution which is a function of the critical effective stress distribution. The crack density coefficient is now time-dependent. For surface flaw analysis the crack density function is expressed as

$$N_S(\sigma(\Psi)) = k_{BS}\ \sigma_{Ieq,0}^{m_S}(\Psi) \tag{107}$$

where k_{BS} and m_s are constants and the critical effective stress, $\sigma_{Ieq,0}$, is expressed as

$$\sigma_{Ieq,0}(\Psi) = \left[\frac{\int_0^{t_f} \sigma_{Ieq}^{N_S}(\Psi,t)\ dt}{B_{BS}} + \sigma_{Ieq}^{N_S-2}(\Psi,t_f) \right]^{\frac{1}{(N_S-2)}} \tag{108}$$

where N_S and B_{BS} are material fatigue parameters. Based on a probability of failure model, a subscripted fatigue parameter, such as B_{BS} for the Batdorf model, is computed. B_{BS} is directly proportional to B. The various model-dependent subscripted fatigue parameters are all directly proprotional to B. They are evaluated by satisfying the requirement that for a uniaxial stress state, all models produce the same probability of failure. For large values of N, all model fatigue parameters tend to B. The relationship between the B subscripted parameters is discussed in the section **Fatigue Parameter Risk of Rupture Compatibility.**

If the boundary load direction and/or location changes with time, the principal stress vectors change direction with respect to a fixed global coordinate system. If this occurs, the permanent reference axis becomes the fixed global coordinate system. The normal and shear stresses are computed with respect to the global coordinate system. By symmetry the projection of the equivalent stress is over half of the perimeter of a unit radius circle, where

$$\sigma_n = l^2 \, \sigma_x + m^2 \, \sigma_y + 2 \, lm \, \tau_{xy} \tag{109}$$

and

$$\tau^2 = (l \, \sigma_x + m \, \tau_{yx})^2 + (l \, \tau_{xy} + m \, \sigma_y)^2 - \sigma_n^2 \tag{110}$$

and l and m are the direction cosines. Symmetry conditions permit the equivalent mode I stress projection over the half of the unit circle. The probability of failure for the Batdorf model is

$$P_{fS}(t_f) = 1 - \exp\left[-\frac{k_{BS}}{\pi} \int_A \int_0^\pi \sigma_{Ieq,0}^{m_S}(\Psi) \, d\alpha \, dA \right] \tag{111}$$

where $\sigma_{Ieq,0}(\Psi)$ is the critical effective stress distribution as given in equation (108). $\sigma_{Ieq,0}(\Psi)$ is dependent on the appropriate fracture criterion, crack shape, and time t_f. The criteria and crack shapes available for time-dependent analysis are identical to those used for fast fracture. The fracture criteria are: Weibull's normal stress averaging (a shear- insensitive case of the Batdorf theory), total coplanar strain energy release rate, and the noncoplanar (Shetty) criterion.

For the Principle of Independent Action (PIA) model the probability of failure is

$$P_{fS}(t_f) = 1 - \exp\left[-k_{wS} \int_A \left(\sigma_{I1,0}^{m_S}(\Psi) + \sigma_{I2,0}^{m_S}(\Psi) \right) dA \right] \tag{112}$$

where

$$\sigma_{Ii,0}(\Psi) = \left[\frac{\int_0^{t_f} \sigma_i^{N_S}(x,y,t) \, dt}{B_{wS}} + \sigma_i^{N_S-2}(x,y,t_f) \right]^{\frac{1}{N_S-2}}$$

and i=1,2. $\sigma_1(x,y,t)$ and $\sigma_2(x,y,t)$ are the principal tensile stress distributions.

.

In proof testing of components, off axis testing (proof test loading axis differs from service loading) frequently occurs requiring a fixed global coordinate system. This occurrence is discussed and analyzed in the **Proof Testing - Off-Axis Loading** section.

The finite element method enables discretization of the surface of the component into incremental area elements. CARES/LIFE evaluates the failure probability at the Gaussian integration points of shell elements or optionally at the element centroids. Using the element integration points subdivides the element into subelements, where each A_i corresponds to the ith subelement. The area of a two-dimensional element or subelement is calculated in similar fashion to the method outlined for equation (105)

$$A = \int_{-1}^{1} \int_{-1}^{1} \det J(r,s) \, dr \, ds \qquad (113)$$

except a two dimensional natural coordinate space is used. Powers et al. (Powers, Starlinger, and Gyekenyesi, 1992) gives further details of the subelementing procedure as used in CARES/LIFE.

The stress state in each subelement is assumed uniform and the numerical formulation of equation (111) is

$$P_{fS}(t_f) = 1 - \exp\left(-\frac{k_{BS}}{\pi} \sum_{i=1}^{n} A_i \left[\int_{0}^{\pi} \sigma_{Ieq,0}^{m_S}(\Psi) \, d\alpha \right]_i \right) \qquad (114)$$

where n is the total of number of subelements. If k_{BS} is element dependent it would appear inside the brackets.

Static Fatigue

Static fatigue is defined as the application of a constant load over a period of time. For static fatigue, the mode I equivalent stress is independent of time, and from equation (97),

$$\sigma_{Ieq,0}(\Psi) = \sigma_{Ieq}^{N-2}(\Psi) \left[\frac{t_f \, \sigma_{Ieq}^2(\Psi)}{B} + 1 \right]^{\frac{1}{N-2}} \tag{115}$$

For volume flaws (by symmetry, integrating over one octant of the unit radius sphere), the probability of failure for the Batdorf model is

$$P_{fV}(t_f) = 1 - \exp\left\{ \frac{-2k_{BV}}{\pi} \int_V \int_0^{\frac{\pi}{2}} \int_0^{\frac{\pi}{2}} \left[\sigma_{Ieq,0}(\Psi) \right]^{m_V} \sin\alpha \, d\alpha \, d\beta \, dV \right\} \tag{116}$$

For the Principle of Independent Action model, the probability of failure is

$$P_{fV}(t_f) = 1 - \exp\left[-k_{wV} \int_V \left(\sigma_{I1,0}^{m_V}(\Psi) + \sigma_{I2,0}^{m_V}(\Psi) + \sigma_{I3,0}^{m_V}(\Psi) \right) dV \right] \tag{117}$$

where

$$\sigma_{Ii,0}(\Psi) = \left[\frac{\sigma_i^{N_V}(x,y,z) \, t_f}{B_{wV}} + \sigma_i^{N_V-2}(x,y,z) \right]^{\frac{1}{N_V-2}}$$

for i=1,2,3.

The probability of failure for surface flaws is analogous to that for volume flaws. For the Batdorf model, the probability of failure is expressed as

$$P_{fS}(t_f) = 1 - \exp\left\{ \frac{-2k_{BS}}{\pi} \int_A \int_0^{\frac{\pi}{2}} \left[\sigma_{Ieq,0}(\Psi) \right]^{m_S} d\alpha \, dA \right\} \tag{118}$$

For the Principle of Independent Action model, the probability of failure is

$$P_{fS}(t_f) = 1 - \exp\left[-k_{wS} \int_A \left(\sigma_{I1,0}^{m_S}(\Psi) + \sigma_{I2,0}^{m_S}(\Psi) \right) dA \right] \tag{119}$$

where

$$\sigma_{Ii,0}(\Psi) = \left[\frac{\sigma_i^{N_S}(x,y)\; t_f}{B_{wS}} + \sigma_i^{N_S-2}(x,y) \right]^{\frac{1}{N_S-2}}$$

for i=1,2.

Dynamic Fatigue

Dynamic fatigue is defined as the application of a constant stress rate $\dot{\sigma}(\Psi)$ over a period of time t. Thus

$$\sigma_{Ieq}(\Psi,t) = \dot{\sigma}(\Psi)\; t \tag{120}$$

From equation (97)

$$\sigma_{Ieq,0}(\Psi) = \left[\frac{\int_0^{t_f} [\dot{\sigma}(\Psi)\; t]^N\; dt}{B} + [\dot{\sigma}(\Psi)\; t_f]^{N-2} \right]^{\frac{1}{N-2}} \tag{121}$$

For $\sigma_{Ieq}(\Psi,t_f) = \dot{\sigma}(\Psi)\; t_f$

$$\sigma_{Ieq,0}(\Psi) = \left[\frac{\sigma_{Ieq}(\Psi,t_f)^N\; t_f}{(N+1)\; B} + \sigma_{Ieq}(\Psi,t_f)^{N-2} \right]^{\frac{1}{N-2}} \tag{122}$$

For volume flaws, the Batdorf probability of failure equation is

$$P_{fV}(t_f) = 1 - \exp\left\{ -\frac{2\; k_{BV}}{\pi} \int_V \int_0^{\frac{\pi}{2}} \int_0^{\frac{\pi}{2}} [\sigma_{Ieq,0}(\Psi)]^{m_V} \sin\alpha\; d\alpha\; d\beta\; dV \right\} \tag{123}$$

For the PIA model

$$P_{fV}(t_f) = 1 - \exp\left[-k_{wV} \int_V \left(\sigma_{I1,0}^{m_V}(\Psi) + \sigma_{I2,0}^{m_V}(\Psi) + \sigma_{I3,0}^{m_V}(\Psi)\right) dV\right] \quad (124)$$

where

$$\sigma_{Ii,0}(\Psi) = \left[\frac{\sigma_i^{N_V}(x,y,z,t_f)\ t_f}{(N_V+1)\ B_{wV}} + \sigma_i^{N_V-2}(x,y,z,t_f)\right]^{\frac{1}{N_V-2}}$$

for i=1,2,3.

For surface flaws, the Batdorf model probability of failure is

$$P_{fS}(t_f) = 1 - \exp\left[-\frac{2\ k_{BS}}{\pi} \int_A \int_0^{\frac{\pi}{2}} \left[\sigma_{Ieq,0}(\Psi)\right]^{m_S} d\alpha\ dA\right] \quad (125)$$

For the PIA model

$$P_{fS}(t_f) = 1 - \exp\left\{-k_{wS} \int_A \left(\sigma_{I1,0}^{m_S}(\Psi) + \sigma_{I2,0}^{m_S}(\Psi)\right) dA\right\} \quad (126)$$

where

$$\sigma_{Ii,0}(\Psi) = \left[\frac{\sigma_i^{N_S}(x,y,t_f)\ t_f}{(N_S+1)\ B_{wS}} + \sigma_i^{N_S-2}(x,y,t_f)\right]^{\frac{1}{N_S-2}}$$

for i=1,2.

Cyclic Fatigue

Cyclic fatigue is the repeated application of a loading sequence. Analysis of the time-dependent probability of failure for a component subjected to various cyclic boundary load conditions is simplified by transforming that type of loading to an equivalent static state. The conversion satisfies the requirement that both systems will cause the same crack growth (Mencik, 1984). Implicit in this conversion is the validity of the crack growth equation (93). The probability of failure is obtained with respect to the transformed static state.

The fatigue parameters can also be determined from cyclic loaded specimens via transformation to an equivalent static state. Since static and cyclic tests can yield different results when determining the fatigue parameters, the type of loading used should simulate as closely as possible the service conditions.

Evans (Evans, 1980) and Mencik (Mencik, 1984) defined g-factors, for various types of cyclic loading, that are used to convert to an equivalent static state. For periodic loading, T is the time interval of one cycle. $\sigma_{Ieq}(\Psi)$ is the equivalent static stress acting over the same time interval, T, as the applied cyclic load $\sigma_{Ieqc}(\Psi,t)$. The equivalent static stress is defined as

$$\sigma_{Ieq}(\Psi) = g(\Psi)^{\frac{1}{N}} \sigma_{ch}(\Psi) \tag{127}$$

where $\sigma_{ch}(\Psi)$ is a characteristic value of $\sigma_{Ieqc}(\Psi,t)$. Over one cycle where both load systems cause the same crack growth

$$\sigma_{Ieq}^{N}(\Psi) \, T = \int_{0}^{T} \sigma_{Ieqc}^{N}(\Psi,t) \, dt \tag{128}$$

where

$$\sigma_{Ieq}^N(\Psi) = \left[\frac{\int_0^T \sigma_{Ieqc}^N(\Psi,t) \, dt}{T} \right] = \sigma_{ch}^N(\Psi) \, g(\Psi) \qquad (129)$$

and the g-factor is

$$g(\Psi) = \left[\frac{\int_0^T \left(\frac{\sigma_{Ieqc}(\Psi,t)}{\sigma_{ch}(\Psi)} \right)^N dt}{T} \right] \qquad (130)$$

In CARES/LIFE, the characteristic value $\sigma_{ch}(\Psi)$ of $\sigma_{Ieqc}(\Psi,t)$ is taken as $\sigma_{Ieqc_{max}}(\Psi)$, the

maximum stress of the periodic load over the cycle time interval T. For a periodic load over a time

t_1

$$\sigma_{Ieq}^N(\Psi) \, t_1 = \int_0^{t_1} \sigma_{Ieqc}^N(\Psi,t) \, dt = t_1 \left[\frac{\int_0^T \sigma_{Ieqc}^N(\Psi,t) \, dt}{T} \right] = g(\Psi) \, \sigma_{Ieqc_{max}}^N(\Psi) \, t_1 \qquad (131)$$

When more than one type of loading is applied to a component, such as a periodic cyclic load and a

static load, the g-factor is based on the effective variation of the combined loading. The g-factor

can vary from element to element and the stress-volume integration is performed over the

hemisphere for volume flaws and on the semi-circle for surface flaws.

For n multiple, but different, cyclic loadings over an interval of time, $t_n = t_f$

$$\sigma_{Ieq}^N(\Psi) \, t_f = \int_0^{t_1} \sigma_1^N(\Psi,t) \, dt + \int_{t_1}^{t_2} \sigma_2^N(\Psi,t) \, dt + \ldots + \int_{t_{n-1}}^{t_n} \sigma_n^N(\Psi,t) \, dt \qquad (132)$$

Thus

$$\sigma_{Ieq}^N(\Psi) \, t_f = \sum_{i=1}^{n} \sigma_{Ieqc_{max,i}}(\Psi)^N \, g_i(\Psi) \, \delta t_i \qquad (133)$$

where

$$\delta t_i = t_i - t_{i-1}$$

and

$$g_i(\Psi) = \left[\frac{\displaystyle\int_0^{T_i} \left(\frac{\sigma_{Ieqc_i}(\Psi,t)}{\sigma_{Ieqc_{max,i}}(\Psi)} \right)^N dt}{T_i} \right]$$

Another approach by Mencik is to define an equivalent static time, t_{es}, during which a characteristic stress ($\sigma_{ch}(\Psi)$ chosen as the maximum stress $\sigma_{Ieqc_{max}}(\Psi)$) would cause the same crack growth as the applied cyclic stress $\sigma_{Ieqc}(\Psi,t)$ during time δt. Thus

$$\sigma_{Ieqc_{max}}^N(\Psi)\, \delta t_{es}(\Psi) = \frac{\delta t}{T} \int_0^T \sigma_{Ieqc}^N(\Psi,t)\, dt = \sigma_{Ieqc_{max}}^N(\Psi)\, g(\Psi)\, \delta t \qquad (134)$$

or

$$\delta t_{es}(\Psi) = g(\Psi)\, \delta t \qquad (135)$$

For multiple, but different, cyclic loading over an interval of time $t_f = \delta t_1 + \delta t_2 + ... + \delta t_n$

$$\sigma_{Ieqc_{max}}^N(\Psi)\, [\delta t_{es1}(\Psi) + \delta t_{es2}(\Psi) + ... + \delta t_{esn}(\Psi)] = \sigma_{Ieqc_{max}}^N(\Psi)\, [\, g_1(\Psi)\, \delta t_1 + g_2(\Psi)\, \delta t_2 + ... + g_n(\Psi)\, \delta t_n\,] \qquad (136)$$

or

$$\sum_{i=1}^{n} \delta t_{esi}(\Psi) = \sum_{i=1}^{n} g_i(\Psi) \delta t_i \tag{137}$$

Mencik (Mencik,1984) lists g-factors for a variety of waveforms. Table 1 lists the g-factors for various loadings and waveforms supported by CARES/LIFE. A simple closed form expression for the sine wave is not available and consequently a numerical evaluation is required.

CARES/LIFE adopts the approach of equation (131) to compute the time-dependent reliability. Equation (131), the static equivalent stress distribution, is substituted into equation (97) where the time t_1 is replaced by t_f. Hence

$$\sigma_{Ieq,0}(\Psi) = \sigma_{Ieqc_{max}}(\Psi) \left[\frac{g(\Psi) \, \sigma^2_{Ieqc_{max}}(\Psi) \, t_f}{B} + 1 \right]^{\frac{1}{N-2}} \tag{138}$$

Formulations for other failure models are analogously developed.

Application of the Paris and Walker Laws

This section will consider the more general case of reliability modeling where the applied loading varies as a function of time. Subcritical crack growth is a complex phenomenon involving a combination of simultaneous and synergistic failure mechanisms. These can be grouped into two classes: static effects and cyclic effects. Static effects refer to the slow propagation of cracks under cyclic stresses and may be explained by the same environmental and corrosive processes responsible for subcritical crack growth under static loads. Cyclic effects are functionally dependent on the number of cycles and on the duration of the cycle. The subcritical crack growth phenomenon can be caused by a variety of effects, such as debris wedging or the degradation of bridging ligaments, but essentially it is based on the accumulation of some type of irreversible damage that tends to enhance the crack growth. Not all materials display cyclic effects. Glasses seem to show only the static effects, while polycrystalline materials are more susceptible to the cyclic effects. Modeling for static effects is well established, while the work for cyclic effects is still evolving. Modeling for cyclic effects in this version of the CARES/LIFE program is based on phenomenological criteria (Paris law and Walker law) traditionally used for metal fatigue.

Using g-factors to obtain component life is an unconservative practice for materials prone to cyclic damage. To empirically model cyclic effects Dauskardt et. al. (Dauskardt, James, Porter, and Ritchie, 1992) (Dauskardt, Marshall, and Ritchie, 1990) suggest the use of the Paris power-law expression (Paris, 1963), which has traditionally been used in metals design. Dauskardt et al. (Dauskardt, Porter, and Ritchie, 1992) use the Walker modification (Walker, 1970) of the Paris law to express the growth increment per cycle (da(Ψ,n)/dn) as

$$\frac{d\ a(\Psi,n)}{dn} = A_o\ K_{Ic_{max}}^{N-Q}(\Psi,n)\ (\Delta K_{Ic}(\Psi,n))^Q \tag{139}$$

.

where

$$K_{Ic_{max}}(\Psi,n) = \sigma_{Ieqc_{max}}(\Psi,n) \ Y \ \sqrt{a(\Psi,n)}$$

and

$$\Delta K_{Ic}(\Psi,n) = \Delta\sigma_{Ieqc}(\Psi,n) \ Y\sqrt{a(\Psi,n)} = [\sigma_{Ieqc_{max}}(\Psi,n) - \sigma_{Ieqc_{min}}(\Psi,n)] \ Y\sqrt{a(\Psi,n)}$$

A_o, N, and Q are the cyclic fatigue parameters determined from experiment. The Paris law is obtained when N and Q are equal in value. The subscripts max and min indicate the maximum and minimum cycle stress, respectively. From equation (139)

$$\sigma_{Ieqc,0}(\Psi,n_f) = \left[\frac{\int_{n=0}^{n_f} [1-R(\Psi,n)]^Q \ \sigma_{Ieqc_{max}}^N(\Psi,n) \ dn}{B} + \sigma_{Ieqc_{max}}^{N-2}(\Psi,n_f) \right]^{\frac{1}{N-2}} \qquad (140)$$

where n_f denotes the number of cycles to failure, B is expressed in units of stress^2 x cycle (B is determined from cyclic data), and

$$R(\Psi,n) = \frac{\sigma_{Ieqc_{min}}(\Psi,n)}{\sigma_{Ieqc_{max}}(\Psi,n)}$$

For a periodic cyclic stress , R and $\sigma_{Ieqc_{max}}$ are independent of n, hence

$$\sigma_{Ieqc,0}(\Psi,n_f) = \sigma_{Ieqc_{max}}(\Psi) \left[\frac{\sigma_{Ieqc_{max}}^2(\Psi) \ [1 - R(\Psi)]^Q \ n_f}{B} + 1 \right]^{\frac{1}{N-2}} \qquad (141)$$

When R = 1 (the static fatigue case) there is no time-dependent degradation of material strength due to cyclic effects. The probability of failure for cyclic fatigue using the Batdorf model for volume flaws is

$$P_{fV}(n_f) = 1 - \exp\left(\frac{-2}{\pi} k_{BV} \int_V \int_0^{\frac{\pi}{2}} \int_0^{\frac{\pi}{2}} \sigma_{Ieqc,0}^{m_V}(\Psi, n_f) \sin\alpha \ d\alpha \ d\beta \ dV\right) \tag{142}$$

Analogously, equations may be derived for the PIA model or for surface flaws.

The Paris law should be used with prudence. The effect of R<0 on the crack growth is assumed negligible. R is assumed to be equal to zero for this case. Assuming that the static effects and cyclic effects are mutually exclusive events, the component reliability can be described as the product of the reliabilities calculated for each of these phenomena:

$$P_{S_{combined}} = P_{S_{static\ effects}} P_{S_{cyclic\ effects}} \tag{143}$$

thus, when R=1 degradation due to static fatigue is accounted for. In the CARES/LIFE code, equation (143) may be implemented for a given component reliability analysis by modeling that component based on two mutually exculusive events. One event is based on strength degradation due to cyclic effects (Paris law) and the second is based on strength degradation due to static effects (Power law). The combined component reliability is calculated from equation (143). If the component is modeled based on one event, then only one degradation mechanism (cyclic or static) can be considered. Other models that consider the combined cyclic and static effects may be incorporated into future versions of CARES/LIFE.

Material Failure Characterization For Static, Cyclic, Or Dynamic Loading

For time-dependent fracture under static or cyclic fatigue loading, failure probability can be expressed in terms of the specimen time to failure t_f by using the two-parameter specimen uniaxial Weibull model (Paluszny, and Nicholls, 1978)

$$P_f(t_f) = 1 - \exp\left[-\left[\frac{\sigma_{I,0}}{\sigma_\theta}\right]^m\right] = 1 - \exp\left[-\left[\frac{\sigma_f^N(\Psi_o)\, g(\Psi_o)\, t_f}{B_u\, \sigma_\theta^{N-2}}\right]^{\tilde{m}}\right] = 1 - \exp\left[-\left[\frac{t_f}{t_\theta}\right]^{\tilde{m}}\right] \qquad (144)$$

where

$$\tilde{m} = \frac{m}{(N-2)}$$

$$t_\theta = \frac{B_u\, \sigma_\theta^{N-2}}{\sigma_f^N(\Psi_o)\, g(\Psi_o)}$$

and

$$\frac{\sigma_f^2(\Psi_o)\, g(\Psi_o)\, t_f}{B_u} >> 1$$

For static loading $g(\Psi) = 1$. At location Ψ_o, $\sigma_f(\Psi_o)$ is the maximum static or cyclic failure stress in the specimen, $g(\Psi_o)$ is the g-factor, σ_θ is the characteristic strength, $\sigma_{I,0}$ is the transformed static inert strength, $\tilde{m}$ is a modified Weibull modulus, and t_θ is the volume or area specimen characteristic time. Henceforth $\sigma_f(\Psi_o)$ is replaced by σ_f, where location at Ψ_o is implied. The characteristic time is analogous to the characteristic strength. Equation (144) allows the specimen time-dependent failure response to be described with a simple Weibull equation which is only a

function of t_f and the empirically determined parameters $\tilde{m}$ and t_θ. Procedures such as least squares or maximum likelihood analysis can be used to estimate these parameters from experimental fracture data as described in the section titled **Estimation of Statistical Material Strength Parameters.**

For static or cyclic fatigue, using the uniaxial time-dependent Weibull distribution for volume flaws with the g-factor approach of equation (130) and for

$$\frac{\sigma^2_{1eqc_{max}}(x,y,z) \ g(x,y,z) \ t_f}{B_{wV}} \ >> \ 1$$

then

$$P_{fV}(t_f) = 1 - exp\left[\frac{-1}{\sigma_{oV}^{\tilde{m}_V}} \int_V \sigma_{1eqc,0}^{\tilde{m}_V}(x,y,z) \ dV \right] \tag{145}$$

where

$$\sigma_{1eqc,0}(x,y,z) = \left(\frac{\sigma^{N_V}_{1eqc_{max}}(x,y,z) \ g(x,y,z) \ t_f}{B_{wV}} \right)^{\frac{1}{N_V-2}}$$

For the case when the g-factor is constant throughout the specimen, henceforth denoted by g, equation (145) can be expressed in terms of the maximum static or cyclic failure stress σ_f in the specimen by multiplying the numerator and denominator by $\sigma_f^{\tilde{m}_V N_V}$. Thus

$$P_{fV}(t_f) = 1 - exp\left[-V_{ef} \left(\frac{t_f}{t_{oV}} \right)^{\tilde{m}_V} \right] \tag{146}$$

where

$$t_{oV} = \frac{B_{wV} \, \sigma_{oV}^{N_V - 2}}{g \, \sigma_f^{N_V}}$$

and

$$V_{ef} = \int_V \left(\frac{\sigma_{1eqc_{max}}(x,y,z)}{\sigma_f} \right)^{\tilde{m}_V N_V} dV \tag{147}$$

The term V_{ef} is the modified effective volume when the applied stress distribution is normalized with respect to σ_f. All expressions previously derived for V_e are still applicable for V_{ef} with the exception that $\tilde{m}_V N_V$ should be substituted for m_V (see section **Fatigue Parameter Risk of Rupture Compatibility**). For constant g-factor , comparing equations (144) and (146) yields the time-dependent scale parameter relationship

$$t_{oV} = t_{\theta V} \, V_{ef}^{1/\tilde{m}_V} \tag{148}$$

The modified effective volume which is used with equation (146) and the PIA model is

$$V_{ef} = \left(\frac{1}{\sigma_f} \right)^{\tilde{m}_V N_V} \int_V \left(\sigma_{1eqc_{max}}^{\tilde{m}_V N_V}(x,y,z) + \sigma_{2eqc_{max}}^{\tilde{m}_V N_V}(x,y,z) + \sigma_{3eqc_{max}}^{\tilde{m}_V N_V}(x,y,z) \right) dV \tag{149}$$

where

$$\sigma_{1eqc_{max}}(x,y,z) \geq \sigma_{2eqc_{max}}(x,y,z) \geq \sigma_{3eqc_{max}}(x,y,z) \geq 0$$

For the Batdorf theory, the modified effective volume analogous with equation (146) is defined as

.

$$V_{ef} = \frac{2\bar{k}_{BV}}{\pi} \int_V \left[\int_0^{\frac{\pi}{2}} \int_0^{\frac{\pi}{2}} \left(\frac{\sigma_{Ieqc_{max}}(\Psi)}{\sigma_f} \right)^{\tilde{m}_V N_V} \sin\alpha \, d\alpha \, d\beta \right] dV \qquad (150)$$

and

$$t_{oV} = \frac{B_{BV} \, \sigma_{oV}^{N_V-2}}{g \, \sigma_f^{N_V}}$$

For surface flaws, the resulting equations are similar to those equations previously derived. Integration is performed over the specimen surface, and the modified effective area A_{ef} is obtained.

$$P_{fS}(t_f) = 1 - \exp\left[-A_{ef} \left(\frac{t_f}{t_{oS}} \right)^{\tilde{m}_S} \right] \qquad (151)$$

where

$$t_{oS} = \frac{B_{wS} \, \sigma_{oS}^{N_S-2}}{g \, \sigma_f^{N_S}}$$

For the uniaxial Weibull distribution

$$A_{ef} = \int_A \left(\frac{\sigma_{Ieqc_{max}}(x,y)}{\sigma_f} \right)^{\tilde{m}_S N_S} dA \qquad (152)$$

The time-dependent scale parameter is

$$t_{oS} = t_{\theta S} \, A_{ef}^{1/\tilde{m}_S} \qquad (153)$$

The modified effective area for the PIA model is

$$A_{ef} = \left(\frac{1}{\sigma_f}\right)^{\bar{m}_s N_s} \int_A \left(\sigma_{1eqc_{max}}^{\bar{m}_s N_s}(x,y) + \sigma_{2eqc_{max}}^{\bar{m}_s N_s}(x,y)\right) dA \tag{154}$$

For the Batdorf theory, the modified effective area is

$$A_{ef} = \frac{2\bar{k}_{BS}}{\pi} \int_A \left[\int_0^{\frac{\pi}{2}} \left(\frac{\sigma_{Ieqc_{max}}(\Psi)}{\sigma_f}\right)^{\bar{m}_s N_s} d\alpha \right] dA \tag{155}$$

and

$$t_{oS} = \frac{B_{BS}\, \sigma_{oS}^{N_s-2}}{g\, \sigma_f^{N_s}}$$

Similar to cyclic fatigue, for dynamic fatigue the specimen time to failure can be expressed using the two parameter Weibull form as

$$P_f = 1 - \exp\left[-\left[\frac{t_f}{t_{\theta d}}\right]^{\bar{m}(N+1)} \right] \tag{156}$$

where

$$t_{\theta d} = \left[\frac{(N + 1)\, B_u\, \sigma_\theta^{N-2}}{\dot{\sigma}_f^{\,N}}\right]^{1/(N+1)}$$

t_f is the time to failure and $t_{\theta d}$ is the characteristic time (subscript d indicates dynamic fatigue). For volume flaws substituting $(N_v + 1)$ for the g-factor and rearranging equation (146) then

$$P_{fV}(t_f) = 1 - \exp\left[-V_{ef}\left(\frac{t_f}{t_{odV}}\right)^{\bar{m}_v(N_v+1)} \right] \tag{157}$$

where

$$t_{odV} = \left[\frac{(N_V + 1)\ B_{wV}\ \sigma_{oV}^{N_V-2}}{\dot\sigma_f^{N_V}} \right]^{1/(N_V+1)} = t_{\theta dV}\ V_{ef}^{\frac{1}{m_V}}$$

Note in equation (157) that σ_f denotes the maximum stress in the specimen and that $\dot\sigma$ is the stressing rate at that location. The derivation for surface flaws follows a similar line of reasoning.

For the Paris law the analogous relation to equation (144) is

$$P_f = 1 - \exp\left[-\left[\frac{n_f}{n_\theta} \right]^{\bar m} \right] \tag{158}$$

where n_f is the cycles to failure and n_θ is a characteristic number of cycles. Similar to equation (145)

$$P_{fV}(n_f) = 1 - \exp\left[\frac{-1}{\sigma_{oV}^{m_V}} \int_V \sigma_{1eq,0}^{m_V}(x,y,z)\ dV \right] \tag{159}$$

where

$$\sigma_{1eq,0}(x,y,z) = \left(\frac{\sigma_{1eqc_{max}}^{N_V}(x,y,z)\ (1 - R)^{N_V}\ n_f}{B_{wV}} \right)^{\frac{1}{N_V-2}}$$

Similar to equation (146) then

$$P_{fV}(n_f) = 1 - \exp\left[-V_{ef}\left(\frac{n_f}{n_{oV}} \right)^{\bar m_V} \right] \tag{160}$$

where

$$n_{oV} = \frac{B_{wV}\, \sigma_{oV}^{N_V-2}}{(1-R)^{N_V}\, \sigma_f^{N_V}} = n_{\theta V}\, V_{ef}^{\frac{1}{m_V}}$$

The derivation for surface flaws follows a similar line of reasoning.

Fatigue Parameter Risk of Rupture Compatibility

To ensure compatibility of failure probabilities the relationships between the fatigue parameters (N and B) and the various failure criterions must be established. From uniaxial test specimen data (simple tension, 3- or 4-point bend) compatibility is derived by equating the risk of rupture of the specimen uniaxial Weibull equation to the uniaxial Weibull, the PIA model, the Weibull normal stress averaging, or the Batdorf shear-sensitive formulation.

For volume flaw analysis, the probabilities of failure for the various approaches mentioned above are:

Specimen Uniaxial Weibull

$$P_f = 1 - \exp\left[-\left(\frac{\sigma_{I,0}}{\sigma_{\theta V}}\right)^{m_V}\right]$$

Uniaxial Weibull

$$P_f = 1 - \exp\left[-k_{wV} \int_V \sigma_{I,0}^{m_V}(x,y,z)\ dV\right]$$

PIA Model

$$P_f = 1 - \exp\left[-k_{wV} \int_V \left(\sum_{i=1}^{3} \sigma_{i,0}^{m_V}(x,y,z)\right) dV\right]$$

Normal Stress Averaging

$$P_f = 1 - \exp\left[-k_{wpV} \int_V \overline{\sigma}_n^{m_V}(x,y,z)\ dV\right]$$

Batdorf Model

$$P_f = 1 - \exp\left[-\frac{2}{\pi} k_{BV} \int_V \int_0^{\frac{\pi}{2}} \int_0^{\frac{\pi}{2}} \sigma_{Ieq,0}^{m_V}(\Psi)\ \sin\alpha\ d\alpha\ d\beta\ dV\right]$$

Subscript 0 denotes transformed stress to time t=0.

The basis for compatibility of failure probabilities is the requirement that all expressions produce the same probability of failure for a uniaxial stress state as that obtained from the specimen uniaxial Weibull equation. The value of N remains invariant, whereas the value of B is adjusted to satisfy this requirement. The approach is similar to that used to obtain the relationships of the crack density coefficients for fast fracture reliability analysis. The most common experimental test specimens used in the evaluation of the fatigue parameters are the uniaxial tension, three-point bend,

and four-point bend geometries. The fatigue parameters N and B are obtained from the data based solely on the maximum stress in the specimen at fracture and the time to failure.

For the specimen uniaxial Weibull equation the time dependent transformation equations are

Static Fatigue

$$\sigma_{I,0} = \left[\frac{\sigma_f^{N_v} \, t_f}{B_{uV}} \right]^{\frac{1}{N_v-2}}$$

Dynamic Fatigue

$$\sigma_{I,0} = \left[\frac{\sigma_f^{N_v} \, t_f}{B_{uV} \, (N_v+1)} \right]^{\frac{1}{N_v-2}}$$

Cyclic Fatigue

$$\sigma_{I,0} = \left[\frac{\sigma_f^{N_v} \, g \, t_f}{B_{uV}} \right]^{\frac{1}{N_v-2}}$$

assuming $\dfrac{\sigma^2 t_f}{B} \gg 1$, where t_f is the time to fracture, g is the g-factor used with cyclic loading, σ_f is the maximum tensile stress in the specimen at fracture, and B_{uV} is the fatigue parameter obtained from the specimen uniaxial Weibull equation. Equating the risk of rupture of the specimen uniaxial Weibull model to the uniaxial Weibull model risk of rupture gives

$$\left(\frac{\sigma_f^{N_v} t_f}{\sigma_{\theta V}^{N_v-2} \, B_{uV}} \right)^{\bar{m}_V} = \int_V \left(\frac{\sigma_1^{N_v}(x,y,z) \, t_f}{B_{wV} \, \sigma_{oV}^{N_v-2}} \right)^{\bar{m}_V N_v} dV \tag{161}$$

then

$$\left(\frac{B_{wV}}{B_{uV}} \right)^{\bar{m}_V} = \frac{1}{V_e} \int_V \left(\frac{\sigma_1(x,y,z)}{\sigma_f} \right)^{\bar{m}_V N_v} dV = \frac{V_{ef}}{V_e} \tag{162}$$

where

$$V_e = \left(\frac{\sigma_{oV}}{\sigma_{\theta V}}\right)^{m_V} = \int_V \left(\frac{\sigma_1(x,y,z)}{\sigma_f}\right)^{m_V} dV \qquad (163)$$

For V_{ef}, the static equivalent stress distribution $\sigma_1(x,y,z)$ is normalized with respect to the maximum equivalent static tensile stress σ_f at t_f. Thus V_{ef} for a given specimen configuration is similar to V_e for the same specimen with the exception that the exponent associated with V_{ef} is $\tilde{m}_V N_V$ whereas the exponent associated with V_e is m_V. When there is no stress gradient then V_e and V_{ef} are equivalent. When stress gradients exist throught the specimen then these terms are not equal. For the three and four-point bend specimen (for three-point bend, the inner span, L_2, is set equal to zero), equating the risk of rupture of the specimen uniaxial Weibull equation with that of the uniaxial Weibull expression

$$B_{wV} = B_{uV} \left[\frac{\frac{wh}{2}(L_1 + \tilde{m}_V N_V L_2)}{V_e(1 + \tilde{m}_V N_V)^2}\right]^{1/\tilde{m}_V} = B_{uV}\left[\frac{V_{ef}}{V_e}\right]^{1/\tilde{m}_V} \qquad (164)$$

where

$$V_e = \left[\frac{wh}{2} \frac{(L_1 + m_V L_2)}{(1 + m_V)^2}\right]$$

and

$$V_{ef} = \left[\frac{wh}{2} \frac{(L_1 + \tilde{m}_V N_V L_2)}{(1 + \tilde{m}_V N_V)^2}\right]$$

For the PIA model the relationship between B_{wV} and B_{uV} is

$$\left(\frac{B_{wV}}{B_{uV}}\right)^{\tilde{m}_V} = \frac{1}{V_e}\int_V \left[\left(\frac{\sigma_1(x,y,z)}{\sigma_f}\right)^{\tilde{m}_V N_V} + \left(\frac{\sigma_2(x,y,z)}{\sigma_f}\right)^{\tilde{m}_V N_V} + \left(\frac{\sigma_3(x,y,z)}{\sigma_f}\right)^{\tilde{m}_V N_V}\right] dV = \frac{V_{ef}}{V_e} \qquad (165)$$

Equating the risk of rupture of the specimen uniaxial Weibull to the Batdorf risk of rupture yields the relationship between B_{BV} and B_{uV}

$$\left(\frac{B_{BV}}{B_{uV}}\right)^{\tilde{m}_V} = \frac{1}{V_e}\left[\frac{2\,\bar{k}_{BV}}{\pi}\int_V\int_0^{\frac{\pi}{2}}\int_0^{\frac{\pi}{2}}\left[\frac{\sigma_{Ieq}(\Psi)}{\sigma_f}\right]^{\tilde{m}_V N_V}\sin\alpha\ d\alpha\ d\beta\ dV\right] \tag{166}$$

where $\sigma_{Ieq}(\Psi)$ represents the static equivalent stress distribution. For the Weibull normal stress averaging method, B_{nwV} is substituted for B_{BV} and $\sigma_{In,0}(\Psi)$ is substituted for $\sigma_{Ieq,0}(\Psi)$.

The relationship between B_{wV} and B_{BV} is established by equating the risk of ruptures for the uniaxial Weibull model and the Batdorf model

$$\left(\frac{B_{wV}}{B_{BV}}\right)^{\tilde{m}_V} = \frac{\int_V\left(\dfrac{\sigma_{Ieq}(x,y,z)}{\sigma_f}\right)^{\tilde{m}_V N_V}dV}{\dfrac{2\,\bar{k}_{BV}}{\pi}\int_V\left[\int_0^{\frac{\pi}{2}}\int_0^{\frac{\pi}{2}}\left(\dfrac{\sigma_{Ieq}(\Psi)}{\sigma_f}\right)^{\tilde{m}_V N_V}\sin\alpha\ d\alpha\ d\beta\right]dV} \tag{167}$$

For the uniaxial stress state this expression becomes strictly a function of the fracture criterion. This can be demonstrated with a shear insensitive fracture criterion (equivalent to the Weibull normal stress averaging method) where

$$\sigma_{Ieq}(\Psi) = \sigma_{Ieq}(x,y,z)\cos^2\alpha \tag{168}$$

so that

$$\left(\frac{B_{wV}}{B_{BV}}\right)^{\tilde{m}_V} = \frac{\int_V\left(\dfrac{\sigma_{Ieq}(x,y,z)}{\sigma_f}\right)^{\tilde{m}_V N_V}dV}{\dfrac{2\,\bar{k}_{BV}}{\pi}\int_V\left(\dfrac{\sigma_{Ieq}(x,y,z)}{\sigma_f}\right)^{\tilde{m}_V N_V}\left[\int_0^{\frac{\pi}{2}}\int_0^{\frac{\pi}{2}}\cos^{2\tilde{m}_V N_V}\alpha\ \sin\alpha\ d\alpha\ d\beta\right]dV} \tag{169}$$

combined with equation (66) then

$$\left(\frac{B_{wV}}{B_{BV}}\right)^{\tilde{m}_V} = \frac{2\,\tilde{m}_V\,N_V + 1}{2\,m_V + 1} \tag{170}$$

For co-linear crack extension with a Griffith crack

$$\sigma_{Ieq}(\Psi) = \sigma_{Ieq}(x,y,z)\,\cos\,\alpha \tag{171}$$

so that

$$\left(\frac{B_{wV}}{B_{BV}}\right)^{\tilde{m}_V} = \frac{\displaystyle\int_V \left(\frac{\sigma_{Ieq}(x,y,z)}{\sigma_f}\right)^{\tilde{m}_V N_V} dV}{\displaystyle\frac{2\,\overline{k}_{BV}}{\pi}\int_V \left(\frac{\sigma_{Ieq}(x,y,z)}{\sigma_f}\right)^{\tilde{m}_V N_V}\left[\int_0^{\frac{\pi}{2}}\int_0^{\frac{\pi}{2}}\cos^{\tilde{m}_V N_V}\alpha\,\sin\,\alpha\,d\alpha\,d\beta\right]dV} \tag{172}$$

combined with equation (68) then

$$\left(\frac{B_{wV}}{B_{BV}}\right)^{\tilde{m}_V} = \frac{\tilde{m}_V\,N_V + 1}{m_V + 1} \tag{173}$$

For an arbitrary fracture criterion expressed as some function of the flaw orientation

$$\sigma_{Ieq}(\Psi) = \sigma_{Ieq}(x,y,z)\,f(\alpha,\beta) \tag{174}$$

then

$$\left(\frac{B_{wV}}{B_{BV}}\right)^{\tilde{m}_V} = \frac{\pi}{2\,\overline{k}_{BV}\left(\displaystyle\int_0^{\frac{\pi}{2}}\int_0^{\frac{\pi}{2}} f^{\tilde{m}_V N_V}(\alpha,\beta)\,\sin\,\alpha\,d\alpha\,d\beta\right)} \tag{175}$$

For surface flaw analysis, the relationship between the specimen uniaxial Weibull fatigue parameter B_{uS} and the uniaxial Weibull B_{wS}, Weibull normal stress averaging B_{nwS} and the Batdorf parameter B_{BS} is obtained in a similar manner to that used for the volume flaw analysis. Equating the risk of rupture of the specimen uniaxial Weibull to the uniaxial Weibull equations

$$\left(\frac{\sigma_f^{N_S} t_f}{\sigma_{\theta S}^{N_S-2} B_{uS}} \right)^{\tilde{m}_S} = \int_A \left(\frac{\sigma_1^{N_S}(x,y) \, t_f}{B_{wS} \, \sigma_{oS}^{N_S-2}} \right)^{\tilde{m}_S N_S} dA \tag{176}$$

then

$$\left(\frac{B_{wS}}{B_{uS}} \right)^{\tilde{m}_S} = \frac{1}{A_e} \int_A \left(\frac{\sigma_1(x,y)}{\sigma_f} \right)^{\tilde{m}_S N_S} dA = \frac{A_{ef}}{A_e} \tag{177}$$

where

$$A_e = \left(\frac{\sigma_{oS}}{\sigma_{\theta S}} \right)^{m_S} = \int_A \left(\frac{\sigma_1(x,y)}{\sigma_f} \right)^{m_S} dA \tag{178}$$

For A_{ef}, the static equivalent stress distribution $\sigma_1(x,y)$ is normalized with respect to the maximum equivalent static tensile stress σ_f at t_f. Thus A_{ef} for a given specimen configuration is similar to A_e for the same specimen with the exception that the exponent associated with A_{ef} is $\tilde{m}_S N_S$ whereas the exponent associated with A_e is m_S. When there is no stress gradient then A_e and A_{ef} are equivalent. When stress gradients exist throught the specimen then these terms are not equal.

For the four-point bend specimen ($L_2=0$ for the three point bend solution)

$$A_e = \frac{(L_1 + m_S L_2) \, (h + w + m_S w)}{(1 + m_S)^2} \tag{179}$$

Equating the risk of rupture of the specimen uniaxial Weibull equation to the uniaxial Weibull formulation

$$B_{wS} = B_{uS} \left[\frac{(L_1 + \tilde{m}_S N_S L_2)(h + w + w \tilde{m}_S N_S)}{A_e (1 + \tilde{m}_S N_S)^2} \right]^{1/\tilde{m}_S} = B_{uS} \left(\frac{A_{ef}}{A_e} \right)^{1/\tilde{m}_S} \tag{180}$$

For the PIA model the relationship between B_{wS} and B_{uS} is

$$\left(\frac{B_{wS}}{B_{uS}} \right)^{\tilde{m}_S} = \frac{1}{A_e} \int_A \left[\left(\frac{\sigma_1(x,y)}{\sigma_f} \right)^{\tilde{m}_S N_S} + \left(\frac{\sigma_2(x,y)}{\sigma_f} \right)^{\tilde{m}_S N_S} \right] dA = \frac{A_{ef}}{A_e} \tag{181}$$

Equating the risk of rupture of the specimen uniaxial Weibull to the Batdorf risk of rupture yields the relationship between B_{BS} and B_{uS}

$$\left(\frac{B_{BS}}{B_{uS}} \right)^{\tilde{m}_S} = \frac{1}{A_e} \left[\frac{2 \, \bar{k}_{BS}}{\pi} \int_A \int_0^{\frac{\pi}{2}} \left[\frac{\sigma_{Ieq}(\Psi)}{\sigma_f} \right]^{\tilde{m}_S N_S} d\alpha \; dA \right] \tag{182}$$

where $\sigma_{Ieq}(\Psi)$ represents the static equivalent stress distribution. For the Weibull normal stress averaging method, B_{nwV} is substituted for B_{BV} and $\sigma_{In,0}(\Psi)$ is substituted for $\sigma_{Ieq,0}(\Psi)$.

The relationship between B_{wS} and B_{BS} is established by equating the risk of ruptures of the uniaxial Weibull model and the Batdorf model

$$\left(\frac{B_{wS}}{B_{BS}} \right)^{\tilde{m}_S} = \frac{\int_A \left(\frac{\sigma_{Ieq}(x,y)}{\sigma_f} \right)^{\tilde{m}_S N_S} dA}{\frac{2 \, \bar{k}_{BS}}{\pi} \int_A \left[\int_0^{\frac{\pi}{2}} \left(\frac{\sigma_{Ieq}(\Psi)}{\sigma_f} \right)^{\tilde{m}_S N_S} d\alpha \right] dA} \tag{183}$$

For the uniaxial stress state this expression becomes strictly a function of the fracture criterion. This can be demonstrated with a shear insensitive fracture criterion (equivalent to the Weibull normal stress averaging method) where   .

$$\sigma_{Ieq}(\Psi) = \sigma_{Ieq}(x,y) \cos^2 \alpha \tag{184}$$

so that

$$\left(\frac{B_{wS}}{B_{BS}}\right)^{\tilde{m}_S} = \frac{\int_A \left(\frac{\sigma_{Ieq}(x,y)}{\sigma_f}\right)^{\tilde{m}_S N_S} dA}{\frac{2 \, \bar{k}_{BS}}{\pi} \int_A \left(\frac{\sigma_{Ieq}(x,y)}{\sigma_f}\right)^{\tilde{m}_S N_S} \left[\int_0^{\frac{\pi}{2}} \cos^{2\tilde{m}_S N_S} \alpha \, d\alpha\right] dA} \tag{185}$$

combined with equation (79) then

$$\left(\frac{B_{wS}}{B_{BS}}\right)^{\tilde{m}_S} = \frac{N_S \, \Gamma \, (\tilde{m}_S N_S) \, \Gamma \left(m_S + \frac{1}{2}\right)}{(N_S - 2) \, \Gamma \left(\tilde{m}_S N_S + \frac{1}{2}\right) \Gamma \, (m_S)} \tag{186}$$

For co-linear crack extension with a Griffith crack

$$\sigma_{Ieq}(\Psi) = \sigma_{Ieq}(x,y) \cos \alpha \tag{187}$$

so that

$$\left(\frac{B_{wS}}{B_{BS}}\right)^{\tilde{m}_S} = \frac{\int_A \left(\frac{\sigma_{Ieq}(x,y)}{\sigma_f}\right)^{\tilde{m}_S N_S} dA}{\frac{2 \, \bar{k}_{BS}}{\pi} \int_A \left(\frac{\sigma_{Ieq}(x,y)}{\sigma_f}\right)^{\tilde{m}_S N_S} \left[\int_0^{\frac{\pi}{2}} \cos^{\tilde{m}_S N_S} \alpha \, d\alpha\right] dA} \tag{188}$$

combined with equation (81) then

.

$$\left(\frac{B_{wS}}{B_{BS}}\right)^{\tilde{m}_S} = \frac{N_S \ \Gamma\left(\frac{\tilde{m}_S N_S}{2}\right) \Gamma\left(\frac{m_S + 1}{2}\right)}{(N_S - 2) \ \Gamma\left(\frac{\tilde{m}_S N_S + 1}{2}\right) \Gamma\left(\frac{m_S}{2}\right)} \tag{189}$$

For an arbitrary fracture criterion expressed as some function of the flaw orientation

$$\sigma_{Ieq}(\Psi) = \sigma_{Ieq}(x,y) \ f(\alpha) \tag{190}$$

then

$$\left(\frac{B_{wS}}{B_{BS}}\right)^{\tilde{m}_S} = \frac{\pi}{2 \ \bar{k}_{BS} \left(\int_0^{\frac{\pi}{2}} f^{\tilde{m}_S N_S}(\alpha) \ d\alpha\right)} \tag{191}$$

Evaluation of Fatigue Parameters from Inherently Flawed Specimens

The lifetime reliability of structural ceramic components depends on the history of the loading, the component geometry, the distribution of pre-existing flaws, and the parameters, N and B, that characterize subcritical crack growth. These crack growth parameters must be measured under conditions representative of the service environment. When determining the fatigue parameters from rupture data of naturally flawed specimens, the statistical effects of the flaw distribution must be considered along with the strength degradation effects of subcritical crack growth. A more direct approach is to calculate fatigue parameters from velocity measurements of an induced crack of known configuration, thereby eliminating the statistical aspects of the flaw population from the experiment. The weakness of this approach, however, is the difficulty of getting a notched or indented specimen to behave in an identical manner as the naturally flawed specimen. CARES/LIFE is developed on the basis that fatigue parameters are most accurately obtained from naturally flawed specimens. In the following discussion, three methods are described to estimate these parameters from fatigue data: the median value technique, a least squares regression technique, and a modification to a method from Jakus (Jakus, Coyne, and Ritter, 1978) known as trivariant regression analysis. These methods are described in terms of volume flaw analysis for static (or steady state cyclic) fatigue and for dynamic (constant stressing rate) fatigue using the power law formulation. The Paris law methodology is given in terms of steady state cyclic loading. Analogous relations for surface flaws are easily developed by replacing the effective volume with the effective area.

Static and cyclic fatigue parameter evaluation

Rearranging equation (146) for static fatigue or steady state cyclic loading at a fixed level of reliability, the specimen time to failure for volume flaws is expressed as a function of the maximum

stress, σ_f, in the specimen (for cyclic loading this corresponds to $\sigma_{Ieqc_{max}}$ at the highest stressed point

in the specimen)

$$t_f = \left\{ \frac{B_{wV} \; \sigma_{oV}^{N_V-2}}{g \left[\dfrac{V_{ef}}{\ell n \left(\dfrac{1}{1-P_{fV}} \right)} \right]^{1/\bar{m}_V}} \right\} \sigma_f^{-N_V}$$ (192)

The g-factor is assumed constant throughout the specimen and for all loading levels. The terms

between the brackets are simplified by replacing them with a constant yielding

$$t_f = A_c \; \sigma_f^{-N_V}$$ (193)

Equation (193) is a convenient expression from which to fit experimental data, thus A_c and N_V can

be considered as material-environmental parameters. Taking the logarithm of equation (193) yields

$$\ell n \; t_f = \ell n \; A_c - N_V \; \ell n \; \sigma_f$$ (194)

Linear regression analysis of the experimental data is used to solve equation (194) for the slope, -

N_V, and the intercept $\ell n \; A_c$. The fatigue parameter estimation techniques in CARES/LIFE estimate

A_c and N_V for a probability of failure fixed at 50% ($P_{fV} = 0.50$).

For the median value technique, CARES/LIFE uses the median value at each individual

stressing level as data points. Using equation (194) and performing least-squares linear regression

on the set of median values estimates the line corresponding to a failure probability of 50% with

slope $-N_V$ and intercept $\ell n \; A_c$. Details of the least squares solution technique are given in Pai

(Pai, and Gyekenyesi, 1988). The median value estimation method is the least efficient fatigue

parameter estimation technique in CARES/LIFE (i.e., the estimated parameter has the largest confidence interval for a given sample size).

Another fatigue parameter estimation method incorporated in CARES/LIFE is referred to as the least squares regression technique. This method is similar to the median value technique except that linear regression using equation (194) is performed with all the fatigue data points (instead of only the median values). The fatigue parameter N_V is obtained from the slope of the regression line. Assuming that the experimental data is at a sufficient number of discrete levels of applied stress, all the data failure times t_{fi} are transformed to an equivalent failure time t_{Ti} at an equivalent single level of stress, σ_T. Equating the failure probabilities calculated from equation (146) for data number i yields

$$t_{Ti} = t_{fi} \left(\frac{\sigma_{fi}}{\sigma_T} \right)^{N_V} \tag{195}$$

where the subscript T indicates a transformed value. In CARES/LIFE, the value of σ_T is the lowest level of applied stress in the data set. With all the data transformed to the various values t_{Ti}, CARES/LIFE performs Weibull parameter estimation as described in the section titled **Estimation of Statistical Material Strength Parameters**, solving equation (144) for $\tilde{m}_V$ and $t_{\theta VT}$. Substituting into equation (193) for a time to failure corresponding to a 50% probability of failure yields

$$A_c = t_{\theta VT} \; \sigma_T^{N_V} \left[\ell n \left(\frac{1}{1-0.50} \right) \right]^{1/\tilde{m}_V} = \frac{B_{wV} \; \sigma_{oV}^{N_V-2}}{g} \left[\frac{\ell n \left(\frac{1}{1-0.50} \right)}{V_{ef}} \right]^{1/\tilde{m}_V} \tag{196}$$

where

$$t_{\theta V T} = \frac{B_{wV} \, \sigma_{oV}^{N_V - 2}}{g \, \sigma_T^{N_V} V_{ef}^{\frac{1}{\tilde{m}_v}}}$$

The third option in CARES/LIFE for estimating fatigue parameters is a modification to a method used by Jakus (Jakus, Coyne, and Ritter, 1978) called trivariant regression analysis. This estimation technique is referred to as the median deviation procedure. In this procedure, the fatigue parameters and Weibull modulus are determined by minimizing the median deviation of the logarithm of the time. The characteristic strength $\sigma_{\theta v}$ is assumed known. From equation (195), the fatigue data is transformed to a single stressing level for an assumed value of N_V. Using equation (144) and the previously mentioned least squares or maximum likelihood estimation methods, the Weibull parameters $\tilde{m}_v$ and $t_{\theta V T}$ are obtained. With these parameters the median value, $t_{T_{0.5}}$, is calculated (i.e., the value for t_T when $P_{fV} = 0.50$). Using the transformed fatigue data as a discrete variable the median deviation is defined as (using absolute values)

$$\text{M.D.} = \frac{1}{k} \sum_{i=1}^{k} \left| \ell n \, t_{T_i} - \ell n \left[t_{\theta V T} \left(\ell n \frac{1}{1 - 0.50} \right)^{1/\tilde{m}_v} \right] \right| = \frac{1}{k} \sum_{i=1}^{k} \left| \ell n \, t_{T_i} - \ell n \, t_{T_{0.50}} \right| \qquad (197)$$

for the k data points. The median deviation, M.D., is a measure of dispersion or scatter about the median. It can also be obtained for the continuous variable defined by the Weibull parameters $\tilde{m}_v$ and $t_{\theta V T}$ for ranked probabilities of failure P_{fi}.

The value of N_V for which the M.D. is a minimum establishes the solution. The scatter of the distribution is measured with the Weibull modulus $\tilde{m}_V$ since for a fixed value of k the expression inside the brackets of equation (198) is a constant. CARES/LIFE minimizes equation (198) by

$$\text{M.D.} = \frac{1}{k} \sum_{i=1}^{k} \left| \ell n \left[t_{\theta VT} \left(\ell n \frac{1}{1-P_{fi}} \right)^{1/\tilde{m}_V} \right] - \ell n \, t_{T_{0.5}} \right|$$

$$= \frac{1}{\tilde{m}_V} \left\{ \frac{1}{k} \sum_{i=1}^{k} \left| \ell n \left[\frac{\ell n \frac{1}{1-P_{fi}}}{\ell n \frac{1}{1-0.5}} \right] \right| \right\}$$

(198)

maximizing $\tilde{m}_V$ versus N_V. This process is iterative, covering an appropriate range of values of N_V.

After a solution for N_V is obtained, equation (196) is used to calculate A_c.

The median deviation procedure was investigated with Monte-Carlo simulations of static fatigue data. For sample sizes of 20 and 30 specimens each, 10,000 simulations were run where the fast fracture Weibull modulus, m, randomly varied between 2.0 and 30.0, N randomly varied between 10.0 and 60.0, and the number of stressing levels randomly varied between 2 and the sample size. The parameters σ_{oV} and B_U were fixed at 100.0 and 10000.0/N+1 , respectively. The results of the simulations were compared to estimates calculated using the median value technique for the same fracture data. Examination of the 90% confidence intervals indicated that the median deviation procedure yielded better results than the median value technique. Using maximum likelihood estimation (MLE) gave better results than using least squares (LS) estimation with the median deviation procedure. For the crack growth exponent, N, the 90% confidence interval from the median deviation procedure (with MLE) was about 70% of the range of the median value 90% confidence interval, with no bias indicated with either estimator. For the crack growth constant, B_U, the 90% confidence interval for the median deviation procedure was dramatically smaller than the median value 90% confidence interval, with negligible bias indicated with the median deviation method and significant negative bias with the median value method.

The fatigue parameter B_{wV} is obtained by comparing equations (192) and (193) for a 50% probability of failure

$$B_{wV} = \frac{A_c \, g}{\sigma_{oV}^{N_V - 2}} \left[\frac{V_{ef}}{\ell n\left(\frac{1}{1-0.50}\right)} \right]^{1/\tilde{m}_V} \tag{199}$$

Alternatively, B_{wV} can be obtained by equating equations (144) and (145)

$$B_{wV} = \frac{t_{\theta V} \, g \, \sigma_f^{N_V} \, V_{ef}^{1/\tilde{m}_V}}{\sigma_{oV}^{N_V - 2}} \tag{200}$$

Information on the underlying inert strength distribution can also be obtained from the fatigue data. Using equation (195) to transform all the fatigue data to a single Weibull distribution and performing least squares or maximum likelihood analysis establishes the parameters $\tilde{m}_V$ and $t_{\theta VT}$.

The fast-fracture Weibull modulus is then solved as

$$m'_V = \tilde{m}_V \, (N_V - 2) \tag{201}$$

where the superscript $'$ denotes a fast-fracture parameter estimated from fatigue data. The fast-fracture characteristic strength $\sigma_{\theta V}$ cannot be estimated from the fatigue data. CARES/LIFE calculates a characteristic strength, $\sigma'_{\theta V}$, based on extrapolation of the fatigue data to a specific failure time. This time is arbitrarily fixed at $1/(N+1)$ seconds for static loading (equivalent to 1.0 second for dynamic loading). From equation (195) then

$$\sigma'_{\theta V} = \sigma_T \, [t_{\theta VT} \, (N_V + 1)]^{1/N_V} \tag{202}$$

Much more statistical uncertainty is associated with the determination of the Weibull modulus than with the characteristic strength for fast-fracture testing.

With the calculated quantities $\sigma'_{\theta v}$ and m'_v, the fatigue data can be transformed to an equivalent inert strength distribution by equating the risk of rupture of equations (55) and (144) for the various transformed fatigue data values

$$\sigma'_{fl_i} = \sigma'_{\theta v} \left(\frac{t_{T_i}}{t_{\theta VT}} \right)^{\frac{1}{N_v - 2}} \tag{203}$$

where σ'_{fl_i} represents the i'th transformed inert fracture strength of the specimen. Plotting the

ranked values σ'_{fl_i} ($\ell n \, \ell n (1/1 - P_{fv})$ versus $\ell n \, \sigma$) gives useful visual information for the analyst

(CARES/LIFE does not include a graphical interface). With $\sigma'_{\theta v}$, m'_v , and the various σ'_{fl_i} values,

CARES/LIFE performs the outlier test and determines the K-S and A-D goodness-of-fit statistics as explained in the section titled **Estimation of Statistical Material Strength Parameters**. The outlier test and goodness-of-fit statistics in this case are also valid for the transformed fatigue data (denoted with subscript T) and the original fatigue data as well. Hence the calculated goodness-of-fit significance levels measure the hypothesis that fatigue data was generated from the parameters N_v, A_c, and m'_v.

Dynamic fatigue parameter evaluation

Fatigue parameter estimation methodology for dynamic fatigue is similar to the power law formulation for static and cyclic fatigue. Rearranging equation (157) for a fixed level of reliability, the specimen failure stress σ_f for volume flaws is expressed as a function of the of the stressing rate $\dot{\sigma}$ at the highest stressed point in the component

$$\sigma_f = \left\{ \frac{(N_V + 1)\, B_{wV}\, \sigma_{oV}^{N_V-2}}{\left[\dfrac{V_{ef}}{\ell n\left(\dfrac{1}{1-P_{fV}}\right)} \right]^{1/\bar{m}_V}} \right\}^{1/(N_V+1)} \dot{\sigma}^{1/(N_V+1)} \tag{204}$$

The terms between the brackets are simplified by replacing them with a constant yielding

$$\sigma_f = A_d\, \dot{\sigma}^{1/(N_V+1)} \tag{205}$$

Equation (205) is a convenient expression from which to fit experimental data, thus A_d and N_V can be considered as material-environmental parameters. Taking the logarithm of equation (205) yields

$$\ell n\, \sigma_f = \ell n\, A_d + \frac{1}{N_V + 1}\, \ell n\, \dot{\sigma} \tag{206}$$

Median value, least squares and the median deviation technique are used to solve equation (206) as previously discussed for static and cyclic loadings.

Assuming that the experimental data is at a sufficient number of discrete levels of stressing rates, all the data failure times t_{fi} are transformed to equivalent failure times t_{T_i} at a fixed stressing rate $\dot{\sigma}_T$. Equating the failure probabilities calculated from equation (156) for data number i yields

$$t_{Ti} = t_{fi} \left(\frac{\dot{\sigma}_i}{\dot{\sigma}_T} \right)^{N_V/(N_V+1)} \tag{207}$$

where the subscript T indicates a transformed value. In CARES/LIFE, the value of $\dot{\sigma}_T$ is the lowest stressing rate in the data set. With all the data transformed to the various values t_{T_i}, CARES/LIFE performs Weibull parameter estimation as described in the section titled **Estimation of Statistical Material Strength Parameters**, solving equation (156) for $\tilde{m}_V(N_V+1)$ and $t_{\theta VT}$.

Substituting into equation (205) for a time to failure corresponding to a 50% probability of failure yields

$$A_d = t_{\theta d V T} \left\{ \dot{\sigma}_T^{N_V} \left[\ell n \left(\frac{1}{1-0.50} \right) \right]^{1/\tilde{m}_V} \right\}^{1/(N_V+1)} = \left\{ (N_V + 1) \ B_{wV} \ \sigma_{oV}^{N_V-2} \left[\frac{\ell n \left(\frac{1}{1-0.50} \right)}{V_{ef}} \right]^{1/\tilde{m}_V} \right\}^{1/(N_V+1)} \quad (208)$$

where

$$t_{\theta d V T} = \left\{ \frac{(N_V + 1) \ B_{wV} \ \sigma_{oV}^{N_V-2}}{\dot{\sigma}_T^{N_V} \ V_{ef}^{1/\tilde{m}_V}} \right\}^{1/(N_V+1)}$$

The median deviation method for estimating fatigue parameters minimizes the median deviation of the logarithm of the time to failure. From equation (207), the fatigue data is transformed to a single stressing rate for an assumed value of N_V. Using equation (156) and the previously mentioned least squares or maximum likelihood estimation methods, the Weibull parameters $\tilde{m}_V(N_V+1)$ and $t_{\theta d V T}$ are obtained. With these parameters the median value, $t_{T_{0.5}}$, is calculated (i.e., the value for t_T when $P_{fV} = 0.50$). Using the transformed fatigue data as a discrete variable the median deviation is defined as

$$\text{M.D.} = \frac{1}{k} \sum_{i=1}^{k} \left| \ell n \ t_{T_i} - \ell n \left[t_{\theta d V T} \left(\ell n \frac{1}{1 - 0.50} \right)^{\frac{1}{\tilde{m}_V(N_V+1)}} \right] \right| = \frac{1}{k} \sum_{i=1}^{k} \left| \ell n \ t_{T_i} - \ell n \ t_{T_{0.50}} \right| \quad (209)$$

for the k data points. The median deviation, M.D., is a measure of dispersion or scatter about the median. It can also be obtained for the continuous variable defined by the Weibull parameters $\tilde{m}_V(N_V+1)$ and $t_{\theta d V T}$ for ranked probabilities of failure P_{fi}.

$$\text{M.D.} = \frac{1}{k} \sum_{i=1}^{k} \left| \ln \left[t_{\theta d V T} \left(\ln \frac{1}{1 - P_{fi}} \right)^{\frac{1}{\tilde{m}_V(N_V+1)}} \right] - \ln t_{T_{0.5}} \right|$$

$$= \frac{1}{\tilde{m}_V(N_V + 1)} \left\{ \frac{1}{k} \sum_{i=1}^{k} \left| \ln \left[\frac{\ln \frac{1}{1-P_{fi}}}{\ln \frac{1}{1-0.5}} \right] \right| \right\} \tag{210}$$

The value of N_V for which the M.D. is a minimum establishes the solution. The scatter of the

distribution is measured with the Weibull modulus $\tilde{m}_V(N_V+1)$ since for a fixed value of k the

expression inside the brackets of equation (210) is a constant. CARES/LIFE minimizes equation

(210) by maximizing $\tilde{m}_V(N_V+1)$ versus N_V. This process is iterative, covering an appropriate range

of values of N_V. After a solution for N_V is obtained, equation (208) is used to calculate A_d.

The median deviation procedure was investigated with Monte-Carlo simulations of dynamic

fatigue data. For sample sizes of 20 and 30 specimens each, 10,000 simulations were run where the

fast fracture Weibull modulus, m, randomly varied between 2.0 and 30.0, N randomly varied

between 10.0 and 60.0, and the number of stressing rates randomly varied between 2 and the sample

size. The parameters σ_{ov} and B were fixed at 100.0 and 10000.0/N+1 , respectively. The results

of the simulations were compared to estimates calculated using the median value technique for the

same fracture data. The conclusions reached with dynamic fatigue simulations were identical to

those obtained with the static fatigue simulations.

The fatigue parameter B_{wv} is obtained by comparing equations (204) and (205) for a 50%

probability of failure

$$B_{wV} = \frac{A_d^{N_V+1}}{(N_V + 1) \, \sigma_{oV}^{N_V-2}} \left[\frac{V_{ef}}{\ell n\left(\frac{1}{1-0.50}\right)} \right]^{1/\tilde{m}_V} \tag{211}$$

Alternatively, B_{wV} can be obtained by equating equations (156) and (157)

$$B_{wV} = \frac{t_{\theta dV}^{N_V+1} \, \dot{\sigma}^{N_V} \, V_{ef}^{1/\tilde{m}_V}}{(N_V + 1) \, \sigma_{oV}^{N_V-2}} \tag{212}$$

Information on the underlying inert strength distribution can also be obtained from the fatigue data. Using equation (207) to transform all the fatigue data to a single Weibull distribution and performing least squares or maximum likelihood analysis establishes the parameters $\tilde{m}_V(N_V+1)$ and $t_{\theta VT}$. The fast-fracture Weibull modulus is then solved as

$$m_V' = \tilde{m}_V \, (N_V-2) \tag{213}$$

where the superscript ' denotes a fast-fracture parameter estimated from fatigue data. The fast-fracture characteristic strength $\sigma_{\theta V}$ cannot be estimated from the fatigue data. CARES/LIFE calculates a characteristic strength, $\sigma_{\theta V}'$, based on extrapolation of the dynamic fatigue data to a specific time. This time is arbitrarily fixed at 1.0 second. From equation (207)

$$\sigma_{\theta V}' = \dot{\sigma} \, t_{\theta dVT}^{(N_V+1)/N_V} \tag{214}$$

Much more statistical uncertainty is associated with the determination of the Weibull modulus than with the characteristic strength for fast-fracture testing.

With the calculated quantities $\sigma_{\theta V}'$ and m_V', the fatigue data can be transformed to an equivalent inert strength distribution by equating the risk of rupture of equations (55) and (156) for the various data values

$$\sigma'_{fl_i} = \sigma'_{\theta V} \left(\frac{t_{T_i}}{t_{\theta dVT}} \right)^{\frac{N_v+1}{N_v-2}} \tag{215}$$

where σ'_{fl_i} represents the i'th transformed inert fracture strength of the specimen. Plotting the

ranked values σ'_{fl_i} (ℓn ℓn($1/1$-P_{fV}) versus ℓn σ) gives useful visual information for the analyst

(CARES/LIFE does not include a graphical interface). With $\sigma'_{\theta V}$, m'_{V}, and the various σ'_{fl_i} values,

CARES/LIFE performs the outlier test and determines the K-S and A-D goodness-of-fit statistics as

explained in the section titled **Estimation of Statistical Material Strength Parameters**. The

outlier test and goodness-of-fit statistics in this case are also valid for the transformed fatigue data

(denoted with subscript T) and the original fatigue data as well. Hence the calculated goodness-of-

fit significance levels measure the hypothesis that fatigue data was generated from the parameters

N_V, A_d, and m'_V.

Cyclic fatigue parameter evaluation

Fatigue parameter estimation for the Paris law is identical to the power law formulation for

cyclic fatigue except that cycles replaces time and the g-factor is replaced with $(1-R)^N$. It is

important to point out that the Paris law as formulated in CARES/LIFE assumes that no crack

extension occurs when loading on the crack face is compressive, hence negative R ratio loading is

equivalent to $R = 0$ loading. For this parameter estimation technique cyclic data is required at two

or more applied loading levels and the R ratio must be held constant for all the data. Rearranging

equation (158) for steady state cyclic loading at a fixed level of reliability, the specimen cycles to

failure for volume flaws is expressed as a function of the maximum static equivalent stress, σ_f, in

the specimen ($\sigma_f = \sigma_{Ieqc_{max}}$ at the highest stressed point in the component)

$$n_f = \left\{ \frac{B_{wV}\, \sigma_{oV}^{N_V - 2}}{(1 - R)^{Q_V} \left[\dfrac{V_{ef}}{\ell n \left(\dfrac{1}{1 - P_{fV}} \right)} \right]^{1/\tilde{m}_V}} \right\} \sigma_f^{-N_V} \tag{216}$$

The terms between the brackets are simplified by replacing them with a constant yielding

$$n_f = A_c\, \sigma_f^{-N_V} \tag{217}$$

Equation (217) is a convenient expression from which to fit experimental data, thus A_c and N_V can be considered as material-environmental parameters. Taking the logarithm of equation (217) yields

$$\ell n\, n_f = \ell n\, A_c - N_V\, \ell n\, \sigma_f \tag{218}$$

Median value, least squares and the median deviation technique are used to solve equation (218) as previously discussed for the power law methodology.

Assuming that the experimental data is at a sufficient number of discrete levels of applied stress, all the data cycles to failure n_{fi} are transformed to an equivalent number of cycles n_{Ti} at an equivalent single level of (maximum) stress, σ_T. Equating the failure probabilities calculated from equation (160) for data number i yields

$$n_{Ti} = n_{fi} \left(\frac{\sigma_{fi}}{\sigma_T} \right)^{N_V} \tag{219}$$

where the subscript T indicates a transformed value. In CARES/LIFE, the value of σ_T is the lowest level of applied (maximum) stress in the data set. With all the data transformed to the various values n_{Ti}, CARES/LIFE performs Weibull parameter estimation as described in the section titled **Estimation of Statistical Material Strength Parameters**, solving equation (158) for $\tilde{m}_V$ and

$n_{\theta VT}$. Substituting into equation (217) for the number of cycles corresponding to a 50% probability of failure yields

$$A_c = n_{\theta VT} \, \sigma_T^{N_v} \left[\ell n \left(\frac{1}{1-0.50} \right) \right]^{1/\bar{m}_v} = \frac{B_{wV} \, \sigma_{oV}^{N_v-2}}{(1 - R)^{Q_v}} \left[\frac{\ell n \left(\dfrac{1}{1-0.50} \right)}{V_{ef}} \right]^{1/\bar{m}_v} \tag{220}$$

where

$$n_{\theta VT} = \frac{B_{wV} \, \sigma_{oV}^{N_v-2}}{(1 - R)^{Q_v} \, \sigma_T^{N_v} \, V_{ef}^{1/\bar{m}_v}}$$

The median deviation method for estimating fatigue parameters minimizes the median deviation of the logarithm of the number of cycles. From equation (219), the fatigue data is transformed to a single stressing level for an assumed value of N_v. Using equation (158) and the previously mentioned least squares or maximum likelihood estimation methods, the Weibull parameters $\bar{m}_v$ and $n_{\theta VT}$ are obtained. With these parameters the median value, $n_{T_{0.5}}$, is calculated (i.e., the value for n_T when $P_{fV} = 0.50$). Using the transformed fatigue data as a discrete variable the median deviation is defined as

$$\text{M.D.} = \frac{1}{k} \sum_{i=1}^{k} \left| \ell n \, n_{T_i} - \ell n \left[n_{\theta VT} \left(\ell n \frac{1}{1 - 0.50} \right)^{1/\bar{m}_v} \right] \right| = \frac{1}{k} \sum_{i=1}^{k} \left| \ell n \, n_{T_i} - \ell n \, n_{T_{0.50}} \right| \tag{221}$$

for the k data points. The median deviation, M.D., is a measure of dispersion or scatter about the median. It can also be obtained for the continuous variable defined by the Weibull parameters $\tilde{m}_V$ and $n_{\theta VT}$ for ranked probabilities of failure P_{fi}.

$$M.D. = \frac{1}{k} \sum_{i=1}^{k} \left| \ell n \left[n_{\theta VT} \left(\ell n \frac{1}{1-P_{fi}} \right)^{1/\tilde{m}_V} \right] - \ell n \; n_{T_{0.5}} \right|$$

$$= \frac{1}{\tilde{m}_V} \left\{ \frac{1}{k} \sum_{i=1}^{k} \left| \ell n \left[\frac{\ell n \frac{1}{1-P_{fi}}}{\ell n \frac{1}{1-0.5}} \right] \right| \right\}$$

(222)

The value of N_V for which the M.D. is a minimum establishes the solution. The scatter of the distribution is measured with the Weibull modulus $\tilde{m}_V$ since for a fixed value of k the expression inside the brackets of equation (222) is a constant. CARES/LIFE minimizes equation (222) by maximizing $\tilde{m}_V$ versus N_V. This process is iterative, covering an appropriate range of values of N_V.

After a solution for N_V is obtained, equation (220) is used to calculate A_c.

The fatigue parameter B_{wV} is obtained by comparing equations (216) and (217) for a 50% probability of failure

$$B_{wV} = \frac{A_c (1 - R)^{Q_V}}{\sigma_{oV}^{N_V-2}} \left[\frac{V_{ef}}{\ell n \left(\frac{1}{1-0.50} \right)} \right]^{1/\tilde{m}_V}$$

(223)

Alternatively, B_{wV} can be obtained by equating equations (158) and (160).

$$B_{wV} = \frac{n_{\theta V} (1 - R)^{Q_V} \sigma_f^{N_V} V_{ef}^{1/\tilde{m}_V}}{\sigma_{oV}^{N_V-2}} \qquad (224)$$

Information on the underlying inert strength distribution can also be obtained from the fatigue data. Using equation (219) to transform all the fatigue data to a single Weibull distribution and performing least squares or maximum likelihood analysis establishes the parameters $\tilde{m}_V$ and $n_{\theta VT}$.

The fast-fracture Weibull modulus is then solved as

$$m_V' = \tilde{m}_V (N_V-2) \qquad (225)$$

where the superscript ' denotes a fast-fracture parameter estimated from fatigue data. The fast-fracture characteristic strength $\sigma_{\theta V}$ cannot be estimated from the fatigue data. CARES/LIFE calculates a characteristic strength, $\sigma'_{\theta V}$, based on extrapolation of the fatigue data to a specific number of cycles. This number is arbitrarily fixed at $1/(N+1)$ cycles.

$$\sigma'_{\theta V} = \sigma_T [n_{\theta VT} (N_V + 1)]^{1/N_V} \qquad (226)$$

Much more statistical uncertainty is associated with the determination of the Weibull modulus than with the characteristic strength for fast-fracture testing.

With the calculated quantities $\sigma'_{\theta V}$ and m'_V, the fatigue data can be transformed to an equivalent inert strength distribution by equating the risk of rupture of equations (55) and (158) for the various data values

$$\sigma'_{fI_i} = \sigma'_{\theta V} \left(\frac{n_{T_i}}{n_{\theta VT}} \right)^{\frac{1}{N_V-2}} \qquad (227)$$

where σ'_{fl_i} represents the i'th transformed inert fracture strength of the specimen. Plotting the

ranked values σ'_{fl_i} ($\ell n\ \ell n(1/1-P_{fv})$ versus $\ell n\ \sigma$) gives useful visual information for the analyst

(CARES/LIFE does not include a graphical interface). With $\sigma'_{\theta v}$, m'_v , and the various σ'_{fl_i} values,

CARES/LIFE performs the outlier test and determines the K-S and A-D goodness-of-fit statistics as

explained in the section titled **Estimation of Statistical Material Strength Parameters**. The

outlier test and goodness-of-fit statistics in this case are also valid for the transformed fatigue data

(denoted with subscript T) and the original fatigue data as well. Hence the calculated goodness-of-

fit significance levels measure the hypothesis that fatigue data was generated from the parameters

N_v, A_c, and m'_v.

Proof Testing Effect on Component Service Probability of Failure

Prior to placing a component in service, confidence that it will perform reliably is usually demonstrated through proof testing. Another method, nondestructive evaluation (NDE), is used to remove components with discernable but unacceptable flaw sizes (Wiederhorn, and Fuller, 1985). Applied NDE is still in its early stages of development and at present not widely accepted because detection of small flaws, which can cause catastrophic failure, is uncertain.

Ideally, the boundary conditions applied to a component under proof testing simulate those conditions the component would be subjected to in service and the proof test loads are appropriately greater in magnitude over a fixed time interval t_p. After proof testing, the survived component is placed in service with greater confidence in its integrity and a predictable minimum service life, t_{min}, with reliability equal to one.

The objective of the following analysis is to predict the attenuated probability of failure of a component in service after proof testing and the minimum life expectancy of the proof tested component. This concept will then be extended to predict the component reliability for off-axis proof testing (misaligned and dissimilar multiaxial loads). All derivations in this section are for static fatigue and volume flaws. If the proof test and service stress distributions are cyclic, the g-factor approach is required to transform the stresses to their equivalent static stresses. Analogous relationships may be developed for the surface flaw solution.

The attenuated probability of failure, P_{faV}, of a component surviving proof testing for time t_p and subjected to an in service equivalent static stress distribution $\sigma_{Ieq}(\Psi)$ over a time interval $(t_q\text{-}t_p)$ is (Weibull, 1939)

$$P_{faV}(t_q) = \frac{P_{fiV}(t_q) - P_{fpV}(t_p)}{1 - P_{fpV}(t_p)} \tag{228}$$

The term $P_{fpV}(t_p)$ is the probability of failure of a survived component subjected to a proof test static equivalent stress distribution, $\sigma_{Ieqp}(\Psi)$, over a time interval denoted by t_p. The term $P_{fiV}(t_q)$ is the probability of failure of a survived component subjected to a proof test static equivalent stress distribution $\sigma_{Ieqp}(\Psi)$ over time interval t_p and an in service static equivalent stress distribution $\sigma_{Ieq}(\Psi)$ over time interval $(t_q - t_p)$. The reliability of the survived component increases as the ratio of the proof test stress to the service stress increases.

For the Batdorf model, the probability of failure of a given component over time interval t_p is

$$P_{fpV}(t_p) = 1 - \exp\left[-\frac{2\,k_{BV}}{\pi}\int_V\int_0^{\pi/2}\int_0^{\pi/2}\left[\sigma_{Ieqp,0}(\Psi)\right]^{m_V}\sin\alpha\ d\alpha\ \ d\beta\ dV\right] \qquad (229)$$

where, from equation (97), the transformed proof test stress distribution over time interval t_p is

$$\sigma_{Ieqp,0}(\Psi) = \left[\frac{\sigma_{Ieqp}^{N_V}(\Psi)\ t_p}{B_{BV}} + \sigma_{Ieqp}^{N_V-2}(\Psi)\right]^{1/(N_V-2)}$$

For the PIA model

$$P_{fpV}(t_p) = 1 - \exp\left[-k_{wV}\int_V (\sigma_{Ip1,0}^{m_V} + \sigma_{Ip2,0}^{m_V} + \sigma_{Ip3,0}^{m_V})\ dV\right] \qquad (230)$$

where

$$\sigma_{Ipi,0}(\Psi) = \left[\frac{\sigma_{pi}^{N_V}(x,y,z)\ t_p}{B_{wV}} + \sigma_{pi}^{N_V-2}(x,y,z)\right]^{1/(N_V-2)}$$

for i=1,2,3. $\sigma_{p1}(x,y,z)$, $\sigma_{p2}(x,y,z)$, and $\sigma_{p3}(x,y,z)$ are the proof test principal tensile stress distributions.

Alternately, the probability of failure based on the Weibull normal stress averaging method is

$$P_{fpv}(t_p) = 1 - \exp\left(-k_{wpV} \int_V \bar{\sigma}_{Ipn}^{m_V}(x,y,z) \ dV\right) \qquad (231)$$

where

$$\bar{\sigma}_{Ipn}^{m_V}(x,y,z) = \frac{\int_A \sigma_{Ipn,0}^{m_V}(\Psi) \ dA}{\int_A dA}$$

and

$$\sigma_{Ipn,0}(\Psi) = \left(\frac{\sigma_{Ipn}^{N_V}(\Psi) \ t_p}{B_{nwV}} + \sigma_{Ipn}^{N_V-2}(\Psi)\right)^{\frac{1}{N_V-2}}$$

$\bar{\sigma}_{Ipn}(x,y,z)$ is the proof test average normal stress from the projection of $\sigma_{Ipn}(\Psi)$, the normal stress, over the surface area of a unit radius sphere (equation(11)).

The probability of failure of a given component over time interval t_q is calculated as follows for the Batdorf model

$$P_{fiv}(t_q) = 1 - \exp\left[\frac{-2 \ k_{BV}}{\pi} \int_V \int_0^{\pi/2} \int_0^{\pi/2} [\sigma_{Ieq,0}(\Psi)]^{m_V} \sin \ \alpha \ d\alpha \ d\beta \ dV\right] \qquad (232)$$

where

$$\sigma_{Ieq,0}(\Psi) = \left[\frac{\sigma_{Ieq}^{N_V}(\Psi) \ (t_q - t_p) + \sigma_{Ieqp}^{N_V}(\Psi) \ t_p}{B_{BV}} + \sigma_{Ieq}^{N_V-2}(\Psi)\right]^{1/(N_V-2)}$$

For the PIA model

$$P_{fiv}(t_q) = 1 - \exp\left[-k_{wV} \int_V (\sigma_{I1,0}^{m_V} + \sigma_{I2,0}^{m_V} + \sigma_{I3,0}^{m_V}) \ dV\right] \qquad (233)$$

where

$$\sigma_{Ii,0}(\Psi) = \left[\frac{\sigma_i^{N_V}(x,y,z)\,(t_q - t_p) + \sigma_{pi}^{N_V}(x,y,z)\,t_p}{B_{wV}} + \sigma_i^{N_V-2}(x,y,z) \right]^{1/(N_V-2)}$$

for i=1,2,3. $\sigma_1(x,y,z)$, $\sigma_2(x,y,z)$, and $\sigma_3(x,y,z)$ are the principal tensile stress distributions.

For the Weibull normal stress averaging method

$$P_{fiV}(t_q) = 1 - \exp\left[-k_{wpV} \int_V \overline{\sigma}_{In}^{m_V}(x,y,z)\,dV \right] \tag{234}$$

where

$$\overline{\sigma}_{In}^{m_V}(x,y,z) = \frac{\int_A \sigma_{In,0}^{m_V}(\Psi)\,dA}{\int_A dA}$$

and

$$\sigma_{In,0}(\Psi) = \left(\frac{\sigma_{In}^{N_V}(\Psi)(t_q - t_p) + \sigma_{Ipn}^{N_V}(\Psi)t_p}{B_{nwV}} + \sigma_{In}^{N_V-2}(\Psi) \right)^{\frac{1}{N_V-2}}$$

$\overline{\sigma}_{In}(x,y,z)$ is the in-service average normal stress from the projection of the normal stress distribution $\sigma_{In}(\Psi)$ over a unit radius sphere. After determining the values of $P_{fiV}(t_q)$ and $P_{fpV}(t_p)$, the service component attenuated probability of failure $P_{faV}(t_q)$ is computed. Depending on the magnitude of the service load and time of application, P_{fiV} can be less than P_{fpV}. For this case, the attenuated probability of failure, P_{faV}, is 0.

The minimum life expectancy of a survived component for a static equivalent stress distribution is obtained by satisfying the condition $P_{fiV}(t_q) = P_{fpV}(t_p)$. For the Batdorf model, equating equations (232) and (229) results in

$\cdot$

$$t_{min} = \frac{B_{BV}}{\sigma_{Ieq}^2(\Psi)} \left[\left(\frac{\sigma_{Ieqp}(\Psi)}{\sigma_{Ieq}(\Psi)} \right)^{N_V-2} - 1 \right]_{min} \tag{235}$$

where the subscript min denotes the smallest value of the term in equation (235) for all Ψ throughout the component. If at any location the component proof test stress level is less than the service stress level, then an assured minimum lifetime t_{min} does not exist and the component can not be guaranteed to survive for any given time during service loading. When the proof test loading is identical to the service loading, except for the magnitude of the loads, then the minimum value for equation (235) occurs at the maximum stressed point in the component. Analogous relations for t_{min} may be obtained for the PIA model and the Weibull normal stress averaging method.

Proof Testing – Off-Axis Loading

Often, the proof test loading does not exactly simulate the loading during service. In such cases the component stress distribution during testing differs from that during service, resulting in what is known as off-axis loading (misaligned and dissimilar loadings). Equation (228) is used to calculate the attenuated failure probability for an off-axis tested component. The Batdorf model or Weibull's normal stress averaging method are applied. Regions where the service stress is compressive do not enter in the computation of P_{fpV}.

As discussed in the section **Time Dependent Reliability Analysis**, for off-axis loading, the load direction and/or load boundary differs from the service load condition. Symmetry of all the finite elements is now with respect to a global coordinate system. For the Batdorf model, the probability of failure for a given component over time interval t_p is then

$$P_{fpV}(t_p) = 1 - \exp \left[\frac{-k_{BV}}{2\pi} \int_V \int_0^{2\pi} \int_0^{\frac{\pi}{2}} [\sigma_{Ieqp,0}(\Psi)]^{m_V} \sin \alpha \ d\alpha \ d\beta \ dV \right] \tag{236}$$

and the probability of failure over time interval t_q is

$$P_{fiV}(t_q) = 1 - \exp\left[-\frac{k_{BV}}{2\pi} \int_V \int_0^{2\pi} \int_0^{\frac{\pi}{2}} [\sigma_{Ieq,0}(\Psi)]^{m_V} \sin\alpha \; d\alpha \; d\beta \; dV \right] \tag{237}$$

where $\sigma_{Ieqp,0}(\Psi)$ and $\sigma_{Ieq,0}(\Psi)$ are the previously defined transformed stress distributions.

Substituting equations (236) and (237) into equation (228) and simplifying yields the expression for the attenuated failure probability

$$P_{faV}(t_q) = 1 - \exp\left[-\frac{k_{BV}}{2\pi} \int_V \int_0^{2\pi} \int_0^{\frac{\pi}{2}} \left[\sigma_{Ieq,0}^{m_V}(\Psi) - \sigma_{Ieqp,0}^{m_V}(\Psi) \right] H(\Psi) \sin\alpha \; d\alpha \; d\beta \; dV \right] \tag{238}$$

where

$$H(\Psi) = 1 \qquad t_{min}(\Psi) < t_q - t_p$$

$$H(\Psi) = 0 \qquad t_{min}(\Psi) \geq t_q - t_p$$

$$H(\Psi) = 1 \qquad \sigma_{Ieq}(\Psi) \geq \sigma_{Ieqp}(\Psi)$$

The Heaviside function is introduced to account for t_{min}, which is now evaluated locally at Ψ.

Users' Guide

This section is a guide to the execution of CARES/LIFE and the preparation of all data files necessary in the reliability analysis. This includes the files associated with the finite element interface, the user input file for the parameter estimation module, and the user input file for the reliability analysis module. Examples of each type of file are presented followed by an explanation of how the variables in the files are designated and/or manipulated. Initially, the finite element interfaces and how they process information are discussed. This information is stored in a neutral data base which is subsequently accessed by the reliability analysis module (and the user if the need arises). As noted later, the user must coordinate the size of the neutral data base and the blank common array before attempting to execute a reliability analysis for a component. The steps required to execute the parameter estimation module are presented along with examples of the input and output files associated with this module. Lastly, the results of a component reliability analysis are stored in an output file, and the format of this output file along with the details regarding how the user manipulates the format are discussed.

Each user is given access to the entire CARES/LIFE source code (interface modules, reliability analysis module, parameter estimation module) so the user can make changes in the code locally. Since all of the modules contained in the CARES/LIFE algorithm are programmed in standard FORTRAN77, the user must have access to a FORTRAN compiler. The algorithm has been programmed in a general fashion, and system specific FORTRAN statements have been avoided.

Finite Element Interface Module

Three interface programs have been developed to process MSC/NASTRAN, ANSYS, and ABAQUS output files. It is left to the user to ensure that the appropriate flags are included in the finite element input file (e.g., bulk data deck) so that all data pertinent to a reliability analysis is included in the finite element output file. The pertinent information is specified in a series of papers

(^Powers.., Edwards.., and Pintz) where the individual interfaces are discussed. Details given in this section apply to the NASCARES interface program. The preparation of the NASTRAN BULK DATA file is described in **MSC/NASTRAN Finite Element Analysis.**

Certain information must appear in the finite element output file for the execution of the interface. The information includes: the temperatures, stresses, and the volume/area of each finite element. The user must ensure that this information is included in the finite element output file. If this information is not provided in the output file, the execution of the interface program terminates.

Before execution of the interface program (given the default name NASCARES.FOR, the user must initially compile and link the interface program on the host system. In addition, the user must compile and link the program each time changes are made to the source code. The most common changes to the source code involve the size of the blank common. The following error

```
"INSUFFICIENT MEMORY ALLOCATION"
"TOTAL MEMORY ALLOCATED"
"MEMORY NEEDED"
```

will be generated if the blank common is not large enough to accommodate the data for the analysis. If this occurs the value of MTOT in the PARAMETER statement must be increased so that it is greater than the memory needed. Another instance where modification of the source code may be necessary, is the assignment the finite element output and the neutral data base file to the proper logical units. These are identified in the source code as LUA = 7 for the finite element output, and LUB = 8 for the neutral data base file. These files are assigned through the use of an "OPEN" statement within the source code. Initially, the file names are assigned interactively. The user is prompted for the filenames when the program is executed. Another option is to delete (or comment out) those lines of code which query the user for the filename and insert the appropriate file names into the OPEN statements. This requires editing the source code and placing the name of the

MSC/NASTRAN output file in the "OPEN" statement assigned to LUA. The "OPEN" statements reside at the beginning of the interface source code, and appear as follows:

```
OPEN(UNIT=LUA,FILE='NASTRAN.OUT',STATUS='OLD')
OPEN(UNIT=LUB,FILE='CARES.NEU',STATUS='NEW')
```

The user replaces "NASTRAN.OUT" with the name of the MSC/NASTRAN output file as it appears in the present working directory. Also, the default name given to the neutral data base file is CARES.NEU. The name of this file can be modified at the discretion of the user. However, throughout this manual the default name is used in reference to the neutral data base. The reader is directed to Section **CARES.NEU File** for a detailed description of the neutral data base file.

CARES.NEU File

The neutral data base (CARES.NEU) is the output file created by either of the finite element interfaces, and it contains several groups of format specific lines (or cards). Note that the user can insert comments at the beginning of the neutral data base in order to document a specific component analysis. Comment lines must begin with the letters COM in the first three spaces of the line. This approach in documenting a specific reliability analysis will not jeopardize the file structure of the neutral data base, and thus halt the execution of a reliability analysis.

An example of the different fields as they appear in CARES.NEU file is provided below. An explanation of the terms associated with each field follows the example. The data fields are identified by the variable names as they appear in the source code of the reliability analysis program (CARES/LIFE).

The following is a brief description of each parameter and data field in the CARES.NEU file.

TITLE CARD - used to identify the CARES.NEU file by providing a short description of the model.

TITLE
Ex. 5: Rotating Annular Disk

FORTRAN format: A80

TITLE - The default title card generated by the interface module identifies the finite element model by obtaining the title from the output. Thus the user must edit the CARES.NEU file after the data base has been created and tailor the title card to a specific component if more detail is required. The default title is also used as the title for postprocessing.

CONTROL CARD - input the parameters for the analysis.

NUMEL	NUMELB	
5	0	

FORTRAN format: 2I5

NUMEL - The number of element groups. All element types: volume, surface, and axisymmetric are included.

NUMELB - Flag for shell element groups with volume processing. If volume processing is performed, the stress in the shell element is assumed to be constant through the thickness.
        0 - No volume processing of shell element groups.
        1 - volume processing of shell element groups.

ELEMENT GROUP CARD - contains three parameters that specify element group information.

INUEG	IEGTYP	IGREL	ISHELL	
1	8	40	0	

FORTRAN format: 4I5

INUEG - identification index of the element group.

IEGTYP - an integer that specifies the element type. This integer is intended to facilitate the visualization of the CARES/LIFE results. The user has the option to assign values which are appropriate for a given application. For the current versions of NASCARES and ABACARES, the element type corresponds to PDA/PATRAN's shape parameter. These values are:
      3 - TRIANGULAR
      4 - QUADRILATERAL
      5 - TETRAHEDRON
      6 - PYRAMID
      7 - PENTAHEDRON (WEDGE)
      8 - HEXAHEDRON (BRICK)

IGREL - an integer that specifies the number of elements within the element group.

ISHELL - Shell element flag.
      0 - volume element group. For subsequent reading of the neutral file on the subelement level, the six components of stress will be anticipated for each integration point.
      1 - surface element group. For subsequent reading of the neutral file on the subelement level, the three in-plane stress components will be anticipated for each integration point.

An Element Group Card appears for each element group. Note that within the element group, the data is categorized at two levels which corresponds to the information contained on the ELEMENT CARD and the SUBELEMENT CARD.

ELEMENT CARD - contains information that identifies each element and includes

IELNUM	ISUBEL	MATINP	MAT2	ELVOL	ELTEMP	ELTHIC
1	27	300	0	0.5000	25.0	0.0

FORTRAN format: 4I5,3E15.6

IELNUM - the element identification integer

ISUBEL - the number of subelements within each element. The number of subelements in each element depends on the Gaussian integration order and the element type.

MATINP - the material identification number for volume processing of this element. This value must match the material identification number (MATID) which is defined in the material control input section of the templet file.

MAT2 - the material identification number for surface processing of this element. This value must match the material identification number (MATID) which is defined in the material control input section of the templet file.

ELVOL - element volume for volume elements or element area for surface elements.

ELTEMP - average element temperature or the temperature at the center of the element.
ELTHIC - element thickness, set equal to zero for volume elements.

SUBELEMENT CARD - contains information that define the subelements of the finite element model. The subelement card has two forms: one for volume elements and the other for surface elements.

VOLUME ELEMENT

ISUNUM	SUBVOL	SUBTEM	SSTR(1)	SSTR(2)	SSTR(3)
1	0.1072	25.0	σ_{xx}	σ_{yy}	σ_{zz}

	SSTR(4)	SSTR(5)	SSTR(6)
	σ_{xy}	σ_{yz}	σ_{zx}

FORTRAN format: I5,5E15.6,/,35X,3E15.6

ISUNUM - the subelement identification integer

SUBVOL - the subelement volume

SUBTEM - the subelement temperature

SSTR(1) - σ_{xx}, the stress component in the x direction

SSTR(2) - σ_{yy}, the stress component in the y direction

SSTR(3) - σ_{zz}, the stress component in the z direction

SSTR(4) - σ_{xy}, the shear stress component in the xy-plane

SSTR(5) - σ_{yz}, the shear stress component in the yz-plane

SSTR(6) - σ_{zx}, the shear stress component in the zx-plane

SURFACE ELEMENT

ISUNUM	SUBVOL	SUBTEM	SSTR(1)	SSTR(2)	SSTR(3)
1	0.03858	25.0	σ_{xx}	σ_{yy}	σ_{xy}

FORTRAN format: I5,5E15.6

    ISUNUM - the subelement identification integer

    SUBVOL - the subelement area

    SUBTEM - the subelement temperature

    SSTR(1) - σ_{xx}, the stress component in the x direction

    SSTR(2) - σ_{yy}, the stress component in the y direction

    SSTR(3) - σ_{xy}, the shear stress component in the xy-plane

Parameter Estimation Module C4PEST

Prior to execution of the parameter estimation module, the user must assign the input and output files to the correct logical units which are specified in the FORTRAN source code. Three files are necessary for parameter estimation: the input, the output, and the file created by C4PEST for subsequent input to C4LIFE. These are identified in the source code as LUA, LUB, and LUF, respectively. These files are assigned through the use of an "OPEN" statement within the source code. Initially, the file names are assigned interactively. The user is prompted for the filenames when the program is executed. Another option is to delete (or comment out) those lines of code which query the user for the filename and insert the appropriate file names into the OPEN statements. This requires editing the source code and placing the name of the file into the appropriate "OPEN" statement. The "OPEN" statements reside at the beginning of the source code, and appear as follows:

```
OPEN(UNIT=LUA,FILE='C4PEST.INP',STATUS='OLD',FORM='FORMATTED')
OPEN(UNIT=LUB,FILE='C4PEST.OUT',STATUS='UNKNOWN')
OPEN(UNIT=LUF,FILE='C4LIFE.INP',STATUS='UNKNOWN')
```

Note that the user replaces "C4PEST.INP", "C4PEST.OUT", and "C4LIFE.INP" with the names of the files as they appear in the present working directory. Throughout this manual the default names are used to reference the files.

C4PEST.INP File

The parameter estimation module requires an input file that contains the failure data, failure mode (i.e., failure caused by volume or surface defects), type of specimen, and the requested estimation method. The data must be entered in the fixed format specified in the **INPUT INFORMATION** section. The following are examples of the necessary data for time-dependent

analyses. Examples for the following are included: Fast-Fracture, Static Fatigue, Cyclic Fatigue, Cyclic Fatigue: Constant R-Ratio, and Effective Volume and Area Computation.

C4PEST.OUT File

The output file for the parameter estimation module is given the default name C4PEST.OUT. Information contained in this file includes a summary of the parameter estimation procedure, the values of the goodness-of-fit statistics for each estimation method, and the Weibull parameters for the different temperature levels.

Templet File Keywords for
Weibull Parameter Estimation With Module C4PEST

Fast-Fracture

Master Control Input:

```
NE      = 0 or 3
NMATS   = []
NMATV   = []
NGP     = --
TIME    = 0 0
INTERP  = --
```

Temperature Independent Material Control Input:

```
MATID  = []
ID1    = []   (ID1 = 4 or 5 is recommended.  If specimen effective volume or area is input then ID1 = 4)
ID4    = []
ID2    = []
ID3    = []
IKBAT  = 1
PR     = --
C      = --
MLORLE = --
OUTLIE = --
```

If parameters are to be obtained from flexure bar specimens (ID1 = 2 or 5)
```
DH    = []
DW    = []
DL1   = []
DL2   = []
```

Temperature Dependent Material Control Input; **The Data Table:**

```
DTABLE.

TEMP   = []
VAGAGE = []   (Used only if ID1 = 1 or 4)
FAST   = []
```

Keywords that are specific to the C4LIFE module are not listed here. The C4PEST module will ignore keywords that are only used with the C4LIFE module. These keywords should also be included in the C4PEST INP file if component reliability analysis will be subsequently performed with the C4LIFE module.

Templet File Keywords for
Fatigue Parameter Estimation With Module C4PEST

Static Fatigue

(Input file C4PEST INP keyword settings)
Key: [] user must specify;   -- default value or user input

Master Control Input:

```
NE      = 0 or 3
NMATS   = []
NMATV   = []
NGP     = --
TIME    = Positive non-zero number   (Seconds)
INTERP  = --
```

Temperature Independent Material Control Input:

```
MATID  = []
IDl    = []   (IDl = 4 or 5 is recommended   If specimen effective volume or area is input then IDl = 4)
ID4    = []
ID2    = []
ID3    = []
IKBAT  = 1
PR     = --
C      = --
MLORLE = --
OUTLIE = --
```

If parameters are to be obtained from flexure bar specimens (IDl = 2 or 5)
```
DH     = []
DW     = []
DL1    = []
DL2    = []
```

Temperature Dependent Material Control Input; The Data Table:

DTABLE:

```
TEMP   = []
SOL    = --
VAGAGE = []   (Used only if IDl = 1 or 4)
VAGTIM = []   (Used only if IDl = 1 or 4)
              (The values input for the VAGTIM and VAGAGE keywords are identical if the specimen is a
              tensile specimen)
RANGE  = Search for solution between [] and [] (Used only if SOL = 2)
STAT   = []   (Static fatigue specimen rupture data)
FAST   = --   (Optional fast-fracture specimen rupture data;  Weibull parameters obtained from this data will
              override Weibull parameters estimated strictly from the fatigue data)
```

Keywords that are specific to the C4LIFE module are not listed here The C4PEST module will ignore keywords that are only used with the C4LIFE module. These keywords should also be included in the C4PEST.INP file if component reliability analysis will be subsequently performed with the C4LIFE module.

Templet File Keywords for
Fatigue Parameter Estimation With Module C4PEST

Dynamic Fatigue

Master Control Input:

```
NE      = 0 or 3
NMATS   = []
NMATV   = []
NGP     = --
TIME    = Positive non-zero number   (Seconds)
INTERP  = --
```

Temperature Independent Material Control Input:

```
MATID  = []
ID1    = []   (ID1 = 4 or 5 is recommended   If specimen effective volume or area is input then ID1 = 4)
ID4    = []
ID2    = []
ID3    = []
IKBAT  = 1
PR     = --
C      = --
MLORLE = --
OUTLIE = --
```

If parameters are to be obtained from flexure bar specimens (ID1 = 2 or 5) .
```
DH    = []
DW    = []
DL1   = []
DL2   = []
```

Temperature Dependent Material Control Input; **The Data Table:**

```
DTABLE

TEMP   = []
SOL    = --
VAGAGE = []   (Used only if ID1 = 1 or 4)
VAGTIM = []   (Used only if ID1 = 1 or 4)
              (The values input for the VAGTIM and VAGAGE keywords are identical if the specimen is a
              tensile specimen)
RANGE  = Search for solution between [] and [] (Used only if SOL = 2)
DYNA   = []   (Dynamic fatigue specimen rupture data)
FAST   = --   (Optional fast-fracture specimen rupture data,  Weibull parameters obtained from this data will
              override Weibull parameters estimated strictly from the fatigue data)
```

Keywords that are specific to the C4LIFE module are not listed here The C4PEST module will ignore keywords that are only used with the C4LIFE module. These keywords should also be included in the C4PEST.INP file if component reliability analysis will be subsequently performed with the C4LIFE module

Templet File Keywords for
Fatigue Parameter Estimation With Module C4PEST
Cyclic Fatigue; R-Ratio is Constant Throughout the Specimen

(Input file C4PEST INP keyword settings)
Key: [] user must specify;   -- default value or user input

Master Control Input:

```
NE     = 0 or 3
NMATS  = []
NMATV  = []
NGP    = --
TIME   = Positive non-zero number   (Seconds or cycles)
INTERP = --
```

Temperature Independent Material Control Input:

```
MATID  = []
ID1    = []   (ID1 = 4 or 5 is recommended.  If specimen effective volume or area is input then ID1 = 4)
ID4    = []
ID2    = []
ID3    = []
IKBAT  = 1
PR     = --
C      = --
MLORLE = --
OUTLIE = --
```

If parameters are to be obtained from flexure bar specimens (ID1 = 2 or 5)
```
DH   = []
DW   = []
DL1  = []
DL2  = []
```

Temperature Dependent Material Control Input; **The Data Table:**

```
DTABLE
```

```
TEMP   = []
SOL    = --
CYCLIC = []   (Power law IWAVE = 1 to 5 ; RCYC = [] ; PERIOD = [] , QCYC = [])
              (Paris law: IWAVE = 0 ; RCYC = [] ; PERIOD = [] , QCYC = 0 0 or blank entry)
              (Walker law: IWAVE = 0 ; RCYC = [] ; PERIOD = [] ; QCYC > 0 0)
VAGAGE = []   (Used only if ID1 = 1 or 4)
VAGTIM = []   (Used only if ID1 = 1 or 4)
              (The values input for the VAGTIM and VAGAGE keywords are identical if the specimen is a
              tensile specimen)
RANGE  = Search for solution between [] and [] (Used only if SOL = 2)
CYCL   = []   (Cyclic fatigue specimen rupture data)
              (Power law: Peak cyclic stress and time to failure in seconds)
              (Paris law and Walker law  Peak cyclic stress and cycles to failure)
FAST   = --   (Optional fast-fracture specimen rupture data, Weibull parameters obtained from this data will
              override Weibull parameters estimated strictly from the fatigue data)
```

Keywords that are specific to the C4LIFE module are not listed here The C4PEST module will ignore keywords that are only used with the C4LIFE module These keywords should also be included in the C4PEST.INP file if component reliability analysis will be subsequently performed with the C4LIFE module.

Templet File Keywords for
Component Reliability Analysis With Module C4LIFE

Effective Volume and Area Computation
of the Finite Element Model

(Input file CARES.INP keyword settings)
Key. [] user must specify; -- default value or user input

One neutral file is required (CARES NEU)

Master Control Input:

```
NE      = 3
IPRINC  = 1
NMATS   = []
NMATV   = []
NGP     = --
NS      = []
IPROOF  = 0
FACTOR  = --
TIME    = 0.0
TIMEPT  = 0 0
```

Temperature Independent Material Control Input:

```
MATID  = []
ID1    = 3
ID4    = []
ID2    = []
ID3    = []
IKBAT  = 1
PR     = --
C      = --

CYCLIC
        IWAVE   = 1
        RCYC    = 1.0
        PERIOD  = 1 0
        QCYC    = 1 0

PFCONV  =       []  (Probability of failure for corresponding load, 0.000001 < PFCONV < 0 999999 )
```

Temperature Dependent Material Control Input:

```
TDEG  = []  (Only one temperature level should be input)
PARAM = []  (the Weibull modulus can be obtained from analysis of specimen data using the C4PEST
            module. The characteristic strength and scale parameter are arbitrary but reasonable
            input values)
```

The calculated effective volume or area is input into the C4PEST module using the VAGAGE or VAGTIM keywords of the Data Table

Reliability Analysis Module C4LIFE

Two data files are required to conduct a reliability analysis of a structural component. They are the user input file and the neutral data base. The CARES.NEU contains the information obtained from the finite element output file and is discussed in the **CARES.NEU** section. The CARES.INP file contains user specified data and is partitioned into three groups, master control input, material control input, and temperature dependent data. The master control input contains a set of control indices which direct the overall program execution. The material control input specifies the material identification parameters. The temperature dependent data segment of the CARES.INP file contains data sets with temperature dependent Weibull parameters. The structure of the CARES.INP file is discussed in the **INPUT INFORMATION** section.

As was indicated previously, the user must coordinate the size of the neutral data base and the blank common array used in the reliability module. The user adapts the amount of memory allocated to the blank common array to the size of the problem and the restrictions of the host computer. The default size of the one dimensional blank common array (identified as MTOT in the source code) is 1,000,000 data entries. The size is specified on the PARAMETER card which is located at the beginning of the source code for the reliability analysis module. This card appears as follows:

PARAMETER (MTOT=100000,NPLV=15)

Note that the amount of the blank common array utilized is displayed in the CARES.OUT file. Thus the user can optimize the value of MTOT.

In addition, the user must assign input and output files utilized by the reliability analysis module through the use of the "OPEN" command. Three files (CARES.INP, CARES.NEU and CARES.OUT) must be assigned to logical units. Initially, the file names are assigned interactively.

The user is prompted for the filenames when the program is executed. Another option is to delete (or comment out) those lines of code which query the user for the filename and insert the appropriate file names into the OPEN statements. This requires editing the source code and placing the names of the files into the "OPEN" statements. Changing the file name requires editing the source code and changing the following statements

```
OPEN(LUA,FILE='C4LIFE.INP',STATUS='OLD',FORM='FORMATTED')
OPEN(LUB,FILE='C4LIFE.OUT',STATUS='UNKNOWN',FORM='FORMATTED')
OPEN(LUC,FILE='CARES.NEU',STATUS='OLD',FORM='FORMATTED')
```

An optional second neutral file may be used to specify a proof test load or as the other extreme load case in a cyclic fatigue problem. This file has the default name "PROOF.NEU" and is defined in the "OPEN" statement

```
OPEN(LUG,FILE='PROOF.NEU',STATUS='OLD',FORM='FORMATTED')
```

If the user requests a PATRAN output file, an "OPEN" statement is provided in the source code for this purpose. The "OPEN" statement is executed if IPOST=1 is specified in the CARES.INP file. This statement appears near the end of the main routine in the reliability analysis module as follows

```
OPEN(LUF,FILE='CARES.PAT',STATUS='UNKNOWN',RECORDTYPE='FIXED',
     FORM='FORMATTED',RECL=80)
```

Note that the default name is CARES.PAT. In addition, the entry "RECL=80" stipulates that the record length (i.e., line format) in the CARES.PAT file is 80 characters in length instead of 132 characters (the standard format for the C4LIFE.OUT file).

.

C4LIFE.INP File

The reliability evaluation module requires an input file that contains the failure data, failure mode (i.e., failure caused by volume or surface defects), type of specimen, and the requested estimation method. The data must be entered in the fixed format specified in the **INPUT INFORMATION** section. This file is also generated by the parameter estimation module. The following are examples of the necessary data for time-dependent analyses. Examples for the following are included: Fast-Fracture, Static Fatigue, Proof Test, Cyclic Fatigue: Constant R-Ratio, and Cyclic Fatigue: R-Ratio varies throughout the component..

C4LIFE.OUT File

The reliability module output file is assigned the default name of CARES.OUT. Information contained in this file include job statistics, component reliability, element group reliabilities, and element reliabilities. The information is presented in this sequential order.

Templet File Keywords for
Component Reliability Analysis With Module C4LIFE

Fast-Fracture

One neutral file is required (CARES.NEU)

Master Control Input:

```
NE      = 3
IPRINC  = 1
NMATS   = []
NMATV   = []
NGP     = --
NS      = []
IPROOF  = 0
FACTOR  = --
TIME    = 0 0
TIMEPT  = 0 0
```

Temperature Independent Material Control Input:

```
MATID   = []
ID1     = 3
ID4     = []
ID2     = []
ID3     = []
IKBAT   = 1
PR      = --
C       = --

CYCLIC.
        IWAVE   = 1
        RCYC    = 1 0
        PERIOD  = 1.0
        QCYC    = 1 0

PFCONV  =       0 0
```

Temperature Dependent Material Control Input:

```
TDEG    = []
PARAM   = []
```

Templet File Keywords for
Component Reliability Analysis With Module C4LIFE

Static Fatigue Load

(Input file CARES.INP keyword settings)
Key: [] user must specify,   -- default value or user input

One neutral file is required (CARES.NEU)

Master Control Input:

```
NE     = 3
IPRINC = 1
NMATS  = []
NMATV  = []
NGP    = --
NS     = []
IPROOF = 0
FACTOR = --
TIME   = []   (Seconds)
TIMEPT = 0 0
```

Temperature Independent Material Control Input:

```
MATID = []
ID1   = 3
ID4   = []
ID2   = []
ID3   = []
IKBAT = 1
PR    = --
C     = --

CYCLIC:
        IWAVE  = 1
        RCYC   = 1 0
        PERIOD = 1 0
        QCYC   = 1 0

PFCONV =     0 0
```

Temperature Dependent Material Control Input:

```
TDEG   = []
PARAM  = []
TPARAM = []
```

Templet File Keywords for
Component Reliability Analysis With Module C4LIFE

Proof Test Load

(Input file CARES.INP keyword settings)
Key   [] user must specify;   -- default value or user must specify

---

Two neutral files are required.   1) CARES NEU - service load,   2) PROOF.NEU - proof test load

---

Master Control Input:

```
NE      = 3
IPRINC  = 2
NMATS   = []
NMATV   = []
NGP     = --
NS      = []
IPROOF  = 1
FACTOR  = 1.0
TIME    = []   (Service load duration in seconds)
TIMEPT  = []   (Proof test load duration in seconds)
```

Temperature Independent Material Control Input:

```
MATID   = []
ID1     = 3
ID4     = []
ID2     = []
ID3     = []
IKBAT   = 1
PR      = --
C       = --

CYCLIC
        IWAVE    = 1
        RCYC     = 10
        PERIOD   = 10
        QCYC     = 10

PFCONV   ≈    00
```

Temperature Dependent Material Control Input:

```
TDEG    = []
PARAM   = []
TPARAM  = []
```

Templet File Keywords for
Component Reliability Analysis With Module C4LIFE

Cyclic Load; R-Ratio is Constant Throughout the Component

(Input file CARES INP keyword settings)

Key: [] user must specify; -- default value or user input

One neutral file is required (CARES NEU) containing peak cyclic stresses

Master Control Input:

```
NE      = 3
IPRINC  = 1
NMATS   = []
NMATV   = []
NGP     = --
NS      = []
IPROOF  = 0
FACTOR  = --
TIME    = []  (Power law seconds)
              (Paris law and Walker law cycles)
TIMEPT  = 0.0
```

Temperature Independent Material Control Input:

```
MATID  = []
ID1    = 3
ID4    = []
ID2    = []
ID3    = []
IKBAT  = 1
PR     = --
C      = --

CYCLIC
       IWAVE   = (Power law  1 < IWAVE < 6)
                 (Paris law and Walker law  IWAVE = 0)
       RCYC    = []
       PERIOD  = [] (Seconds)
       QCYC    = []

PFCONV   =    0.0
```

Temperature Dependent Material Control Input:

```
TDEG   = []
PARAM  = []
TPARAM = []  (For the Walker law to be invoked the value of Q must be specified  A blank or zero
             entry defaults to the power law or Paris law)
```

Templet File Keywords for
Component Reliability Analysis With Module C4LIFE

Cyclic Load; R-Ratio Varies Throughout the Component

(Input file CARES INP keyword settings)
Key. [] user must specify; -- default value or user input

Two neutral files are required. 1) CARES NEU - containing maximum cyclic stresses, 2) PROOF.NEU - containing minimum cyclic stresses

---

Master Control Input:

```
NE      = 3
IPRINC  = 2
NMATS   = []
NMATV   = []
NGP     = --
NS      = []
IPROOF  = 1
FACTOR  = 1.0
TIME    = []   (Power law. seconds)
                (Paris law and Walker law  cycles)
TIMEPT  = TIME  (The values input for the TIMEPT and TIME keywords must be identical)
```

Temperature Independent Material Control Input:

```
MATID   = []
ID1     = 3
ID4     = []
ID2     = []
ID3     = []
IKBAT   = 1
PR      = --
C       = --

CYCLIC:
        IWAVE   = (Power law  1 < IWAVE < 6)
                  (Paris law and Walker law: IWAVE = 0)
        RCYC    = 1.0   (This input is ignored when two neutral files are used)
        PERIOD  = [] (Seconds)
        QCYC    = []

PFCONV   =     0.0
```

Temperature Dependent Material Control Input:

```
TDEG    = []
PARAM   = []
TPARAM  = []   (For the Walker law to be invoked the value of Q must be specified.  A blank or
                zero entry defaults to the power law or Paris law)
```

Summary

To summarize, the following abbreviated checklist is provided so that the user can quickly identify difficulties when executing the modules contained in the CARES/LIFE algorithm.

Interface Module:

Assure the parameter MTOT is large enough to process the neutral data base.

Assure all proper information is contained in the finite element output file.

Assign the finite element output file to the correct logical unit.

Assure the source code has been compiled and linked free of errors after all changes have been made to the interface module source code.

Parameter Estimation Module:

Assign C4PEST.INP and C4PEST.OUT to the proper logical units in the parameter estimation source code.

Assure that the failure data appears in the correct format in the C4PEST.INP file.

Assure the source code has been compiled and linked free of errors after all changes have been made to the parameter estimation module source code.

Reliability Module:

Assure the parameter MTOT is large enough to process the neutral data base.

Assign CARES.NEU and CARES.INP to the correct logical units.

Check the C4LIFE.INP file such that the data corresponds to values contained in the CARES.NEU file.

Assure the source code has been compiled and linked free of errors after all changes have been made to the reliability analysis module source code.

Example Problems
Fast-Fracture Example Problems

Example 1 - Statistical Material Parameter Estimation

To validate the methods used to estimate statistical material parameters from fast-fracture data, we compared results from the fracture of four-point bend bars broken at NASA Lewis and analyzed by the CARES/LIFE parameter estimation module C4PEST with results independently obtained by Bruckner-Foit and Munz (Bruckner-Foit, and Munz, 1988) for the International Energy Agency (IEA) Annex II, Subtask 4 (Tennery, 1987). The IEA Annex II agreement is focused on cooperative research and development among the United States, West Germany, and Sweden in the areas of structural ceramics. Subtask 4 of the agreement addresses mechanical property measurement methods with initial research concentrating solely on four-point flexure testing. Three different materials were analyzed, namely a hot isostatic pressed (HIPped) silicon carbide (SiC) from Elektroschmelzwerke Kempten (ESK), West Germany, a HIPped silicon nitride (Si_3N_4) from ASEA CERAMA, Sweden; and a sintered silicon nitride from GTE WESGO, USA, although only results from the ESK and ASEA materials are discussed herein.

In November 1986, 400 HIPped SiC flexure bars from West Germany were distributed by Oak Ridge National Laboratory (ORNL) (Oakridge, Tennessee) to the five participating U.S. laboratories, including NASA Lewis. The bars were fractured at these laboratories and the fracture stress data sets were returned to ORNL as complete data without censoring for different failure modes. Shortly thereafter, 400 Si_3N_4 bars from Sweden were also received by ORNL and subsequently distributed to the same U.S. laboratories for fracture testing. Again, the fracture stress data sets were returned to ORNL as complete samples. The number of specimens of a particular material given to each U.S. laboratory was 80. The specimens had cross-sectional dimensions of 3.5 mm in width and 4.5 mm in height. The specimens were tested in four-point bending with an outer

span of 40 mm and an inner span of 20 mm. The nominal loading rate was 0.5 mm/min, and the testing temperature was approximately 20 °C.

Details of the statistical analyses of these data sets are given in references by Bruckner-Foit and Munz (Bruckner-Foit, and Munz, 1988), and Tennery (Tennery, 1987). The results of the 80 silicon carbide flexure bars tested at NASA Lewis, which are shown in table E1-T1, were analyzed with the C4PEST module to calculate the maximum likelihood estimates (MLE's) of the Weibull parameters. The Weibull parameter values from CARES/LIFE, summarized in table E1-T2, match the predictions from Bruckner-Foit and Munz (Bruckner-Foit, and Munz, 1988) reasonably well. The SiC fracture data are plotted in figure E1-F1 along with the proposed Weibull line and the Kanofsky-Srinivasan 90-percent confidence bands. Since all of the data are within the 90-percent bands and the goodness-of-fit significance levels are high, it is concluded that the fracture data show good Weibull behavior.

ASEA CERAMA HIPped Si_3N_4 bars (Tennery, 1987) from Sweden were also fractured at NASA Lewis, and subsequently, the statistical material parameters were estimated with CARES/LIFE by using the maximum likelihood method. A comparison of the Si_3N_4 results with those from Bruckner-Foit and Munz (Bruckner-Foit, and Munz, 1988)is also shown in table E1-T2. Agreement between estimates from the two sources is excellent. When the 80 ASEA silicon nitride bars were analyzed by the CARES/LIFE code as a complete sample, the significance levels of 54 and 35 percent from the Kolmogorov-Smirnov and Anderson-Darling goodness-of-fit tests, respectively, were relatively low, indicating a questionable fit to the proposed Weibull distribution. The lower significance level for the Anderson-Darling test indicated greater deviation occurring in the low strength region of the distribution. From the outlier test included in the CPEST module, the highest strength fracture stress was detected to be an outlier at the 1-percent significance level. Several of the lower strengths were flagged as outliers at various significance levels (1, 5, or 10

percent). Figure E1-F2 shows a Weibull plot of the data. From the figure it appears that the data are bimodal with an outlier point at the highest strength.

Because of the observed trends, the data were re-analyzed assuming a censored distribution and removing the highest strength outlier point ($\sigma_f = 817.2$ MPa) as bad data. Although it is possible that both failure modes were surface induced, for the sake of this example it is assumed that the low-strength failures were predominantly due to volume flaws and that the high-strength specimens fractured predominantly because of surface flaws. Since results from fractography of the individual specimens to identify the various failure modes were not available, the fracture origins had to be arbitrarily assigned prior to parameter estimation. Note that identifying individual specimen flaw origins is especially important for small sample sizes where a plot of the data does not yield clear trends. However, for the NASA Lewis Si_3N_4 data, the sample size was large, and clear trends could be observed, although extra care would be required to determine if the trends were surface flaw or volume flaw based. From inspection of figure E1-F2, we decided to assign the lowest nine strengths as due to volume flaws and the remainder as due to surface flaws. An input (templet) file for the C4PEST module was prepared and is provided on diskette along with the output file from the module. The cracks were arbitrarily assumed to be Griffith cracks, and the total strain energy release rate fracture criterion was used. This assumption was used only in the calculation of k_{BS} and k_{BV}. The K-S significance level increased from 0.54 to 0.68, and the A-D significance level increased from 0.35 to 0.58. This improvement supports the initial assumption of bimodal behavior. The value of $\hat{m}$ changed from 13.4 for the complete sample to $\hat{m}_S = 22.8$ and $\hat{m}_S = 4.13$. The value of $\hat{\sigma}_\theta$ changed from 686 MPa for the complete sample to $\hat{\sigma}_{\theta S} = 692$ MPa and $\hat{\sigma}_{\theta V} = 1128$ MPa for the surface and volume flaw distributions, respectively. Further improvements in the goodness-of-fit scores may be gained by correctly identifying the failure mode of the fracture origins.

From equation (68) the normalized Batdorf crack density coefficient for volume flaws is (m_V + 1) = 4.13 + 1 = 5.13, and from equations (58) and (60) the scale parameter σ_{oV} is 17.9 MPa (m)$^{3/4.13}$. For surface flaws the normalized Batdorf crack density coefficient is 6.05, whereas σ_{oS} calculated by using equations (71) and (73) is 461.3 MPa (m)$^{2/22.8}$.

For the Si_3N_4 fracture data from NASA Lewis, we have obtained goodness-of-fit significance levels as high as 0.78 and 0.88 for the K-S and A-D tests, respectively, by assuming a particular bimodal flaw distribution. For this case, 13 volume flaws were assumed, and the MLE's were $\hat{m}_S$ = 21.0, $\hat{m}_S$ = 6.79, $\hat{\sigma}_{\theta S}$ = 693 MPa, and $\hat{\sigma}_{\theta S}$ = 876 MPa. The 13 volume flaws did not correspond to the 13 lowest fracture strengths. On the basis of these goodness-of-fit scores, it is concluded that the data show good bimodal Weibull behavior.

It should be noted from figure E1-F2 that the assumed volume flaw distribution dominates the failure response at low probabilities of failure. Therefore, in component design, it is essential to properly account for competing failure modes; otherwise nonconservative design predictions may result.

TABLE E1-T1. EXTREME FIBER FRACTURE STRESSES OF ESK HIPped SILICON CARBIDE (SiC) BARS

Flexure bar	Strength, MPa	Flexure bar	Strength, MPa
1	281.2	41	516.2
2	291.0	42	519.8
3	358.2	43	527.6
4	385.4	44	530.7
5	389.0	45	530.7
6	390.8	46	545.7
7	391.8	47	548.8
8	402.8	48	552.7
9	412.5	49	559.6
10	413.3	50	562.4
11	413.9	51	563.3
12	417.8	52	566.1
13	418.2	53	566.5
14	426.9	54	570.1
15	437.6	55	572.8
16	440.0	56	575.0
17	441.0	57	576.1
18	442.5	58	580.0
19	443.8	59	582.6
20	444.9	60	588.0
21	446.2	61	588.6
22	451.5	62	591.0
23	452.1	63	591.0
24	452.7	64	593.3
25	470.4	65	598.7
26	474.1	66	599.6
27	475.5	67	610.0
28	475.5	68	612.7
29	479.2	69	619.9
30	483.5	70	619.9
31	484.8	71	622.2
32	486.2	72	622.3
33	488.6	73	640.5
34	492.5	74	649.0
35	493.2	75	657.2
36	496.0	76	660.0
37	505.7	77	664.3
38	511.9	78	673.5
39	512.5	79	673.9
40	513.8	80	725.3

TABLE E1-T2. WEIBULL PARAMETERS, KOLMOGOROV-SMIRNOV, AND ANDERSON-DARLING TEST RESULTS FOR FOUR-POINT BEND BAR FRACTURE DATA DETERMINED BY THE MAXIMUM LIKELIHOOD METHOD

[All estimates are biased estimates; 80 complete samples per material.]

Material type	Source of data	Shape parameter, $\hat{m}$	90-percent confidence limits on $\hat{m}$		Characteristic strength $\hat{\sigma}_0$, MPa	90-percent confidence limits on $\hat{\sigma}_0$, MPa		K-S test statistic, D	K-S test significance level, α, percent	A-D test significance level, α, percent
			Upper	Lower		Upper	Lower			
SiC (ESK)	CARES	6.48	7.38	5.52	556	573	539	0.070	83	86
SiC (ESK)	Ref. 57	6.59	7.65	5.61	556	574	539	.063	(a)	(a)
Si₃N₄ (ASEA)	CARES	13.39	15.25	11.42	686	696	676	.0901	54	35
Si₃N₄ (ASEA)	Ref. 57	13.40	15.3	11.4	686	696	676	.088	(a)	(a)

[a]Not available.
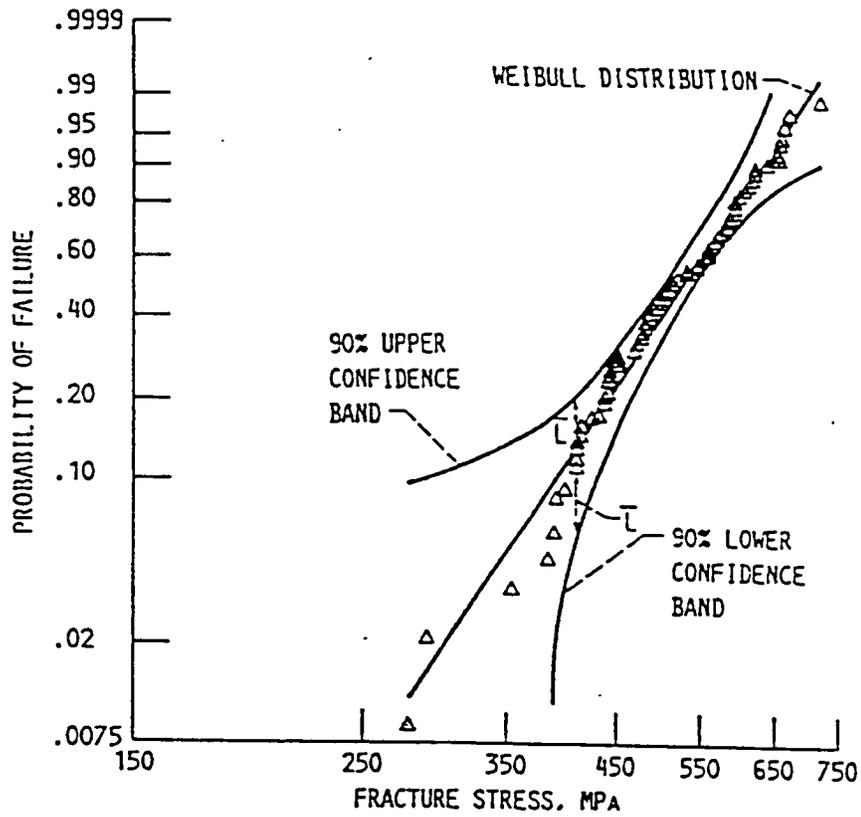
Figure E1-F1.--90-percent confidence bands about the Weibull line for ESK HIPped silicon carbide (SiC). (Fracture stress data generated at NASA Lewis; not all data points shown; $\overline{L}$=0.0829.)
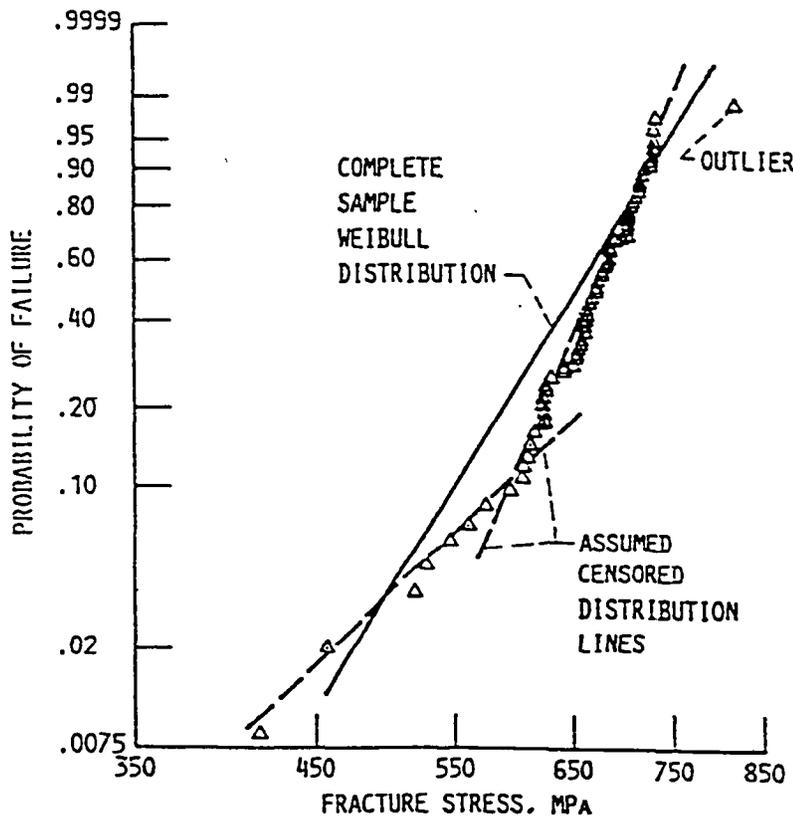
Figure E1-F2.--Complete sample, assumed censored sample Weibull distributions, and outlier in ASEA CERAMA HIPped silicon nitride (Si₃N₄). (Fracture stress data generated at NASA Lewis; not all data points shown.)

Example 2 - Internally Heated and Pressurized Tube

Jadaan, et.al. (Jadaan, 1990) (Shelleman, 1991) (Jadaan, Shelleman, Conway, Mecholsky, and Tressler, 1991) (Shelleman, Jadaan, Conway, and Mecholsky, 1991) conducted experimental and analytical studies on Reaction Bonded Silicon Carbide (SCRB210) tubular components at Penn State. Ten long tubes (660 mm long, 17.1 mm inner radius, and 21.9 mm outer radius) were rapidly pressurized to failure at 1200°C in order to evaluate their fast-fracture strength distribution. O-ring and C-ring coupon specimens (9.5 mm wide, 17.1 mm inner radius, and 21.9 mm outer radius), cut from the same lot of tubes, were fractured by diametrally compressing them to failure at temperatures ranging from room temperature to 1200°C. The resulting O-ring and C-ring strength distributions were used to calculate the Weibull parameters, m, σ_{oS}, and σ_{oV} for the SCRB210 material.

In this example, the C4LIFE module of the CARES/LIFE code was used to calculate the predicted failure probabilities for the long tubes using the Weibull parameters of the diametrically compressed O-ring and C-ring specimens (see Tables E2-T1 and E2-T2). The Weibull moduli were calculated from strength data using least-squares analysis. The C4PEST module (one of the three modules comprising the CARES/LIFE Code) was utilized to calculate the Weibull moduli and characteristic strengths. Subsequently, a scale parameter at a given temperature was calculated from m and σ_o corresponding to that temperature in association with effective area and volume expressions obtained from references 1-4. The Weibull moduli and scale parameters were then input into the C4PEST code to calculate the Batdorf coefficients. The C4PEST module was also used to specify the fracture criterion and flaw shape to be used for failure probability calculation.

The long tube components were tested in a tube burst test facility (Shelleman, Jadaan, Butt, Tressler, Hellman, and Mecholsky, 1992). This facility consisted mainly of four components: (1) pressure seals, (2) end plates, (3) water cooled end caps (152.4 mm long), and (4) containment or

test chamber. The long tube component was mounted vertically in the test chamber and supported at the ends by the water cooled end caps. The pressure seals were inserted into the open ends of the tubes. This methodology of supporting and pressure sealing the tubes allowed them to expand freely in the axial direction, thus preventing the development of axial stresses due to thermal expansion. A heating element was suspended from the upper pressure seal inside the tube and connected to a temperature controller. A thermocouple was also suspended from the upper pressure seal to measure the temperature at the inner surface of the tube. Thermocouples were also placed at the outer surface along the axial direction of the tube at six locations. Figure E2-F1 shows a typical thermal profile for a tested tube. The lower pressure seal contained an opening connected to a pressure booster. For more details regarding the design and operation of the burst test apparatus, see Shelleman, et al.

Fracture surface analysis (fractography) was performed on the reconstructed tubes after failure to determine the type of dominant flaws causing failure. Fractographic analysis is a necessary component of reliability analysis, in order to determine whether area, volume, or combined (area and volume) reliability analysis should be performed. The SCRB210 tubes were highly decorated with silicon nodules at the inner surfaces of the tubes, remnant from fabrication. These silicon nodules induced a more severe flaw population at the inner surfaces of the tubes than through the volumes or outer surfaces of the tubes. Indeed, upon fractographic examination of reconstructed tube fragments, failure was found to be dominantly induced by flaws located at the inner surfaces of the tubes. Therefore, surface area reliability analysis was used to predict the failure probabilities for the tubes.

The MSC/NASTRAN finite element program was utilized to calculate the thermomechanical stresses for the internally heated and pressurized tubes at 1200°C. Symmetry conditions allow modeling of one quarter of the tube, and thus, 4 segments were required to make up the entire

tubular component. A total of 540 solid elements (HEXA) and 270 shell elements (QUAD8) were used (figure E2-F2). The shell elements, used with surface flaw reliability analysis, were placed at the inner and outer surfaces of the tubes. The shell elements shared common nodes with the solid elements. These two-dimensional elements are used by the CARES/LIFE code only to identify external surfaces and obtain corresponding in-plane stresses and areas. The contribution of these elements to the overall stiffness of the model was negligible. The thickness of the shell elements was 1.0×10^{-6} mm and only membrane properties were assigned to these elements via the PSHELL BULK DATA card. Four layers of equally sized solid elements were used to model the bulk of the tube. Three elements were used in the circumferential direction. Note that the entire volume and surface area of the tube are stressed in tension.

The tangential stresses at the inner surface of the tube from MSC/NASTRAN finite element analysis were found to be within 5% of the closed form solution. Fifteen Gauss integration points (NGP=15) were used for the reliability analysis with CARES/LIFE. The values for Poisson's ratio and thermal coefficient of expansion were 0.16 and 4.6×10^{-6} °C^{-1}, respectively. The Young's modulus was temperature dependent with a value of 378, 326, and 304 GPa at 25, 1100, and 1200°C, respectively. A radial temperature gradient of 6°C was assumed constant along the entire length of the tube.

After completing the finite element analysis and creating the MSC/NASTRAN output file (containing the element stresses and temperatures) the NASCARES module was used to create a neutral file. This neutral file contained the subelement stresses, volumes (or surface areas for the shell elements), and temperatures. Subsequently, the C4LIFE module read the data base from the neutral file for reliability analysis. Furthermore, the C4LIFE program read the data base stored in the output file, CARES.INP, of the parameter estimation module, C4PEST. Finally, the main

reliability program, C4LIFE, performed the reliability calculations by calculating the survival probability and risk of rupture intensities for all subelements.

The manner in which the tubes were supported and pressurized is important from an analytical point of view. Because the tubes are not axially restrained, a predominantly uniaxial tensile stress state results. The tensile axial stresses are negligible compared to the tangential tensile stresses. The radial stresses are compressive, and thus do not contribute to the failure probability analysis. Since the stress state is essentially uniaxial, then all fracture criteria/flaw shapes should yield similar failure probabilities (All failure probability fracture criteria collapse to the Weibull criterion for uniaxial stress states). This expected result was used to verify the CARES/LIFE code. Table E2-T3 shows the predicted failure probability, based on various fracture criteria and flaw shapes, for a typical tube. As can be seen from table E2-T3, all fracture criteria predicted essentially equal failure probabilities as expected.

Table E2-T4 shows the experimental and predicted failure probabilities for the ten tested tubes. Experimental failure probabilities were calculated using the equation $P_f=(i-0.5)/N$ where i is the tube rank number and N is the total number of specimens. The predicted failure probabilities were calculated at the inner and outer surfaces of the tubes. Failure probabilities corresponding to failures associated with flaws located at the inner surfaces of the tubes were calculated using the O-ring specimen Weibull parameters. Failure probabilities corresponding to failures associated with flaws located at the outer surfaces of tubes were calculated using the Weibull parameters obtained from testing C-ring specimens in compression. This is because the O-ring test samples flaws located at the inner surface of the tube, while the C-ring in compression test samples flaws located at the outer surface of the tube. As stated previously, the inner surfaces of the tubes are highly decorated with silicon nodules while the outer surfaces are smooth and homogeneous. This variability of the inner surface flaw population resulted in large scatter in the strength data for the

O-ring specimens, and thus a low Weibull modulus (see Table E2-T2). The combination of low Weibull moduli and maximum stresses occurring at the inner surfaces of the tubes resulted in high calculated failure probabilities at the inner surfaces compared to those at the outer surfaces of the tubes (Table E2-T4). The combined failure probability (last column of Table E2-T4) is the overall failure probability taking into account both the inner and outer surface areas of the tubes.

Figure E2-F3 shows the experimental failure probability data for the ten tubes as a function of internal pressure at failure. Figure E2-F3 also includes the combined predicted failure probability curve for the tubes calculated using the CARES/LIFE code. As shown in figure E2-F3, the experimental failure probabilities compare very well with the predicted failure probabilities.

TABLE E2-T1. AVERAGE STRENGTHS AND WEIBULL PARAMETERS
FOR SCRB210 O-RING SPECIMENS

Temperature (°C)	Number of Specimens	Average Strength (MPa)	Characteristic Strength[+] (σ_o) (MPa)	Weibull* Modulus (m)	Area Scale* Parameter (σ_{oS}) (MPa.m$^{2/m}$)
25	26	242.9±50.4	263.6	5.3	46.5
800	20	250.6±54.8	275.2	4.5	37.4
1000	20	283.0±42.4	301.9	7.2	79.0
1200	21	300.1±44.6	320.9	6.9	79.9

+   Characteristic strength corresponds to the O-ring specimen strength value at 63.2% failure probability

*   m, σ_o, and σ_{oA} are calculated from strength data based on least square analysis.

TABLE E2-T2. AVERAGE STRENGTHS AND WEIBULL PARAMETERS FOR SCRB210 C-RING SPECIMENS TESTED IN COMPRESSION

Temperature (°C)	Number of Specimens	Average Strength (MPa)	Characteristic Strength[+] (σ_o) (MPa)	Weibull* Modulus (m)	Area Scale* Parameter (σ_{oS}) (MPa.m$^{2/m}$)
25	22	239.2±39.7	255.8	6.8	73.6
800	20	240.6±29.6	253.7	9.1	98.4
1000	26	275.9±48.9	298.4	5.7	68.6
1200	20	318.7±29.8	331.8	12.1	160.7

+   Characteristic strength corresponds to the C-ring specimen strength value at 63.2% failure probability

*   m, σ_o, and σ_{oA} are calculated from strength data based on least square analysis.
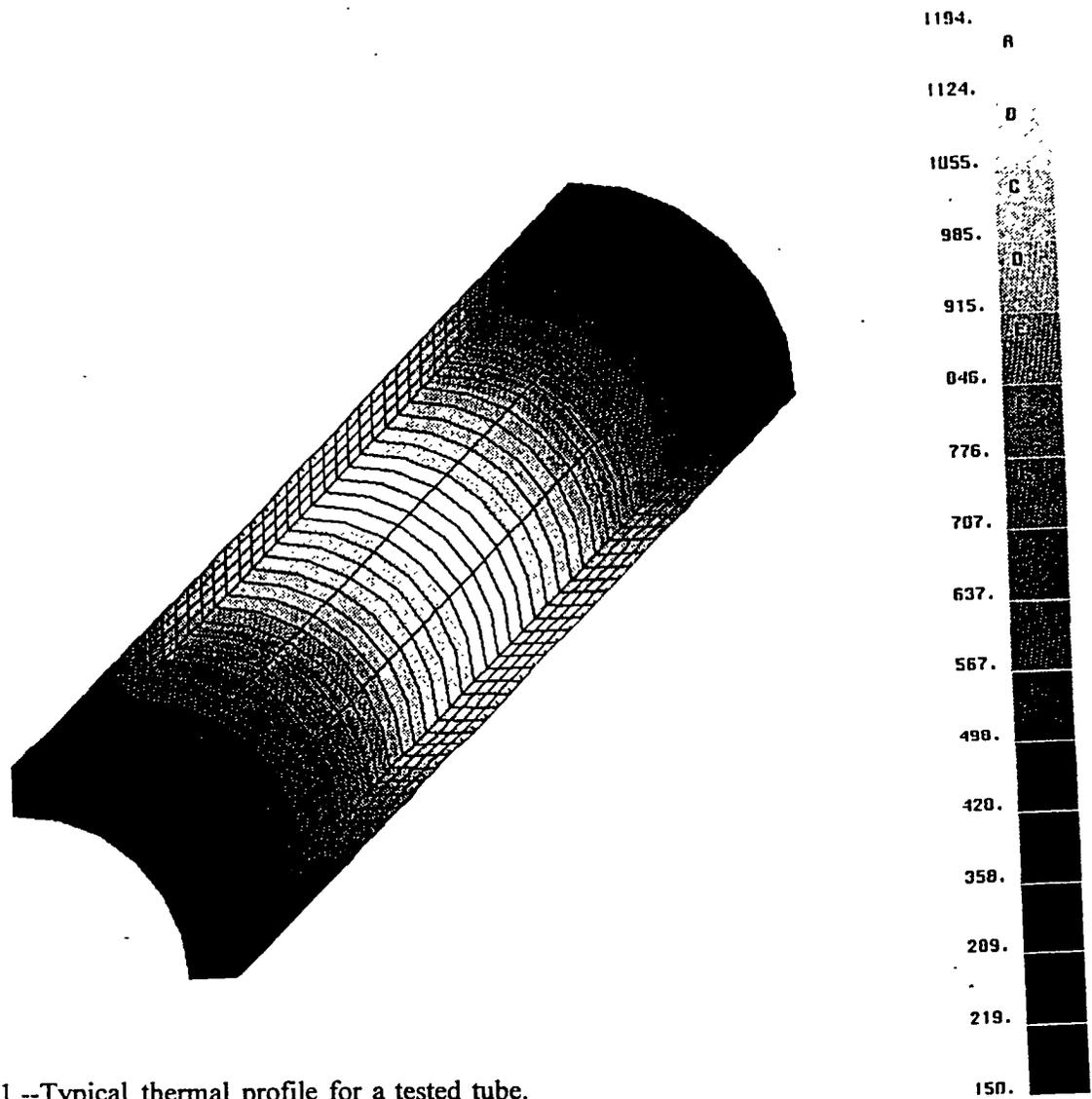
Figure E2-F1.--Typical thermal profile for a tested tube.
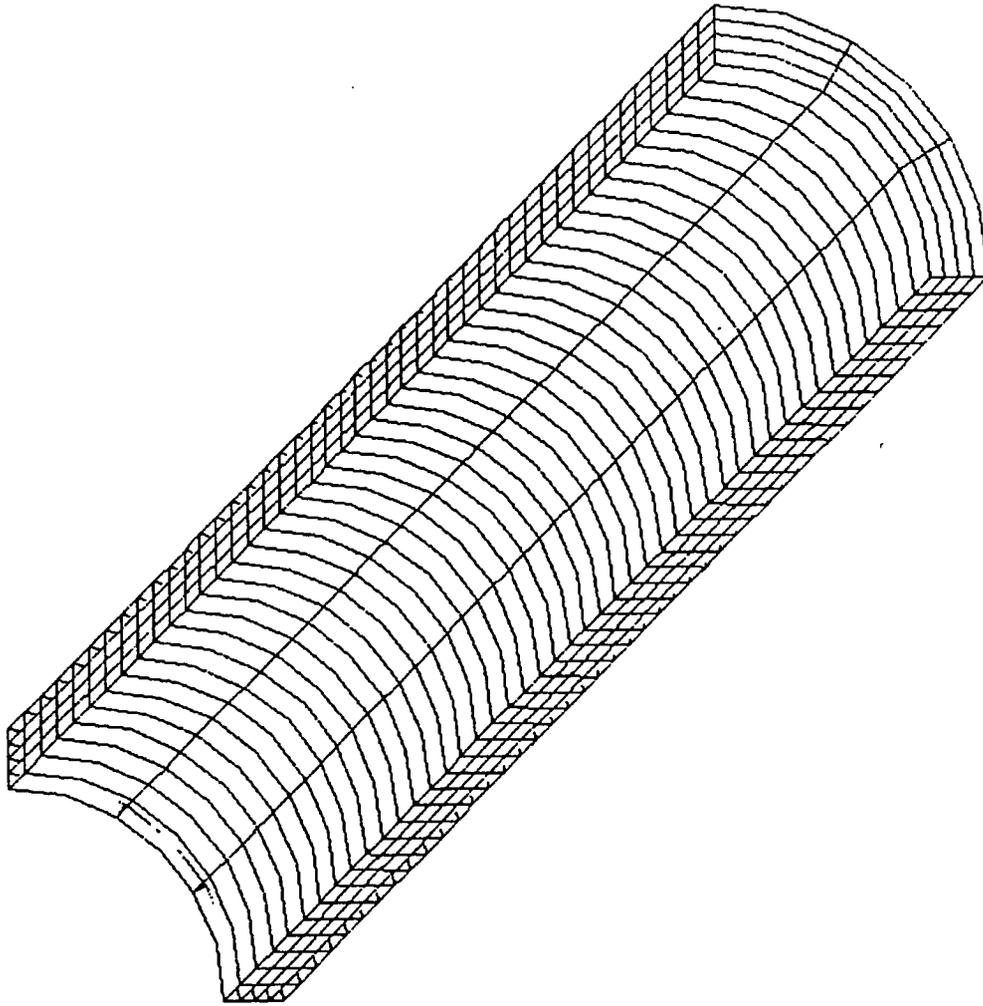
Figure E2-F2.--Tubular component with finite element mesh.

TABLE E2-T3. CARES/LIFE PREDICTED FAILURE PROBABILITIES FOR A TYPICAL
INTERNALLY HEATED AND PRESSURIZED SCRB210 TUBE CALCULATED BASED ON
VARIOUS FRACTURE CRITERIA AND FLAW SHAPES.

(pressure at failure = 19 MPa, experimental failure probability = 0.45)

Fracture Criterion and Flaw Shape	Predicted Failure Probability P_{fA}
Normal Stress Averaging Method	0.465
PIA Criterion	0.470
Energy Release Rate Criterion (Griffith Crack)	0.470
Noncoplanar Strain Energy Release Rate Criterion $\overline{C} = 0.80$ (Semi-Circular Surface Crack)	0.476

TABLE E2-T4. EXPERIMENTAL AND PREDICTED FAILURE PROBABILITIES FOR INTERNALLY HEATED AND PRESSURIZED SCRB210 TUBES

Energy release rate criterion
(Surface flaw analysis)

Rank (i)	Pressure at Failure (MPa)	Max. Stress at Failure (MPa)	Experimental Failure Probability (i-0.5)/N	CARES/LIFE Predicted Failure Probability, P_{fs}		
				Inner Surface	Outer Surface	Combined
1	13.8	53.4	0.05	0.110	0.001	0.111
2	14.5	56.1	0.15	0.140	0.001	0.141
3	17.7	70.1	0.25	0.353	0.004	0.355
4	18.6	73.9	0.35	0.429	0.005	0.437
5	19.0	75.7	0.45	0.467	0.006	0.470
6	20.7	83.0	0.55	0.621	0.010	0.624
7	23.8	96.3	0.65	0.864	0.024	0.868
8	24.0	97.0	0.75	0.876	0.026	0.880
9	24.2	98.4	0.85	0.891	0.028	0.894
10	28.9	119.3	0.95	0.996	0.090	0.996
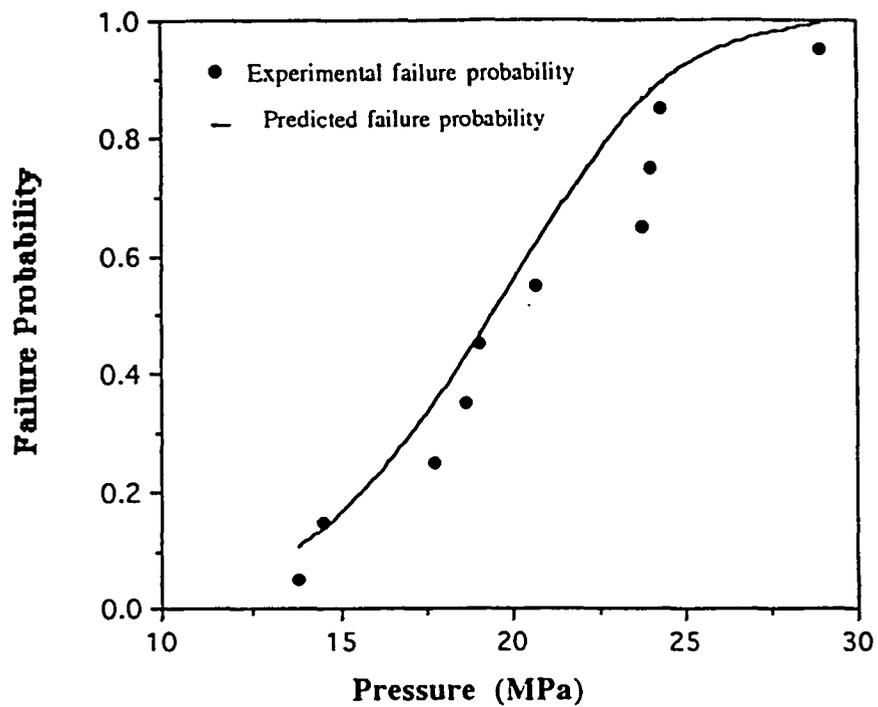
Figure E2-F3.--Experimental and predicted failure probabilities for the ten tubes as a function of internal pressure at failure.

Example Problems
Time-Dependent Example Problems

Example 3 - Fatigue Parameter Estimation

This example demonstrates the determination of Weibull and fatigue parameters from multiaxially loaded specimen rupture data. In addition, Weibull parameters evaluated using fast-fracture data will be contrasted to Weibull parameters estimated from fatigue data. Ring-on-ring loaded square plate specimens made from soda-lime glass were prepared and fractured under dynamic fatigue loading in a distilled water environment at the NASA Lewis Research Center. Ring-on-ring loading induces an equibiaxial stress state within the inner loading ring. The plate specimens measured 50 mm x 50 mm and had an average thickness, h, of 1.50 mm.

The maximum fracture stress at the specimen center was computed using the fracture load, P, and the equation given by Shetty et al. (Shetty, Rosenfield, Bansal, and Duckworth, 1980)

$$\sigma_f = \frac{3\ P}{4\ \pi\ h^2} \left[2\ (1 + v)\ \ell n\ \left[\frac{r_o}{r_i} \right] + \frac{(1 - v)\ (r_o^2 - r_i^2)}{R_s^2} \right] \tag{1}$$

where the diagonal half length, R_s, was 35.92 mm, the inner radius, r_i, was 5.02 mm, the outer radius, r_o, was 16.09 mm, and Poisson's ratio, v, was 0.25. Figure E3-F1 shows the fracture strengths of the 121 specimens loaded at the stressing rates of 0.02, 0.20, 2.00, and 20.00 MPa/s. In addition, 30 specimens were tested in fast fracture in an inert environment of silicon oil. All flaw origins resided on the specimen surface (surface flaws).

Using the CARES/LIFE parameter estimation module, the fast-fracture Weibull parameters and the fatigue parameters were determined. For the fast-fracture strengths measured in silicon oil the Weibull modulus, m_S, and characteristic strength, $\sigma_{\theta S}$, were estimated to be 2.871 and 394.2 MPa, respectively, using the maximum likelihood technique. The least-squares method

produced estimates of 2.675 and 395.3 MPa, respectively. For the fatigue data, the crack growth exponent, N_S, was determined with the median value, least-squares, and the median deviation techniques. The inert strength Weibull modulus, m'_S, and a characteristic strength, $\sigma'_{\theta S}$, were estimated from the fatigue data using equations (201) and (202), respectively. Using equation (203) the fatigue data was transformed to an equivalent inert strength distribution. The ranked data (median ranking (Pai, and Gyekenyesi, 1988)) is plotted in figure E3-F2, along with the ranked inert strengths of the fast-fracture specimens. The transformed inert strengths in the figure were determined using the parameters obtained from the median deviation analysis utilizing equation (194) and the maximum likelihood method utilizing equation (144). The solid line represents the transformed fatigue distribution with $m'_S = 2.344$ and $\sigma'_{\theta S} = 387.4$ MPa. The dashed line represents the fast fracture strengths with $m_S = 2.871$ and $\sigma_{\theta S} = 394.2$ MPa. Figure E3-F2 supports the assumption that the fatigue data and the inert strength data are generated from the same flaw population.

The specimen effective areas, A_{ef} and A_e, were evaluated numerically using equations (155) and (75), respectively, with the CARES/LIFE component reliability analysis module and a finite element model of the specimen. Because of symmetry, only one quarter of the specimen was modeled using brick and wedge elements as shown in figure E3-F3. Quadrilateral and triangular shell elements were attached to the faces of the solid elements corresponding to the specimen external surfaces. The shell elements contributed negligible stiffness to the model. For this example, the Batdorf model with the G_T (total strain energy release rate) fracture criterion and a Griffith crack was used in the numerical evaluation. The scale parameter σ_{oS} and the fatigue constant B_{BS} were calculated from equations (71) and (200), respectively. Table E3-T1 lists the

results of this analysis for the option using Weibull parameters estimated from the fatigue data.

Table E3-T2 lists the results for the option using the Weibull parameters from the fast-fracture data.

The scale parameter values in tables E3-T1 and E3-T2 show a significant variation. Because of the low value of the Weibull modulus, the small differences in the estimated values translate to large differences in the scale parameter. The characteristic strengths estimated from the fatigue data and the fast-fracture data were all within ±7.0 MPa of the value of 394.0 MPa (the fast-fracture value of $\sigma_{\theta S}$ from maximum likelihood estimation) for all methods of estimation.

Summary of the Preparation and Program Execution
Steps for the Glass Plate Example Problem

(See file contents table in **Example Guide** section for file descriptions)

• Prepare input file 3_PEST.INP for execution with module C4PEST. This file contains the dynamic fatigue data consisting of the specimen stressing rates and the failure stresses (at the center of the specimen). Optionally include the fast-fracture data of the plate specimens in the Data Table. Because the specimen geometry is not a beam in flexure or a tensile specimen, the effective area must be numerically evaluated using a finite element model of the specimen. Since the specimen effective area is unknown the 3_PEST.INP input file is prepared using the tensile specimen option (**ID1** = 4). The effective area, A_e, and the stress-normalized effective area, A_{ef}, are assigned a default value of 1.0 (see keywords **VAGAGE** and **VAGTIM** in the Data Table). For this problem the **PFCONV** keyword should also be activated in the Master control Input (see the comments regarding preparation of the finite element model, below). If the specimen geometry was a beam in flexure or a tensile specimen, then A_e and A_{ef} are automatically evaluated and the user could directly proceed with component reliability evaluation following the execution of the C4PEST module.

• Execute the C4PEST module with input file 3_PEST.INP and obtain the output file 3_PEST.OUT. Examine the 3_PEST.OUT file and obtain the Weibull modulus m and the fatigue exponent N. Calculate the modified Weibull modulus $\tilde{m}$ = Nm/(N-2). Editing the 3_PEST.INP input file, prepare another section of the Material Control Input with a new data table including the modified Weibull modulus $\tilde{m}$ (using the **PARAM** keyword). Do not include any specimen rupture data in this table. Arbitrary values are input for the Weibull scale parameter σ_o and the

characteristic strength σ_θ (input of the value of the characteristic strength of the specimen data is recommended for both of these parameters). Again assume a tensile specimen geometry (**ID1** = 4) and input 1.0 for A_e and A_{ef} (keywords **VAGAGE** and **VAGTIM** in the Data Table). The fracture criterion and crack geometry should be consistent with the other Material Control Input section previously prepared.

• Again execute the C4PEST module with the now modified input file 3_PEST.INP, obtain the output file 3_PEST.OUT and the data file 3_LIFE.INP.

• Prepare a finite element model of the specimen and loading configuration (in this case MSC/NASTRAN input file 3_NAS.INP). The magnitude of the loading is recommended to correspond to some finite probability of failure of the specimen. A good choice is to specify loading corresponding to the specimen characteristic strength σ_θ. In this case the keyword **PFCONV** in the Master Control Input of file 3_PEST.INP (or also 3_LIFE.INP) would be assigned the value $P_f = 0.63212$.

• Execute the finite element program (in this case MSC/NASTRAN) and obtain the output file (in this case file 3_NAS.OUT).

• Prepare a neutral file by executing the appropriate interface module NASCARES, ABACARES, or ANSCARES (in this case the file 3.NEU is obtained from execution of the NASCARES module).

• Execute the C4LIFE module with the input control file 3_LIFE.INP and the neutral file 3.NEU. Examine the output file 3_LIFE.OUT (obtained from executing module C4LIFE) and obtain the calculated effective area A_e associated with Weibull modulus m, and the stress

normalized effective area A_{ef} associated with the modified Weibull modulus $\tilde{m}$.

• Again, edit the file 3_PEST.INP. For the Data Table containing the specimen rupture data, input the correct values for A_e and A_{ef} using the **VAGAGE** and **VAGTIM** keywords.

• Execute the C4PEST module with input file 3_PEST.INP. The output files 3_PEST.OUT and 3_LIFE.INP now contain the correct fatigue and Weibull parameters.

• Perform component reliability analysis with module C4LIFE. Since the specimen had induced multiaxial stresses, the reliability analysis must be performed using the same fracture criterion and flaw geometry as that used to obtain the fatigue and Weibull parameters.
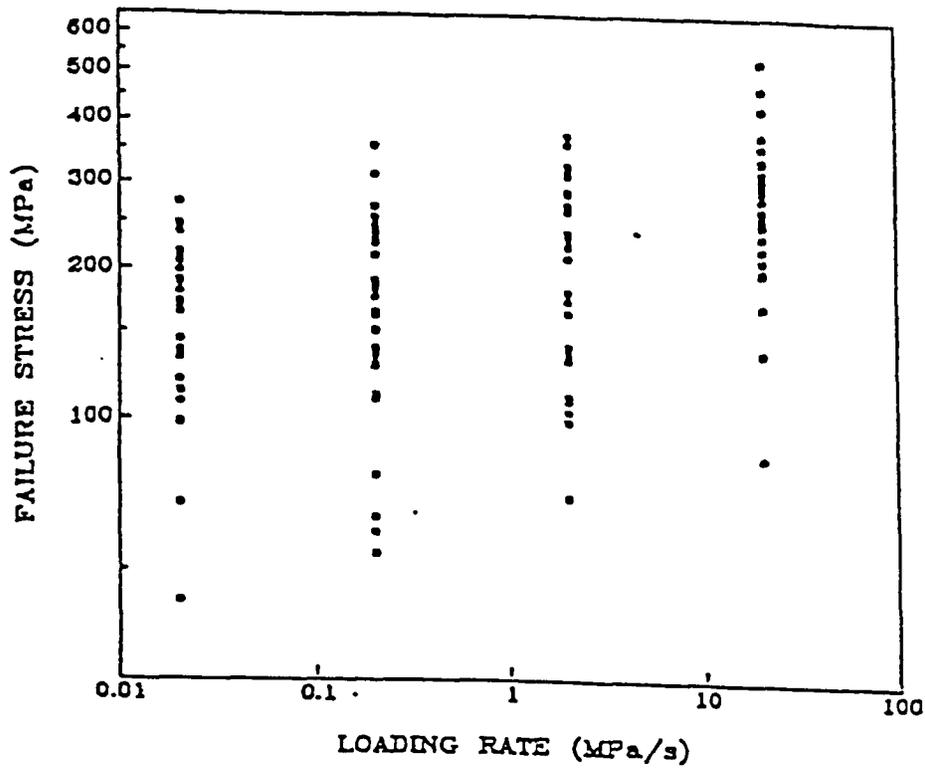
Figure E3-F1.--Dynamic fatigue fracture strengths for the ring-on-ring loaded soda-lime glass square plate specimens.
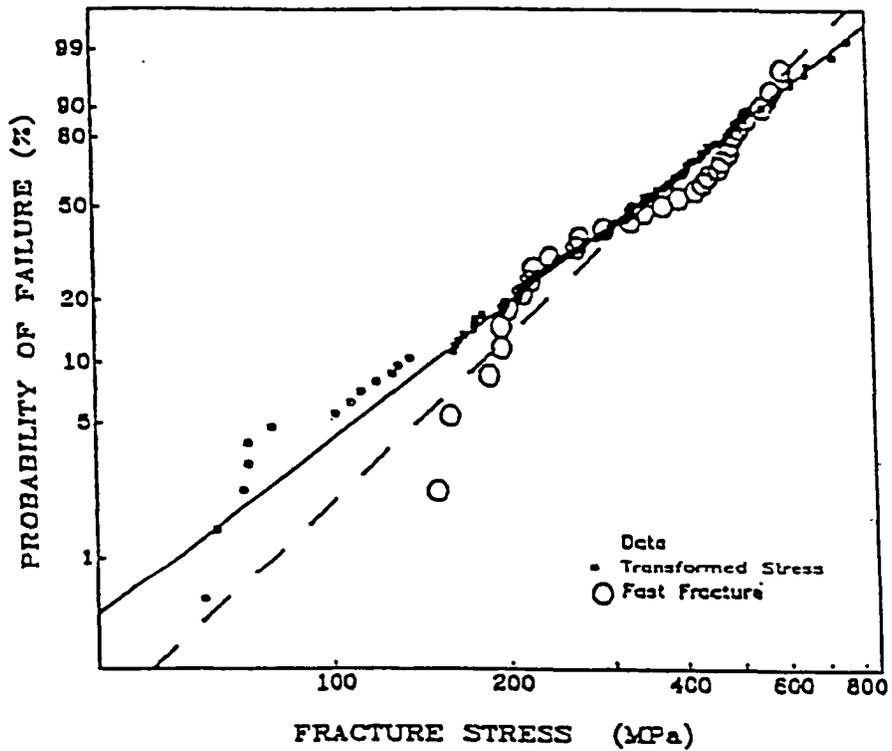
Figure E3-F2.--Soda-lime glass fatigue data transformed to an equivalent inert strength distribution versus inert strengths measured in silicon oil. The solid line and the dashed are maximum likelihood estimations of the respective distributions.
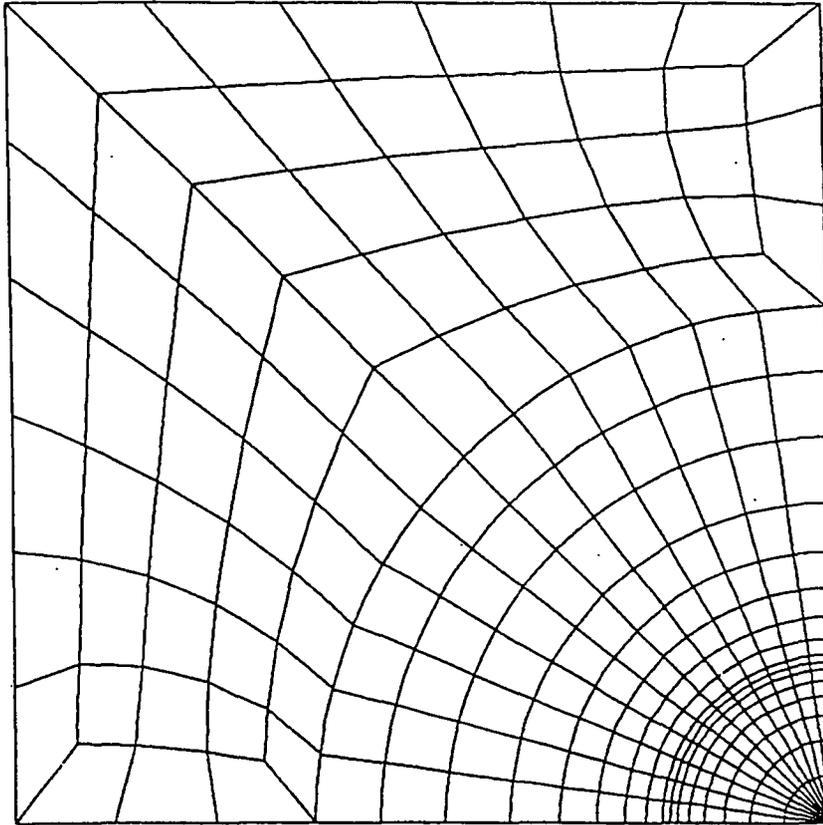
Figure E3-F3.--Finite element mesh for the ring-on-ring loaded square plate specimen. The finite element model reproduces one quarter of the total specimen geometry.

TABLE E3-T1. PARAMETERS ESTIMATED FROM FATIGUE DATA

Method	Fatigue exponent, N_S	Fatigue constant, B_{BS} $MPa^2 \cdot s$	Weibull modulus, m'_S	Scale parameter, σ'_{oS} $MPa \cdot mm^{2/m_s}$
Median Value	12.60	4 445	2.279	5 904
Least Squares	11.24	6 337	2.208	6 707
Median Deviation	11.88	5 994	2.344	5 443

TABLE E3-T2. PARAMETERS ESTIMATED FROM FATIGUE AND FAST-FRACTURE DATA

Method	Fatigue exponent, N_S	Fatigue constant, B_{BS} $MPa^2 \cdot s$	Weibull modulus, m_S	Scale parameter, σ_{oS} $MPa \cdot mm^{2/m_s}$
Median Value	12.60	3 225	2.675	3 915
Least Squares	11.24	8 527	2.675	3 915
Median Deviation	11.88	6 064	2.871	3 305

TABLE E3-T3. SODA-LIME-SILICA GLASS ESTIMATED PARAMETERS

Surface flaws (water environment)

Batdorf theory, G_t fracture criterion, Griffith crack

(Weibull parameters estimated from inert strength data measured in silicon oil environment)

Method	N_S	$\ell n\ A_d$	B_{wS}/B_{BS} MPa^2-sec	m_S	$\sigma_{\theta S}$ MPa	A_e mm^2	A_{ef} mm^2	σ_{oS} MPa-mm$^{2/m}$
Median Deviation	11.88	5.377	7935./ 6064.	2.871	394.2	448.0	421.4	3305.

m_S = Weibull modulus

A_e = effective area

A_{ef} = stress-normalized effective area

A_d = fatigue constant

$\sigma_{\theta S}$ = characteristic strength

σ_{oS} = Weibull scale parameter

B_{wS} = Weibull fatigue constant

B_{BS} = Batdorf fatigue constant

N_S = fatigue exponent

TABLE E3-T4. SODA-LIME-SILICA GLASS ESTIMATED PARAMETERS

Surface flaws (water environment)
Batdorf theory, G_t fracture criterion, Griffith crack

Method	N_s	$\ell n\ A_d$	B_{wS}/B_{BS} MPa^2-sec	m_s'	σ_{0S}' MPa	A_e mm^2	A_{ef} mm^2	σ_{oS}' MPa-mm$^{2/m}$
Median Deviation	11.88	5.377	8234./ 5994.	2.344	387.4	490.2	451.4	5443.

m_s' = Weibull modulus
A_e = effective area
A_{ef} = stress-normalized effective area

A_d' = fatigue constant
σ_{0S}' = characteristic strength
σ_{oS}' = Weibull scale parameter

B_{wS} = Weibull fatigue constant
B_{BS} = Batdorf fatigue constant
N_s = fatigue exponent

Example 4 - Cyclic Fatigue and R-ratio Sensitivity

This example demonstrates the determination of Weibull and fatigue parameters from cyclically loaded specimen rupture data. In addition, reliability predictions using the power law will be contrasted to predictions based on the Walker equation for various levels of R-ratio.

This work is based on experiments performed by Liu and Chen (Liu, and Chen, 1991) using 3-mol%-Yttria-Stabilized Zirconia (3Y-TZP). The data is sparse and is used only to demonstrate the capability of the CARES/LIFE program.

Cyclic fatigue experiments for various levels of R-ratio were performed on tensile specimens. Five specimens each were tested at R-ratio values of 0.8, 0.5, and 0.0, while six specimens were tested at an R-ratio value of -1.0. A triangular cyclic stress wave form was used, at a frequency of 1 Hz, for 10^5 cycles or until failure occurred. The tensile specimens had a 16.0 mm gauge length and a 6.0 mm gauge diameter. Fractographic examination showed that failure most frequently occurred at or near the surface and the failure origins were pore type flaws.

Fast-fracture testing was performed using 4-point bending specimens. A total of 11 specimens are used in this analysis with an inner load span of 4.0 mm, an outer load span of 13.6 mm, an average width of 2.577 mm, and an average height of 1.384 mm. Specimens that significantly deviated from these dimensions were not included in this analysis. Fractography of the 4-point bending specimens indicated that failure occurred from surface or near surface flaws.

The analysis performed with the CARES/LIFE code assumed that failure was due to surface flaws. Using the CARES/LIFE parameter estimation module the fast-fracture Weibull parameters and the fatigue parameters were determined. The maximum likelihood estimates (MLE's) of the Weibull parameters from the 4-point bend specimens were Weibull modulus m = 14.02, characteristic strength $\sigma_{\theta S}$ = 901.6 MPa, and scale parameter σ_{oS} = 1079.0 Mpa $\cdot$ mm$^{0.1427}$. These values were used in the subsequent calculations for the fatigue parameter B_{wS}. The fatigue

parameters were estimated using the median deviation technique and they are shown in Table E4-T1 for the various R-ratio levels and crack growth laws. The g-factor for the power law formulation with the sawtooth waveform and a positive R-ratio is

$$g = \frac{1 - R^{N+1}}{(1 - R)(N + 1)} \tag{1}$$

while for a negative R-ratio

$$g = \frac{1}{(1 - R)(N + 1)} \tag{2}$$

For the Walker crack growth law, Liu and Chen (Liu, and Chen, 1991) determined that a value of Q = 2.0 for the R-ratio sensitivity exponent was a best fit to the experimental data. Since the CARES/LIFE code does not estimate the value of Q from experimental data, the value of 2.0 for Q was used for this analysis.

Specimens that did not fail (runout data) were not considered in the parameter estimation analysis, although an exception was made for the one specimen at R = 0.0. This runout data was included because another specimen did rupture at this corresponding level of applied stress. From the analysis of Liu and Chen (Liu, and Chen, 1991) the fatigue exponent for all the data was estimated to be N = 21.0. From Table E4-T1, the average value of the fatigue exponent is N = 20.0.

For this example problem the fatigue parameters estimated for R = 0.8 are used to predict the median (P_{fs} = 0.5) cycles to failure versus the range of the applied stresses, $\Delta\sigma$, for the tensile specimen geometry. These predictions are shown in Figs. E4-F1 and E4-F2 for the power law and the Walker formulation, respectively, for the various R-ratios corresponding to the experimental data. The results were obtained using a finite element model of the gauge area of the tensile

specimen and performing the subsequent reliability analysis for various peak stresses and R-ratios. The finite element model consisted of a single shell element loaded in uniform tension and with an area equal to the specimen gauge area. The reliability analysis used the noncoplanar strain energy release rate criterion with a Griffith crack, although for the uniaxial stress state all the failure criteria in CARES/LIFE are normalized to yield an identical failure probability.

In Fig. E4-F1 the power law is used with the sawtooth loading waveform to predict the effect of changing the R-ratio. Since the fatigue parameters for R = 0.8 are used in the reliability analysis, the median line prediction for R = 0.8 shown in the figure is in good agreement with the rupture data, as expected. However, as the R-ratio becomes smaller the deviation from the data tends to increase. This trend is not apparent for R = 0.5, but it is apparent for the 0.0 and -1.0 values of R-ratio. In this case the deviation from the data progresses in a non conservative manner (material strength is over predicted). These results for the 0.0 and -1.0 R-ratios seem to indicate that some cyclic degradation is present.

In Fig. E4-F2 the Walker formulation with Q = 2.0 is used to predict the effect of changing the R-ratio. The fatigue parameters for R = 0.8 are used and there is good agree-ment between the median line prediction for this R-ratio and the fatigue data. Good correlation to the data is also achieved for the 0.0 and -1.0 values of the R-ratio. Some discrepancy is noted for the R = 0.5 specimen data, however, the deviation is on the conservative side (material strength is under predicted). The results from Fig. E4-F2 reasonably correlate with those of Liu and Chen (Liu, and Chen, 1991) and support their conclusion that cyclic fatigue degradation has occurred. Figure E4-F2 also shows the results using the Paris law. In this case the predictions for all the R-ratios occur on the same line (The R = 0.8 median line).

The experimental data apparently showed increased fatigue degradation due to the presence of compressive stresses (negative R-ratio). The traditional fracture mechanics approach assumes that

the presence of compressive stress does not enhance crack growth. This is assumed true for the power law formulation shown in Fig. E4-F1. With the Walker formulation this assumption means that the median line for $R = -1.0$ would superimpose on the $R = 0.0$ median line. However to achieve correlation to the experimental data, the line shown in Fig. E4-F2 for $R = -1.0$ is calculated on the basis that there is further material degradation when compressive stress is present. The current version of the CARES/LIFE code is constructed so that no additional material strength degradation is predicted if compressive cyclic stresses are present (negative R-ratios), unless the direct R-ratio input option is used. In that case the code issues an appropriate warning message. If cyclic fatigue reliability analysis is being performed using the option of simultaneously processing two finite element results files, then if a negative R-ratio is encountered at a particular element the code automatically resets the value to zero.

TABLE E4-T1. PARAMETERS ESTIMATED FROM CYCLIC FATIGUE DATA OF ZIRCONIA

R-Ratio	Fatigue exponent, N_S	Power law constant, B_{wS}, $MPa^2 \cdot s$	Walker eq. constant, B_{wS}, $MPa^2 \cdot cycle$	Paris law constant, B_{wS}, $MPa^2 \cdot cycle$
0.8	19.88	$5.995 \ (10)^5$	$1.011 \ (10)^5$	$3.225 \ (10)^{-8}$
0.5	19.20	$1.892 \ (10)^6$	$4.776 \ (10)^6$	$3.174 \ (10)^1$
0.0	15.13	$2.532 \ (10)^5$	$4.083 \ (10)^6$	$4.083 \ (10)^6$
-1.0	25.79	$6.829 \ (10)^1$	$1.464 \ (10)^4$	$2.131 \ (10)^{11}$
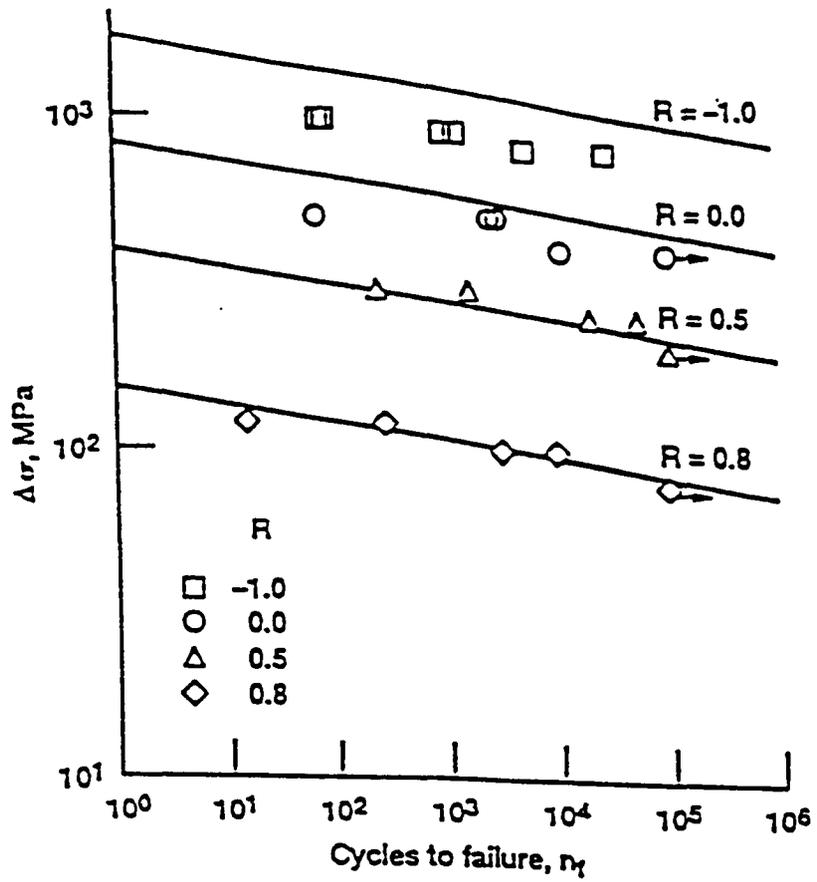
Figure E4-F1.--Stress amplitude-failure cycle (S-N) curve of 3Y-TZP. Median lines are extrapolated from R = 0.8 data using the power law.
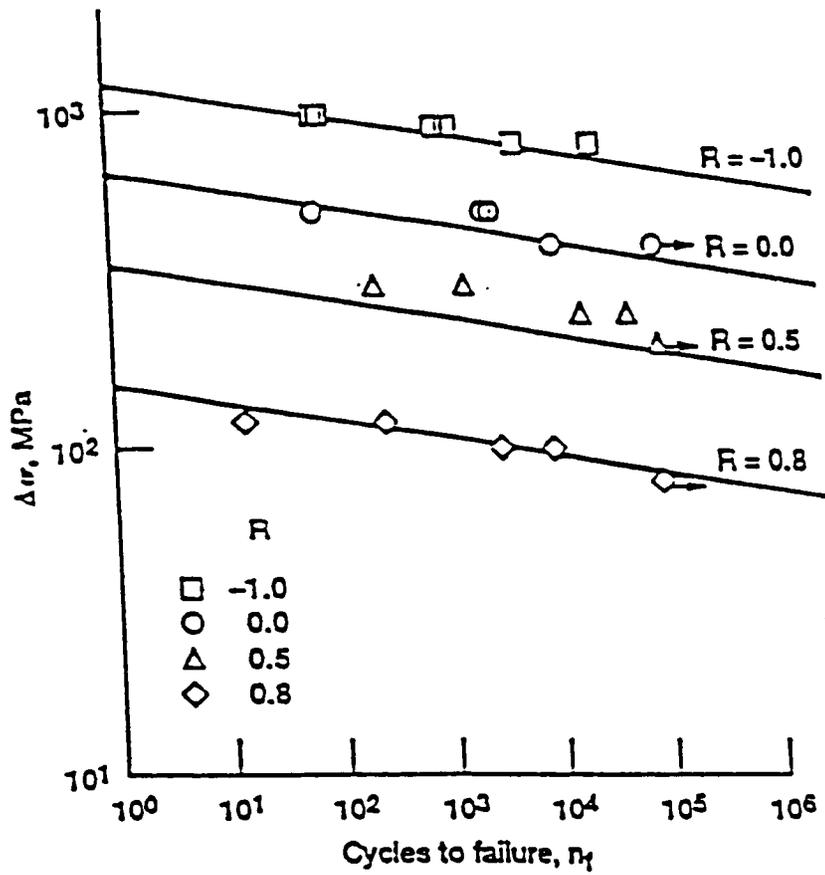
Figure E4-F2.--Stress amplitude-failure cycle (S-N) curve of 3Y-TZP. Median lines are extrapolated from R = 0.8 data using the Walker equation.

Example 5 - Isothermal Rotating Annular Disk

This example illustrates the use of the CARES/LIFE program modules for the time-dependent reliability analysis of a silicon nitride (NC-132) annular disk rotating at various constant and cyclic angular speeds. The module C4LIFE is used to compute the probability of failure of the annular disk rotating at constant speeds for both fast fracture (t=0) and time-dependent (static fatigue) analyses. The problem is then repeated to determine the time-dependent probability of failure for the annular disk rotating at various sinusoidal cyclic angular speeds. Results are presented for various fracture criteria and crack geometries using the PIA and Batdorf models for both volume flaw and surface flaw analyses.

The disk inside diameter was 0.0127 m, the outside diameter was 0.08255 m, and the disk was 0.0038 m thick (fig. E5-F1). Analysis was performed on the annular rotating disk at a uniform 1000°C temperature. The material/environmental fatigue parameters, N=30 and B=320 MPa^2 hr, necessary for time-dependent reliability analysis were estimated using NC-132 data at 1000°C (^Quinn, and Quinn, 1983). The same fatigue parameters were used for both volume flaw and surface flaw analyses. Weibull material parameters independently evaluated at room temperature from four-point bend tests of 85 specimens were assumed to be valid for the 1000°C analysis. For the given "A-size" bar geometry (w = 0.00635 m, h = 0.003175 m, L$_1$ = 0.01905 m, and L$_2$ = 0.009525 m), the Weibull modulus, m$_V$, was 7.65 and the characteristic strength, $\sigma_{\theta V}$, was 808 MPa (^Swank, and Williams, 1981). For volume flaws, equations (56) and (60) are used to calculate the Weibull scale parameter, σ_{oV} = 74.79 MPa (m)$^{3/7.65}$. Assuming that fractures in the four-point bend specimens were caused by surface flaws, the Weibull modulus, m$_S$, was 7.65, the characteristic strength, $\sigma_{\theta S}$, was 808 MPa, and the surface scale parameter, σ_{oS}, calculated from equations (69) and (73), was 232.0 MPa (m)$^{2/7.65}$. Other required material properties include a Young's modulus of 289 GPa, a Poisson's ratio of 0.219, and a material mass density of 3.25x10^3 kg/m^3.

Seven disks were tested in fast fracture and the experimental disk Weibull modulus obtained was 4.95. This value differed considerably from the 7.65 value (^Swank, and Williams, 1981) based on four-point bend specimen data. A better agreement between disk and four-point bend specimen Weibull slopes would lead to improved predictions in failure probabilities for the entire range. Estimation of parameters from small sample sets greatly increases potential deviation from the true population parameters. Confidence limits are used to measure the intrinsic uncertainties in parameter estimates from finite sample sizes. The 90-percent confidence limits on m can be obtained from Thoman, et al. (^Thoman, Bain, and Antle, 1969) For the 85 four-point bend specimens, with m_v = 7.65, the calculated limits are 6.56 and 8.68. Similarly, for the seven fractured disks and the estimated m_v of 4.95, the 90-percent confidence limits are 2.27 and 6.98. Excluding potential experimental errors, it is possible that the rotating disks and the four-point bend specimens broke because of the same flaw population since their 90-percent confidence limits overlap between 6.56 and 6.98. Therefore, it cannot be concluded with absolute certainty that the disks broke from a different flaw population than the four-point bend bars unless further testing is performed. The apparent differences between prediction and experiment are not significant enough to cause rejection of the hypothesis that the bars and disks broke because of the same flaw population.

MSC/NASTRAN finite element models of the annular disk were created for several constant rotational speeds between 60 000 rpm and 120 000 rpm. For volume flaw analysis, the MSC/NASTRAN finite element model of the disk consisted of brick elements and used the structured solution sequence 114, static cyclic symmetry analysis. Because of symmetry, only eight HEXA elements were used in one 15° sector of the model (fig. E5-F1). Each element spanned both the thickness and circumferential directions. For surface flaw analysis, the same MSC/NASTRAN finite element analysis was performed as for volume flaws with the addition of QUAD8 shell elements to identify external surfaces of the model. The shell elements shared common nodes with

the solid elements. The contribution of these elements to the overall stiffness of the model was negligible. The thickness of the shell elements was 1.0×10^{-6} m and only membrane properties were assigned to these elements via the PSHELL BULK DATA card in MSC/NASTRAN. The various constant angular rotations considered were applied via RFORCE and LOADCYH BULK DATA cards. The stresses and element volumes calculated using the finite element model were both within approximately 1 percent of the available closed-form solution for this problem. A model with twice as many elements along the radial direction was also analyzed to check mesh convergence, and the resulting stresses were extremely close to those obtained with only eight HEXA elements.

After each MSC/NASTRAN finite element analysis was executed, and the MSC/NASTRAN output files were created, the NASCARES module was used to create a neutral file for each angular speed considered. The information contained in the neutral files (the element/subelement stresses, volumes/areas, and temperatures) was read by the C4LIFE module for subsequent volume flaw and surface flaw reliability analyses. The number of Gauss points used in the numerical integration for reliability was set to 15 (NGP = 15). The shear-sensitive IKBAT = 1 option, with $\overline{C} = 0.82$, was used when performing the reliability analysis to calculate the normalized Batdorf crack density coefficient based on the various fracture criteria and crack geometries selected.

For the annular disk rotating at various constant angular speeds, reliability calculations were made as a function of disk rotational speed and time for several fracture criteria and crack configurations. The fast-fracture (t=0) and time-dependent (static fatigue) analyses were performed at constant rotational speeds between 60 000 and 120 000 rpm to cover the entire range of failure probabilities predicted by the fracture models within CARES/LIFE.

Fast-fracture and time-dependent probability of failure results for the annular disk rotating at constant angular speeds are shown in tables E5-T1 and E5-T2 for volume flaw analysis and surface flaw analysis, respectively. As expected, these results show that the probability of failure increases

with both increasing angular speed and time. For a given constant angular speed and time, failure probabilities obtained by surface flaw analysis are considerably less than those obtained by volume flaw analysis for all fracture models, indicating that failure would most likely occur due to volume flaws. The main reason for the greatly decreased failure estimates for surface flaw analysis is the much higher equivalent surface Weibull scale parameter, σ_{os}. Figure E5-F2 is a Weibull plot of time-dependent probability of failure results for the annular disk rotating at various constant angular speeds using the noncoplanar strain energy release rate fracture criterion with the Batdorf model. For this case, volume flaw analysis was performed assuming a penny-shaped crack geometry, and surface flaw analysis assumed a semi-circular crack geometry. The importance of postmortem fractography to identify the nature of the fracture-causing flaws is evident from the two widely different sets of answers shown in figure E5-F2 for the volume flaw and surface flaw analyses.

The problem was repeated for the annular disk rotating at various sinusoidal cyclic angular speeds. Reliability calculations for the rotating annular disk were made as a function of cyclic rotational speed and time for various fracture criteria and crack geometries. Two approaches were used to determine the probability of failure for the cyclic fatigue problem. For the first approach, reliability analysis was performed for two sinusoidal cyclic angular speed variations: (1) 60 000 rpm to 70 000 rpm and (2) 60 000 rpm to 80 000 rpm. In this approach, reliability calculations were made based on a user input R-ratio and a stress distribution throughout the disk based on the maximum cyclic stresses. The second approach was used to verify the results of the first reliability analysis for the 60 000 rpm to 80 000 rpm cycle. In this approach, the sinusoidal cyclic angular speed variation was transformed to an equivalent constant angular speed, and reliability analysis was performed for the equivalent static stress distribution.

For the first approach, the procedure outlined above was followed to perform the MSC/NASTRAN finite element analyses and create the neutral files required for subsequent reliability analysis with CARES/LIFE. For each cyclic angluar speed considered, the module

C4LIFE was used with one neutral file (containing information relative to the maximum rotational speed for the cycle) to calculate the time-dependent probability of failure for both volume flaw and surface flaw analyses. The reliability analysis was performed using the power law with the period of one cycle equal to 36 seconds (0.01 hr). Since the stress distribution in a rotating annular disk is directly proportional to the square of the angular speed, the QCYC keyword was used to assign the value of 2.0 to the loading waveform exponent. This value is used by the C4LIFE module to determine the g-factor associated with the given waveform. The ratio of the minimum to the maximum cycle stress (in this case, the square of the ratio of the minimum to the maximum rotational speed) was specified using the CYCLIC keyword in the C4LIFE input file.

For this approach, reliability calculations for the rotating annular disk were made as a function of cyclic rotational speed and time for two sinusoidal cyclic angular speed variations of 60 000 rpm to 70 000 rpm and 60 000 rpm to 80 000 rpm. Results from these analyses are shown in tables E5-T3 and E5-T4 for volume flaw analysis and surface flaw analysis, respectively, for various fracture criteria and crack geometries. Figure E5-F3 is a Weibull plot of time-dependent probability of failure results for the annular disk rotating at a sinusoidal cyclic angular speed varying from 60 000 rpm to 80 000 rpm over a period of 0.01 hr using the noncoplanar strain energy release rate fracture criterion with the Batdorf model. For this case, volume flaw analysis was performed assuming a penny-shaped crack geometry, and surface flaw analysis assumed a semi-circular crack geometry. As expected, the reliability predictions for the disk rotating at this particular cyclic angular speed are between the predicted reliabilities for constant angular speeds of 60 000 rpm and 80 000 rpm. Also, as observed for the annular disk rotating at constant angular speeds, failure probabilities obtained by surface flaw analysis are lower than those obtained by volume flaw analysis for all fracture models.

To verify the results of the above analysis, the sinusoidal cyclic load condition for the 60 000 rpm to 80 000 rpm cycle was transformed to an equivalent static load condition, and reliability

analysis was performed for the equivalent static problem. As discussed in the section **Cyclic Fatigue,** transforming a periodic cyclic load condition to an equivalent static load condition is based on satisfying the requirement that both systems produce the same crack growth. An equivalent constant angular speed, ω_{eq}, which satisfies this requirement is calculated for the given cycle

$$\omega_{eq} = \left[\frac{\int_0^T \left[\left(\frac{\omega_{max} + \omega_{min}}{2} \right) + \left(\frac{\omega_{max} - \omega_{min}}{2} \right) \sin\frac{2\pi t}{T} \right]^{2N} dt}{T} \right]^{\frac{1}{2N}}$$

where T is the period of one cycle, N is the fatigue crack growth exponent, t is the service time, ω_{max} is the maximum rotational speed in the cycle, and ω_{min} is the minimum rotational speed in the cycle. The equivalent constant angular speed calculated for the 60 000 rpm to 80 000 rpm cycle was 77 485.20 rpm. For this equivalent constant angular speed, the procedure outlined previously was followed to perform an MSC/NASTRAN finite element analysis and create the neutral file required for subsequent reliability analysis. The module C4LIFE was then used to perform time-dependent reliability analysis for the equivalent constant angular speed problem. Overall, the results of this analysis agreed with the results presented for the cyclic analysis in tables E5-T3 and E5-T4. For short service times, however, the results deviate slightly from those presented in tables E5-T3 and E5-T4, due to the presence of the fast-fracture term which appears in the calculation of the transformed equivalent stress distribution (equation (97)). As the service time increases, the influence of this fast-fracture term diminishes.

To verify the equivalence of the two approaches employed for performing the reliability analysis for the 60 000 rpm to 80 000 rpm sinusoidal cyclic angular speed variation, the g-factors associated with each of the two approaches were compared. For the first approach, the g-factor calculated for the 60 000 rpm to 80 000 rpm cycle using the C4LIFE reliability analysis module was g = 0.147322. For the second approach, the equivalent constant angular speed was used to calculate the g-factor

$$g = \left[\left(\frac{\omega_{eq}}{\omega_{max}} \right)^2 \right]^N$$

For this case, the g-factor calculated was g = 0.147138. Since the difference in the values of the g-factors obtained for the two approaches is essentially negligible, the equivalence of the two approaches is verified.
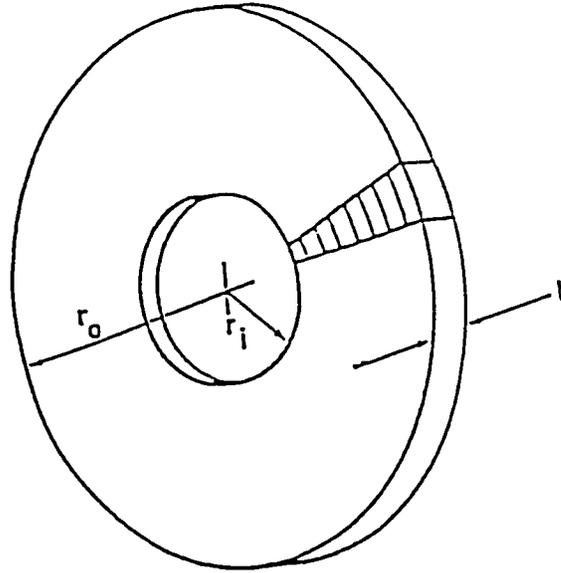
Figure E5-F1.--Rotating annular disk with 15° sector finite element mesh. Inner disk radius, r_i, 6.35 mm; outer disk radius, r_o, 41.28 mm; disk thickness, t, 3.80 mm.

TABLE E5-T1. FAILURE PROBABILITIES OF A ROTATING ANNULAR DISK-CONSTANT RPM VALUES-VOLUME FLAW ANALYSIS

[NGP=15; IKBAT=1; m_V=7.65; σ_{ov}=74.79 MPa(m)$^{3/7.65}$; N=30; B=320 MPa^2 hr]

Angular Speed, rpm	Service Time, hrs	CARES/LIFE Failure Probability				
		PIA criterion	Batdorf Model Noncoplanar strain energy release rate criterion ($\overline{C}$=0.82)		Batdorf Model Energy release rate criterion G_T	
			Griffith crack	Penny-shaped crack	Griffith crack	Penny-shaped crack
60 000	0.0	0.0002101	0.0001920	0.0001817	0.0002307	0.0002209
	0.1	0.0003598	0.0003268	0.0003095	0.0003911	0.003751
	1.0	0.0006488	0.0005882	0.0005573	0.0007033	0.0006748
	10.0	0.001211	0.001098	0.001040	0.001313	0.001260
	100.0	0.002270	0.002058	0.001950	0.002460	0.002360
	1000.0	0.004254	0.003857	0.003655	0.004610	0.004423
70 000	0.0	0.002219	0.002028	0.001920	0.002437	0.002333
	0.1	0.004408	0.004001	0.003791	0.004785	0.004590
	1.0	0.008071	0.007320	0.006936	0.008746	0.008392
	10.0	0.01505	0.01365	0.01294	0.01630	0.01565
	100.0	0.02804	0.02545	0.02413	0.03036	0.02914
	1000.0	0.05196	0.04721	0.04479	0.05619	0.05397
80 000	0.0	0.01699	0.01554	0.01471	0.01865	0.01786
	0.1	0.03829	0.03479	0.03299	0.04147	0.03982
	1.0	0.06971	0.06340	0.06017	0.07533	0.07238
	10.0	0.1266	0.1155	0.1097	0.1364	0.1313
	100.0	0.2242	0.2056	0.1959	0.2405	0.2320
	1000.0	0.3789	0.3506	0.3357	0.4032	0.3905
90 000	0.0	0.09869	0.09058	0.08595	0.1078	0.1035
	0.1	0.2349	0.2155	0.2055	0.2520	0.2431
	1.0	0.3922	0.3632	0.3479	0.4171	0.4042
	10.0	0.6067	0.5708	0.5513	0.6363	0.6211
	100.0	0.8263	0.7954	0.7776	0.8500	0.8380
	1000.0	0.9625	0.9490	0.9404	0.9715	0.9671
100 000	0.0	0.4060	0.3787	0.3627	0.4356	0.4217
	0.1	0.7771	0.7436	0.7246	0.8036	0.7901
	1.0	0.9392	0.9210	0.9097	0.9519	0.9456
	10.0	0.9947	0.9914	0.9890	0.9966	0.9957
	100.0	0.9999	0.9999	0.9998	1.0000	1.0000
	1000.0	1.0000	1.0000	1.0000	1.0000	1.0000
110 000	0.0	0.8934	0.8707	0.8558	0.9145	0.9050
	0.1	0.9992	0.9985	0.9978	0.9996	0.9994
	1.0	1.0000	1.0000	1.0000	1.0000	1.0000
	10.0	1.0000	1.0000	1.0000	1.0000	1.0000
	100.0	1.0000	1.0000	1.0000	1.0000	1.0000
	1000.0	1.0000	1.0000	1.0000	1.0000	1.0000
120 000	0.0	0.9998	0.9996	0.9993	0.9999	0.9999
	0.1	1.0000	1.0000	1.0000	1.0000	1.0000
	1.0	1.0000	1.0000	1.0000	1.0000	1.0000
	10.0	1.0000	1.0000	1.0000	1.0000	1.0000
	100.0	1.0000	1.0000	1.0000	1.0000	1.0000
	1000.0	1.0000	1.0000	1.0000	1.0000	1.0000

TABLE E5-T2. FAILURE PROBABILITIES OF A ROTATING ANNULAR
DISK-CONSTANT RPM VALUES-SURFACE FLAW ANALYSIS

[NGP=15; IKBAT=1; m_S=7.65; σ_{oS}=232.0 MPa(m)$^{2/765}$; N=30; B=320 MPa^2 hr]

Angular Speed, rpm	Service Time, hrs	CARES/LIFE Failure Probability			
		PIA criterion	Batdorf Model Noncoplanar strain energy release rate criterion ($\overline{C}$=0.82)		Batdorf Model Energy release rate criterion G_T
			Griffith crack	Semi-circular crack	Griffith crack
60 000	0.0	0.00003677	0.00003389	0.00003502	0.00003843
	0.1	0.00006674	0.00006183	0.00006370	0.00006923
	1.0	0.0001214	0.0001125	0.0001158	0.0001257
	10.0	0.0002269	0.0002103	0.0002165	0.0002349
	100.0	0.0004254	0.0003943	0.0004060	0.0004405
	1000.0	0.0007979	0.0007396	0.0007615	0.0008262
70 000	0.0	0.0003888	0.0003584	0.0003703	0.0004063
	0.1	0.0008223	0.0007620	0.0007848	0.0008523
	1.0	0.001515	0.001404	0.001446	0.001569
	10.0	0.002835	0.002628	0.002706	0.002936
	100.0	0.005311	0.004924	0.005069	0.005499
	1000.0	0.009940	0.009217	0.009489	0.01029
80 000	0.0	0.002995	0.002761	0.002853	0.003130
	0.1	0.007258	0.006728	0.006928	0.007520
	1.0	0.01343	0.01246	0.01282	0.01391
	10.0	0.02502	0.02321	0.02389	0.02590
	100.0	0.04642	0.04310	0.04435	0.04803
	1000.0	0.08531	0.07932	0.08157	0.08820
90 000	0.0	0.01802	0.01662	0.01717	0.01882
	0.1	0.04878	0.04529	0.04661	0.05049
	1.0	0.08899	0.08276	0.08511	0.09201
	10.0	0.1603	0.1495	0.1536	0.1655
	100.0	0.2795	0.2620	0.2686	0.2878
	1000.0	0.4593	0.4344	0.4439	0.4709
100 000	0.0	0.08713	0.08060	0.08317	0.09087
	0.1	0.2447	0.2290	0.2349	0.2522
	1.0	0.4079	0.3848	0.3936	0.4189
	10.0	0.6257	0.5978	0.6086	0.6386
	100.0	0.8417	0.8189	0.8278	0.8518
	1000.0	0.9685	0.9595	0.9631	0.9722
110 000	0.0	0.3242	0.3031	0.3115	0.3360
	0.1	0.7372	0.7103	0.7207	0.7495
	1.0	0.9179	0.9014	0.9080	0.9249
	10.0	0.9908	0.9870	0.9886	0.9922
	100.0	0.9998	0.9997	0.9998	0.9999
	1000.0	1.0000	1.0000	1.0000	1.0000
120 000	0.0	0.7731	0.7452	0.7566	0.7878
	0.1	0.9961	0.9942	0.9950	0.9968
	1.0	1.0000	0.9999	1.0000	1.0000
	10.0	1.0000	1.0000	1.0000	1.0000
	100.0	1.0000	1.0000	1.0000	1.0000
	1000.0	1.0000	1.0000	1.0000	1.0000

Figure E5-F2.--Time-dependent probability of failure for annular disk rotating at constant angular speeds. Analysis performed using the noncoplanar strain energy release rate fracture criterion with the Batdorf model. Solid lines denote volume flaw analysis (penny-shaped crack); dashed lines denote surface flaw analysis (semi-circular crack).

TABLE E5-T3. FAILURE PROBABILITIES OF A ROTATING ANNULAR
DISK-CYCLIC RPM VALUES-VOLUME FLAW ANALYSIS

[NGP=15; IKBAT=1; m_v=7.65; σ_{ov}=74.79 MPa(m)$^{3/765}$; N=30; B=320 MPa^2 hr]

Angular Speed, rpm	Service Time, hrs	CARES/LIFE Failure Probability				
		PIA criterion	Batdorf Model Noncoplanar strain energy release rate criterion ($\overline{C}$=0.82)		Batdorf Model Energy release rate criterion G_T	
			Griffith crack	Penny-shaped crack	Griffith crack	Penny-shaped crack
60 000-70 000	0.01	0.002352	0.002147	0.002033	0.002579	0.002
	0.10	0.003072	0.002795	0.002647	0.003347	0.003
	1.00	0.005246	0.004759	0.004510	0.005690	0.005
	10.00	0.009706	0.008802	0.008341	0.01052	0.010
	100.00	0.01811	0.01643	0.01557	0.01961	0.018
	1000.00	0.03370	0.03059	0.02901	0.03647	0.035
60 000-80 00	0.01	0.01824	0.01667	0.01578	0.01998	0.019
	0.10	0.02455	0.02235	0.02118	0.02671	0.025
	1.00	0.04228	0.03841	0.03643	0.04577	0.043
	10.00	0.07715	0.07019	0.06663	0.08334	0.080
	100.00	0.1397	0.1275	0.1212	0.1505	0.144
	1000.00	0.2459	0.2257	0.2152	0.2635	0.254

TABLE E5-T4. FAILURE PROBABILITIES OF A ROTATING ANNULAR
DISK-CYCLIC RPM VALUES-SURFACE FLAW ANALYSIS

[NGP=15; IKBAT=1; m_s=7.65; σ_{oS}=232.0 MPa(m)$^{2/7\ 65}$; N=30; B=320 MPa^2 hr]

Angular Speed, rpm	Service Time, hrs	CARES/LIFE Failure Probability			
		PIA criterion	Batdorf Model Noncoplanar strain energy release rate criterion ($\overline{C}$=0.82)		Batdorf Model Energy release rate criterion G_T
			Griffith crack	Semi-circular crack	Griffith crack
60 000- 70 000	0.01	0.0004175	0.0003854	0.0003979	0.0004357
	0.10	0.0005642	0.0005223	0.0005384	0.0005863
	1.00	0.0009815	0.0009096	0.0009367	0.001017
	10.00	0.001824	0.001691	0.001741	0.001889
	100.00	0.003415	0.003166	0.003260	0.003537
	1000.00	0.006397	0.005930	0.006106	0.006623
60 000- 80 00	0.01	0.003268	0.003018	0.003116	0.003410
	0.10	0.004564	0.004227	0.004356	0.004740
	1.00	0.008036	0.007450	0.007670	0.008324
	10.00	0.01491	0.01383	0.01424	0.01544
	100.00	0.02778	0.02577	0.02653	0.02875
	1000.00	0.05147	0.04780	0.04918	0.05325
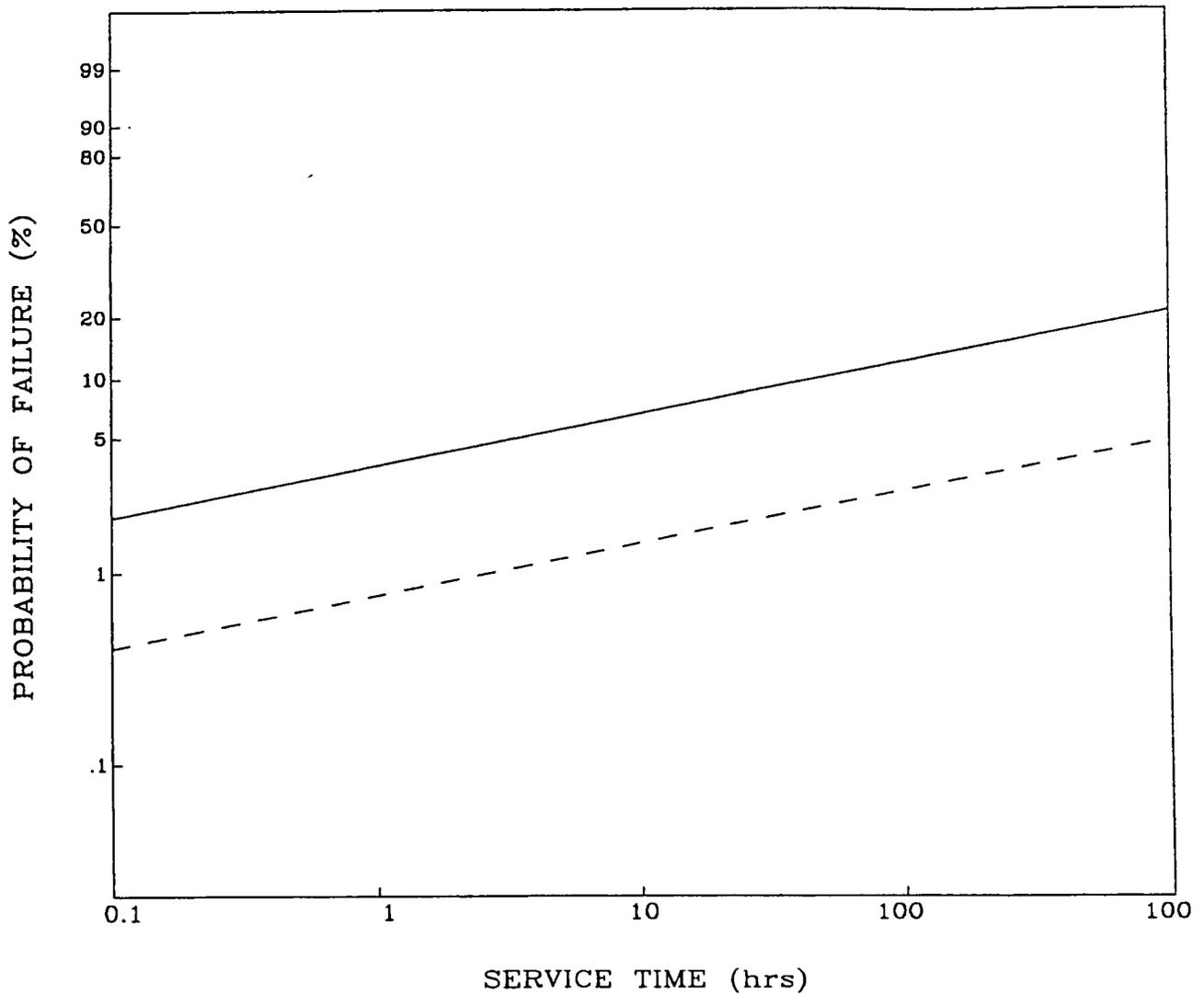
Figure E5-F3.--Time-dependent probability of failure for annular disk rotating at sinusoidal cyclic speed varying from 60 000 rpm to 80 000 rpm (period = 0.01 hr). Analysis performed using the noncoplanar strain energy release rate fracture criterion with the Batdorf model. Solid lines denote volume flaw analysis (penny-shaped crack); dashed lines denote surface flaw analysis (semi-circular crack).

Example 6 - Thermomechanically Loaded Rotating Annular Disk

This example illustrates the use of the CARES/LIFE program modules for the time-dependent reliability analysis of an annular disk subjected to a thermomechanical load at various constant angular speeds. The module C4LIFE is used to compute the probability of failure of the annular disk for both fast fracture (t=0) and time-dependent (static fatigue) analyses. Results are presented for the noncoplanar strain energy release rate fracture criterion using the Batdorf model for both volume flaw (penny-shaped crack geometry) and surface flaw (semi-circular crack geometry) analyses.

The annular disk analyzed in this example is a modified version of that in **Example 5– Isothermal Rotating Annular Disk**. The disk inside diameter was 0.0127 m, the outside diameter was 0.08255 m, and the disk was 0.0038 m thick (fig. E6-F1). The finite element mesh geometry was identical to that in example 5. For example 5, the disk was entirely made of silicon nitride and the analysis was performed at a constant temperature. For this example, the disk was composed of three materials: silicon nitride, silicon carbide, and steel. Elements were assigned material properties accordingly, and a radial variation in temperature was imposed.

MSC/NASTRAN finite element models of the disk were created for each constant angular speed considered. The MSC/NASTRAN finite element model of the disk for volume flaw analysis consisted of brick elements and used the structured solution sequence 114, static cyclic symmetry analysis. Because of symmetry, only eight HEXA elements were used in one 15° sector of the finite element model (fig. E6-F1). Each element spanned both the thickness and circumferential directions. For surface flaw analysis, the same MSC/NASTRAN analysis was performed as for volume flaws with the addition of QUAD8 shell elements to identify external surfaces of the model. The shell elements shared common nodes with the solid elements. The contribution of these elements to the overall stiffness of the model was negligible. The thickness of the shell elements

was 1.0 x 10^{-6} m and only membrane properties were assigned to these elements via the PSHELL

BULK DATA card in MSC/NASTRAN.

For this example, the disk consisted of three materials: two were ceramics and one was

metal. The material properties were assigned via PSHELL, PSOLID, MAT1, MATT1, and

TABLEM1 cards in the MSC/NASTRAN BULK DATA. The MAT1 card assumes temperature-

independent material properties. The MATT1 and TABLEM1 cards are employed to define

temperature-dependent material properties. Only the PSHELL and PSOLID cards are required for

postprocessing with CARES/LIFE. For this example, the innermost solid element was sintered

silicon carbide with an assigned MAT1 material ID of 302. The three shell elements (100, 110, and

130) that shared nodes with this element were also assigned to material ID 302. Temperature-

dependent material properties (Sturmer, Schulz, and Wittig, 1991) shown in table E6-T1 were

assigned to material ID 302 via MATT1 and TABLEM1 cards in the MSC/NASTRAN BULK

DATA. Temperature-independent material properties assigned to the silicon carbide include a

Poisson's ratio of 0.160 and a material mass density of 3.420x10^3 kg/m^3. The outermost HEXA

element was assigned to MAT1 material ID 301 and had temperature-independent material

properties consistent with steel: a Young's modulus of 20.69 GPa, a Poisson's ratio of 0.3, a

material mass density of 7.834x10^3 kg/m^3, and a thermal expansion coefficient of 3.70x10^{-6} °C^{-1}.

The three shell elements (107, 117, and 120) that shared nodes with this element also had material

ID 301. The remaining 6 solid and 12 shell elements were silicon nitride with an assigned MAT1

material ID of 300. The required temperature-independent material properties assigned to the silicon

nitride include a Young's modulus of 289 GPa, a Poisson's ratio of 0.219, a material mass density

of 3.25x10^3 kg/m^3, and a thermal expansion coefficient of 3.083x10^{-6} °C^{-1}.

For this example, a thermal gradient that varied with the disk radius was imposed on the

nodes. The temperature varied from 1093°C at the inner bore to 704°C at the outside periphery.

The gradient was approximately linear, and the loads were arbitrarily imposed. The thermal loads were assigned via TEMP and LOADCYN BULK DATA cards. The various constant angular rotations considered were applied via RFORCE and LOADCYH BULK DATA cards.

After each MSC/NASTRAN finite element analysis was executed, and the MSC/NASTRAN output files were created, the NASCARES module was used to create a neutral file for each angular speed considered. The information contained in the neutral files (the element/subelement stresses, volumes/areas, and temperatures) was read by the C4LIFE module for subsequent volume flaw and surface flaw reliability analyses.

The Weibull and fatigue parameters needed for the reliability analyses are given in tables E6-T2 and E6-T3. For the silicon nitride, the temperature-dependent Weibull parameters were assumed based on values obtained for the Weibull modulus at room temperature (Swank, and Williams, 1981)(Nemeth, Manderscheid, and Gyekenyesi, 1990) The temperature-dependent material/environmental fatigue parameters necessary for the time-dependent reliability analysis were estimated using values obtained for silicon nitride (NC-132) data at 1000°C (Quinn, and Quinn, 1983). The parameters were directly input at temperature levels of 538°C, 816°C, and 1093°C. For the sintered silicon carbide, the Weibull and fatigue parameters were obtained from Sturmer, et al. (Sturmer, Schulz, and Wittig, 1991) based on four-point bend test specimen geometry with w = 0.005 m, h = 0.004 m, L_1 = 0.040 m, and L_2 = 0.020 m. Weibull parameters at room temperature were assumed valid for the temperature-dependent analyses. Temperature-dependent fatigue parameters were estimated from this data and directly input at the three temperature levels given above. Material 301 was steel and was subsequently ignored in the reliability analysis by not specifying it in either the Master Control Input or the Material Control Input.

For the thermomechanically loaded annular disk rotating at various constant angular speeds, reliability calculations were made as a function of disk rotational speed and time for the fracture

criterion and crack configurations considered. The number of Gauss points used in the numerical integration for reliability was set to 15 (NGP = 15). The shear-sensitive IKBAT = 1 option, with = 0.82, was used when performing the reliability analysis to calculate the normalized Batdorf crack density coefficient based on the fracture criterion and crack geometries selected. Fast-fracture (t=0) and time-dependent (static fatigue) reliability analyses were performed at constant rotational speeds of 2000 rpm, 3000 rpm, 6000 rpm, and 10 000 rpm to examine the range of failure probabilities predicted by the C4LIFE program module.

Fast-fracture and time-dependent probability of failure results for the annular disk rotating at constant angular speeds are given in tables E6-T4 and E6-T5 for volume flaw analysis and surface flaw analysis, respectively. Figure E6-F2 is a Weibull plot of time-dependent probability of failure results for the annular disk rotating at various constant angular speeds. These results were obtained using the noncoplanar strain energy release rate fracture criterion with the Batdorf model. Volume flaw analysis was performed assuming a penny-shaped crack geometry, and surface flaw analysis assumed a semi-circular crack geometry. As expected, these results show that the probability of failure increases with both increasing angular speed and time. For a given constant angular speed and time, failure probabilities obtained by surface flaw analysis are considerably less than those obtained by volume flaw analysis, indicating that failure would most likely occur due to volume flaws.

.
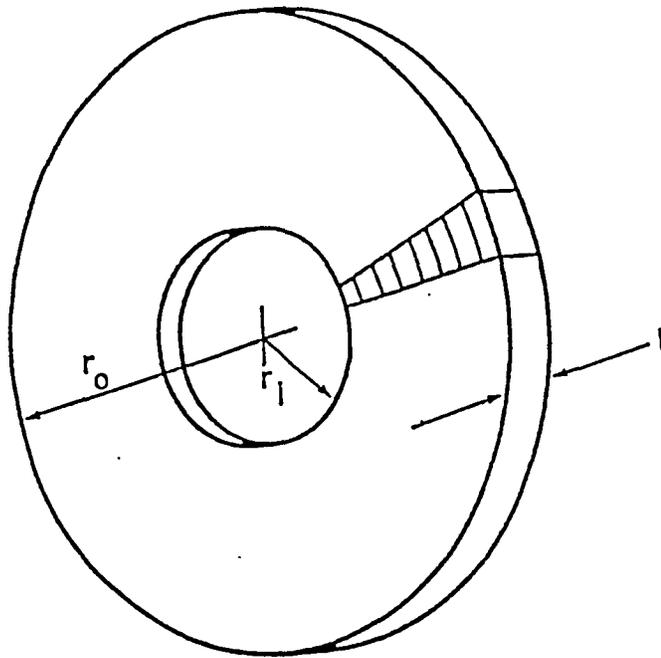
Figure E6-F1.--Thermomechanically loaded rotating annular disk with 15° sector finite element mesh. Inner disk radius, r_i, 6.35 mm; outer disk radius, r_o, 41.28 mm; disk thickness, t, 3.80 mm.

TABLE E6-T1. TEMPERATURE-DEPENDENT MATERIAL PROPERTIES
FOR SILICON CARBIDE

Temperature °C	E GPa	α °C^{-1}
599.85	422.6	1.678x10^{-6}
799.85	419.0	1.678x10^{-6}
999.85	415.4	1.689x10^{-6}
1199.85	411.8	1.728x10^{-6}

TABLE E6-T2. WEIBULL AND FATIGUE PARAMETERS FOR SILICON NITRIDE (NC-132)

Temperature °C	m_v	σ_{ov} MPa(m)$^{3/m_v}$	N_v	B_{Bv} MPa²hr	m_s	σ_{oS} MPa(m)$^{2/m_s}$	N_s	B_{Bs} MPa²hr
538	7.65	91.120	30	320	7.65	205.582	30	200
816	10.00	114.539	28	310	9.00	213.379	28	180
1093	12.00	110.104	26	290	10.00	165.375	26	170

TABLE E6-T3. WEIBULL AND FATIGUE PARAMETERS FOR SILICON CARBIDE

Temperature °C	m_v	σ_{ov} MPa(m)$^{3/m_v}$	N_v	B_{Bv} MPa²hr	m_s	σ_{oS} MPa(m)$^{2/m_s}$	N_s	B_{Bs} MPa²hr
538	8.6	49.678	56	1275	8.6	134.357	56	520
816	8.6	49.678	47	1850	8.6	134.357	47	750
1093	8.6	49.678	38	520	8.6	134.357	38	210

TABLE E6-T4. FAILURE PROBABILITIES FOR THERMOMECHANICALLY LOADED ROTATING ANNULAR DISK (VOLUME FLAW ANALYSIS)

Noncoplanar strain energy release rate criterion
Batdorf model
(Penny-shaped crack)

[NGP=15; IKBAT=1; $\bar{C}$=0.82]

Service time, hrs	CARES/LIFE Failure Probability			
	Angular speed, rpm			
	2 000	3 000	6 000	10 000
0.0	0.4691	0.4728	0.4937	0.5489
0.1	0.6909	0.6951	0.7178	0.7740
1.0	0.8624	0.8654	0.8820	0.9191
10.0	0.9665	0.9678	0.9743	0.9866
30.0	0.9877	0.9883	0.9912	0.9962
50.0	0.9930	0.9933	0.9952	0.9981
100.0	0.9971	0.9973	0.9981	0.9994
300.0	0.9995	0.9995	0.9997	0.9999
500.0	0.9998	0.9998	0.9999	1.0000
700.0	0.9999	0.9999	1.0000	1.0000
900.0	0.9999	0.9999	1.0000	1.0000
1000.0	1.0000	1.0000	1.0000	1.0000

TABLE E6-T5. FAILURE PROBABILITIES FOR THERMOMECHANICALLY LOADED ROTATING ANNULAR DISK (SURFACE FLAW ANALYSIS)

Noncoplanar strain energy release rate criterion
Batdorf model
(Semi-circular crack)

[NGP=15; IKBAT=1; $\bar{C}$=0.82]

Service time, hrs	CARES/LIFE Failure Probability			
	Angular speed, rpm			
	2 000	3 000	6 000	10 000
0.0	0.1405	0.1436	0.1615	0.2108
0.1	0.3084	0.3148	0.3509	0.4453
1.0	0.4720	0.4804	0.5267	0.6392
10.0	0.6719	0.6809	0.7285	0.8303
30.0	0.7667	0.7750	0.8176	0.9010
50.0	0.8076	0.8153	0.8543	0.9269
100.0	0.8580	0.8647	0.8978	0.9547
300.0	0.9223	0.9270	0.9493	0.9824
500.0	0.9448	0.9486	0.9659	0.9897
700.0	0.9571	0.9602	0.9745	0.9930
900.0	0.9649	0.9676	0.9798	0.9949
1000.0	0.9679	0.9704	0.9818	0.9956
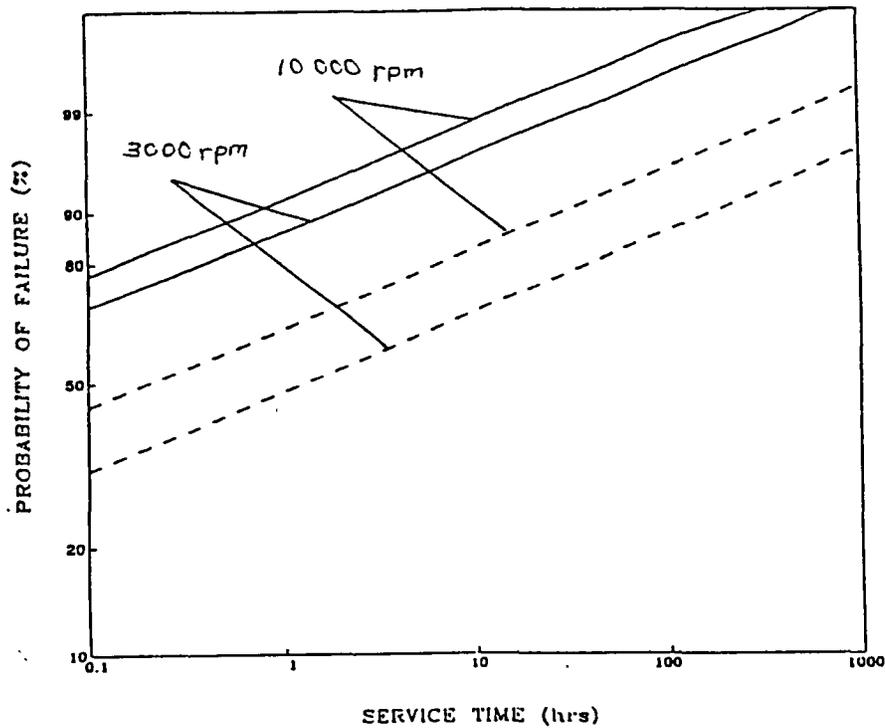
Figure E6-F2.--Time-dependent probability of failure for thermomechanically loaded annular disk rotating at constant angular speeds. Analysis performed using the noncoplanar strain energy release rate fracture criterion with the Batdorf model. Solid lines denote volume flaw analysis (penny-shaped crack); dashed lines denote surface flaw analysis (semi-circular crack).

Example 7 - Proof Testing

This problem illustrates the use of the CARES/LIFE program modules for determining the time-dependent reliability of a silicon nitride (NC-132) beam (Fig. E7-F1) subjected to a pure bend service load after being proof tested in pure bend or pure tension for various time periods. As discussed in the section **Proof Testing Effect on Component Service Probability of Failure**, proof testing components allows weaker specimens to be eliminated from the strength distribution. Thus, a component can be placed in service with greater confidence in its integrity. In this example, the resulting attenuated probability of failure as a function of time is computed using the noncoplanar strain energy release rate fracture criterion with the Batdorf model for both volume flaw (penny-shaped crack geometry) and surface flaw (semi-circular crack geometry) analyses. Based on a service load having a fast fracture probability of failure of approximately 0.03, four combinations of proof test loading and service loading were considered: (1) The beam was proof tested under a pure bend load condition and then subjected to an in-service pure bend load condition which produces a maximum stress 25% lower than the maximum proof test stress. (2) The beam was proof tested under a pure bend load condition and then subjected to an in-service pure bend load condition which produces a maximum stress 25% higher than the maximum proof test stress. (3) The beam was proof tested under a pure tension load condition and then subjected to an in-service pure bend load condition which produces a maximum stress 25% lower than the maximum proof test stress. (4) The beam was proof tested under a pure tension load condition and then subjected to an in-service pure bend load condition which produces a maximum stress 25% higher than the maximum proof test stress. Cases (1) and (2) were designed to illustrate the ideal situation, where the boundary conditions applied to a component under proof testing identically simulate those conditions the component is subjected to in service, and differ only in magnitude. Cases (3) and (4) illustrate off-axis proof test loading, i.e., the proof test and service loads are misaligned (pure tension vs. pure bending).

The beam dimensions are given in figure E7-F1. Analysis was performed on the beam at a uniform 1000°C temperature. The material/environmental fatigue parameters, N=30 and B=320 MPa^2 hr, necessary for time-dependent reliability analysis were estimated using NC-132 data at 1000°C (Quinn, and Quinn, 1983). The same fatigue parameters were used for both volume and surface flaw analyses. Weibull material parameters independently evaluated at room temperature from four-point bend tests of 85 specimens were assumed to be valid for the 1000°C analysis. For volume flaw analysis, the Weibull modulus, m_V, was 7.65 (Swank, and Williams, 1981) (Nemeth, Manderschied, and Gyekenyesi, 1990). The Weibull scale parameter, calculated using equations (56) and (60), was $\sigma_{oV} = 74.79$ MPa (m)$^{3/7.65}$. For surface flaw analysis, the Weibull modulus, m_S, was 7.65 and the scale parameter, calculated from equations (69) and (73), was σ_{oS}=232.0 MPa (m)$^{2/7.65}$. Other required material properties include a Young's modulus of 289 GPa and a Poisson's ratio of 0.219.

MSC/NASTRAN finite element models of the beam were created for both volume flaw and surface flaw analyses for each of the service and proof test load conditions considered. The MSC/NASTRAN finite element analyses used the structured solution sequence 101, static analysis. Because of symmetry, only one quarter of the beam was modeled for each finite element analysis, as indicated in figure E7-F1. For volume flaw analysis, the finite element mesh of the quarter beam consisted of twenty HEXA elements in the length (x) direction, eight HEXA elements in the height (y) direction, and one HEXA element in the thickness (z) direction. For surface flaw analysis, the same MSC/NASTRAN finite element model was used as for volume flaws with the addition of QUAD8 shell elements to identify external surfaces of the model. The shell elements shared common nodes with the solid elements. The contribution of these elements to the overall stiffness of the model was negligible. The thickness of the shell elements was 1.0x10^{-6} m, and only membrane properties were assigned to these elements via the PSHELL BULK DATA card in MSC/NASTRAN. The pure bend load conditions were induced in the beam by prescribing

displacements in the longitudinal direction which are proportional to the y-coordinate of the beam at x=L. The pure tension load conditions were induced in the beam by applying a uniform tensile force at x=L. For case (1), the beam was proof tested under a pure bend load condition producing a maximum stress of 722.5 MPa and then subjected to a pure bend service load condition producing a maximum stress of 578.0 MPa. For case (2), the beam was proof tested under a pure bend load condition producing a maximum stress of 433.5 MPa and then subjected to a pure bend service load condition producing a maximum stress of 578.0 MPa. For case (3), the beam was proof tested under a pure tension load condition producing a maximum stress of 722.5 MPa and then subjected to a pure bend service load condition producing a maximum stress of 578.0 MPa. For case (4), the beam was proof tested under a pure tension load condition producing a maximum stress of 433.5 MPa and then subjected to a pure bend service load condition producing a maximum stress of 578.0 MPa.

After the MSC/NASTRAN finite element analyses were executed, and the MSC/NASTRAN output files were created, the NASCARES module was used to create a neutral file for each load condition. The information contained in the neutral files (the element/subelement stresses, volumes/areas, and temperatures) was read by the C4LIFE module for subsequent volume flaw and surface flaw reliability analyses. The number of Gauss points used in the numerical integration for reliability was set to 15 (NGP=15). The option IPROOF=1 was invoked to consider the neutral files for both the service load and proof test load conditions simultaneously. The shear-sensitive IKBAT=1 option, with $\overline{C}$ = 0.82, was used when performing the reliability analysis to calculate the normalized Batdorf crack density coefficient based on the fracture criterion and crack geometries selected.

Time-dependent reliability calculations were made for each of the four combinations of service and proof test loading considered. Attenuated probability of failure results were obtained for

proof test times of 0.1, 1.0, 10.0, and 100.0 hours. In addition, the time-dependent probability of failure results for the beam without proof testing prior to service loading were calculated.

For cases (1) and (2), the proof test and service load conditions differed only in magnitude. These two cases were chosen to examine the predicted attenuated reliability of a component in service after being proof tested at stresses 25% above and 25% below the maximum expected service stress. Time-dependent reliability analysis results for case (1) are given in tables E7-T1 and E7-T2 for volume flaws and surface flaws, respectively. Figure E7-F2 is a Weibull plot of the time-dependent probability of failure results obtained for various proof test times examined in case (1). This plot shows the attenuation which occurs in the time-dependent probability of failure as a result of proof testing. Time-dependent reliability analysis results for case (2) are given in tables E7-T3 and E7-T4 for volume flaws and surface flaws, respectively. The results for case (2) indicate that proof testing at stresses 25% lower than the maximum stress expected in service does improve component integrity. However, this improvement is essentially insignificant when compared with the results from case (1) where the components are proof tested at stresses 25% greater than the maximum stress expected in service. For both of the cases where the proof test load conditions identically simulate the service load conditions, the probability of failure observed for surface flaw analysis is greater than that for volume flaw analysis, due to the specimen geometry and the Weibull material parameters.

For cases (3) and (4), the proof test and service load conditions differed not only in magnitude, but also in direction of application (i.e., off-axis proof testing). The predicted attenuated reliability of a component in service after off-axis proof testing at stresses 25% above and 25% below the maximum expected service stress was examined. Time-dependent reliability analysis results for case (3) are given in tables E7-T5 and E7-T6 for volume flaws and surface flaws, respectively. Figure E7-F3 is a Weibull plot of the time-dependent probability of failure results obtained for various proof test times examined in case (3). As in figure E7-F2, this plot also shows

the attenuation which results from proof testing. Time-dependent reliability analysis results for case (4) are given in tables E7-T7 and E7-T8 for volume flaws and surface flaws, respectively. Figure E7-F4 is a Weibull plot of the results obtained for various proof test times examined in case (4). For clarity of presentation, the results shown in this figure are for volume flaw analysis only; the results for surface flaw analysis are similar, although greater in magnitude, as observed in case (3). These results indicate that proof testing at stresses 25% below the maximum stress expected in service also improves component integrity for off-axis proof test loading. However, as observed previously, these improvements are small compared to those obtained when components are proof tested at stresses 25% greater than the maximum stress expected in service. Also, as observed previously in cases (1) and (2), the probability of failure observed for surface flaw analysis is greater than that for volume flaw analysis in cases (3) and (4), due to the specimen geometry and the Weibull material parameters. In addition, for all of the off-axis proof tested specimens in cases (3) and (4), the probability of failure observed for surface flaw analysis is much higher than that for volume flaw analysis. This observation is expected, due to the different stress distributions induced in the beam by the service and proof test load conditions for this case.

The results obtained for the four cases considered in this example illustrate how proof testing enables a component to be placed in service with greater confidence in its integrity. Furthermore, these results show that component integrity is sensitive to the particular proof test and service loads that are applied.
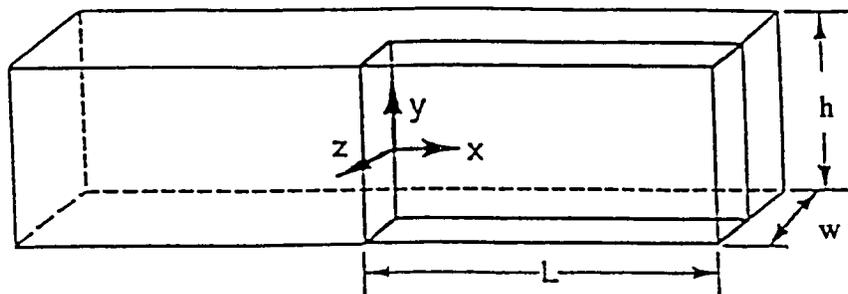
Figure E7-F1.--Silicon nitride (NC-132) beam. Length, L, 10.0 mm; height, h, 4.0 mm; width, w, 1.0 mm.

TABLE E7-T1. FAILURE PROBABILITIES FOR PROOF-TESTED BEAM--CASE 1 (VOLUME FLAW ANALYSIS)

Batdorf Model
Noncoplanar strain energy release rate criterion
(Penny-shaped crack)

[NGP=15; IKBAT=1; $\overline{C}$=0.82; m_V=7.65; σ_{ov}=74.79 MPa(m)$^{3/7.65}$; N=30; B=320 MPa^2 hr]

Service time, hrs	CARES/LIFE Failure Probability				
	Proof test time, t_p, hrs				
	No proof testing	0.1	1.0	10.0	100.0
0.0	0.02836	0.0000	0.0000	0.0000	0.0000
0.1	0.09214	0.0000	0.0000	0.0000	0.0000
1.0	0.1654	0.0007664	0.0001447	0.00002717	0.000005097
10.0	0.2876	0.01798	0.003541	0.0006680	0.0001254
100.0	0.4706	0.1362	0.03558	0.007039	0.001330
1000.0	0.6976	0.4607	0.2418	0.06608	0.01324

TABLE E7-T2. FAILURE PROBABILITIES FOR PROOF-TESTED BEAM--CASE 1 (SURFACE FLAW ANALYSIS)

Batdorf Model
Noncoplanar strain energy release rate criterion
(Semi-circular crack)

[NGP=15; IKBAT=1; $\overline{C}$=0.82; m_S=7.65; σ_{oS}=232.0 MPa(m)$^{2/7.65}$; N=30; B=320 MPa^2 hr]

Service time, hrs	CARES/LIFE Failure Probability				
	Proof test time, t_p, hrs				
	No proof testing	0.1	1.0	10.0	100.0
0.0	0.03105	0.0000	0.0000	0.0000	0.0000
0.1	0.1046	0.0000	0.0000	0.0000	0.0000
1.0	0.1868	0.001074	0.0002028	0.00003807	0.000007141
10.0	0.3215	0.02077	0.004091	0.0007721	0.0001449
100.0	0.5169	0.1544	0.04063	0.008055	0.001522
1000.0	0.7445	0.5066	0.2715	0.07522	0.01513
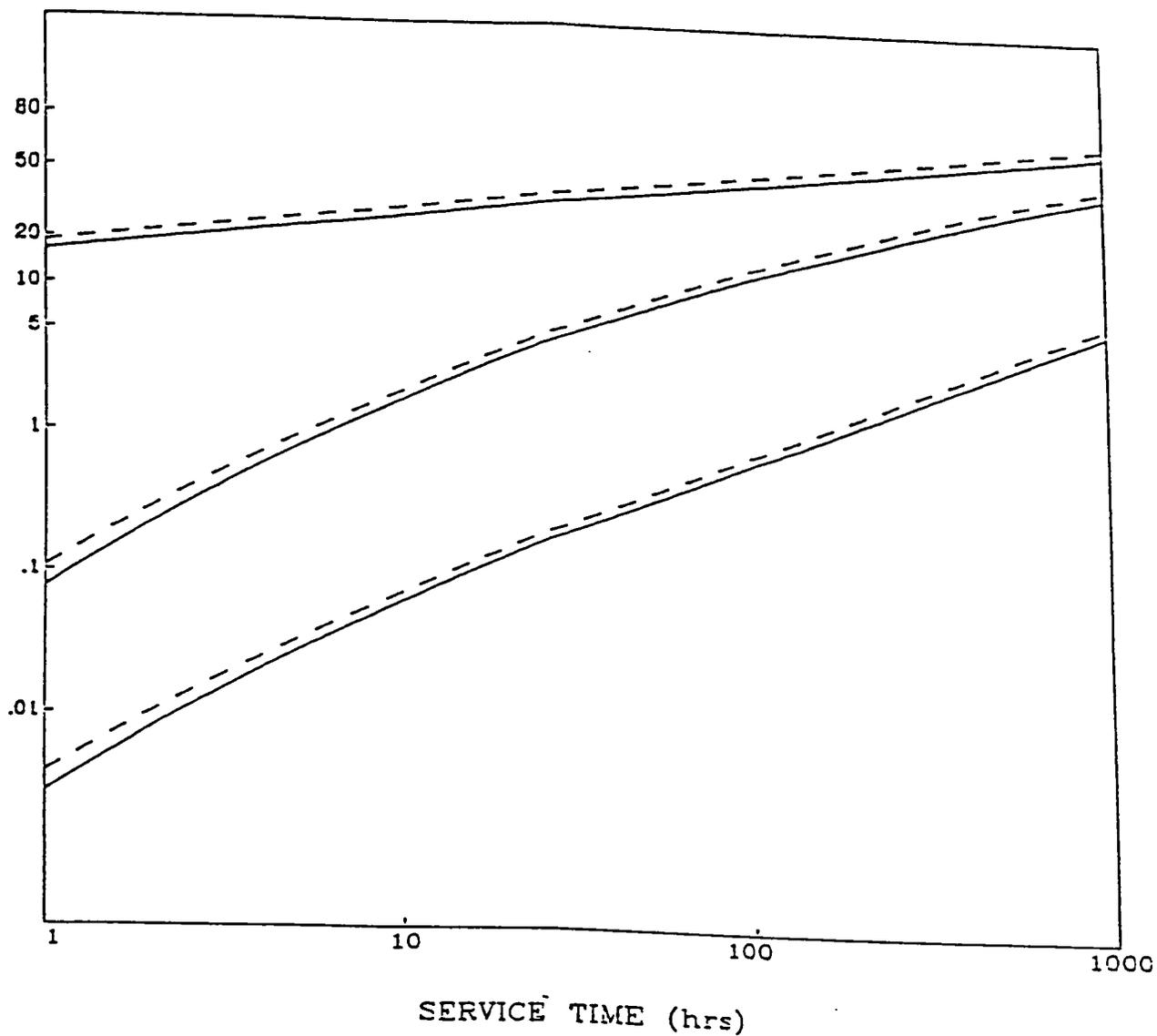
Figure E7-F2.--Probability of failure vs. service time for case (1). Solid lines denote volume flaw analysis; dashed lines denote surface flaw analysis; (t_p = proof test time).

TABLE E7-T3. FAILURE PROBABILITIES FOR PROOF-TESTED
BEAM--CASE 2 (VOLUME FLAW ANALYSIS)

Batdorf Model
Noncoplanar strain energy release rate criterion
(Penny-shaped crack)

[NGP=15; IKBAT=1; $\tilde{C}$=0.82; m_V=7.65; σ_{oV}=74.79 MPa(m)$^{3/7\,65}$; N=30; B=320 MPa^2 hr]

Service time, hrs	CARES/LIFE Failure Probability				
	Proof test time, t_p, hrs				
	No proof testing	0.1	1.0	10.0	100.0
0.0	0.02836	0.01952	0.01271	0.004884	0.001107
0.1	0.09214	0.08378	0.07652	0.06298	0.04006
1.0	0.1654	0.1577	0.1510	0.1383	0.1144
10.0	0.2876	0.2810	0.2753	0.2643	0.2435
100.0	0.4706	0.4657	0.4615	0.4533	0.4378
1000.0	0.6976	0.6939	0.6915	0.6868	0.6779

TABLE E7-T4. FAILURE PROBABILITIES FOR PROOF-TESTED BEAM--CASE 2 (SURFACE FLAW ANALYSIS)

Batdorf Model
Noncoplanar strain energy release rate criterion
(Semi-circular crack)

[NGP=15; IKBAT=1; $\bar{C}$=0.82; m_S=7.65; σ_{oS}=232.0 MPa(m)$^{2/7.65}$; N=30; B=320 MPa^2 hr]

Service time, hrs	CARES/LIFE Failure Probability				
	Proof test time, t_p, hrs				
	No proof testing	0.1	1.0	10.0	100.0
0.0	0.03105	0.02099	0.01331	0.004876	0.001076
0.1	0.1046	0.09520	0.08698	0.07165	0.04563
1.0	0.1868	0.1782	0.1707	0.1565	0.1297
10.0	0.3215	0.3143	0.3080	0.2961	0.2732
100.0	0.5169	0.5118	0.5073	0.4988	0.4825
1000.0	0.7445	0.7418	0.7395	0.7350	0.7263

TABLE E7-T5. FAILURE PROBABILITIES FOR PROOF-TESTED BEAM--CASE 3 (VOLUME FLAW ANALYSIS)

Batdorf Model
Noncoplanar strain energy release rate criterion
(Penny-shaped crack)

[NGP=15; IKBAT=1; $\overline{C}$=0.82; m_V=7.65; σ_{oV}=74.79 MPa(m)$^{3/7.65}$; N=30; B=320 MPa^2 hr]

Service time, hrs	CARES/LIFE Failure Probability				
	Proof test time, t_p, hrs				
	No proof testing	0.1	1.0	10.0	100.0
0.0	0.02836	0.0000	0.0000	0.0000	0.0000
0.1	0.09214	0.0000	0.0000	0.0000	0.0000
1.0	0.1654	0.0000	0.0000	0.0000	0.0000
1.125	0.1703	0.00001733	0.000003264	0.0000006125	0.0000001149
1.25	0.1748	0.00006652	0.00001253	0.000002351	0.0000004411
1.5	0.1829	0.0001908	0.00003595	0.000006747	0.000001266
2.0	0.1962	0.0004538	0.00008561	0.00001607	0.000003015
5.0	0.2446	0.002075	0.0003937	0.00007394	0.00001387
10.0	0.2876	0.004739	0.0009076	0.0001707	0.00003202
100.0	0.4706	0.04773	0.01046	0.002003	0.0003767
1000.0	0.6976	0.2461	0.09026	0.02006	0.003854

TABLE E7-T6. FAILURE PROBABILITIES FOR PROOF-TESTED BEAM--CASE 3 (SURFACE FLAW ANALYSIS)

Batdorf Model
Noncoplanar strain energy release rate criterion
(Semi-circular crack)

[NGP=15; IKBAT=1; $\overline{C}$=0.82; m_S=7.65; σ_{os}=232.0 MPa(m)$^{2/7.65}$; N=30; B=320 MPa^2 hr]

Service time, hrs	CARES/LIFE Failure Probability				
	Proof test time, t_p, hrs				
	No proof testing	0.1	1.0	10.0	100.0
0.0	0.03105	0.00000006397	0.00000006397	0.00000006397	0.00000006397
0.1	0.1046	0.0000001124	0.0000001124	0.0000001124	0.0000001124
1.0	0.1868	0.0008089	0.0001529	0.00002886	0.000005581
1.125	0.1923	0.001011	0.0001912	0.00003606	0.000006935
1.25	0.1973	0.001229	0.0002325	0.00004382	0.000008397
1.5	0.2062	0.001671	0.0003163	0.00005958	0.00001136
2.0	0.2211	0.002558	0.0004853	0.00009134	0.00001734
5.0	0.2745	0.007800	0.001499	0.0002822	0.00005321
10.0	0.3215	0.01621	0.003180	0.0006001	0.0001130
100.0	0.5169	0.1253	0.03204	0.006315	0.001193
1000.0	0.7445	0.4459	0.2239	0.05968	0.01189
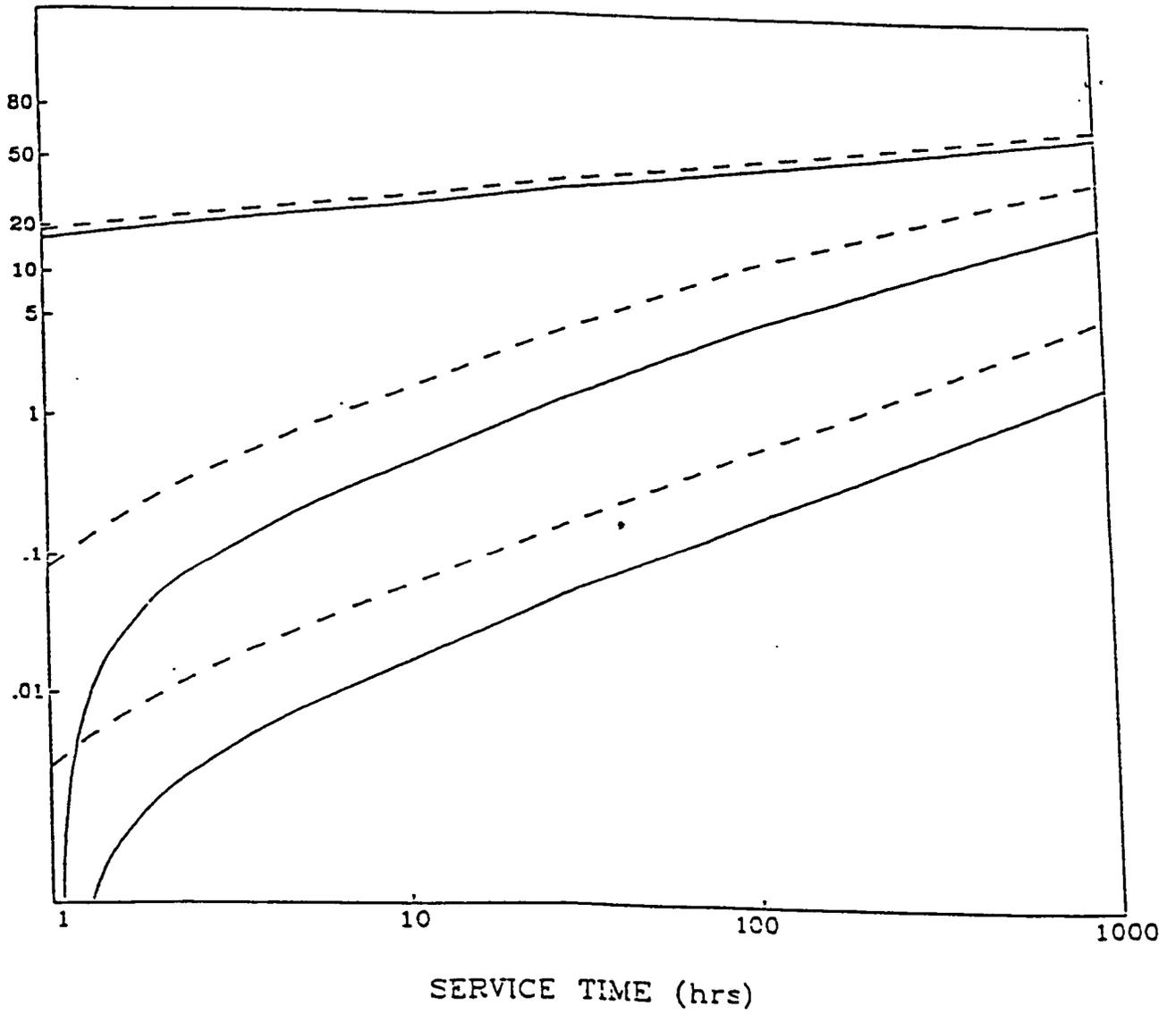
Figure E7-F3.--Probability of failure vs. service time for case (3). Solid lines denote volume flaw analysis; dashed lines denote surface flaw analysis; (t_p = proof test time).

TABLE E7-T7. FAILURE PROBABILITIES FOR PROOF-TESTED BEAM--CASE 4 (VOLUME FLAW ANALYSIS)

Batdorf Model
Noncoplanar strain energy release rate criterion
(Penny-shaped crack)

[NGP=15; IKBAT=1; $\overline{C}$=0.82; m_V=7.65; σ_{oV}=74.79 MPa(m)$^{3/7.65}$; N=30; B=320 MPa^2 hr]

| Service time, hrs | CARES/LIFE Failure Probability | | | | |
| | Proof test time, t_p, hrs | | | | |
	No proof testing	0.1	1.0	10.0	100.0
0.0	0.02836	0.01050	0.004926	0.001367	0.0002749
0.1	0.09214	0.06751	0.05379	0.03543	0.01682
1.0	0.1654	0.1392	0.1227	0.09817	0.06511
10.0	0.2876	0.2622	0.2452	0.2177	0.1762
100.0	0.4706	0.4497	0.4349	0.4101	0.3690
1000.0	0.6976	0.6838	0.6740	0.6572	0.6285

TABLE E7-T8. FAILURE PROBABILITIES FOR PROOF-TESTED BEAM--CASE 4 (SURFACE FLAW ANALYSIS)

Batdorf Model
Noncoplanar strain energy release rate criterion
(Semi-circular crack)

[NGP=15; IKBAT=1; $\overline{C}$=0.82; m_S=7.65; σ_{oS}=232.0 MPa(m)$^{2/7.65}$; N=30; B=320 MPa^2 hr]

Service time, hrs	CARES/LIFE Failure Probability				
	Proof test time, t_p, hrs				
	No proof testing	0.1	1.0	10.0	100.0
0.0	0.03105	0.01787	0.01062	0.003659	0.0007885
0.1	0.1046	0.08966	0.07925	0.06228	0.03769
1.0	0.1868	0.1720	0.1612	0.1431	0.1132
10.0	0.3215	0.3082	0.2982	0.2809	0.2514
100.0	0.5169	0.5068	0.4990	0.4854	0.4613
1000.0	0.7445	0.7389	0.7345	0.7266	0.7124
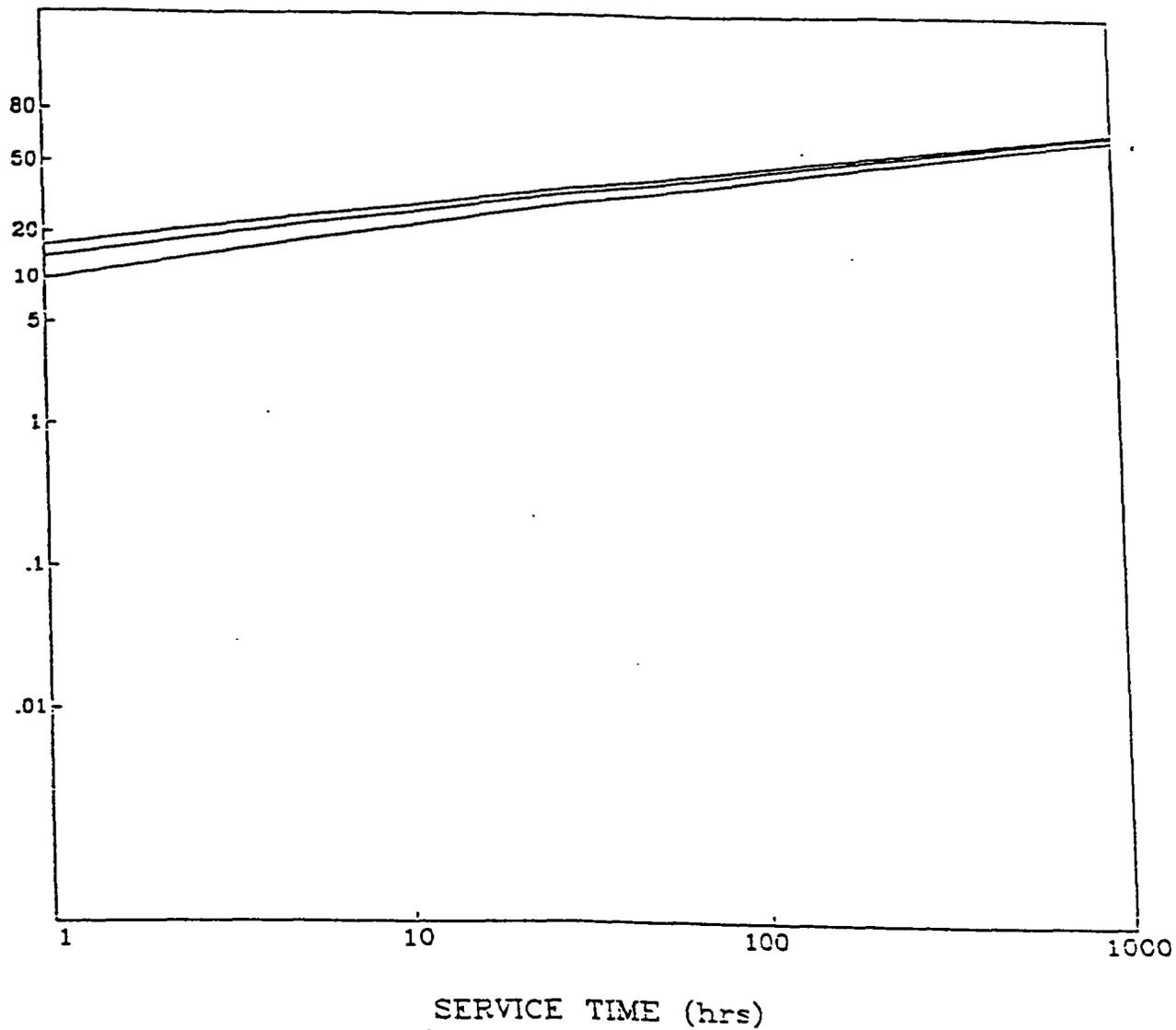
Figure E7-F4.--Probability of failure vs. service time for volume flaw analysis for case (4); (t_p = proof test time).

Example Guide

This section is intened to aid the user in preparing the files associated with the finite element analysis, the finite element interface, the parameter estimation module, and the reliability analysis module for execution of the example problems presented in this manual. The disks included with the CARES/LIFE program contain sample files associated with each example problem. These files typically represent one complete execution of the CARES/LIFE program. Also included are the input and output files for a finite element analysis (using MSC/NASTRAN) where required, and where disk space permits. The following tables provide a list of the files which are included, along with a brief description of the contents of each file. Additional information may be obtained by referring to the individual example problems presented in this manual.

Example 1 - Statistical Material Parameter Estimation

Filename	Contents	Description
1_PEST.INP	C4PEST module input file	This file contains the input required to estimate Weibull statistical material parameters from 4-point bend fast-fracture data with module C4PEST.
1_PEST.OUT	C4PEST module output file	This file contains the results of the C4PEST statistical material parameter estimation.

Example 2 - Internally Heated and Pressurized Tube

Filename	Contents	Description
2_NAS.INP	NASTRAN input file	This file contains the input required to perform an MSC/NASTRAN finite element analysis for an internally heated and pressurized tube.
2_NAS.OUT[1]	NASTRAN output file	This file contains the output from an MSC/NASTRAN finite element analysis of an internally heated and pressurized tube.
2.NEU[2]	NASCARES module output file	This file is a neutral data base containing the element/subelement stresses, temperatures, and volumes/areas for subsequent reliability analysis with module C4LIFE. This file is obtained when the results of the MSC/NASTRAN finite element analysis are processed by the NASCARES interface module.
2_PEST.INP	C4PEST module input file	This file contains the specimen rupture data required to estimate the fast-fracture statistical material parameters using module C4PEST.
2_PEST.OUT	C4PEST module output file	This file contains the results of the fast-fracture statistical material parameter estimation using module C4PEST.
2_LIFE.INP	C4PEST module output file C4LIFE module input file	This file contains the input required to perform a fast-fracture surface area reliability analysis for an internally heated and pressurized tube with module C4LIFE. This file is obtained when the parameter estimation module C4PEST is executed.
2_LIFE.OUT	C4LIFE module output file	This file contains the results of the C4LIFE surface area reliability analysis for an internally heated and pressurized tube.

[1] This file is not provided due to disk space limitations.
[2] This file only contains shell element information (for surface flaw analysis). The entire file is not given due to disk space limitations.

Example 3 - Fatigue Parameter Estimation

Filename	Contents	Description
3_NAS.INP	NASTRAN input file	This file contains the input required to perform an MSC/NASTRAN finite element analysis for a ring-on-ring loaded square plate specimen.
3_NAS.OUT[1]	NASTRAN output file	This file contains the output from an MSC/NASTRAN finite element analysis of a ring-on-ring loaded square plate specimen.
3.NEU[2]	NASCARES module output file	This file is a neutral data base containing the element/subelement stresses, temperatures, and volumes/areas for subsequent reliability analysis with module C4LIFE. This file is obtained when the results of the MSC/NASTRAN finite element analysis are processed by the NASCARES interface module.
3_PEST.INP	C4PEST module input file	This file contains the input required for module C4PEST to determine the fast-fracture Weibull parameters and the fatigue parameters.
3_PEST.OUT	C4PEST module output file	This file contains the results of the parameter estimation using module C4PEST.
3_LIFE.INP	C4PEST module output file C4LIFE module input file	This file contains the input required for module C4LIFE to numerically evaluate the specimen effective areas and to calculate the scale parameter σ_{oS} and the fatigue constant B_{Bs} using Weibull parameters estimated from fatigue and fast-fracture data. This file is obtained when the parameter estimation module C4PEST is executed.
3_LIFE.OUT	C4LIFE module output file	This file contains the results obtained from the C4LIFE reliability analysis module to estimate the specimen effective area. The calculated value is manually input into file 3_PEST.INP using keywords VAGAGE and VAGTIM.

[1] This file is not provided due to disk space limitations.
[2] This file only contains shell element information (for surface flaw analysis). The entire file is not given due to disk space limitations.

Example 4 - Cyclic Fatigue and R-ratio Sensitivity

Filename	Contents	Description
4.NEU	NASCARES module output file	This file is a neutral data base containing the element/subelement stresses, temperatures, and volumes/areas for subsequent reliability analysis with module C4LIFE. This file contains the output for a single shell element loaded in uniform tension with an area equal to the specimen gauge area. Although this file was manually constructed, it represents the results obtained when a finite element analysis is processed by an interface module.
4_PEST_A.INP 4_PEST_B.INP 4_PEST_C.INP	C4PEST module input files	These files contain the input required for module C4PEST to determine the fast-fracture Weibull parameters and the fatigue parameters. The "A" file contains the specimen rupture data for all R-ratios. The "B" file contains the specimen rupture data for R = 0.8 and uses the Walker law. The "C" file contains the specimen rupture data for R = 0.8 and uses the power law.
4_PEST_A.OUT 4_PEST_B.OUT 4_PEST_C.OUT	C4PEST module output files	These files contain the results of the parameter estimation using module C4PEST for the "A", "B", and "C" files.
4_LIFE_B.INP 4_LIFE_C.INP	C4PEST module output files C4LIFE module input files	These files contain the input required to perform a reliability analysis with module C4LIFE. These files are obtained when the parameter estimation module C4PEST is executed for the "A", "B", and "C" files.
4_LIFE_B.OUT 4_LIFE_C.OUT	C4LIFE module output files	These files contain the results of the C4LIFE reliability analysis using the Walker law (file "A") and the power law (file "B") extrapolated for R = 0.0 stress ratio.

Example 5A - Isothermal Rotating Annular Disk (Constant Angular Speed)

Filename	Contents	Description
5A_NAS.INP	NASTRAN input file	This file contains the input required to perform an MSC/NASTRAN finite element analysis for an annular disk rotating at a constant angular speed of 90 000 rpm.
5A_NAS.OUT	NASTRAN output file	This file contains the output from an MSC/NASTRAN finite element analysis of an annular disk rotating at a constant angular speed of 90 000 rpm.
5A.NEU	NASCARES module output file	This file is a neutral data base containing the element/subelement stresses, temperatures, and volumes/areas for subsequent reliability analysis with module C4LIFE. This file is obtained when the results of the MSC/NASTRAN finite element analysis are processed by the NASCARES interface module.
5A_LIFE.INP	C4LIFE module input file	This file contains the input required for module C4LIFE to perform a time-dependent reliability analysis for an annular disk rotating at a constant angular speed of 90 000 rpm.
5A_LIFE.OUT	C4LIFE module output file	This file contains the results of the C4LIFE time-dependent reliability analysis for an annular disk rotating at a constant angular speed of 90 000 rpm.

Example 5B - Isothermal Rotating Annular Disk (Cyclic Angular Speed)

Filename	Contents	Description
5B_NAS.INP	NASTRAN input file	This file contains the input required to perform an MSC/NASTRAN finite element analysis for an annular disk rotating at 80 000 rpm (the maximum cyclic speed for a sinusoidal cyclic angular speed varying from 60 000 rpm to 80 000 rpm).
5B_NAS.OUT	NASTRAN output file	This file contains the output from an MSC/NASTRAN finite element analysis of an annular disk rotating at a 80 000 rpm (the maximum cyclic speed for a sinusoidal cyclic angular speed varying from 60 000 rpm to 80 000 rpm).
5B.NEU	NASCARES module output file	This file is a neutral data base containing the element/subelement stresses, temperatures, and volumes/areas for subsequent reliability analysis with module C4LIFE. This file is obtained when the results of the MSC/NASTRAN finite element analysis are processed by the NASCARES interface module.
5B_LIFE.INP	C4LIFE module input file	This file contains the input required for module C4LIFE to perform a time-dependent reliability analysis for an annular disk rotating at a sinusoidal cyclic angular speed varying from 60 000 rpm to 80 000 rpm.
5B_LIFE.OUT	C4LIFE module output file	This file contains the results of the C4LIFE time-dependent reliability analysis for an annular disk rotating at a sinusoidal cyclic angular speed varying from 60 000 rpm to 80 000 rpm.

Example 6 - Thermomechanically Loaded Rotating Annular Disk

Filename	Contents	Description
6_NAS.INP	NASTRAN input file	This file contains the input required to perform an MSC/NASTRAN finite element analysis for a thermomechanically loaded annular disk rotating at a constant angular speed of 3000 rpm.
6_NAS.OUT	NASTRAN output file	This file contains the output from an MSC/NASTRAN finite element analysis of a thermomechanically loaded annular disk rotating at a constant angular speed of 3000 rpm.
6.NEU	NASCARES module output file	This file is a neutral data base containing the element/subelement stresses, temperatures, and volumes/areas for subsequent reliability analysis with module C4LIFE. This file is obtained when the results of the MSC/NASTRAN finite element analysis are processed by the NASCARES interface module.
6_LIFE.INP	C4LIFE module input file	This file contains the input required for module C4LIFE to perform a time-dependent reliability analysis for a thermomechanically loaded annular disk rotating at a constant angular speed of 3000 rpm.
6_LIFE.OUT	C4LIFE module output file	This file contains the results of the C4LIFE time-dependent reliability analysis for a thermomechanically loaded annular disk rotating at a constant angular speed of 3000 rpm.

Example 7 - Proof Testing

Filename	Contents	Description
7_PT_NAS.INP	NASTRAN input file	This file contains the input required to perform an MSC/NASTRAN finite element analysis for a beam subjected to a pure tension proof test load condition.
7_SB_NAS.INP	NASTRAN input file	This file contains the input required to perform an MSC/NASTRAN finite element analysis for a beam subjected to a pure bend service load condition.
7_PT_NAS.OUT[1]	NASTRAN output file	This file contains the output from an MSC/NASTRAN finite element analysis of a beam subjected to a pure tension proof test load condition.
7_SB_NAS.OUT[1]	NASTRAN output file	This file contains the output from an MSC/NASTRAN finite element analysis of a beam subjected to a pure bend service load condition.
7_PT.NEU	NASCARES module output file	This file is a neutral data base containing the element/subelement stresses, temperatures, and volumes/areas for the proof test load condition for subsequent reliability analysis with module C4LIFE. This file is obtained when the results of the MSC/NASTRAN finite element analysis are processed by the NASCARES interface module.
7_SB.NEU	Neutral file created by NASCARES module	This file is a neutral data base containing the element/subelement stresses, temperatures, and volumes/areas for the service load condition for subsequent reliability analysis with module C4LIFE. This file is obtained when the results of the MSC/NASTRAN finite element analysis are processed by the NASCARES interface module.
7_LIFE.INP	C4LIFE module input file	This file contains the input required for module C4LIFE to perform a time-dependent reliability analysis including the results of proof testing.
7_LIFE.OUT	C4LIFE module output file	This file contains the results of the C4LIFE time-dependent reliability analysis including the effects of proof testing.

[1]This file is not provided due to disk space limitations.

Appendix A
Cyclic Fatigue (g-factor) Examples

Example 1: Simple Boundary Periodic Rectangular Loading (Table 1)

$$g = \frac{\int_0^{t_1+t_{11}} \left(\frac{\sigma_{Ieqc}(t)}{\sigma_1}\right)^N dt}{t_1+t_{11}} = \frac{t_1 + \left(\frac{\sigma_{11}}{\sigma_1}\right)^N t_{11}}{t_1+t_{11}}$$

where

$$\sigma_{Ieq} = \sigma_1 \left[\frac{t_1 + \left(\frac{\sigma_{11}}{\sigma_1}\right)^N t_{11}}{t_1+t_{11}}\right]^{\frac{1}{N}}$$

Note: If the cyclic loading is a force instead of a stress, force P_1 replaces σ_1, and P_{11} replaces σ_{11}.

The equivalent static boundary force P_{eq} replaces σ_{Ieq} and

$$P_{eq} = P_1 \left[\frac{t_1 + \left(\frac{P_{11}}{P_1}\right)^N t_{11}}{t_1 + t_{11}}\right]^{\frac{1}{N}} = P_1 \, g^{\frac{1}{N}}$$

From this equivalent static boundary load σ_{Ieq} (or P_{eq}), we compute the stress distribution throughout the component (specimen), $\sigma_{Ieq}(\Psi)$. To obtain the probability of failure of a component at time $t=t_0$, the transformation of $\sigma_{Ieq}(\Psi)$ at some time t_0 to its equivalent value $\sigma_{Ieq,0}(\Psi)$ at $t=0$ is

$$\sigma_{Ieq,0}(\Psi) = \left[\frac{\sigma_{Ieq}^N(\Psi)\, t_0}{B} + \sigma_{Ieq}^{N-2}(\Psi)\right]^{\frac{1}{N-2}}$$

From this transformed boundary load, the probability of failure is obtained for time $t=t_0$, using the appropriate equation.

Example 2: Sinusoidal Loading (Table 1)

$$\sigma_{Ieqc}(t) = \left[\frac{\sigma_1 + \sigma_{11}}{2} + \frac{\sigma_1 - \sigma_{11}}{2} \sin \frac{2\pi t}{T} \right]$$

where

$$g = \frac{\int_0^T \left[\frac{\sigma_1 + \sigma_{11}}{2\sigma_1} + \frac{\sigma_1 - \sigma_{11}}{2\sigma_1} \sin \frac{2\pi t}{T} \right]^N dt}{T}$$

and

$$\sigma_{Ieq} = \sigma_1 \, g^{\frac{1}{N}}$$

As in example 1 , if the loads are forces P_1 and P_{11} then

$$P_{eqc}(t) = \left[\frac{P_1 + P_{11}}{2} + \frac{P_1 - P_{11}}{2} \sin \left(\frac{2\pi t}{T} \right) \right]$$

$$g = \frac{\int_0^T \left[\frac{P_1 + P_{11}}{2 P_1} + \frac{P_1 - P_{11}}{2 P_1} \sin \left(\frac{2\pi t}{T} \right) \right]^N dt}{T}$$

and the equivalent static load P_{eq} is

.

$$P_{eq} = P_1 \, g^{\frac{1}{N}}$$

Since N is a non-integer value, g is evaluated numerically.

To obtain the probability of failure at time $t=t_0$, as in Example 1, we compute the stress distribution $\sigma_{Ieq}(\Psi)$ throughout the component based on the equivalent static boundary stress σ_{Ieq} (or the equivalent static boundary load, P_{eq}) at location Ψ_0. Next, $\sigma_{Ieq}(\Psi)$ is transformed to $\sigma_{Ieq,0}(\Psi)$. From this transformed stress distribution, the probability of failure is obtained using the appropriate equation.

Appendix B
Neutral File Setup

```
THERMOMECHANICALLY LOADED ANNULAR DISK
COM   EXAMPLE #4 FROM THE CARES USERS MANUAL
COM
COM   EXAMPLE NEUTRAL FILE
COM
    2    0
COM      FORMAT (2I5)
COM   NUMEL  = 2   : NUMBER OF ELEMENT GROUPS
COM   NUMELB = 0   : FLAG FOR SHELL ELEMENT GROUPS WITH VOLUME PROCESSING
COM                 NUMELB STILL IN EXPERIMENTAL STAGES!!
COM                 FOR THIS CASE - NO VOLUME PROCESSING OF SHELL ELEMENT GROUPS
    1    8    8    0
COM      FORMAT (4I5)
COM   INUEG  = 1   : GROUP NUMBER
COM   IEGTYP = 8   : ELEMENT TYPE --- EQUIVALENT TO PATRAN'S SHAPE PARAMETER
COM                    2 = BAR               (NOT USED WITH CARES)
COM                    3 = TRIANGLE
COM                    4 = QUADRILATERAL
COM                    5 = TETRAHEDRON
COM                    6 = PYRAMID
COM                    7 = PENTAHEDRON (WEDGE)
COM                    8 = HEXAHEDRON (BRICK)
COM   IGREL  = 8   : NUMBER OF ELEMENTS IN THIS GROUP
COM   ISHELL = 0   : SHELL ELEMENT FLAG
    1   27  302    0   0.539957E-03    0.197500E+04    0.000000E+00
COM      FORMAT (4I5,3E15.6)
COM   IELNUM =       1  : ELEMENT NUMBER
COM   ISUBEL =      27  : NUMBER OF SUBELEMENTS
COM   MATINP =     302  : MATERIAL NUMBER FOR VOLUME FLAW ANALYSIS
COM   MAT2   =       0  : MATERIAL NUMBER FOR SURFACE FLAW ANALYSIS
COM   ELVOL  = .00054   : ELEMENT VOLUME
COM   ELTEMP = 1975.0   : ELEMENT TEMPERATURE
COM   ELTHIC =    0.0   : ELEMENT THICKNESS (SET TO ZERO FOR VOLUME ELEMENTS)
    1   0.107827E-04    0.199436E+04   -0.242574E+04   -0.438490E+05   -0.495269E+04
                                       -0.361891E+04   -0.299505E+03    0.307790E+04
COM      FORMAT (I5,5E15.6,/,35X,3E15.6)
COM   ISUNUM =       1  : SUBELEMENT NUMBER
COM   SUBVOL = .00001   : SUBELEMENT VOLUME
COM   SUBTEM = 1994.4   : SUBELEMENT TEMPERATURE
COM   SSTR(L),L=1,6     : STRESSES          SIGX            SIGY            SIGZ
COM                                         SIGXY           SIGYZ           SIGZX
    2   0.185592E-04    0.197500E+04   -0.411254E+04   -0.343776E+05    0.946542E+04
                                       -0.251220E+04    0.240778E+03   -0.217892E+04
    3   0.124163E-04    0.195564E+04   -0.579934E+04   -0.249061E+05    0.238835E+05
                                       -0.140549E+04    0.781060E+03   -0.743573E+04
    4   0.171642E-04    0.199437E+04   -0.242574E+04   -0.438490E+05   -0.495269E+04
                                       -0.122070E-03    0.000000E+00    0.307790E+04
    5   0.295430E-04    0.197500E+04   -0.411254E+04   -0.343776E+05    0.946542E+04
                                        0.000000E+00    0.000000E+00   -0.217892E+04
    6   0.197646E-04    0.195564E+04   -0.579934E+04   -0.249061E+05    0.238835E+05
                                       -0.152588E-04    0.476837E-05   -0.743573E+04
    7   0.107827E-04    0.199436E+04   -0.242574E+04   -0.438490E+05   -0.495269E+04
                                        0.361892E+04    0.299505E+03    0.307790E+04
    8   0.185589E-04    0.197500E+04   -0.411254E+04   -0.343776E+05    0.946542E+04
                                        0.251220E+04   -0.240778E+03   -0.217892E+04
    9   0.124161E-04    0.195564E+04   -0.579934E+04   -0.249061E+05    0.238835E+05
```

```
                                            0.140549E+04  -0.781060E+03  -0.743573E+04
     10    0.172524E-04    0.199437E+04   -0.242574E+04  -0.438490E+05  -0.495269E+04
                                           -0.361892E+04  -0.762939E-05   0.915527E-04
     11    0.296951E-04    0.197500E+04   -0.411254E+04  -0.343776E+05   0.946542E+04
                                           -0.251220E+04   0.953674E-05  -0.106812E-03
     12    0.198662E-04    0.195564E+04   -0.579934E+04  -0.249061E+05   0.238835E+05
                                           -0.140549E+04  -0.286102E-05  -0.209808E-03
     13    0.274625E-04    0.199436E+04   -0.242574E+04  -0.438490E+05  -0.495269E+04
                                            0.000000E+00   0.000000E+00   0.122070E-03
     14    0.472688E-04    0.197500E+04   -0.411254E+04  -0.343776E+05   0.946542E+04
                                            0.000000E+00   0.000000E+00   0.610352E-04
     15    0.316233E-04    0.195564E+04   -0.579934E+04  -0.249061E+05   0.238835E+05
                                            0.000000E+00  -0.190735E-05  -0.320435E-03
     16    0.172523E-04    0.199437E+04   -0.242574E+04  -0.438490E+05  -0.495269E+04
                                            0.361891E+04   0.000000E+00   0.000000E+00
     17    0.296945E-04    0.197500E+04   -0.411254E+04  -0.343776E+05   0.946542E+04
                                            0.251220E+04  -0.152588E-04  -0.122070E-03
     18    0.198660E-04    0.195564E+04   -0.579934E+04  -0.249061E+05   0.238835E+05
                                            0.140549E+04  -0.381470E-05  -0.732422E-03
     19    0.107826E-04    0.199436E+04 . -0.242574E+04  -0.438490E+05  -0.495269E+04
                                           -0.361891E+04   0.299505E+03  -0.307790E+04
     20    0.185594E-04    0.197500E+04   -0.411254E+04  -0.343776E+05   0.946542E+04
                                           -0.251221E+04  -0.240778E+03   0.217892E+04
     21    0.124163E-04    0.195564E+04   -0.579934E+04  -0.249061E+05   0.238835E+05
                                           -0.140549E+04  -0.781060E+03   0.743573E+04
     22    0.171642E-04    0.199437E+04   -0.242574E+04  -0.438490E+05  -0.495269E+04
                                           -0.122070E-03   0.000000E+00  -0.307790E+04
     23    0.295430E-04    0.197500E+04   -0.411254E+04  -0.343776E+05   0.946542E+04
                                            0.000000E+00   0.000000E+00   0.217892E+04
     24    0.197646E-04    0.195564E+04   -0.579934E+04  -0.249061E+05   0.238835E+05
                                           -0.152588E-04  -0.381470E-05   0.743573E+04
     25    0.107826E-04    0.199436E+04   -0.242574E+04  -0.438490E+05  -0.495269E+04
                                            0.361891E+04  -0.299505E+03  -0.307790E+04
     26    0.185591E-04    0.197500E+04   -0.411254E+04  -0.343776E+05   0.946542E+04
                                            0.251220E+04   0.240778E+03   0.217892E+04
     27    0.124161E-04    0.195564E+04   -0.579934E+04  -0.249061E+05   0.238835E+05
                                            0.140549E+04   0.781060E+03   0.743573E+04
      2    27   300     0  0.137444E-02    0.192500E+04   0.000000E+00
      1    0.262589E-04    0.194436E+04   -0.181920E+04  -0.754958E+05  -0.213713E+05
                                           -0.618627E+04   0.290242E+03  -0.257061E+04

        .
        .
        .

     27   -0.565651E-03    0.131127E+04   -0.111869E+04  -0.230136E+03  -0.194717E+04
                                           -0.985361E+02  -0.836775E+01  -0.749014E+02
      2     4    18     1
    100     9     0   302  0.359971E-02    0.197500E+04   0.100000E-05
COM       FORMAT (4I5,3E15.6)
COM    IELNUM =     100  : ELEMENT NUMBER
COM    ISUBEL =       9  : NUMBER OF SUBELEMENTS
COM    MATINP =       0  : MATERIAL NUMBER FOR VOLUME FLAW ANALYSIS
COM    MAT2   =     302  : MATERIAL NUMBER FOR SURFACE FLAW ANALYSIS
COM    ELVOL  = .00360  : ELEMENT AREA
COM    ELTEMP = 1975.0  : ELEMENT TEMPERATURE
COM    ELTHIC = 1.0E-6  : ELEMENT THICKNESS
      1    0.258785E-03    0.199436E+04    0.715319E+03  -0.410745E+05   0.432249E+03
COM       FORMAT (I5,5E15.6)
COM    ISUNUM =       1  : SUBELEMENT NUMBER
COM    SUBVOL = .00026  : SUBELEMENT AREA
COM    SUBTEM = 1994.4  : SUBELEMENT TEMPERATURE
COM    SSTR(L),L=1,3    : STRESSES          SIGX           SIGY           SIGXY
      2    0.445423E-03    0.197500E+04   -0.592114E+04  -0.363226E+05   0.398923E+03
```

3	0.297991E-03	0.195564E+04	-0.125576E+05	-0.315707E+05	0.365598E+03
4	0.411939E-03	0.199436E+04	0.715319E+03	-0.410745E+05	0.000000E+00
5	0.709031E-03	0.197500E+04	-0.592114E+04	-0.363226E+05	0.000000E+00
6	0.474350E-03	0.195564E+04	-0.125576E+05	-0.315707E+05	-0.381470E-05
7	0.258784E-03	0.199436E+04	0.715319E+03	-0.410745E+05	-0.432249E+03
8	0.445415E-03	0.197500E+04	-0.592114E+04	-0.363226E+05	-0.398923E+03
9	0.297990E-03	0.195564E+04	-0.125576E+05	-0.315707E+05	-0.365598E+03
101 9 0 300	0.916289E-02	0.192500E+04	0.100000E-05		
1	0.630212E-03	0.194436E+04	0.650431E+04	-0.673899E+05	0.293382E+03
.					
.					
.					
7	0.450427E-02	0.130000E+04	0.639825E+03	-0.100347E+04	0.509900E+00
8	0.177071E-02	0.130000E+04	0.639825E+03	-0.100347E+04	0.000000E+00
9	0.524055E-02	0.130000E+04	0.639825E+03	-0.100347E+04	-0.509900E+00
130 9 0 302	0.981743E-02	0.200000E+04	0.100000E-05		
1	0.759243E-03	0.200000E+04	-0.437730E+05	-0.796470E+04	0.105466E+02
2	0.120858E-02	0.200000E+04	-0.437730E+05	-0.796470E+04	0.000000E+00
3	0.759245E-03	0.200000E+04	-0.437730E+05	-0.796470E+04	-0.105466E+02
4	0.121479E-02	0.200000E+04	-0.437730E+05	-0.796470E+04	0.000000E+00
5	0.193372E-02	0.200000E+04	-0.437730E+05	-0.796470E+04	0.000000E+00
6	0.121479E-02	0.200000E+04	-0.437730E+05	-0.796470E+04	-0.119209E-06
7	0.759241E-03	0.200000E+04	-0.437730E+05	-0.796470E+04	-0.105466E+02
8	0.120858E-02	0.200000E+04	-0.437730E+05	-0.796470E+04	0.000000E+00
9	0.759246E-03	0.200000E+04	-0.437730E+05	-0.796470E+04	0.105466E+02

.

APPENDIX C
SYMBOLS

A   surface area; material-environmental fatigue constant

A^2 Anderson-Darling goodness-of-fit test statistic

a   crack half length; penny-shaped crack radius; radius of semi-circular surface crack

B   risk of rupture; subcritical crack growth constant

b   the intersection of a line with the ordinate axis

$\overline{C}$ Shetty's constant in mixed-mode fracture criterion

c   the contour of a unit radius circle in two-dimensional principal stress space

D   Kolmogorov-Smirnov goodness-of-fit test statistic defined as D^+ or D^-, whichever is the largest

D^+, D^- Kolmogorov-Smirnov goodness-of-fit test statistic

E   Young's modulus of elasticity

F(x)   cumulative distribution function of a random variable

$F_N(x)$ empirical distribution function

G   strain energy release rate

g   g-factor

H   step function

h   total height of four-point bend bar with rectangular cross section

i   ranking of ordered fracture data in statistical analysis

J   Jacobian operator

K   stress intensity factor

K(n)   Kanofsky-Srinivasan confidence band factors

k   crack density coefficient; any counter

L	likelihood function
L_1	length between outer loads in four-point bending
L_2	length between symmetrically applied inner loads in four-point bending
ℓ,m,n	direction cosines of oblique plane normal in principal stress space for the Cauchy infinitesimal tetrahedron
m	Weibull modulus, or shape parameter
N	material-environmental fatigue constant; Weibull crack density function; number of flaws per unit volume or area
n	number of links in a structure; any counter; number of cycles; number of four-point bend specimens at a given temperature
P	load applied to four-point bend bar specimen
P_f	cumulative failure probability
P_1	probability of existence in incremental volume or area of a crack with strength $\leq \sigma_{cr}$
P_2	probability of crack with strength $\leq \sigma_{cr}$ being so oriented that $\sigma_e \geq \sigma_{cr}$
R	ratio of minimum to maximum effective stress in a loading cycle
r	number of remaining specimens in censored data analysis
r,s,t	finite element natural coordinates
r_i	inside radius
r_0	outside radius
T	period of one cycle
t	time; thickness
t_0	time-dependent scale parameter
V	volume
v	velocity

w	total width of four-point bend bar with rectangular cross section
x	any variable
X	ordered statistics
x,y,z	Cartesian coordinate directions
Y	crack geometry factor
Z_i	predicted failure probability at the fracture strength of the ith specimen
α	angle between σ_n and the stress σ_1; significance level
β	angle between σ_n projection and the stress σ_2 in plane perpendicular to σ_1
Γ	gamma function which is tabulated in mathematical handbooks
Δ	increment
δ	increment
ν	material Poisson's ratio
π	3.1416
Σ	applied multidimensional stress state
σ	applied stress distribution; the traction or stress vector on oblique plane of Cauchy infinitesimal tetrahedron
σ_o	Weibull scale parameter
$\sigma_1, \sigma_2, \sigma_2$	tensor stress components; principal stresses ($\sigma_1 \geq \sigma_2 \geq \sigma_3$)
τ	shear stress acting on oblique plane whose normal is determined by angles α and β
Ψ	spatial location (x,y,z) and orientation (α,β) in a component
Ω	solid angle in three-dimensional principal stress space for which $\sigma_e \geq \sigma_{cr}$
ω	angle in two-dimensional principal stress space for which $\sigma_e \geq \sigma_{cr}$; angular speed

Subscripts:

a	applied or service load

B	Batdorf
c	cyclic; critical
ch	characteristic
cr	critical
d	dynamic fatigue
e	effective
ef	effective
eq	equivalent
f	failure; fracture
g	gage
I	inert
I	crack opening mode
II	crack sliding mode
III	crack tearing mode
i	i'th; combined service and proof test loading
max	maximum
min	minimum
n	normal; normal stress averaging
p	polyaxial; proof test
Q	total or combined
s	survival; service
S	surface
T	transformed
u	uniaxial

V volume

w Weibull

θ characteristic

Superscripts:

ʹ inert distribution parameter estimated from fatigue data

^ estimated parameter

~ modified parameter

‾ normalized quantity

·

REFERENCES

A   Abernethy, R.B. et al.: Weibull Analysis Handbook. PWA&GPD-FR-17579, Pratt and Whitney Aircraft, Nov. 1983. (Avail. NTIS, AD-A143100).

B   Baratta, F.I.; Matthews, W.T.; and Quinn, G.D.: Errors Associated with Flexure Testing of Brittle Materials. MTL-TR-87-35, U.S. Army Materials Technology Laboratory, Watertown, MA, July 1987. (Avail. NTIS, AD-A187470).

Barnett, R.L., et al.: Fracture of Brittle Materials Under Transient Mechanical and Thermal Loading. U.S. Air Force Flight Dynamics Laboratory. AFFDL-TR-66-220, Mar. 1967.

Batdorf, S.B.; and Crose, J.G.: A Statistical Theory for the Fracture of Brittle Structures Subjected to Nonuniform Polyaxial Stresses. J. Appl. Mech., vol. 41, no. 2, June 1974, pp. 459-464.

Batdorf, S.B.: Fracture Statistics of Polyaxial Stress States. Fracture Mechanics, N. Perrone, et al., eds., University Press of Virgina, 1976, pp. 579-591.

Batdorf, S.B.: Some Approximate Treatments of Fracture Statistics for Polyaxial Tension. Int. J. Fract., vol. 13, no. 1, Feb. 1977, pp. 5-11.

Batdorf, S.B.; and Heinisch, H.L., Jr.: Weakest Link Theory Reformulated for Arbitrary Fracture Criterion. J. Am. Ceram. Soc., vol. 61, no. 7-8, July-Aug. 1978, pp. 355-358.

Batdorf, S.B.; and Heinisch, H.L., Jr.: Fracture Statistics of Brittle Materials with Surface Cracks. Eng. Frac. Mech., vol. 10, 1978, pp. 831-841.

Batdorf, S.B.: "Fundamentals of the Statistical Theory of Fracture". Fracture Mechanics of Ceramics, vol. 3, eds. Bradt, R.C.; Hasselman, D.P.H; Lange, F. F.: Plenum Press, N.Y.,1978, pp 1-30.

Batdorf, S.B.: Comparison of the Best Known Fracture Criteria. Absorbed Specific Energy and/or Strain Energy Density Criterion, G. Sih, E. Czoboly, and F. Gillemot, eds., Martinus Nijhoff Publishers, 1982, pp. 243-251.

Bathe, K.J.: Finite Element Procedures in Engineering Analysis. Prentice-Hall, Englewood Cliffs, New Jersey. 1982.

Boehm, F.: A Stress-Strength Interference Approach to Fast and Delayed Fracture Reliability Analysis for Ceramic Components. Ph.D. dissertation, Northwestern University, U.S.A., 1989.

Boulet, J.A.M.: An assessment of the State of the Art in Predicting the Failure of Ceramics. ORNL/SUB-86-57598/1, Mar. 1988.

Brockenbrough, J.R.; Forsythe, L.E.; and Rolf, R.L.: Reliability of Brittle Materials in Thermal Shock. J. Am. Ceram. Soc., vol. 69, no. 8, Aug. 1986, pp. 634-637. (Alcoa Laboratories, Rept. No. 52-85-22).

Bruckner-Foit, A.; and Munz, D.: Statistical Analysis of Flexure Strength Data, IEA Annex II, Subtask 4. Institute fur Zuverlassigkeit und Schadenskunde in Maschinenbau University of Karlsruhe, P.O. Box 3640, D-7500 Karlsruhe, West Germany, 1988.

Bruckner-Foit, A; Heger, A.; and Munz, D.: Effect of Proof Testing on the Failure Probability of Multiaxially Loaded Ceramic Components. Life Prediction Methodologies and Data for Ceramic Materials, ASTM STP 1201. Brinkman, C.R.; Duffy, S.F., eds., to be published.

C   Carnahan, B.; Luther, H.A.; and Wilkes, J.D.: Applied Numerical Methods, John Wiley and Sons, Inc. 1969.

Case, W.R.; and Vandegrift, R.E.: Accuracy of Three Dimensional Solid Finite Elements. Twelfth NASTRAN Users' Colloquium, NASA CP-2328, 1984, pp. 26-46.

Ceramic Technology for Advanced Heat Engines Project, Semiannual Progress Report Oct. 1986-Mar. 1987. ORNL/TM-10469, Martin Marietta Energy Systems Inc., Oak Ridge, TN, 1987.

D   D'Agostino, R.B.; and Stephens, M.A., eds.: Goodness-of-Fit Techniques. Marcel Dekker, 1986, pp. 97-193.

Daniels, H.E.: The Statistical Theory of the Strength of Bundles of Threads. I. Proc. R. Soc. London A, vol. 183 1945, pp. 405-435.

Dauskardt, R.H.; Marshall, D.B.; and Ritchie, R.O.: Cyclic Fatigue Crack Propagation in Mg-PSZ Ceramics. J. Am. Cer. Soc., vol. 73, no.4, 1990, pp. 893-903.

Dauskardt, R.H.; James, M.R.; Porter, J.R.; and Ritchie, R.O.: Cyclic Fatigue-Crack Growth in a SiC-Whisker-Reinforced Alumina Ceramic Composite: Long- and Small-Crack Behavior. J. Am. Ceram. Soc., vol. 75, no. 4, 1992, pp.759-771.

Davies, D.G.S.: The Statistical Approach to Engineering Design in Ceramics. Proc. Br. Ceram. Soc., no. 22, 1973, pp. 429-452.

DeSalvo, G.J.: Theory and Structural Design Application of Weibull Statistics, WANL-TME-2688, Westinghouse Astronuclear Lab., 1970.

Dukes W.H.: Handbook of Brittle Material Design Technology, AGARDograph 152, AGARD, Paris, France, 1971.

E   Edwards, M. J.; Powers, L. M.; Stevenson, I.: ABACARES, ABAQUS Users' conference Proceedings, Providence, RI, May 1992.

Erdogan, F.; and Sih, G.C.: Crack Extension in Plates Under Plane Loading and Transverse Shear. J. of Basic Engineering, vol. 85, 1963, pp. 519-527.

Evans, A.G.; and Wiederhorn, S.M.: Crack Propagation and Failure Prediction in Silicon Nitride at Elevated Temperature. J. of Mat. Sci., vol. 9, 1974, pp. 270-278.

Evans, A.G.; and Wiederhorn, S.M.: Proof Testing of Ceramic Materials-An Analytical Basis for Failure Prediction. Int. J. of Fracture, vol. 10, no. 3, 1974.

Evans, A.G.; and Jones, R.L.: Evaluation of a Fundamental Approach for the Statistical Analysis of Fracture, J. Am. Ceram. Soc., vol. 61, no. 3-4, Mar.-Apr. 1978, pp. 156-160.

Evans, A.G.:Fatigue in Ceramics. Int. J. of Fracture, Dec. 1980, pp.485-498.

F Fett, T.; and Munz, D.: Differences Between Static and Cyclic Fatigue Effects in Alumina. submitted to J. of Mat. Sci. Letters, 1992.

Frenkel, J.I.; and Kontorova, T.A.: A Statistical Theory of the Brittle Strength of Real Crystals. J. Phys. USSR, vol. 7 no. 3, 1943, pp. 108-114.

Freudenthal, A.M.: Statistical Approach to Brittle Fracture. Fracture, An Advanced Treatise, Vol. 2, Mathematical Fundamentals, H. Liebowitz, ed., Academic Press, 1968, pp. 591-619.

G Giovan, M.N.; and Sines, G.: Biaxial and Uniaxial Data for Statistical Comparison of a Ceramic's Strength. J. Am. Ceram. Soc., vol. 62, no. 9, Sept. 1979, pp. 510-515.

Griffith, A.A.: The Phenomena of Rupture and Flow in Solids. Philos. Trans. R. Soc. London A, vol. 221, 1921, pp. 163-198.

Griffith, A.A.: The Theory of Rupture. Proceedings of the 1st International Congress for Applied Mechanics, C.B. Biezeno and J.M. Burgers, eds., Delft, 1924, pp. 55-63.

Gross, B., and Gyekenyesi, J.P.: Weibull Crack Density Coefficient for Polydimensional Stress States, J. Am. Ceram. Soc., vol. 72, no. 3, Mar. 1989, pp. 506-507.

Gyekenyesi, J.P.: SCARE: A Postprocessor Program to MSC/NASTRAN for the Reliability Analysis of Structural Ceramic Components. J. Eng. Gas Turbines Power, vol. 108, no. 3, July 1986, pp. 540-546.

Gyekenyesi, J.P.; and Nemeth, N.N.: Surface Flaw Reliability Analysis of Ceramic Components with the SCARE Finite Element Postprocessor Program. J. Eng. Gas Turbines Power, vol. 109, no. 3, July 1987, pp. 274-281.

H Hamada, S.; and Teramae, T.: Reliability Evaluation System for Ceramic Gas Turbine Components. Japan Soc. of Mat. Sci. Jrnl., (ISSN 0514-5163), vol.39, Jan. 1990, pp. 76-81.

Hamanaka, J.; Suzuki, A.; and Saki, K.: Structural Reliability Evaluation of Ceramic Components. J. of the European Ceram. Soc., 1990, pp. 375-381.

Hellen, T.K.; and Blackburn, W.S.: Calculation of Stress Intensity Factors for Combined Tensile and Shear Loading. Int. J. of Frac., vol. 11, 1975, pp. 605-613.

Horibe, S.; and Hirahara, R.: Cyclic Fatigue of Ceramic Materials: Influence of Crack Path and Fatigue Mechanisms. Acta Metall. Mater., vol. 39, no. 6, 1991, pp. 1309-1317.

I   Ichikawa, M.: Proposal of an Approximate Analytical Expression of Maximum Energy Release Rate of a Mixed Mode Crack in Relation to Reliability Evaluation of Ceramic Components. Japan Soc. of Mat. Sci. Jrnl. (ISSN 0514-5163), vol. 40, Feb. 1991, pp. 224-227.

J   Jadaan, O.M., "Fast Fracture and Lifetime Prediction of Ceramic Tubular Components," Ph.D. Thesis, the Pennsylvania State University, University Park, PA, December 1990.

Jadaan, O.M., Shelleman, D.L., Conway, J.C., Mecholsky, J.J., and Tressler, R.E., "Prediction of the Strength of Ceramic Tubular Components: I. Analysis," Journal of Testing and Evaluation, Vol. 19, No. 3, May 1991.

Jakus, K.; Coyne, D.C.; and Ritter, J.E.: Analysis of Fatigue Data for Lifetime Predictions for Ceramic Materials. J. of Mat. Sci., vol. 13, 1978, pp. 2071-2080.

Johnson, C.A.; and Tucker, W.T.: Advanced Statistical Concepts of Fracture in Brittle Materials. Ceramic Technology Project Bimonthly Technical Progress Report to DOE Office of Transportation Technologies, December 1991 - January 1992. ORNL/CF-92/53, UCN-2383 (3 6-88), pp. 101-112.

Johnson, L.G.: Analysis of Data Which Include Suspended Item. The Statistical Treatment of Fatigue Experiments. Elsevier Publishing Co., 1964, pp. 37-41.

K   Kanofsky, P.; and Srinivasan, R.: An Approach to the Construction of Parametric Confidence Bands on Cumulative Distribution Functions. Biometrika, vol. 59, no. 3, 1972, pp. 623-631.

Kontorova, T.A.: A Statistical Theory of Mechanical Strength. J. Tech. Phys. (USSR), vol. 10 1940, pp. 886-890.

L   Lamon, J.: Statistical Approaches to Failure for Ceramic Reliability Assessment, J. Am. Ceram. Soc., vol. 71, no. 2, Feb. 1988, pp. 106-112.

Lamon, J.: Ceramics Reliability-Statistical Analysis of Multiaxial Failure Using the Weibull Approach and the Multiaxial Elemental Strength Models, ASME Paper 88-GT-147, 1988.

Liu, K.C.; and Brinkman, C.R.: Tensile Cyclic Fatigue of Structural Ceramics. Proceedings of the 23rd Automotive Technology Development Contractors' Coordination Meeting, Society of Automotive Engineers, Warrendale, PA, 1986, pp. 279-284.

Liu, S. Y.; and Chen, I. W.: "Fatigue of Yttria-Stabilized Zirconia: I, Fatigue Damage, Fracture Origins, and Lifetime Prediction", Journal of the American Ceramic Society, Vol. 74, No. 6, pp. 1197-1205, 1991.

M   Margetson, J.: A Statistical Theory of Brittle Failure for an Anisotropic Structure Subjected to a Multiaxial Stress State, AIAA Paper 76-632, July 1976.

Mencik, J.: Rationalized Load and Lifetime of Brittle Materials. Communications of the Am. Cer. Soc., vol. 67, March 1984, pp. 110-116.

N   Neal, D.; Vangel, M.; and Todt, F.: Statistical Analysis of Mechanical Properties. Engineered Materials Handbook, Vol. 1, Composites, ASM International, Metals Park, OH, 1987, pp. 302-307.

Nelson, W.: Weibull and Extreme Value Distributions. Applied Life Data Analysis. Wiley, 1982, pp. 333-395.

Nemeth, N.N.; Manderscheid, J.M.; and Gyekenyesi, J.P.:Ceramics Analysis and Reliability Evaluation of Structures (CARES). NASA TP-2916, 1990.

O   Okabe, N.; Hirata, H.; and Muramatsu, M.: Study on Application of Unified Estimation for Ceramic Strength to Reliability Design. J. of Japan Soc. of Mat. Sci., vol. 39, 1990, pp. 393-399.

P   Pai, S.S.; and Gyekenyesi, J.P.: Calculation of the Weibull Strength Parameters and Batdorf Flaw Density Constants for Volume and Surface-Flaw-Induced Fracture in Ceramics, NASA TM-100890, 1988.

Palaniswamy, K., and Knauss, W.G., 1978, On the Problem of Crack Extension in Brittle Solids Under General Loading, Mech. Today, vol. 4, pp. 87-148.

Paluszny, A.; and Wu, W.: Probabilistic Aspects of Designing with Ceramics. J. Eng. Power, vol. 99, no. 4, Oct. 1977, pp. 617-630.

Paluszny, A.; and Nicholls, P.F.: "Predicting Time-Dependent Reliability of Ceramic Rotors". Ceramics for High Performance Applications-II. Burke, J.J.; Lenoe, E.N.; Katz, N.R., eds. Chesnut Hill, Massachusetts, Brook Hill, 1978, pp. 95-112.

Paris, P.C.; Erdogan, F.: A Critical Analysis of Crack Propagation Laws. J. Basic Eng., Trans. ASME, vol. 85, 1963, pp.528-534.

Paris, P.C.; and Sih, G.C.: Stress Analysis of Cracks. ASTM STP 381, 1965, pp. 30-83.

Paul, B.; and Mirandy, L.: An improved Fracture Criterion for Three-Dimensional Stress States, J. Eng. Mater. Technol., vol. 98, no. 2, Apr. 1976, pp. 159-163.

Petrovic, J.J.; and Stout, M.G.: Multiaxial Loading Fracture of Al_2O_3 Tubes: II, Weibull Theory and Analysis. J. Am. Ceram. Soc., vol. 67, no. 1, Jan., 1984, pp. 18-23.

Pierce, F.T.: "The Weakest Link" Theorems of the Strength of Long and of Composite Specimens. Text. Inst. J., vol. 17, 1926, pp. T355-T368.

Pintz, A.; Abumeri, G.H.; and Manderscheid, J.M.: CARES-ANSYS Structural Ceramics Reliability Analysis-Users Manual. NASA CR (not officially published).

Powers, L.M.; Starlinger, A.; and Gyekenyesi, J.P.: Ceramic Component Reliability With the Restructured NASA/CARES Computer Program. NASA TM _____, 1992

Q   Quinn, G. D., and Quinn, J. B., "Slow Crack Growth in Hot-Pressed Silicon Nitride", Fracture Mechanics of Ceramics. Bradt, R. C., Evans, A. G., Hasselman, D. P. H, and Lange, F. F., eds., Plenum Publishing Corp., Vol. 6, 1983, pp. 603-636.

R   Rufin, A.C.: A Study of Statistical Failure Prediction Models for Brittle Materials Subjected to Multiaxial States of Stress, M.S. Thesis Univ. Washington, 1981.

Rufin, A.C.; Samos, D.R.; and Bollard, R.J.H.: Statistical Failure Prediction Models for Brittle Materials. AIAA J., vol. 22, no. 1, Jan. 1984, pp. 135-140.

S   Samos, D.R.: Experimental Investigation and Probability of Failure Analysis of Pressure Loaded Alumina Discs, M.S. Thesis, Univ. of Washington, 1982.

Schaeffer, H.G.: MSC/NASTRAN Primer: Static and Normal Modes Analysis. 2nd ed., Schaeffer Analysis Inc., Mount Vernon, NH, 1979.

Service, T.H.; and Ritter, J.E.; Proof Testing to Assure Reliability of Structural Ceramics. Fracture Mechanics of Ceramics, Volume 7- Composties, Impact, Statistics, and High-Temperature Phenomena. Bradt, R.C.; Evans, A.G.; Hasselman, D.P.H.; and Lange, F.F., 1985, pp.255-264.

Shelleman, D.L., "Test Methodology for Tubular Ceramic Components (Fast Fracture Strength Study)," Ph.D. Thesis, The Pennsylvania State University, University Park, PA, May 1991.

Shelleman, D.L., Jadaan, O.M., Conway, J.C., and Mecholsky, J.J., " Prediction of the Strength of Ceramic Tubular Components: II. Experimental Verification," Journal of Testing and Evaluation, Vol. 19, No. 3, May 1991.

Shelleman, D.L., Jadaan, O.M., Butt, D.P., Tressler, R.E., Hellman, J.R., and Mecholsky, J.J., "High Temperature Tube Burst Test Apparatus," Journal of Testing and Evaluation, Vol. 20, No. 4, July 1992.

Shetty, D.K.; et al.: A Biaxial-Flexure Test for Evaluating Ceramic Strengths, J. Am. Ceram. Soc., vol. 66, no. 1, pp. 36-42, Jan. 1983.

Shetty, D. K.; Rosenfield, A. R.; Bansal, G. K.; and Duckworth, W. H.: Biaxial Flexure Test for Ceramics, Journal of the American Ceramic Society, Vol. 59, No. 12, pp. 1193-1197, 1980).

Shetty, D.L.; Rosenfield, A.R.; and Duckworth, W.H.: Statistical Analysis of Size and Stress State Effects on the Strength of an Alumina Ceramic. Methods for Assessing the Structural Reliability of Brittle Materials; ASTM-STP-844, S.W. Frieman and C.M. Hudson, eds., American Society for Testing and Materials, 1984, pp. 57-80.

Shetty, D.K.: Mixed-Mode Fracture Criteria for Reliability Analysis and Design with Structural Ceramics. J. Eng. Gas Turbines Power, vol. 109, no. 3, July 1987, pp. 282-289.

Shetty, D.K.; and Rosenfield, A.R.: Slow Crack Growth in Glass in Combined Mode I and Mode II loading. Scripta Metallurgica et Materialia, vol. 25, 1991, pp. 997-1002

Shih, T.T.: An Evaluation of the Probabilistic Approach to Brittle Design. Eng. Fract. Mech., vol. 13, no. 2, 1980, pp. 257-271.

Sih, G.C.: Handbook of Stress Intensity Factors. Lehigh University, 1973.

Sih, G.C.: Strain-Energy-Density Factor Applied to Mixed-Mode Crack Problems. Int. J. of Frac., vol. 10, 1974, pp.305-321.

Smith, F.W.; Emery, A.F.; and Kobayashi, A.S.: Stress Intensity Factors for Semi-Circular Cracks. J. Appl. Mech., vol. 34, no. 4, Dec. 1967, pp. 953-959.

Smith F.W.; and Sorenson, D.R.: Mixed-Mode Stress Intensity Factors for Semielliptical Surface Cracks. NASA CR-134684, 1974.

Stefansky, W.: Rejecting Outliers in Factorial Designs. Technometrics, vol. 14, no. 2, May 1972, pp. 469-479.

Stout, M.G.; and Petrovic, J.J.: Multiaxial Loading Fracture of AL_2O_3 Tubes: I, Experiments, J. Am. Ceram. Soc., vol. 67, no. 1, Jan. 1984, pp. 14-18.

Sturmer, G.; Methodische Ansatze zur Konstruktiven Gestaltung Keramischer Flammrohrelemente von Brennkammern. Ph.D. dissertation, University of Karlsruhe, Germany, 1991.

Sturmer, G.; Schulz, A.; and Wittig, S.: Life Time Prediction for Ceramic Gas Turbine Components. ASME Preprint 91-GT-96, June 1991.

Swank, L.R.; and Williams, R.M.: Correlation of Static Strengths and Speeds of Rotational Failure of Structural Ceramics. Am. Ceram. Soc. Bull., vol. 60, no. 8, Aug. 1981, pp. 830-834.

T   Tennery, V.J.: IEA Annex II Management, Subtask 4 Results. Ceramic Technology for Advanced Heat Engines Project, Semiannual Progress Report, Oct. 1986-Mar. 1987. ORNL/TM-10469, Martin Marietta Energy Systems, Inc., Oak Ridge, TN, 1987.

Thiemeier, T.: Lebensdauervorhersage fur Keramische Bauteile Unter Mehrachsiger Beanspruchung, Ph.D. disseration, University of Karlsruhe, Germany, 1989.

Thoman, D.R.; Bain, L.J.; and Antle, C.E.: Inferences on the Parameters of the Weibull Distribution. Technometrics, vol. 11, no. 3, Aug. 1969, pp. 445-460.

Tracy, P.G.; et al.: On Statistical Nature of Fracture, Int. J. Fract., vol. 18, no. 4, Apr. 1982, pp. 253-277.

W   Walker, K.: Effects of Environmental and Complex Load History on Fatigue Life. ASTM STP 462. American Society for Testing and Materials, Philadelphia, PA., 1970, p. 1.

Weibull, W.: A Statistical Theory of the Strength of Materials. Ingeniors Vetenskaps Akademien Handlinger, No. 151, 1939.

Weibull, W.: The Phenomenon of Rupture in Solids. Ingeniors Ventenskaps Akademien Handlinger, No. 153, 1939.

Weibull, W.: A Statistical Distribution Function of Wide Applicability, J. Appl. Mech., vol. 18, no. 3, Sept. 1951, pp. 293-297.

Wertz, J.L., and Heitman, P.W.: Predicting the Reliability of Ceramic Turbine Components. Advanced Gas Turbine Systems for Automobiles, SAE-SP-465, Society of Automotive Engineers, 1980, pp. 69-77.

Wiederhorn, S.M.: Fracture Mechanics of Ceramics. Bradt, R.C., Hasselurau, D.P., and Lang, F.F., eds., Plenum, New York, 1974, pp. 613-646.

Wiederhorn, S.M: Reliability, Life Prediction, and Proof Testing of Ceramics. Ceramics for High-Performance Applications. Burke, J.J.; Gorum, A.E.; and Katz, R.N., eds., 1974, pp.633-663.

Wiederhorn, S.M.; Tighe, N.J.: Proof Testing of Hot Pressed Silicon Nitride. J. Mater. Sci., vol. 13, 1978, pp. 1781-1793.

Wiederhorn, S.M.; Fuller, E.R.; and Thomson, R.: Micromechanisms of Crack Growth in Ceramics and Glasses in Corrosive Environments. Metal Science, August-September 1980, pp. 450-458.

Wiederhorn, S.M.; and Fuller, E.R., Jr.: Structural Reliability of Ceramic Materials. Materials Science and Engineering, vol. 71, 1985, pp. 169-186.
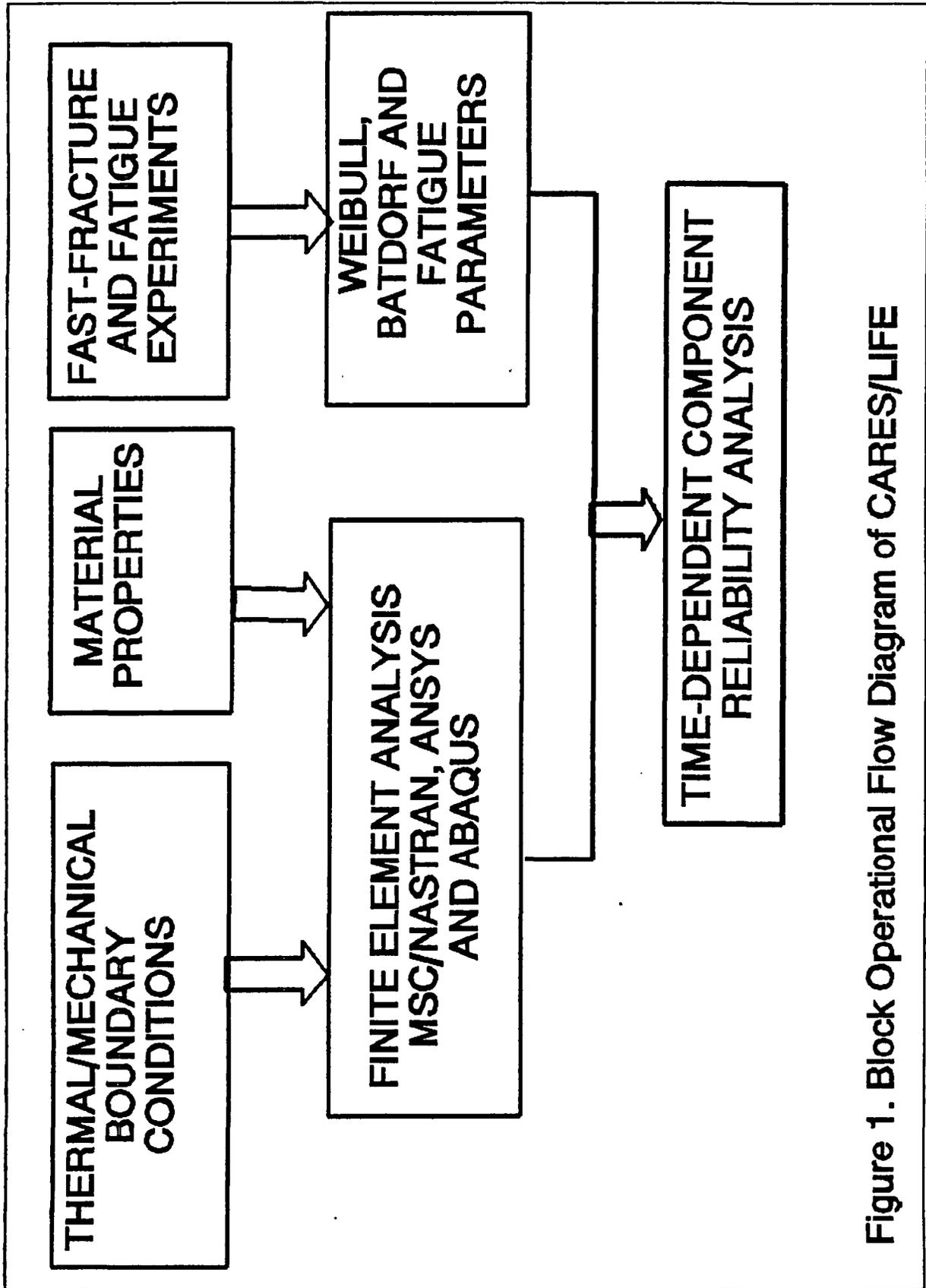
Figure 1. Block Operational Flow Diagram of CARES/LIFE
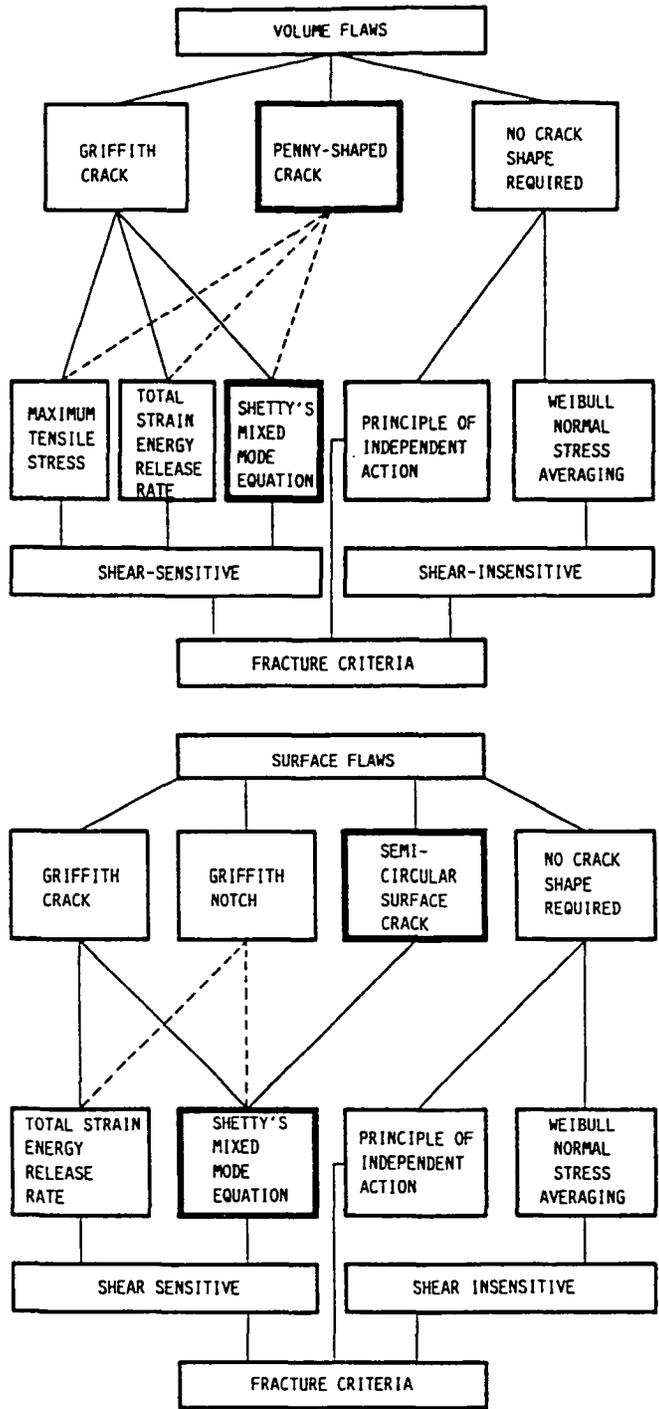
Figure 2.—Available failure criteria and crack shapes.

```
                    ┌─────────────────────────────────┐
                    │ COMPONENT GEOMETRY, LOADING      │
                    │ AND MATERIAL PROPERTIES          │
                    └─────────────────────────────────┘
                                   │
                        ┌──────────────────────┐
                        │ MODEL GENERATION     │──────────────── interactive
                        │ [PATRAN]             │                 pre- and
                        └──────────────────────┘                 post-
                        ┌──────────────────────┐                 processing
                        │ HEAT TRANSFER ANALYSIS│───────────────
                        └──────────────────────┘
                                   │
                              Temperature
                              at each node
                                   │
                        ┌──────────────────────┐
                        │ ELEMENT STRESS       │
                        │ ANALYSIS             │
                        │ [MSC/NASTRAN]        │────────────────
                        │ [ANSYS]              │
                        │ [ABAQUS]             │
                        └──────────────────────┘
                                   │
                              FEA output file:
                              nodal stresses,
                              temperatures, and
                              element connectivity
```

┌──────────────────────┐   ┌──────────────────────┐
│ FRACTURE STRENGTH   │   │ NEUTRAL FILE CREATION │
│ DATA, FLAW TYPES   │   │ [NASCARES]   │
│ AND   │   │ [ANSCARES]   │
│ FRACTURE CRITERIA   │   │ [ABACARES]   │
└──────────────────────┘   └──────────────────────┘

  Control or templet   Neutral data base
  file: files:
  {C4PEST.INP}   {CARES.NEU}
                                   {PROOF.NEU}

┌──────────────────────┐
│ ESTIMATE WEIBULL   │
│ AND FATIGUE   │
│ PARAMETERS   │
│ [C4PEST]   │
└──────────────────────┘

  Control or templet
  file:
  {CARES.INP}

              ┌─────────────────────────────────────┐
              │ CERAMICS ANALYSIS AND RELIABILITY   │
              │ EVALUATION OF STRUCTURES   │
              │ [C4LIFE]   │
              └─────────────────────────────────────┘

              {CARES.OUT}   {CARES.PAT}

      ┌──────────────────────┐   ┌──────────────────────┐
      │ VOLUME, SURFACE AND │   │ ELEMENT RISK OF   │
      │ COMPONENT RELIABILITY│   │ RUPTURE INTENSITIES │
      └──────────────────────┘   └──────────────────────┘

Figure 3 - Block diagram for the analysis and time-dependent reliability
           evaluation of ceramic components. This analysis includes the
           CARES/LIFE integrated design program, finite element analysis, and
           PATRAN PLUS pre- and post-processing.

```
                    --- CARES/LIFE TEMPLET INPUT FILE ---

                            VERSION 4.0

    ******************************************************************
    *                                                                *
    *     RELIABILITY PREDICTION FOR BRITTLE MATERIAL STRUCTURES     *
    *        --- FAST-FRACTURE AND TIME-DEPENDENT MODELING ---       *
    *                                                                *
    ******************************************************************

                        MASTER CONTROL INPUT

    TITLE        : PROBLEM TITLE (ECHOED IN CARES OUTPUT)
    ------------------------------------------------------------------
    SAMPLE INPUT FOR CARES/LIFE
    ------------------------------------------------------------------


    NE           : CONTROL INDEX FOR FINITE ELEMENT POSTPROCESSING
      *-*          (DEFAULT: NE = 0)
       3           0 : EXPERIMENTAL DATA ANALYSIS ONLY
      *-*          3 : COMPONENT RELIABILITY ANALYSIS WITH NEUTRAL FILE
                       DATA BASE

    IPRINC       : CONTROL INDEX FOR ELEMENT STRESS OUTPUT
      *-*          (DEFAULT: IPRINC=1)
       1           1 : USE PRINCIPAL STRESSES
      *-*          2 : USE ELEMENT OR MATERIAL COORDINATE SYSTEM STRESSES.
                       THIS OPTION IS RECOMMENDED FOR MATERIALS MODELED
                       WITH THE BATDORF THEORY.  WHEN TWO NEUTRAL FILES
                       ARE READ (IPROOF = 1) THEN IPRINC SHOULD BE SET
                       TO THIS VALUE

    NMATS        : NUMBER OF MATERIALS FOR SURFACE FLAW ANALYSIS
      *--*         (NMATS+NMATV < 101)
       01          (DEFAULT: NMATS = 0)
      *--*


    NMATV        : NUMBER OF MATERIALS FOR VOLUME FLAW ANALYSIS
      *--*         (NMATS+NMATV < 101)
       00          (DEFAULT: NMATV = 0)
      *--*


    IPRINT       : CONTROL INDEX FOR STRESS OUTPUT
      *-*          (DEFAULT: IPRINT = 0)
       1           0 : DO NOT PRINT ELEMENT STRESSES AND/OR FRACTURE DATA
      *-*          1 : PRINT ELEMENT STRESSES AND/OR FRACTURE DATA

    NGP          : NUMBER OF GAUSSIAN QUADRATURE POINTS (15 OR 30 OR 50)
      *--*         (DEFAULT: NGP = 15)
       15
      *--*
```

Figure 4. Master Control Input section of the templet file

```
NS          : NUMBER OF SEGMENTS IN SYMMETRY PROBLEM
  *---*       (DEFAULT: NS = 1)
   001
  *---*


IPROOF      : CONTROL INDEX FOR RELIABILITY ANALYSIS WITH NEUTRAL FILES
  *-*         (DEFAULT: IPROOF = 0)
   0          0 : READ ONLY ONLY ONE NEUTRAL FILE;
  *-*             EITHER STATIC OR CYCLIC LOADING RELIABILITY ANALYSIS
                  (NO PROOF TESTING IS CONSIDERED)
              1 : READ TWO NEUTRAL FILES;
                  INCLUDE THE EFFECTS OF PROOF TESTING OR CYCLIC LOADING
                  IN THE RELIABILITY ANALYSIS


IPOST       : CONTROL INDEX FOR PATRAN DATA FILE
  *-*         (DEFAULT: IPOST = 0)
   0          0 : DO NOT WRITE ELEMENT RISK OF RUPTURE INTENSITIES
  *-*         1 : WRITE ELEMENT RISK OF RUPTURE INTENSITIES


INTERP      : CONTROL INDEX FOR TEMPERATURE INTERPOLATED PARAMETERS
  *-*         (DEFAULT: INTERP = 0)
   0          0 : DO NOT WRITE INTERPOLATED MATERIAL PARAMETERS
  *-*         1 : WRITE INTERPOLATED MATERIAL PARAMETERS


FACTOR      : LOAD FACTOR FOR WHICH TO MULTIPLY ELEMENT STRESSES
----------    (DEFAULT: FACTOR = 1.0)
000001.000
----------


TIME        : SERVICE LIFE FOR RELIABILITY ANALYSIS OF THE FIRST NEUTRAL
----------    FILE IN UNITS OF SECONDS OR CYCLES (DEFAULT: TIME = 0.0)
000001.000
----------


TIMEPT      : DURATION OF THE PROOF TEST LOAD IN SECONDS OR NUMBER
----------    OF SERVICE CYCLES FOR RELIABILITY ANALYSIS USING THE SECOND
000000.00     NEUTRAL FILE (REQUIRES THAT IPROOF = 1).  FOR CYCLIC FATIGUE
----------    THIS INPUT SHOULD BE IDENTICAL TO THE VALUE INPUT FOR THE
              TIME KEYWORD (DEFAULT: TIMEPT = 0.0)


*****************************************************************
$ENDX       : END OF MASTER CONTROL INPUT
*****************************************************************
```

Figure 4. – Concluded

MATERIAL CONTROL INPUT

```
TITLE        : MATERIAL TITLE (ECHOED IN CARES OUTPUT)
-----------------------------------------------------------------------
SAMPLE INPUT FOR SURFACE FLAW ANALYSIS
-----------------------------------------------------------------------


MATID        : MATERIAL IDENTIFICATION NO. FROM THE FINITE ELEMENT
*-------*      MATERIAL PROPERTY CARD (IF POSTPROCESSING IS NOT
 0000300       BEING PERFORMED THIS ENTRY SHOULD BE SOME UNIQUE NO.)
*-------*      (NO DEFAULT)

ID1          : CONTROL INDEX FOR EXPERIMENTAL DATA
   *-*         (NO DEFAULT)
    5          1 : UNIFORM UNIAXIAL TENSILE SPECIMEN TEST DATA
   *-*         2 : FOUR-POINT BEND TEST DATA
               3 : DIRECT INPUT OF THE REQUIRED PARAMETERS
               4 : CENSORED DATA FOR SUSPENDED ITEM ANALYSIS OF
                   UNIFORM UNIAXIAL TENSILE SPECIMEN TEST DATA
               5 : CENSORED DATA FOR SUSPENDED ITEM ANALYSIS OF
                   FOUR-POINT BEND TEST DATA

ID4          : CONTROL INDEX FOR VOLUME OR SURFACE FLAW ANALYSIS
   *-*         (NO DEFAULT)
    2          1 : VOLUME
   *-*         2 : SURFACE

ID2          : CONTROL INDEX FOR FRACTURE CRITERION
   *-*         (NO DEFAULT)
    5          1 : NORMAL STRESS FRACTURE CRITERION
   *-*             (SHEAR-INSENSITIVE CRACK)
               2 : MAXIMUM TENSILE STRESS CRITERION (VOLUME FLAW ONLY)
               3 : COPLANAR STRAIN ENERGY RELEASE RATE CRITERION
                   (G SUB T)
               4 : WEIBULL PIA MODEL
               5 : SHETTY'S SEMI-EMPIRICAL CRITERION (NONCOPLANAR SERR)

ID3          : CONTROL INDEX FOR CRACK GEOMETRY
   *-*         (NO DEFAULT)
    4          1 : GRIFFITH CRACK (VOLUME FLAW OR SURFACE FLAW)
   *-*         2 : PENNY-SHAPED CRACK (VOLUME FLAW ONLY)
               3 : GRIFFITH NOTCH (SURFACE FLAW ONLY)
                   (ID2 = 3 OR 5 IS REQUIRED)
               4 : SEMICIRCULAR CRACK (SURFACE FLAW ONLY)
                   (ID2 = 5 IS REQUIRED)

IKBAT        : CONTROL INDEX FOR METHOD OF CALCULATING BATDORF CRACK
   *-*         DENSITY COEFFICIENT (K SUB B) FROM TEST DATA
    1          (DEFAULT: IKBAT = 1)
   *-*         0 : SHEAR-INSENSITIVE METHOD (MODE I FRACTURE ASSUMED)
               1 : SHEAR-SENSITIVE METHOD (FRACTURE ASSUMED TO OCCUR
                   ACCORDING TO THE FRACTURE CRITERION AND CRACK SHAPE
                   SELECTED BY THE ID2 AND ID3 INDICES)
```

Figure 5. Material Control Input section of the templet file

```
PR              : POISSON'S RATIO
----------        (DEFAULT: PR = 0.25)
00000.2500
----------


C               : CONSTANT FOR SEMI-EMPIRICAL MIXED-MODE FRACTURE CRITERIA
----------        (KI/KIC)+(KII/(C*KIC))**2 = 1      REF. D.K.SHETTY
00000.8000        OBSERVED VALUES RANGE FROM 0.8 TO 2. (REF. D.K. SHETTY)
----------        NOTE: AS C APPROACHES INFINITY, PREDICTED FAILURE
                  PROBABILITIES APPROACH NORMAL STRESS CRITERION VALUES
                  (DEFAULT C = 1.0)

CYCLIC          : CYCLIC FATIGUE BASED COMPONENT RELIABILITY EVALUATION
---*-*----
        1       : CRACK GROWTH LAW AND WAVE FORM (IWAVE) (DEFAULT: IWAVE = 1)
---*-*----
1.00000000      : R-RATIO OF MIN/MAX CYCLE STRESS (RCYC) (DEFAULT: RCYC = 1.0)
----------
1.00000000      : PERIOD (IN SECONDS) OF A CYCLE (PERIOD) (DEFAULT: PERIOD = 1.0)
----------
1.00000000      : EXPONENT OF POWER LAW WAVE FORM (QCYC) (DEFAULT: QCYC = 1.0).
----------
```

```
            ------------------------------------------------
            IWAVE = 0 :   PARIS LAW OR WALKER LAW
                  = 1 :   POWER LAW; STATIC LOAD
                  = 2 :   POWER LAW; SQUARE WAVE
                  = 3 :   POWER LAW; SAWTOOTH WAVE
                  = 4 :   POWER LAW; 1/2 SINE WAVE
                  = 5 :   POWER LAW; SINE WAVE
            ------------------------------------------------
```

NOTE: 1) THE R-RATIO INPUT (RCYC) ASSUMES THAT
          THE R-RATIO IS CONSTANT THROUGHOUT THE
          COMPONENT. THIS INPUT VALUE IS IGNORED
          IF A SECOND NEUTRAL FILE IS SPECIFIED
          (IPROOF = 1) WHERE RCYC IS THEN CALCULATED
          FOR EACH ELEMENT.

      2) THE WAVE FORM EXPONENT (QCYC) IS USED WITH
          THE POWER LAW (IWAVE > 1). THE G-FACTOR IS
          DETERMINED FOR THE SELECTED WAVE FORM RAISED TO
          THE QCYC EXPONENT. FOR EXAMPLE; IF A ROTATING
          COMPONENT HAS A SINUSIODAL VARIATION IN ANGULAR
          SPEED, THE STRESS IS DIRECTLY PROPORTIONAL TO THE
          SQUARE OF THE ANGULAR SPEED AND QCYC IS SET
          TO A VALUE OF 2.0

```
MLORLE          : CONTROL INDEX FOR METHOD OF CALCULATING WEIBULL
  *-*             PARAMETERS FROM THE EXPERIMENTAL FRACTURE DATA
  0               (DEFAULT: MLORLE = 0)
  *-*             0 : MAXIMUM LIKELIHOOD
                  1 : LEAST-SQUARES LINEAR REGRESSION
```

Figure 5. -Continued

```
OUTLIE        : SIGNIFICANCE LEVEL FOR WHICH OUTLIERS ARE TO
----------      BE DETECTED. INPUT IS IN PERCENT AND MUST BE BETWEEN
00000010.0      THE RANGE OF 0.1 PERCENT TO 10.0 PERCENT
----------      (DEFAULT OUTLIE = 10.0)


PFCONV        : FAILURE PROBABILITY TO CALCULATE THE WEIBULL SCALE
----------      PARAMETER FOR THE FINITE ELEMENT MODEL
0.00000000      ---> (ASSUMES MATERIAL PARAMETERS ARE CONSTANT VERSUS
----------           TEMPERATURE; ONLY ONE TEMPERATURE DATA SET IS INPUT)
                (DEFAULT PFCONV = 0.0 ,THUS QUANTITY NOT CALCULATED)
                NOTE:  0.0 < PFCONV < 1.0


DH            : HEIGHT OF THE FOUR-POINT BEND BAR
----------      (NO DEFAULT)
00002.1000
----------


DL1           : OUTER LOAD SPAN OF THE FOUR-POINT BEND BAR
----------      (NO DEFAULT)
00040.0000
----------


DL2           : INNER LOAD SPAN OF THE FOUR-POINT BEND BAR
----------      (NO DEFAULT)
00020.0000
----------


DW            : WIDTH OF THE FOUR-POINT BEND BAR
----------      (NO DEFAULT)
00002.8000
----------


*********************************************************************
$ENDM         : END OF TEMPERATURE-INDEPENDENT MATERIAL CONTROL INPUT
*********************************************************************
```

Figure 5. Concluded

TEMPERATURE-DEPENDENT MATERIAL CONTROL INPUT DATA
FOR THE ABOVE MATERIAL

!!!
PLEASE NOTE THE FOLLOWING:
  1. TEMPERATURE-DEPENDENT DATA SETS MUST BE ARRANGED IN ASCENDING ORDER
     ACCORDING TO TEMPERATURE (ONE DATA TABLE PER TEMPERATURE).
  2. FRACTURE STRESSES FOR A GIVEN TEMPERATURE CAN BE INPUT IN
     ARBITRARY ORDER.
  3. REGARDLESS OF THE FRACTURE ORIGIN LOCATION, THE FRACTURE STRESS
     INPUT VALUE IS THE EXTREME FIBER STRESS WITHIN THE INNER LOAD SPAN
     OF THE MOR BAR.
!!!

------------> DATA TABLE; EXPLANATION OF INPUT

         TEST : TYPE OF DATA TO BE INPUT.
                : BLANK CHARACTERS DEFAULT TO THE SETTING OF THE
                  IMMEDIATLY PRECEDING VALUE (THIS APPLIES TO
                  TEST AND FIELD1 ONLY FOR THE FAST, STAT, CYCL, AND
                  DYNA KEYWORDS)
         CYCL   : CYCLIC FATIGUE SPECIMEN DATA
                  FIELD1 : MAGNITUDE OF FATIGUE STRESS
                           (MAXIMUM CYCLE STRESS)
                  FIELD2 : LEAVE BLANK OR LIFETIME TO FAILURE
                           (UNITS OF SECONDS FOR POWER LAW)
                           (UNITS OF CYCLES FOR PARIS AND WALKER LAWS)
                  FIELD3 : LEAVE BLANK OR LIFETIME TO FAILURE
                           (UNITS OF SECONDS FOR POWER LAW)
                           (UNITS OF CYCLES FOR PARIS AND WALKER LAWS)
         CYCLIC : CYCLIC FATIGUE DATA (IWAVE)
                  (INPUT IN ALPHA-NUMERIC "FLAW" FIELD)
                      0 : PARIS LAW OR WALKER LAW
                      1 : DIRECT INPUT OF G-FACTOR
                      2 : POWER LAW; SQUARE WAVE
                      3 : POWER LAW; SAWTOOTH WAVE
                      4 : POWER LAW; 1/2 SINE WAVE
                      5 : POWER LAW; SINE WAVE

                  FIELD1 : R-RATIO OF MIN/MAX CYCLE STRESS OR
                           DIRECT INPUT OF G-FACTOR
                  FIELD2 : PERIOD OF THE CYCLE (SECONDS)
                  FIELD3 : WALKER R-RATIO SENSITIVITY EXPONENT
                           OR EXPONENT OF POWER LAW WAVE FORM (QCYC)

         WHEN QCYC IS SET TO ZERO BY THE USER AND THE WALKER OR
         PARIS LAW IS SELECTED, CARES/LIFE AUTOMATICALLY
         DEFAULTS QCYC TO THE VALUE OF THE FATIGUE EXPONENT N,
         WHICH DEFINES THE PARIS LAW.

         Figure 6. Temperature Dependent Material Control Input
                   section of the templet file

WHEN THE WAVE FORM EXPONENT (QCYC) IS USED WITH THE
POWER LAW (IWAVE > 1), THEN THE G-FACTOR IS DETERMINED FOR
THE SELECTED WAVE FORM RAISED TO THE QCYC EXPONENT.
FOR EXAMPLE; IF A ROTATING COMPONENT HAS A SINUSIODAL
VARIATION IN ANGULAR SPEED, THE STRESS IS DIRECTLY
PROPORTIONAL TO THE SQUARE OF THE ANGULAR SPEED AND
QCYC IS SET TO A VALUE OF 2.0

```
DYNA    : DYNAMIC FATIGUE (CONSTANT STRESS RATE) SPECIMEN DATA
            FIELD1 : MAGNITUDE OF STRESS RATE (STRESS/SECOND)
            FIELD2 : LEAVE BLANK OR ULTIMATE FAILURE STRESS
                        OF SPECIMEN
            FIELD3 : LEAVE BLANK OR ULTIMATE FAILURE STRESS
                        OF SPECIMEN
FAST    : FAST FRACTURE
            FIELD1 : LEAVE BLANK OR SPECIMEN FRACTURE STRESS
            FIELD2 : LEAVE BLANK OR SPECIMEN FRACTURE STRESS
            FIELD3 : LEAVE BLANK OR SPECIMEN FRACTURE STRESS
PARAM   : DIRECT INPUT OF FAST-FRACTURE WEIBULL PARAMETERS
            FIELD1 : WEIBULL MODULUS OR SHAPE PARAMETER
            FIELD2 : WEIBULL SCALE PARAMETER
            FIELD3 : WEIBULL CHARACTERISTIC STRENGTH
RSTRES  : RESIDUAL STRESSES IN THE MATERIAL COORDINATE SYSTEM
            FIELD1 : X STRESS COMPONENT (3-D AND 2-D)
            FIELD2 : Y STRESS COMPONENT (3-D AND 2-D)
            FIELD3 : Z STRESS COMPONENT (3-D ONLY)
+STRES  : RESIDUAL STRESSES IN THE MATERIAL COORDINATE SYSTEM
            FIELD1 : XY STRESS COMPONENT (3-D AND 2-D)
            FIELD2 : YZ STRESS COMPONENT (3-D ONLY)
            FIELD3 : ZX STRESS COMPONENT (3-D ONLY)
RANGE   : SEARCH RANGE TO FIND THE FATIGUE EXPONENT N WHEN
            THE MEDIAN DEVIATION TECHNIQUE IS SPECIFIED
            (SOL = 2 )
            (THE DEFAULT RANGE IS 2.1 TO 150.0)
            FIELD1 : BOUNDARY OF SEARCH RANGE
            FIELD2 : BOUNDARY OF SEARCH RANGE
            FIELD3 : LEAVE BLANK
SOL     : SOLUTION METHOD FOR THE TIME-DEPENDENT DATA
            (INPUT IN ALPHA-NUMERIC "FLAW" FIELD)
                    0 : MEDIAN VALUE LEAST SQUARES REGRESSION
                    1 : LEAST SQUARES REGRESSION
                    2 : MEDIAN DEVIATION ITERATION
STAT    : STATIC FATIGUE (CONSTANT STRESS) SPECIMEN DATA
            FIELD1 : MAGNITUDE OF FATIGUE STRESS
            FIELD2 : LEAVE BLANK OR TIME TO FAILURE (SECONDS)
            FIELD3 : LEAVE BLANK OR TIME TO FAILURE (SECONDS)
TEMP    : TEMPERATURE OF SET (ONE ASSIGNMENT PER DATA TABLE)
            FIELD1 : TEMPERATURE
            FIELD2 : LEAVE BLANK
            FIELD3 : LEAVE BLANK
TPARAM  : DIRECT INPUT OF TIME-DEPENDENT PARAMETERS
            FIELD1 : FATIGUE CRACK GROWTH EXPONENT N
            FIELD2 : FATIGUE CONSTANT B SUB W,
                        (STRESS**2*SECOND) OR (STRESS**2*CYCLE)
            FIELD3 : LEAVE BLANK OR WALKER R-RATIO
                        SENSITIVITY EXPONENT
```

Figure 6. -Continued

```
          VAGTIM : TIME-DEPENDENT EFFECTIVE VOLUME OR AREA
                   FIELD1 : EFFECTIVE VOLUME OR AREA
                   FIELD2 : LEAVE BLANK
                   FIELD3 : LEAVE BLANK
          VAGAGE : FAST-FRACTURE EFFECTIVE VOLUME OR AREA
                   FIELD1 : EFFECTIVE VOLUME OR AREA
                   FIELD2 : LEAVE BLANK
                   FIELD3 : LEAVE BLANK
          $ENDD  : END OF DATA MARKER FOR THE DATA TABLE


   FLAW : FRACTURE ORIGIN (ONLY FOR FAST, STAT, CYCL, AND
          DYNA KEYWORDS)
               : BLANK CHARACTER DEFAULTS TO FLAW TYPE INDICATED BY
                 THE ID4 KEYWORD
             S : SURFACE FLAW
             U : UNKNOWN FLAW (COMPETING FAILURE MODE OR RUN OUT)
             V : VOLUME FLAW
```

```
DTABLE       : DATA TABLE (FAST-FRACTURE, STATIC OR DYNAMIC FATIGUE)
-TEST-I-FLAW-I-----FIELD1------I-----FIELD2------I-----FIELD3------I
TEMP                0.100000E+04
SOL     2
RANGE               3.000000E+00      1.000000E+02
FAST                0.102300E+04
                    0.101100E+04
                    0.972000E+03
                    0.943000E+03
                    0.941000E+03
                    0.927000E+03
                    0.921000E+03
                    0.917000E+03
                    0.916000E+03
                    0.915000E+03
                    0.889000E+03
                    0.883000E+03
                    0.883000E+03
                    0.876000E+03
                    0.866000E+03
                    0.784000E+03
                    0.781000E+03
STAT    S           0.700000E+03      0.576000E+02
        S           0.650000E+03      0.432000E+02
        S           0.650000E+03      0.504000E+02
        S           0.650000E+03      0.792000E+02
        S           0.600000E+03      0.313200E+02
        S           0.600000E+03      0.900000E+02
        S           0.600000E+03      0.198000E+03
        S           0.550000E+03      0.360000E+04
        S           0.550000E+03      0.115200E+05
        S           0.550000E+03      0.176400E+05
        S           0.500000E+03      0.972000E+03
        S           0.500000E+03      0.648000E+04
        S           0.500000E+03      0.248040E+06
```

Figure 6. -Continued

```
          U           0.500000E+03      0.109620E+08
          U           0.450000E+03      0.508680E+07
          U           0.450000E+03      0.115704E+08
          S           0.400000E+03      0.296640E+07
          U           0.400000E+03      0.120024E+08
          U           0.400000E+03      0.124236E+08
STAT      S           0.750000E+03      0.608400E+01
          S           0.700000E+03      0.900000E+01
          S           0.700000E+03      0.273600E+02
          S           0.650000E+03      0.360000E+01
          S           0.650000E+03      0.370800E+02
          S           0.650000E+03      0.122400E+03
          S           0.600000E+03      0.756000E+03
          S           0.600000E+03      0.169200E+03
          S           0.600000E+03      0.345600E+03
          S           0.550000E+03      0.121680E+04
          S           0.550000E+03      0.219600E+04
          S           0.550000E+03      0.144000E+04
          S           0.500000E+03      0.100800E+05
          S           0.500000E+03      0.288000E+04
          S           0.500000E+03      0.255600E+04
          S           0.450000E+03      0.124344E+07
          S           0.450000E+03      0.173124E+08
          S           0.450000E+03      0.181152E+08
          S           0.700000E+03      0.504000E+01
$ENDD
-TEST-I-FLAW-I-----FIELD1------I-----FIELD2------I-----FIELD3------I
              END OF DATA FOR THE ABOVE TEMPERATURE


DTABLE      : DATA TABLE (FAST-FRACTURE, STATIC OR DYNAMIC FATIGUE)
-TEST-I-FLAW-I-----FIELD1------I-----FIELD2------I-----FIELD3------I
TEMP                0.110000E+04
SOL       2
STAT      S           0.650000E+03      0.108000E+02
          S           0.650000E+03      0.183600E+02
          S           0.650000E+03      0.396000E+02
          S           0.600000E+03      0.309600E+02
          S           0.600000E+03      0.504000E+02
          S           0.600000E+03      0.648000E+02
          S           0.550000E+03      0.576000E+02
          S           0.550000E+03      0.165600E+03
          S           0.550000E+03      0.194400E+03
          S           0.500000E+03      0.576000E+03
          S           0.500000E+03      0.972000E+03
          S           0.500000E+03      0.374400E+04
          S           0.450000E+03      0.136800E+05
          S           0.450000E+03      0.144000E+05
          S           0.450000E+03      0.208800E+05
          S           0.400000E+03      0.324000E+05
          S           0.400000E+03      0.385200E+05
          S           0.400000E+03      0.208080E+06
          S           0.400000E+03      0.248400E+06
          S           0.350000E+03      0.134280E+07
          S           0.350000E+03      0.176760E+07
```

Figure 6. -Continued

```
          S       0.350000E+03      0.203400E+07
          U       0.300000E+03      0.828000E+07
          U       0.300000E+03      0.118944E+08
$ENDD
-TEST-I-FLAW-I-----FIELD1------I-----FIELD2------I-----FIELD3------I
            END OF DATA FOR THE ABOVE TEMPERATURE


DTABLE      : DATA TABLE (FAST-FRACTURE, STATIC OR DYNAMIC FATIGUE)
-TEST-I-FLAW-I-----FIELD1------I-----FIELD2------I-----FIELD3------I
TEMP                0.120000E+04
SOL     2
STAT    S           0.600000E+03      0.360000E+01
        S           0.545000E+03      0.154800E+02
        S           0.545000E+03      0.201600E+02
        S           0.545000E+03      0.252000E+02
        S           0.500000E+03      0.972000E+02
        S           0.500000E+03      0.972000E+02
        S           0.500000E+03      0.147600E+03
        S           0.450000E+03      0.205200E+03
        S           0.450000E+03      0.237600E+03
        S           0.450000E+03      0.601200E+03
        S           0.400000E+03      0.154800E+04
        S           0.400000E+03      0.158400E+04
        S           0.400000E+03      0.277200E+04
        S           0.350000E+03      0.709200E+04
        S           0.350000E+03      0.108720E+05
        S           0.350000E+03      0.277200E+05
        S           0.317000E+03      0.205200E+05
        S           0.317000E+03      0.219600E+05
        S           0.317000E+03      0.302400E+05
        S           0.317000E+03      0.392400E+05
        S           0.317000E+03      0.410400E+05
        S           0.317000E+03      0.691200E+05
        S           0.250000E+03      0.442800E+06
        S           0.250000E+03      0.558000E+06
        S           0.248000E+03      0.540000E+06
        S           0.200000E+03      0.218888E+07
        S           0.200000E+03      0.236880E+07
        S           0.200000E+03      0.213480E+07
        S           0.200000E+03      0.191880E+07
        S           0.266000E+03      0.279000E+06
STAT    S           0.317000E+03      0.385200E+05
        S           0.317000E+03      0.554400E+05
        S           0.317000E+03      0.525600E+05
        S           0.317000E+03      0.345600E+05
        S           0.350000E+03      0.684000E+04
        S           0.350000E+03      0.756000E+04
        S           0.350000E+03      0.122400E+05
        S           0.350000E+03      0.136800E+05
        S           0.350000E+03      0.140400E+05
        S           0.350000E+03      0.126000E+05
```

Figure 6. -Continued

```
        S          0.250000E+03     0.489600E+06
        S          0.250000E+03     0.511200E+06
        S          0.250000E+03     0.540000E+06
$ENDD
-TEST-I-FLAW-I-----FIELD1------I-----FIELD2------I-----FIELD3------I
          END OF DATA FOR THE ABOVE TEMPERATURE


**********************************************************************
$ENDT      : END OF DATA FOR THE ABOVE MATERIAL
**********************************************************************
```

Figure 6. -Concluded

```
TEMP
----------
 1000.0000
----------


PARAM
*--------M--------*-------SP--------*
   0.1611065200E+02  0.1210912550E+04
*-----------------*-----------------*


TPARAM
*--------N--------*--------B--------*
   0.3113000000E+02  0.8027108872E+03
*-----------------*-----------------*



TEMP
----------
 1100.0000
----------


PARAM
*--------M--------*-------SP--------*
   0.2770502294E+02  0.1036704873E+04
*-----------------*-----------------*


TPARAM
*--------N--------*--------B--------*
   0.1836900000E+02  0.4116402524E+05
*-----------------*-----------------*



TEMP
----------
 1200.0000
----------


PARAM
*--------M--------*-------SP--------*
   0.1969015533E+02  0.1141176912E+04
*-----------------*-----------------*


TPARAM
*--------N--------*--------B--------*
   0.1215720002E+02  0.6478040059E+05
*-----------------*-----------------*


*******************************************************************
$ENDT
*******************************************************************
```

Figure 7. Temperature Dependent Material Control Input
style for module C4LIFE
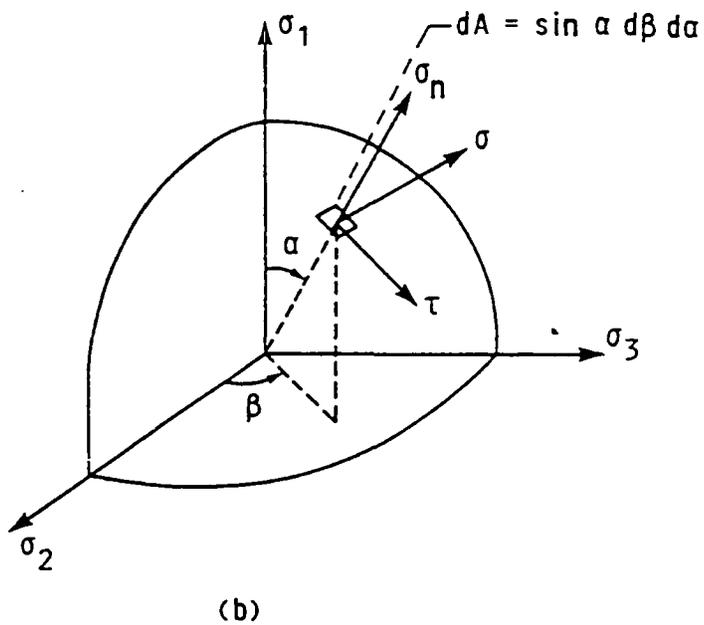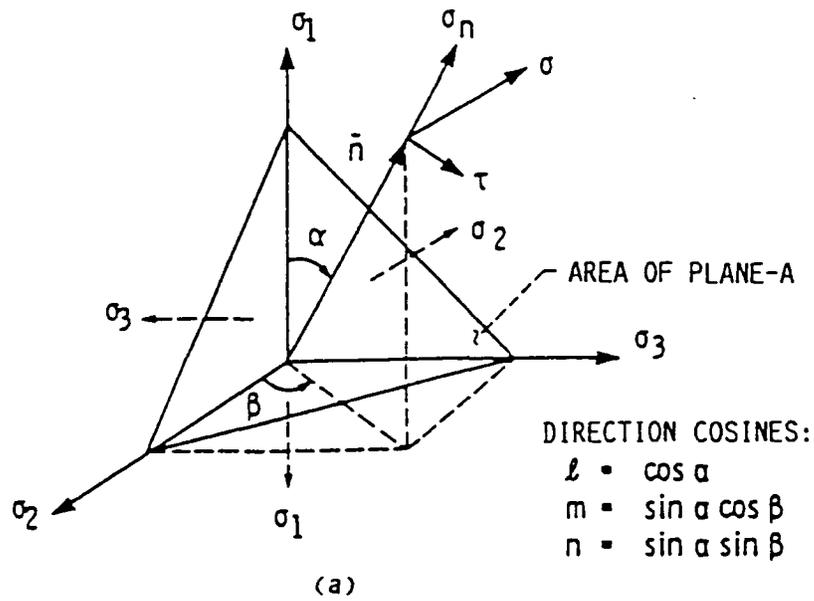
(a) In principal stress space.
(b) Projected onto a plane tangent to the unit radius sphere.

Figure 8.—Stresses on Cauchy infinitesimal tetrahedron.
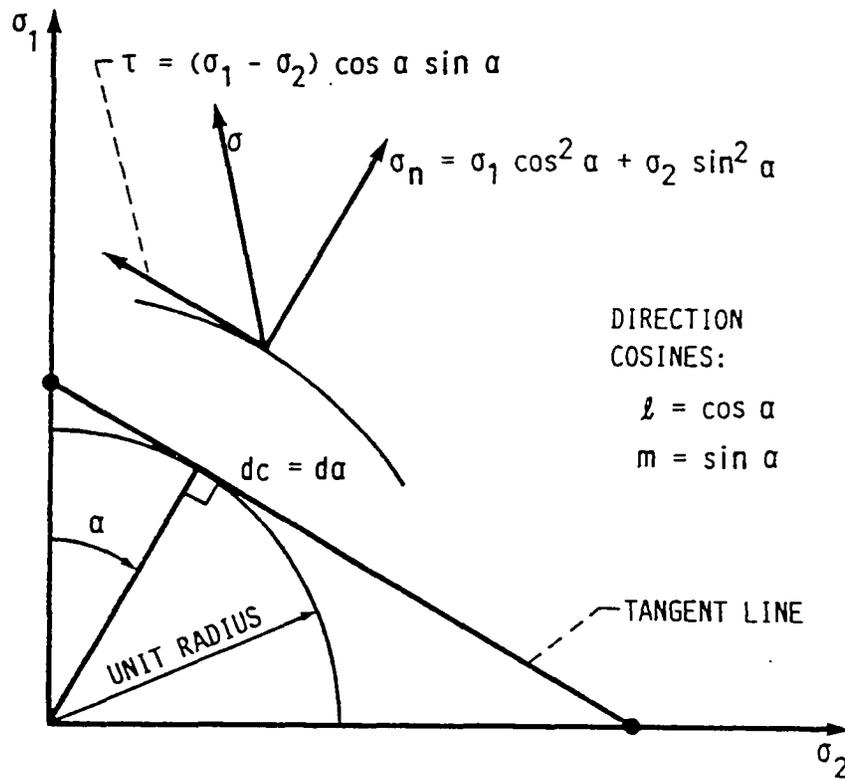
Figure 9.—Normal and shear stress as a function of α projected onto a tangent line to the unit radius circle (in principal stress space).
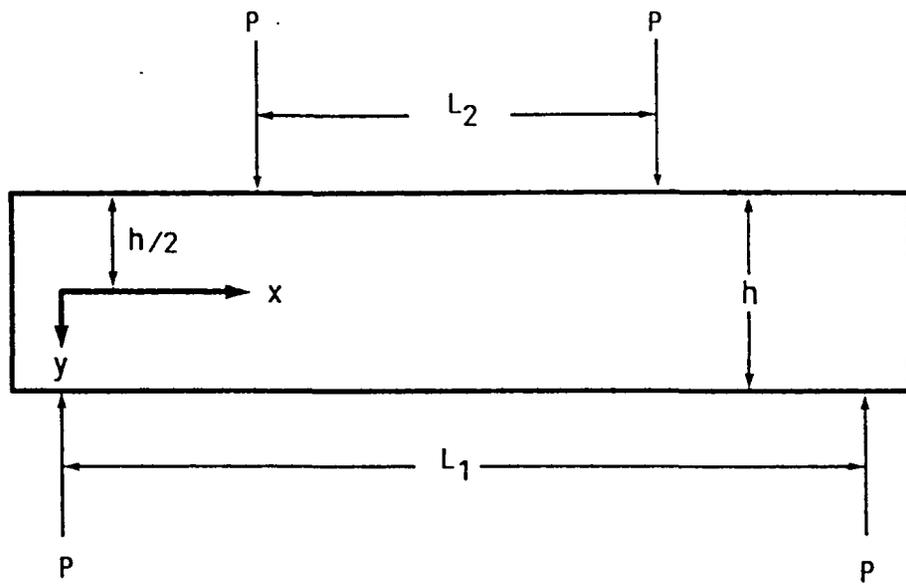
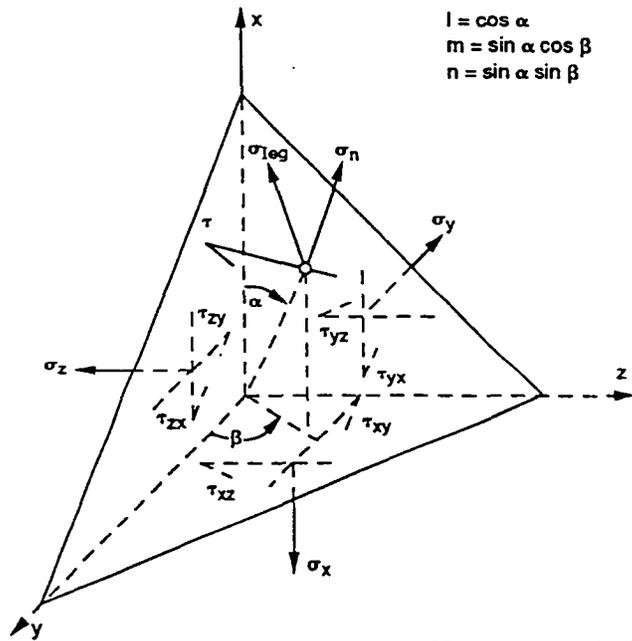Figure 10—Four-point bend specimen geometry (beam width is *w*).
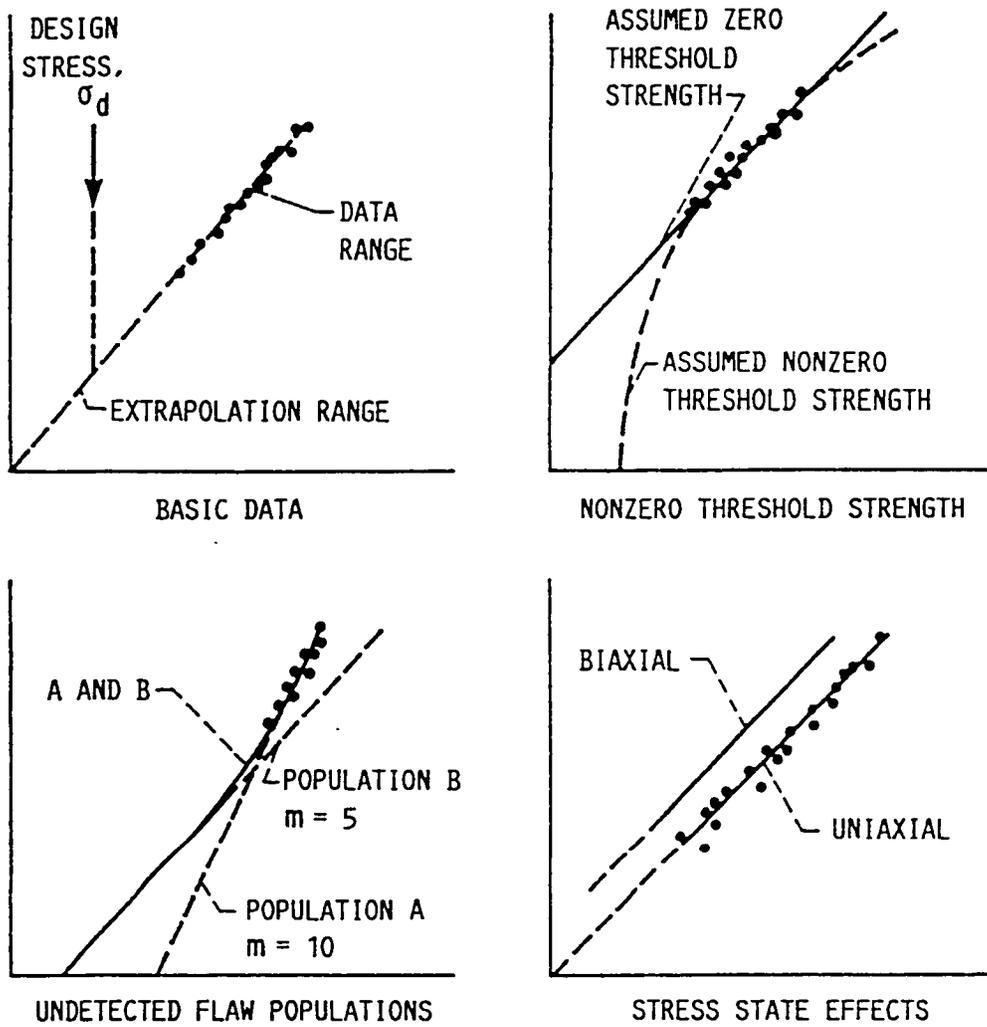
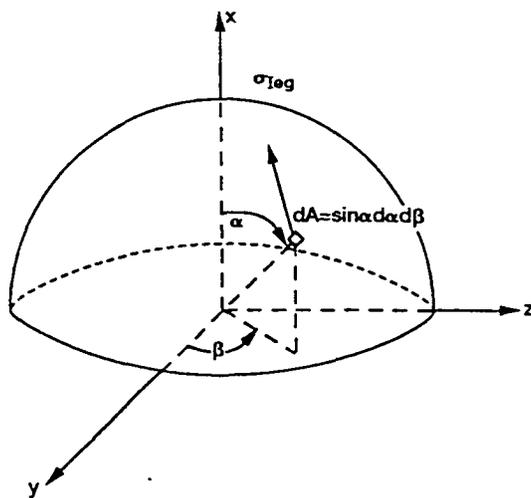Figure 11.—Limitations of experimental data extrapolation and statistical approach to design.

$$\sigma_n = l\sigma_x + m\sigma_y + n\sigma_z + 2(lm\tau_{xy} + mn\tau_{yz} + nl\tau_{zx})$$

$$\tau = \sqrt{(l\sigma_x + m\tau_{yx} + n\tau_{zx})^2 + (l\tau_{xy} + m\sigma_y + n\tau_{zy})^2 + (l\tau_{xz} + m\tau_{yz} + n\sigma_z)^2 - \sigma_n^2}$$

(a) Cauchy stress components on infinitesimal Tetraledron.

(b) Globial Coordinate System.

Figure 12.—Projection of equivalent stress onto upper half of a unit radius sphere in the global-coordinate system.

TABLE 1. g-FACTORS

$$H(t,C) = 1 \quad \text{for } t \geq C$$
$$H(t,C) = 0 \quad \text{for } t < C$$
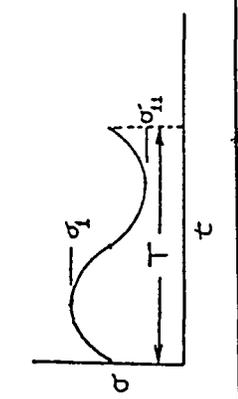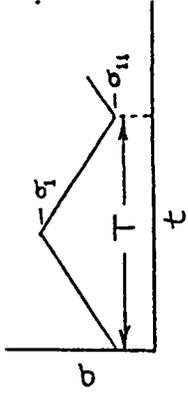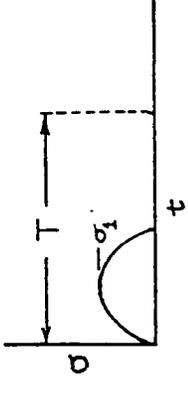$$\sigma_{11} \geq 0$$

Loading Function $\sigma_{leqc}(t)$	g-Factor $$g = \frac{1}{T}\int_0^T \left(\frac{\sigma_{leqc}(t)}{\sigma_{leqc_{max}}}\right)^N dt$$	Waveform
Static Fatigue $\sigma_{leqc} = \text{constant}$	1	
Dynamic Fatigue $\sigma_{leqc}(t) = \dot{\sigma}\, t$	$\dfrac{1}{N+1}$	
Cyclic Square Wave $\sigma_{leqc}(t) = \sigma_1[H(t,0)-H(t,t_1)] + \sigma_{11}[H(t,t_1)-H(t,T)]$	$\dfrac{t_1 + \left(\dfrac{\sigma_{11}}{\sigma_1}\right)^N t_{11}}{t_1 + t_{11}}$	
Sine Wave $\sigma_{leqc}(t) = \left(\dfrac{\sigma_1-\sigma_{11}}{2}\right)\sin\left(\dfrac{2\pi t}{T}\right) + \left(\dfrac{\sigma_1+\sigma_{11}}{2}\right)$	$\dfrac{1}{T}\int_0^T \left[\dfrac{\sigma_1+\sigma_{11}+(\sigma_1-\sigma_{11})\sin\left(\dfrac{2\pi t}{T}\right)}{2\,\sigma_1}\right]^N dt$	
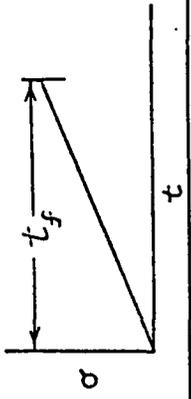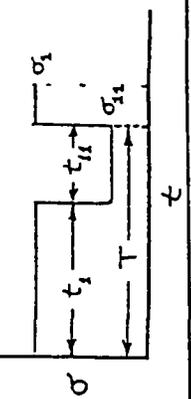
TABLE 1. g-FACTORS (Cont.)

$H(t,C) = 1 \quad \text{for } t \geq C$

$H(t,C) = 0 \quad \text{for } t < C$

$\sigma_{11} \geq 0$

Loading Function $\sigma_{leqc}(t)$	g-Factor $$g = \frac{1}{T}\int_0^T \left(\frac{\sigma_{leqc}(t)}{\sigma_{leqc_{max}}}\right)^N dt$$	Waveform
Cyclic Saw Tooth Wave $$\sigma_{leqc}(t) = \left(\frac{2(\sigma_1-\sigma_{11})t}{T}+\sigma_{11}\right)\left[H(t,0)-H\left(t,\frac{T}{2}\right)\right]$$ $$+\left(\frac{-2(\sigma_1-\sigma_{11})t}{T}+2\sigma_1-\sigma_{11}\right)\left[H\left(t,\frac{T}{2}\right)-H(t,T)\right]$$	$$\frac{\sigma_1-\sigma_{11}\left(\dfrac{\sigma_{11}}{\sigma_1}\right)^N}{(N+1)(\sigma_1-\sigma_{11})}$$	
Positive Half Pulse of Sine Wave $$\sigma_{leqc}(t) = \left(\sigma_1 \sin\left(\frac{2\pi t}{T}\right)\right)\left[H(t,0)-H\left(t,\frac{T}{2}\right)\right]$$	$$\frac{\Gamma\left(\dfrac{N+1}{2}\right)}{\sqrt{\pi}\, N\, \Gamma\left(\dfrac{N}{2}\right)}$$	

NOTE:

When $\sigma_{11} < 0$, the value of the g-factor is generally obtained numerically, integrating over the time interval where $\sigma_{Ieqc}(t) \geq 0$. The following simple example illustrates how CARES/LIFE handles this case. Given a saw tooth cyclic wave defined by (t, σ) over time interval T as $(0, \sigma_{11})$, $(\frac{T}{2}, \sigma_1)$, and (T, σ_{11}) with

$$R = \frac{\sigma_{11}}{\sigma_1} = -\frac{1}{3}$$

The interval where $\sigma_{Ieqc}(t) \geq 0$ is

$$\left(\frac{1}{1 + \left|\frac{\sigma_{11}}{\sigma_1}\right|} \right) T = \frac{3}{4} \frac{T}{4}$$

Hence

$$g = \frac{2}{T} \int_{\frac{T}{8}}^{\frac{T}{2}} \left[\frac{\frac{2(\sigma_1 - \sigma_{11})t}{T} + \sigma_{11}}{\sigma_1} \right]^N dt = \frac{2}{T} \int_{\frac{T}{8}}^{\frac{T}{2}} \left[\frac{2(1-R)t}{T} + R \right]^N dt$$

Thus, the resulting g-factor is

$$g = \frac{3}{4(N+1)}$$

341

REPORT DOCUMENTATION PAGE

Public reporting burden for this collection of information is estimated to average 1 hour per response, including the time for reviewing instructions, searching existing data sources, gathering and maintaining the data needed, and completing and reviewing the collection of information. Send comments regarding this burden estimate or any other aspect of this collection of information, including suggestions for reducing this burden, to Washington Headquarters Services, Directorate for Information Operations and Reports, 1215 Jefferson Davis Highway, Suite 1204, Arlington, VA 22202-4302, and to the Office of Management and Budget, Paperwork Reduction Project (0704-0188), Washington, DC 20503.

1. AGENCY USE ONLY (Leave blank)	2. REPORT DATE	3. REPORT TYPE AND DATES COVERED
	February 2003	Technical Memorandum

4. TITLE AND SUBTITLE

CARES/LIFE Ceramics Analysis and Reliability Evaluation of Structures Life Prediction Program

6. AUTHOR(S)

Noel N. Nemeth, Lynn M. Powers, Lesley A. Janosik, and John P. Gyekenyesi

5. FUNDING NUMBERS

WBS-22-708-31-09

7. PERFORMING ORGANIZATION NAME(S) AND ADDRESS(ES)

National Aeronautics and Space Administration
John H. Glenn Research Center at Lewis Field
Cleveland, Ohio 44135-3191

8. PERFORMING ORGANIZATION REPORT NUMBER

E-13748

9. SPONSORING/MONITORING AGENCY NAME(S) AND ADDRESS(ES)

National Aeronautics and Space Administration
Washington, DC 20546-0001

10. SPONSORING/MONITORING AGENCY REPORT NUMBER

NASA TM—2003-106316

11. SUPPLEMENTARY NOTES

This document was initially released in 1993. The formal numbered publication was delayed until 2003. Noel N. Nemeth, Lesley A. Janosik, and John P. Gyekenyesi, NASA Glenn Research Center; Lynn M. Powers, Case Western Reserve University, Cleveland, Ohio 44106. Responsible person, Noel N. Nemeth, organization code 5920, 216-433-3215.

12a. DISTRIBUTION/AVAILABILITY STATEMENT

Unclassified - Unlimited
Subject Category: 39   Distribution: Nonstandard

Available electronically at http://gltrs.grc.nasa.gov

This publication is available from the NASA Center for AeroSpace Information, 301-621-0390.

12b. DISTRIBUTION CODE

13. ABSTRACT (Maximum 200 words)

This manual describes the Ceramics Analysis and Reliability Evaluation of Structures Life Prediction (CARES/LIFE) computer program. The program calculates the time-dependent reliability of monolithic ceramic components subjected to thermomechanical and/or proof test loading. CARES/LIFE is an extension of the CARES (Ceramic Analysis and Reliability Evaluation of Structures) computer program. The program uses results from MSC/NASTRAN, ABAQUS, and ANSYS finite element analysis programs to evaluate component reliability due to inherent surface and/or volume type flaws. CARES/LIFE accounts for the phenomenon of subcritical crack growth (SCG) by utilizing the power law, Paris law, or Walker law. The two-parameter Weibull cumulative distribution function is used to characterize the variation in component strength. The effects of multiaxial stresses are modeled by using either the principle of independent action (PIA), the Weibull normal stress averaging method (NSA), or the Batdorf theory. Inert strength and fatigue parameters are estimated from rupture strength data of naturally flawed specimens loaded in static, dynamic, or cyclic fatigue. The probabilistic time-dependent theories used in CARES/LIFE, along with the input and output for CARES/LIFE, are described. Example problems to demonstrate various features of the program are also included.

14. SUBJECT TERMS

Life (durability); Fatigue life; Reliability analysis; Reliability; Fracture strength; Structural analysis; Component reliability; Finite element method; Ceramics

15. NUMBER OF PAGES

350

16. PRICE CODE

17. SECURITY CLASSIFICATION OF REPORT	18. SECURITY CLASSIFICATION OF THIS PAGE	19. SECURITY CLASSIFICATION OF ABSTRACT	20. LIMITATION OF ABSTRACT
Unclassified	Unclassified	Unclassified	